U.S. DEPARTMENT OF COMMERCE
National Technical Information Service

PB-260 498

Particulate Collection Problems in Converting to Low Sulfur Coals

Southern Research Inst, Birmingham, Ala

Prepared for

Industrial Environmental Research Lab, Research Triangle Park, N C

. Oct 76

TECHNICAL REPORT DATA

(Please read Instructions on the reverse before completing)

1. REPORT NO.
EPA-600/7-76-016

2.

3. RECIPIENT'S ACCESSION NO.
PB-260 498

4. TITLE AND SUBTITLE
CONFERENCE ON PARTICULATE COLLECTION PROBLEMS IN CONVERTING TO LOW SULFUR COALS

5. REPORT DATE
October 1976

6. PERFORMING ORGANIZATION CODE

7. AUTHOR(S)
G. B. Nichols (Compiler)

8. PERFORMING ORGANIZATION REPORT NO.

9. PERFORMING ORGANIZATION NAME AND ADDRESS
Southern Research Institute
2000 Ninth Avenue, South
Birmingham, Alabama 35205

10. PROGRAM ELEMENT NO.
EHE624

11. CONTRACT/GRANT NO.
68-02-2114

12. SPONSORING AGENCY NAME AND ADDRESS
EPA, Office of Research and Development
Industrial Environmental Research Laboratory
Research Triangle Park, NC 27711

13. TYPE OF REPORT AND PERIOD COVERED
Proceedings; 1-9/76

14. SPONSORING AGENCY CODE
EPA-ORD

15. SUPPLEMENTARY NOTES IERL-RTP Project Officer for this report is D. C. Drehmel, Mail Drop 61. 919/549-8411 Ext 2925.

16. ABSTRACT These proceedings present papers that discuss problems encountered in burning low-sulfur coal in electrical utility power plant boilers. Operating experience with electrostatic precipitators (ESPs), fabric filter baghouses, and wet scrubbers for control of fly ash stack emissions and techniques for improving performance are described. Increasing the collection efficiency of ESPs for high-resistivity fly ash by adding conditioning agents (e.g., sulfur trioxide, sulfuric acid, ammonium sulfate, sulfamic acid, and ammonia) to the flue gas is discussed, as are possible mechanisms for their action. Experiments are described on the reentrainment of fly ash as the result of rapping ESP collection electrodes. A mathematical model is described that calculates the collection efficiency of an ESP as a function of particle size and operating conditions. A mathematical model is also presented for fabric filter action; it incorporates a model of collection efficiency and a non-linear model of fabric drag. Fractional collection efficiency data for submicron fly ash particles are given for a baghouse. Performance data are also presented for wet scrubbers collecting fly ash and in one experiment include the chemical composition (e.g., content of trace elements) of the uncollected fly ash. A multiple-stream process is described for cleaning coal to produce fractions of low and medium sulfur contents by specific gravity differences.

17. KEY WORDS AND DOCUMENT ANALYSIS

a. DESCRIPTORS		b. IDENTIFIERS/OPEN ENDED TERMS	c. COSATI Field/Group	
Air Pollution	Fly Ash	Air Pollution Control	13B	
Dust Collectors	Mathematical Models	Stationary Sources	13A	12A
Coal	Fabrics	Particulate	21D	11E
Combustion	Flue Gases	Low-Sulfur Coal	21B	
Electric Power Plants		Baghouses	10B	
Electrostatic Precipitators		Fabric Filters		
		Coal Cleaning		

18. DISTRIBUTION STATEMENT
Unlimited

19. SECURITY CLASS *(This Report)*
Unclassified

20. SECURITY CLASS *(This page)*
Unclassified

21. NO. OF PAGES
257

22. PRICE
$9.00

EPA Form 2220-1 (9-73)

PB 260 498

EPA

U.S. Environmental Protection Agency
Office of Research and Development

Industrial Environmental Research
Laboratory
Research Triangle Park, North Carolina 27711

EPA-600/7-76-016
October 1976

CONFERENCE ON PARTICULATE COLLECTION PROBLEMS IN CONVERTING TO LOW SULFUR COALS

Interagency
Energy-Environment
Research and Development
Program Report

REPRODUCED BY
NATIONAL TECHNICAL
INFORMATION SERVICE
U. S. DEPARTMENT OF COMMERCE
SPRINGFIELD, VA. 22161

RESEARCH REPORTING SERIES

Research reports of the Office of Research and Development, U.S. Environmental Protection Agency, have been grouped into seven series. These seven broad categories were established to facilitate further development and application of environmental technology. Elimination of traditional grouping was consciously planned to foster technology transfer and a maximum interface in related fields. The seven series are:

1. Environmental Health Effects Research
2. Environmental Protection Technology
3. Ecological Research
4. Environmental Monitoring
5. Socioeconomic Environmental Studies
6. Scientific and Technical Assessment Reports (STAR)
7. Interagency Energy-Environment Research and Development

This report has been assigned to the INTERAGENCY ENERGY-ENVIRONMENT RESEARCH AND DEVELOPMENT series. Reports in this series result from the effort funded under the 17-agency Federal Energy/Environment Research and Development Program. These studies relate to EPA's mission to protect the public health and welfare from adverse effects of pollutants associated with energy systems. The goal of the Program is to assure the rapid development of domestic energy supplies in an environmentally--compatible manner by providing the necessary environmental data and control technology. Investigations include analyses of the transport of energy-related pollutants and their health and ecological effects; assessments of, and development of, control technologies for energy systems; and integrated assessments of a wide range of energy-related environmental issues.

REVIEW NOTICE

This report has been reviewed by the participating Federal Agencies, and approved for publication. Approval does not signify that the contents necessarily reflect the views and policies of the Government, nor does mention of trade names or commercial products constitute endorsement or recommendation for use.

This document is available to the public through the National Technical Information Service, Springfield, Virginia 22161.

EPA-600/7-76-016
October 1976

CONFERENCE ON PARTICULATE COLLECTION PROBLEMS IN CONVERTING TO LOW SULFUR COALS

G.B. Nichols, Compiler

Southern Research Institute
2000 Ninth Avenue South
Birmingham, Alabama 35205

Contract No. 68-02-2114
Program Element No. EHE624

EPA Project Officer: Dennis C. Drehmel

Industrial Environmental Research Laboratory
Office of Energy, Minerals, and Industry
Research Triangle Park, NC 27711

Prepared for

U.S. ENVIRONMENTAL PROTECTION AGENCY
Office of Research and Development
Washington, DC 20460

ABSTRACT

The papers in these proceedings discuss problems encountered in burning low-sulfur coal in electrical utility power plant boilers. Operating experience with electrostatic precipitators, fabric filter baghouses, and wet scrubbers for control of fly ash stack emissions and techniques for improving performance are described. Increasing the collection efficiency of electrostatic precipitators for high-resistivity fly ash by adding conditioning agents (e.g., sulfur trioxide, sulfuric acid, ammonium sulfate, sulfamic acid, and ammonia) to the flue gas is discussed, as are possible mechanisms for their action. Experiments on the reentrainment of fly ash as the result of rapping precipitator collection electrodes are described. A mathematical model that calculates the collection efficiency of an electrostatic precipitator as a function of particle size and operating conditions is described. A mathematical model is also presented for fabric filter action; it incorporates a model of collection efficiency and a non-linear model of fabric drag. Fractional collection efficiency data for sub-micron fly ash particles are given for a baghouse. Performance data are also presented for wet scrubbers collecting fly ash and in one experiment include the chemical composition (e.g., content of trace elements) of the uncollected fly ash. A multiple-stream process is described for cleaning coal to produce fractions of low and medium sulfur contents by specific gravity differences.

CONTENTS

Abstract iii

Acknowledgements iv

Figures. vii

Tables xii

Introduction
John K. Burchard 1

Paper 1. Operating Experience with ESP Conditioning in Relation to an Electrostatic Precipitator Upgrading Program
Scott H. Cragle 3

Paper 2. Sulfur Trioxide Injection at State Line Station
Ronald Cook and Michael Trykoski 20

Paper 3. Discussion and Comparison of Clinch River and Glen Lyn Plant Electrostatic Precipitators
W. J. Buchanan 30

Paper 4. The MCCS Coal Cleaning Plant at Homer City Station
Willard A. Crandall 36

Paper 5. Electrostatic Precipitator Options for Collection of High Resistivity Fly Ash
L. E. Sparks 58

Paper 6. Mathematical Modelling of Fine Particle Collection by Electrostatic Precipitation
John P. Gooch and Jack R. McDonald 68

Paper 7. Techniques for Conditioning Fly Ash
Edward B. Dismukes 107

Paper 8. Rapping Reentrainment Studies
Herbert W. Spencer, III 123

Paper 9. Fabric Filtration Performance Model
Douglas W. Cooper and Vladimir Hampl 149

CONTENTS (Continued)

Paper 10. Operating Experience and Performance at the Sunbury Baghouse
Harry Spagnola and James H. Turner 186

Paper 11. Scrubber Experience at Mohave
John M. Johnson, Dale G. Jones, Alexander Weir, Jr.,
W. Carl Martin, and Seymour Calvert 208

Paper 12. Evaluation of a Particulate Scrubber on a Full Scale Utility Boiler
D. S. Ensor, L. E. Sparks, S. Calvert, D. V. Wallon,
and K. S. Campbell 225

Metric Conversion Factors 244

FIGURES

Figure Page

PAPER 1

1 Optical density vs. grain loading, Montour Unit 1 . . . 6
2 Apollo injection locations (temperature full load - temperature half load) 9
3 Selected resistivity data with and without LPA-402 conditioning 13

PAPER 2

1 Sulfur burning flue gas conditioning system, State Line Unit 3 22
2 Effect of conditioning level on collection efficiency, State Line Unit 3 23
3 Corona power input as a function of SO_3 addition . . . 24
4 Flow diagram, flue gas conditioning unit 26

PAPER 4

1 New multi-stream coal cleaning process, Homer City Electric Generating Station 41
2 Effect of size on quality of 1.3 sp. gr. float product 42
3 Effect of specific gravity of separation on sulfur content of cleaned coal 43
4 Homer City - MCCS simplified diagram 45
5 Homer City - MCCS simplified diagram, coal cleaning circuits 46
6 MCCS coal sulfur balance 50
7 MCCS coal heat content balance 51
8 Photo of Homer City MCCS plant during construction . . 52
9 Photo of Homer City MCCS plant during construction . . 53

PAPER 6

1 "F" as a function of ideal efficiency and gas flow standard deviation 78
2 Degradation from 99.9% efficiency with sneakage 80
3 Correction factor for by-pass sneakage when N_S=5 . . . 81
4 Effect of reentrainment on the efficiency of a four-section precipitator designed for a no-reentrainment efficiency as indicated for a monodisperse particulate 83

Figure Page

PAPER 6 (Continued)

5 Schematic drawing of the laboratory precipitator . . 85
6 Inlet particle size distributions from Brink data . . 86
7 Experimentally measured and ideal calculated fractional collection efficiencies in the laboratory precipitator 88
8 Experimentally measured, ideal calculated, and sneakage-corrected fractional collection efficiencies for a current density of 53.8 nA/cm^2 and a gas velocity of 0.72 m/sec in the laboratory precipitator 89
9 Experimentally measured, ideal calculated, and sneakage-corrected fractional collection efficiencies for a current density of 26.9 nA/cm^2 and a gas velocity of 0.72 m/sec in the laboratory precipitator 90
10 Experimental and theoretical data for a wire of radius 1.488 x 10^{-3}m 91
11 Effective migration velocities for a full-scale precipitator on a coal-fired boiler 93
12 Fractional collection efficiencies for a full-scale precipitator on a coal-fired power boiler 94
13 Computed performance curves at 5 nA/cm^2 94
14 Computed performance curves at 10 nA/cm^2 95
15 Computed performance curves at 15 nA/cm^2 96
16 Computed performance curves at 20 nA/cm^2 97
17 Computed performance curves at 40 nA/cm^2 98
18 Computed performance curves for "hot" precipitator . 99
19 Measured and theoretical fractional efficiency . . . 100
20 Effective migration velocity vs particle diameter . . 100
21 Computed and measured data from pilot precipitator . 102
22 Computed and measured data from pilot precipitator . 103
23 Comparison of measured and computed fractional collection efficiencies 104

PAPER 7

1 Electrical resistivity of fly ash as a function of temperature or water vapor concentration 110
2 Concentration of sulfur trioxide as a function of sampling location or temperature 111
3 Acidity and sulfate content of fly ash as functions of temperature and water vapor concentration . . . 112
4 Resistivity as a function of the concentration of injected sulfur trioxide 113

FIGURES (Continued)

Figure Page

PAPER 7 (Continued)

5 Concentration of sulfur trioxide as a function of gas temperature at the outlet of a precipitator 115
6 Reduction of rapping reentrainment by ammonia 119
7 Rapidity of the effect of ammonia on the voltage of a precipitator 120

PAPER 8

1 Block diagram of experimental layout for a rapping reentrainment study 126
2 Schematic of diluter for real time particle sizing system 129
3 Extractive sampling system for real time system . . . 129
4 Percent emissions due to rapping for particles with diameters of 1 to 20 μm 131
5 Cumulative percent distribution for rapping puffs, rapping intervals of 12, 32, and 52 minutes, pilot test 131
6 Particle size distributions for inlet particulate, outlet particulate with rapping, outlet particulate without rapping, and average effective distribution for rapping puffs 133
7 Fractional efficiencies as function of particle diameter for half normal current density test. Test location Number 3 133
8 Average efficiencies for FluiDyne pilot precipitator for various rapping intervals 134
9 Dust removal efficiency versus time interval between raps 134
10 Precipitator efficiency at Test location Number 1 as a function of the rapping interval 137
11 Percent of dust collected on precipitator plates emitted from pilot precipitator due to rapping . . 137
12 Spatial distribution of particles in rapping puff . . 139
13 Rapping puffs at the exit plane of the pilot precipitator, upstream and downstream raps 140

PAPER 9

1 Schematic of n-compartment baghouse 151
2 Theoretical and experimental curves of glass fiber filter 158
3 Theoretical and experimental curves of Dacron-type filter 158
4 Baghouse simulation program flow chart 165
5 Fabric filter cake, resting on fabric 166

FIGURES (Continued)

Figure | Page

PAPER 9 (Continued)

6 Schematic of flow model for analysis of impaction and interception 171
7 Test run No. 5: 15-bag simulation pressure versus time graph 174
8 Test run No. 5: baghouse simulation individual flow rate graph 174
9 Test run No. 13a baghouse simulation penetration . . 175
10 Test run No. 13b: baghouse simulation penetration versus time graph; single bag, nonlinear drag, with pinholes 179
11 Test run No. 15 baghouse simulation penetration versus time graph; single bag, nonlinear drag, without pinholes 180
12 Test run No. 16 baghouse simulation penetration versus time graph; three bags, nonlinear drag, with pinholes 180

PAPER 10

1 Location of dust removal equipment 188
2 Baghouse general arrangement 190
3 Gas flow through baghouse compartments during normal operation and cleaning 191
4 Differential pressure chart - indicating a damper malfunction on 2A baghouse 198
5 Installing filter bag 200
6 Bolometer chart - indicating a bag failure in compartment No. 14 of No. 2B baghouse 201
7 Baghouse performance at Sunbury Steam Electric Station 206

PAPER 11

1 170 MW Vertical module (4-stage TCA). 210
2 170 MW Horizontal module (4-stage). 211
3 Inlet vs. outlet grain loading, 170 MW horizontal module 213
4 Inlet vs. outlet grain loading, 170 MW vertical TCA module 214
5 Inlet vs. outlet grain loading, 170 MW vertical PPA module 214
6 Effect of turndown ratio on particulate removal . . . 215
7 Effect of liquid flow rate on vertical TCA module particulate removal 216
8 Effect of liquid flow rate on horizontal module particulate removal 217
9 Overall penetration as predicted by impaction collection theory 219

FIGURES (Continued)

Figure Page

PAPER 11 (Continued)

10 Comparison of power requirements to produce a given "cut diameter" 221

PAPER 12

1 Scrubber system 227
2 Combined penetrations for diffusion battery and cascade impactor (December 10, 1974) 231
3 Combined penetrations of diffusion battery and cascade impactor (December 11, 1974) 232
4 Combined penetrations for diffusion battery and cascade impactor (December 12, 1974) 232
5 Scrubber penetrations for selected elements 234
6 Cherokee No. 3 scrubber accumulative availability from start-up to November 1974 240
7 Cherokee No. 3 scrubber accumulative availability from start-up to November 1974 averaged over the previous year on a running basis 242

TABLES

Table Page

PAPER 1

1 Design Data on Precipitators Included in PL's Particulate Compliance Program 5
2 Montour: LPA-40 Performance 7
3 Montour No. 2: LPA-402A Performance 11

PAPER 2

1 Typical Coal and Ash Analysis Arch Mineral No. 1 . . . 21
2 State Line Station Generating Units 25
3 Summary of State Line Test Results 29

PAPER 3

1 Precipitator Design Parameters 31
2 Percent of Total Coal Tonnage Delivered in Two Sulfur Ranges 33
3 Fly Ash Analysis 34

PAPER 4

1 Participants in Homer City MCCS Project 38
2 Typical Coal Analyses 48
3 Homer City Generating Station Alternative SO_2 Control Strategies(cost comparison) 48
4 Homer City Generating Station Alternative SO_2 Control Strategies(estimated materials consumed) 49
5 Homer City Generating Station Alternative SO_2 Control Strategies(estimated effluent comparison) 49
6 Ambient Air Quality SO_2 Concentrations (Forecast) . . . 49
7 Concurrent Research & Development Programs 54

PAPER 5

1 Electrostatic Precipitator Specific Collector Area Required for 99.5% Particle Collection for Various Current Densities 61
2 Partial List of Conditioning Agents 63
3 Effect of Conditioning on Efficiency 64

TABLES (Continued)

Table Page

PAPER 6

1 Typical Inlet and Outlet Particle Size Data for Wet ESP Experiments 87

PAPER 7

1 Equilibrium Distribution of Oxidized Forms of Sulfur at Various Gas Temperatures 108
2 Reduction of Rapping Reentrainment by Sulfur Trioxide 118

PAPER 8

1 Percentage Contribution of Rapping Reentrainment to Total Emissions 130
2 Effect of Rapping Reentrainment on Efficiency for Rapping Losses Accounting for 20%, 30%, 40% and 50% of Emissions for Various Overall Efficiencies . . . 142
3 Effect of Rapping Reentrainment on Performance for Various Reentrainment Percentages as a Function of Number of Sections and a Constant Collection Efficiency Per Section 143

PAPER 9

1 Technical Data - Fabric Filters Selected for Verification 159
2 Experimental Data - Fabric Filters Selected for Verification 160
3 Test Run No. 13A Baghouse Simulation Input Data . . . 176
4 Approximate Sunbury Fly Ash Size Distribution 177
5 Parameters for Five Boilers Using Fabric Filtration . 183

PAPER 10

1 Typical Plant Coal Analysis 187
2 Menardi Filter Bag, Style No. 601T 192
3 Cleaning/Sweep Cycle Time Sequence 193
4 Bag Failures 202
5 Installation, Operation and Maintenance Costs 203

PAPER 11

1 Operating Conditions at Design Gas Flowrate 212

PAPER 12

1 Scrubber Collection Efficiency 230
2 Penetration of Elements Through the Scrubber 233
3 Particle Penetration Summary. 235
4 Comparison of Mobile Bed Studies 236

INTRODUCTION

John K. Burchard
Environmental Protection Agency
Industrial Environmental Research Laboratory

The purpose of this conference is to discuss the problems involved in firing low sulfur coal and to explore the impact of various control strategies. Federal standards for power plants were established in December, 1971, and include sulfur dioxide and particulate matter. At that time, switching to low sulfur coal appeared to be the answer to the sulfur oxides problem. However, switching presented the problem of transportation of coal from areas richest in low sulfur coal, the western United States, to areas requiring the highest usage, the eastern United States.

An additional specific disadvantage in using low sulfur coal, in utilities equipped with electrostatic precipitators for pollution control, is a corresponding decrease in collection efficiency because of the increase in ash resistivity. At normal precipitator temperatures, around 300°F (150°C), fly ash resistivity is rather strongly inversely proportional to the sulfur trioxide concentration in the emissions. The SO_3 concentration will depend on the sulfur content of the coal, the boiler operating conditions, and the chemical composition of the fly ash.

In general, therefore, high sulfur coal gives higher SO_3 concentrations and lower resistivity, and a given electrostatic precipitator will perform better on high sulfur coal than on low sulfur coal. Therefore, switching to low sulfur coal means reduced efficiency and increased particulate emissions.

This is the problem to be discussed for the next two days. The latest data on performance analysis of electrostatic precipitators will be presented as well as alternative methods of particulate collection, such as bag houses and scrubbers.

PAPER 1

OPERATING EXPERIENCE WITH ESP CONDITIONING IN RELATION TO AN ELECTROSTATIC PRECIPITATOR UPGRADING PROGRAM

Scott H. Cragle
Pennsylvania Power and Light Co.

ABSTRACT

This report summarizes the major areas of an ongoing electrostatic precipitator (ESP) upgrading program at Pennsylvania Power and Light Co. Particular emphasis is placed on the area of flue gas conditioning including eighteen months of operating experience with Apollo Chemical Corporation products, a planned SO_3 injection trial, and other potential agents.

Results of ongoing trials of Apollo products at Montour SES on two 750 MW bituminous coal fired units are presented. Performance data, operating problems and cost information are covered. Eight chemical formulations have been injected into various combinations of four locations in efforts to improve product performance, solve air heater plugging problems and improve distribution of the product on the fly ash. A significant reduction of emissions on a difficult fly ash has been noted although only half as great a reduction as originally expected based on tests run with a good collecting fly ash. Air heater plugging problems have been eliminated.

The report also covers some of the practical considerations and potential problems that can occur in evaluating proprietary additives.

Also, the report briefly summarizes projects on six of the Company's ESPs including work in the following areas: fuel quality effects; flue gas conditioning; rappers; voltage controls; sectionalizing; gas flow distribution; operating and maintenance and additional dust collector capacity.

INTRODUCTION

Pennsylvania Power and Light Company (PL) began a series of efforts to upgrade its existing electrostatic precipitator (ESP) capacity in mid-1973. At that time it had become apparent that the particulate emissions from the two new boilers at PL's

Montour station did not meet consistently acceptable levels. The Montour station has two 750 MW units with pulverized bituminous coal boilers. The ESPs were built in a chevron configuration and designed for a 99.4% efficiency for coals with a 1.5% to 3.0% sulfur and an efficiency of 99% for coals with a 1.0% to 1.5% sulfur content. More detailed information is shown in Table 1.

INITIAL PERFORMANCE TESTS (9/73 - 11/73)

An initial series of efficiency tests on Unit 1 resulted in efficiencies from 90.9% to 95.4%. A compliance test by the Pennsylvania Department of Environmental Resources showed emissions 9 to 10 times the emission limit of 0.1 $lb/10^6$ Btu. Another series of outlet tests was run to determine the effect of the sulfur content of the different fuels burned at the plant and also to determine the feasibility of using the two recently installed Lear Siegler opacity monitors as indicators of ESP performance.

The tests showed a relation between optical density and dust flow from the precipitator (Figure 1). As a result of this test, the monitors have become an integral tool in monitoring precipitator performance. The tests showed that the ESPs performed within regulation with certain high sulfur fuels, but performed poorly with the low sulfur fuel from our Greenwich Mine, a major fuel source for the plant. The test points are numbered on Figure 1 in the order that the tests were performed. Tests 1 through 4 show that we didn't observe the full effect of a low sulfur coal until it had been burned for several consecutive days. This was due to the residual fly ash in the ESP. Tests 5 through 8 indicate that the good effects from a high sulfur coal were not noticed on the first day after burning a low sulfur coal, but only on the second and third day. Test 8 was a lower sulfur coal, but high levels of SO_3 were reported during the test, possibly due to a high vanadium content in the ash.

EXPERIENCE WITH THE APOLLO FLY ASH CONDITIONING AGENT

Based on the test results, we viewed flue gas treatment to be the major solution to the ESP performance problem at Montour. Ongoing work done in other areas is covered briefly later in the paper. After a short study (1/74) of conditioning alternatives, we chose Apollo (2/74) on the basis of a low first cost and a short three month lead time for installation. We thought that Apollo would be a quick, low cost demonstration of the effectiveness of fly ash treatment on our problem fuels. Other alternatives required large capital investments and nearly a one year lead time to set up any demonstration.

TABLE 1. DESIGN DATA ON PRECIPITATORS INCLUDED IN PL'S PARTICULATE COMPLIANCE PROGRAM

Unit	Rating, MW		Flow, acfm × 10^3	SCA, $ft^2/10^3$ acfm	Face Velocity, ft.sec	Treatment Time, sec	Typical Fuels	
							S,%	Ash,%
Brunner Island 1	350	Research Cottrell (1961)	550	180	4.2	4.5	1.5-2.5	12-25
		Buell (1965)	550	180	5.2	3.5	1.5-2.5	12-25
Brunner Island 3	750	Western (1969)	2,300	204	5.3	4.6	1.5-2.5	12-25
Montour 1	750	Western (1972)	2,300	204	5.3	4.6	0.8-2.5	12-30
Montour 2	750	Western (1973)	2,300	204	5.3	4.6	0.8-2.5	12-30
Martins Creek 1	160	Buell (1968)	600	274	4.3	6.2	2.0-2.5	12-30
Martins Creek 2	160	Buell (1968)	600	274	4.3	6.2	2.0-2.5	12-30

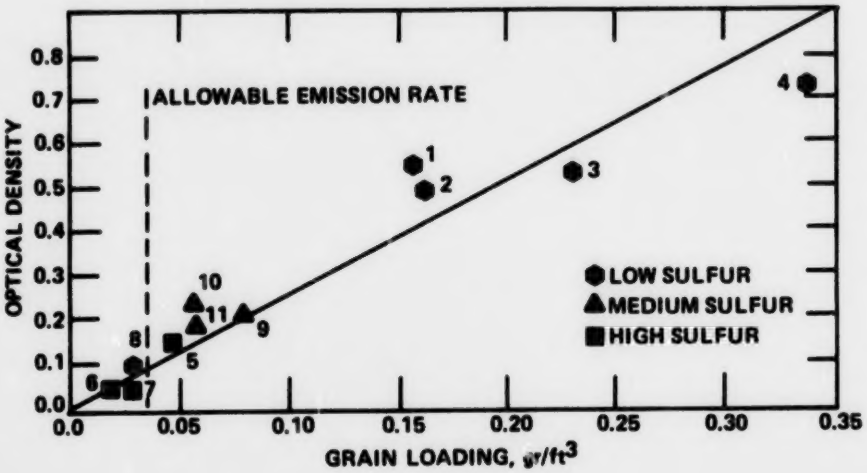

Figure 1. Optical density vs. grain loading, Montour Unit 1, November 1973

Our initial plans were for the trial to last three months on one 750 MW unit. The cost projection was \$150,000 (20¢/kW) to install the system and \$90,000 for three months of chemical supply. The system has now been expanded to both Montour units for a cumulative capital cost of about \$400,000 (\$200,000 per unit or 27¢/kW). The cost of chemicals to treat both units is \$650,000 per year (0.0067¢/kWh).

Performance - LPA - 40® (9/74 - 1/75)

All conclusions about ESP performance in this report are based on data taken by PL personnel.

The Apollo product used in the initial testing was LPA-40. This was a sulfamic acid (PL analysis) based multicomponent product that is injected into the flue gas upstream of the boiler economizer. Through breakdown to NH_3 and SO_3 it is intended to affect fly ash resistivity, agglomeration, and space charge in the flue gas.

Because of a 3 month strike at PL, initial operation of the Apollo system was delayed until September, 1974. We quickly discovered that we were limited to injecting less than 0.1 gal/ton of coal (25 gal/hr) because of increased pressure drop across the Ljungstrom air heaters. A series of emission tests were run at this feed rate, and two opacity monitors made continuous observations. Table 2 shows the improvement that occurred with this Apollo additive using our regulated emission limit (0.1 lb/10^6 Btu) as a base line (1x). Emissions were reduced by 30-45%.

TABLE 2. MONTOUR: LPA-40 PERFORMANCE

Fuel	Ash,%	Sulfur,%	LPA-40	Emissions
Greenwich	18	1.0	------	6× - 9×
Greenwich	18	1.0	0.1 gal/ton	4× - 5×
Oneida	18	2.5	------	1× - 2×
Oneida	14	2.5	------	1× (Base)

Internal inspection of the air heater showed no adverse effects related to the high pressure drop. Whenever treatment was shut off for a few days the pressure drop would return to normal. Most likely, the plugging was due to unvaporized product on the air heater or recombination of vaporized product to ammonium bisulfate.

During the next phase of the test program, our efforts were centered on reducing the air heater plugging to allow higher treatment rates. These five approaches were taken (in chronological order):

1. Product Atomization (10/74) - Air atomized nozzles were added to the system to assist in faster breakdown of the product. No major improvement resulted from this change.

2. Flow Distribution Tests (11/74) - We suspected uneven treatment of the flue gases might be a significant problem because of the location of the injection ports (Figure 2, Phase I). Tests run at the inlet of the air heater showed evidence that 80% of the gas stream was getting uniform treatment and 20% of the gas stream was receiving lower than normal concentrations of the product. We are not certain if this situation improves upstream of the precipitator. Even if it is a significant problem, no ready solution is available to us to allow more even treatment of the flue gas.

3. LPA - 40, Neutral Formulation (11/74) - Apollo changed the major component of their product from sulfamic acid to ammonium sulfate (results of PL analysis) indicating that the new product decomposed faster. No significant improvement in performance resulted from the change of product.

4. Flue Gas Temperature at the Point of Injection (1/75-4/75) - Flue gas temperature at the point of injection is apparently critical to the application of LPA - 40. Injecting the product into the flue gas stream at too high a temperature results in the chemical combination of the products with the fly ash. Also, production of SO_3 at high temperatures is not useful because the SO_3 will convert to SO_2 by the nature of the SO_2 - SO_3 chemical equilibrium. Injecting at too low a temperature, the product does not decompose as completely and as rapidly as necessary and air heater plugging results. Our problem was low temperature at the injection point.

   At the start of the program Apollo indicated that the ideal temperature of injection was 800-1000° F. Following their change to the neutral formulation, Apollo

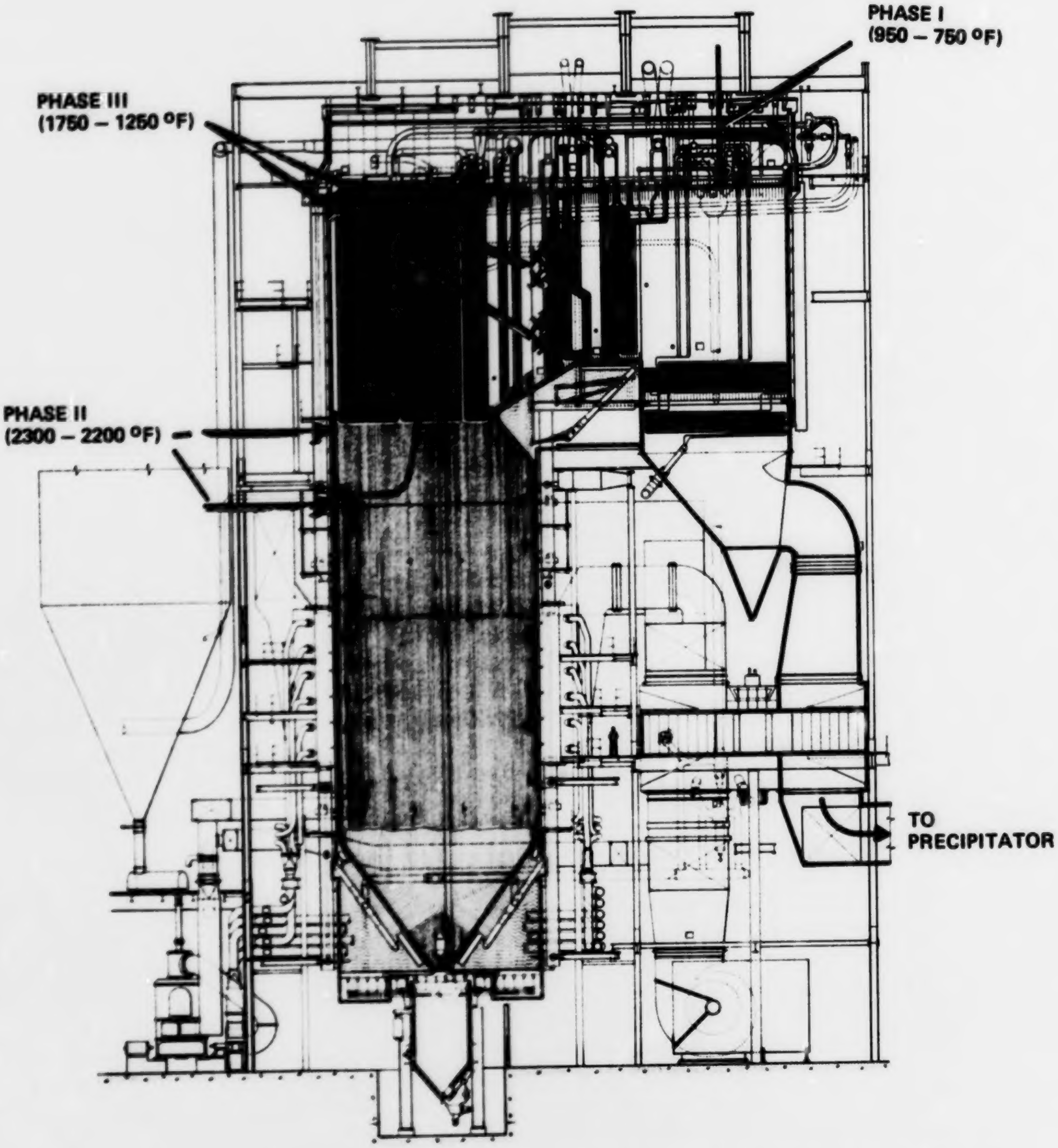
PHASE I
(950 – 750 °F)
PHASE III
(1750 – 1250 °F)
PHASE II
(2300 – 2200 °F)
TO
PRECIPITATOR

Figure 2. Apolln injection locations (temperature full load – temperature half load)

indicated that they had seen good results at injection temperatures above 1200° F and that temperatures as high as 1500° F would be optimum for their product. Currently they believe the optimum temperature is 1250-1300° F.

Figure 2, a boiler cross section, shows the locations we have injected LPA-40 with the associated flue gas temperatures for both full boiler load and half boiler load. Note how the temperature varies with load.

Phase I (950-750° F) - This is the original penthouse location where we have had the best results so far. Injection here at the rate of 0.1 gal/ton resulted in air heater plugging.

Phase II (2300-2200° F) - Injection above the firing zone at high rates (0.4 gal/ton) had no effect. No effect was seen on precipitator performance and no air heater plugging occurred.

Phase III (1650 - 1250° F, upper ports; 1750 - 1350° F, lower ports) - Injection into the side of the boiler into the superheat area showed no effect at full load. No effect was observed on precipitator performance and no air heater plugging occurred.

Phase IV - The problem of finding an injection point with the right temperature caused the next phase of testing. Product was injected through the Phase I location during periods of high boiler load and injected into the Phase III location during periods of low boiler load in an attempt to keep the injection temperatures acceptable. This approach was intended to reduce the chance of air heater plugging while providing continuous treatment of the fly ash at all boiler loads. No improvement in precipitator performance or in the plugging problem resulted from this approach.

5. Revised Apollo Chemical Formulations (5/75 - Present)

LPA 401, Catalytic Formulation - This is the LPA-40 formulation with a metal added to cause faster breakdown. This formulation caused more air heater plugging problems than the normal LPA-40.

LPA 402, Agglomerator Formulation - This formulation contains an organic compound in trace quantities. Results with this have been good. Air heater plugging has been eliminated and ESP performance has been equivalent to LPA-40.

LPA 403, Combination of LPA 401 and 402 - No trial was run due to the problems with 401.

LPA 404, Non-Ammoniated Formulation SO_3 Release Agent - This was designed to produce SO_3 only. Results with this chemical showed no improvements in SO_3 concentration in the flue gas or improvement of the in-situ resistivity of the fly ash.

LPA 405, Another Non-Ammoniated Formulation - This is similar to 404, but has not been tried due to handling concerns resulting from its low pH of 1.0.

LPA 402A, Agglomerator Formulation - This is similar to 402 only with a different organic compound. It is more volatile than 402. Results with this chemical seem identical to those with 402 and it is the formulation presently being used.

Performance - LPA 402 and 402A

Table 3 shows results for Unit 2 with LPA 402A in the same format as Table 2 shows results for LPA 40 on Unit 1. The Unit 2 precipitator in general performs better than Unit 1 due to some variations in physical flow arrangement. The results indicate that 402 and 402A are similar performers to LPA 40 in the Montour boilers when injected at the penthouse location.

During April and May, 1976, a series of ESP efficiency tests are being run on Montour 2. The tests are being run with high sulfur coal, low sulfur coal, and low sulfur coal conditioned with LPA-402A.

TABLE 3. MONTOUR NO. 2: LPA-402A PERFORMANCE

Fuel	Ash,%	Sulfur,%	LPA-402A	Emissions
Greenwich	20	1.3	-------	4× - 12×
Greenwich			0.1 gal/ton	1.5× - 2×
Oneida	12	2.4	-------	0.6×

Resistivity

Figure 3 plots in-situ resistivity taken by Apollo and Southern Research Institute using a point to plane probe. These were taken at various times during our test program. The scatter of the data is evident in this graph and, as a result, it is difficult to make conclusive statements about it. By looking at selected points, we have noticed certain trends, however. Increased sulfur content of the fuel has the expected effect of lowering the resistivity. Lower temperatures seem to produce lower resistivities as expected. The school of thought at PL, which has not been fully investigated, is that lower flue gas temperatures may help the performance of the Apollo flue gas treatment by lowering the resistivity. In general, for a low sulfur fuel, it seems that the Apollo LPA 402 treatment lowers the resistivity about one-half of an order of magnitude from the low 10^{11} ohm-cm to the high 10^{10} ohm-cm.

At this point our data on available SO_3 in the flue gas is incomplete. Apollo picks up most of the sulfur compounds in hopper samples of fly ash.

It is difficult to draw conclusions from either resistivity analysis or SO_3 analysis because of the variable sulfur content of fuel burned at Montour. Monitoring minute-to-minute changes in the sulfur content of the coal is difficult.

GENERAL OBSERVATIONS

These are some suggestions that will be helpful to a company considering a test program with a proprietary chemical flue gas conditioning additive.

1. PL has found that trials planned to be quick and inexpensive can turn out to be more involved than initially anticipated. If you are using expediency for justification of a choice of a certain alternative, be certain that your trial program will be expedient.

2. Prior to the start of a test program, define the ground rules for the evaluation program.

   a. What is the expected mechanism of action of the additive?

   b. What parameters will be used to measure the performance of the additive (resistivity, SO_3 concentration, NH_3 concentration, fly ash analysis, etc.)? Ideally you will set up a program to measure the additive's effect in more ways than just precipitator performance. In this way you can determine if changes in ESP operation are due to the additive or other parameters. Also it will be easier to troubleshoot any lack of performance.

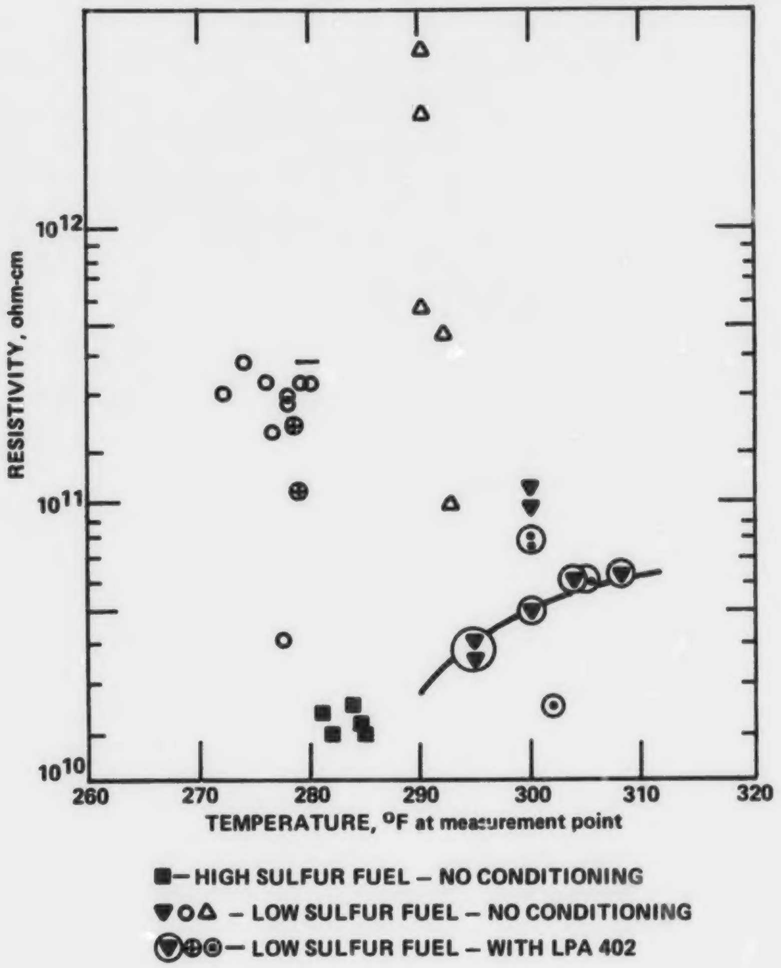

Figure 3. Selected resistivity data with and without LPA-402 conditioning

3. Get a commitment from the vendor prior to the program as to the "ideal" temperature and location for injection of the product. If possible, investigate the temperature (and its variation with boiler load) at proposed injection locations before installing ports and starting the trial.

4. Be sure your injection system is capable of adequate distribution of the additive in the flue gas. Cutting corners in this area may well limit the success of your trial.

5. Use great care in installing the injection system and, if possible, observe its operation (injecting water) from inside the boiler during an outage. An unfortunate error in our installation resulted in 16 economizer leaks and a six day unit outage.

6. To demonstrate the capabilities of the ESP, arrange to burn some higher sulfur fuels and test the units under ideal resistivity conditions.

7. If your system is installed during an annual outage, allow the boiler to become dirty before testing emissions and drawing conclusions on the performance of an additive product. PL's Chem Lab feels that a clean boiler after an outage acts as a catalytic bed in the conversion of SO_2 to SO_3. During the period following an outage the higher levels of SO_3 result in somewhat better precipitator performance. Also the precipitator is usually cleaner following an outage.

   Also, note any modifications that are made during an outage to the boiler such as addition of economizer or other tube surface to the boiler. These may affect the amount of SO_3 formed by catalytic action or they may affect the temperature (thus resistivity) of the fly ash.

8. Often, ESP performance improvements attributed to additives are due, in part, to changes in other parameters. Data in this report was taken by PL under carefully controlled conditions to minimize this problem.

   a. During both baseline and additive testing, maintain uniform operating conditions in the boiler (coal quality, excess air, gas temperature, mill classifier setting, etc.). Variations in these parameters can cloud your results.

Continuous reading SO_2 and opacity monitors have been a useful tool in quickly determining relative changes in these parameters. Absolute values from these instruments depend on monitor reliability and maintenance.

b. Familiarize yourself with the operation of the ESP. Use consistent set points for rappers and automatic voltage controls (at sparking threshold) during all testing. Observe the power levels during emission testing to detect any abnormal conditions that may invalidate results of that particular test.

9. At Montour we have found that changes in the type of coal burned in the boiler do not have the full effect on the precipitator for a number of days. Be careful not to draw positive or negative conclusions too soon after adjusting any operating parameter.

10. By following these guidelines and being open-minded towards alternate chemical formulations and injection locations, recommended by the supplier, PL has benefited with improved performance. Try to identify all possible approaches before the start of the trial.

SUMMARY

The original plan for the Apollo trial was a quick, simple, and inexpensive demonstration with hopes for impressive results. Although the trial turned out to be long, involved, and costly with less than spectacular results, day to day emissions at the Montour plant have been reduced significantly through the use of Apollo.

PL'S PARTICULATE COMPLIANCE PROGRAM (1/75 - Present)

PL's particulate compliance program is a series of trials in 8 investigative areas on six of PL's precipitators.

Starting with the formation of a 5-man Air Quality Project Team in January, 1975, PL started a two-year investigative program to bring its units into full day-to-day compliance with Pennsylvania air quality regulations. In the past, PL had attempted to have ESPs comply by making modifications that seemed most promising. Often, too many changes were made to a unit at one time. This made it difficult to determine what, if any, improvement was gained, and if the changes could be applied to other units with similar problems. Previous work done on Montour No. 1 is a prime example. This work included:

1. Modification of rapper shafts and the rapping program.
2. Adjustment of electrode control set points.
3. Trials with updated high voltage controls on sections of the precipitator.
4. Installation of turning vanes in an attempt to improve gas flow distribution.
5. Experimentation with adding weight to the electrode wire tensioning weights.
6. Collecting plate realignment and wire support frame stabilization.
7. Blending of high sulfur coal with low sulfur coal at the mine in order to raise the overall sulfur level of the coal.
8. Adjustments to operating parameters such as excess oxygen and flue gas temperature.
9. Apollo fly ash conditioning trial.

The combination of concurrent changes made it extremely difficult, if not impossible, to reasonably evaluate the effect of any single change. The intent of the present program is to produce as conclusive a result as possible about the effects of various modifications that will be made. Table 1 lists the design parameters of the six precipitators.

This is a brief summary of the work in each investigative area.

1. Fuel Quality Effect

   The root of the problem with precipitators is often the type of fuel burned. PL uses a wide variety of coals ranging from 10% to 30% ash and from 0.8% to 2.5% sulfur. A study is being done on all of the six units to determine the effects of the various fuels on the dust collector performance. At the end of the study PL will consider the economics and practicality of achieving compliance by controlling the quality of fuel shipped to our plants. This approach is possible by using the capabilities of cleaning plants at our mines and coal blending.

2. Flue Gas Conditioning

a. Apollo - Use of the Apollo product will continue unless a more effective gas conditioning system is demonstrated or additional collecting capacity is installed at Montour. PL has an agreement with Pennsylvania regulatory authorities to continue any reasonable activity that lowers emissions at Montour.

b. SO_3 injection, Brunner Island Unit 1 - A Wahlco SO_3 injection utilizing a liquid SO_2 vaporizer system will go into trial service on this unit during August, 1976. A series of tests with the SO_3 injection will be run to get data similar to that in Tables 2 and 3. With this data, we hope to assess how effective such a system would be at Montour in comparison to the Apollo system. The total capital cost of the trial system of this 350 MW boiler is $445,000 ($1.28/kW) and the expected cost for liquid SO_2 during the six month trial period will be about $70,000 (.0058¢/kWh). Any permanent installation of this system will include a sulfur burner resulting in $400,000 additional capital cost and a reduction of chemical cost by a factor of 5 or 6. We expect to have results available from this trial by October 1, 1976.

c. Trimex, Martins Creek 2 - PL's Research and Development group is sponsoring this trial in an effort to demonstrate the feasibility of reducing SO_2 emissions from the boiler. An offshoot of this trial may be conditioning of the fly ash. After almost five months of testing our Chem Lab reports that the Trimex chemical has shown no effect on the SO_2 emissions or on the performance of the ESPs.

d. Other Additives - Although no additional trials are planned, PL is investigating the use of triethylamine, concentrated ammoniacal liquor, Betz proprietary additives, and Nalco proprietary additives. A trial with Nalco's experimental catalytic additive was cancelled after we had unsuccessful laboratory trials.

3. Rappers

Internal inspection of many of PL's precipitators equipped with the vibrating rappers have shown heavy dust buildups on the plates. On one of the two Montour Unit 2 precipitators, the vibrating rappers have been replaced with impact rappers. The new rappers' performance is being evaluated.

4. Voltage Controls

Because of the wide variety of fuels burned at PL's plants, we have found that the automatic voltage controls on many of the units are not capable of following the varying conditions in the ESPs. Eight thyristor controls manufactured by L. L. Little are being installed on one of the two precipitators at Brunner Island Unit 3. We hope to evaluate any improvement in the efficiency of the precipitator, any reduction in burnout of wires, and the general ability of the control to follow changes in operating conditions.

5. Sectionalizing

The precipitators at Martins Creek have a relatively high degree of sectionalization and offer a certain amount of flexibility in allowing quick modification of their sectionalizing arrangement. Experiments are being run with varying amounts of plate area per TR set to determine what possible benefit may be gained by increasing the sectionalization of the precipitators on other PL units and future units. This work is in progress at present.

6. Gas Flow Distribution

The Brunner Island 3 precipitator and Montour 1 and 2 precipitators are built with a chevron inlet configuration. There is evidence that the flow distribution is not uniform over the face of the precipitator. Field tests have been run to determine the flow distribution and a model study is being conducted to determine if improvement is possible. If modifications are made, efficiency tests before and after the modifications will be run to determine the effect of improvement in flow distribution.

7. Operating and Maintenance

A complete review of operating and maintenance procedures is being conducted throughout the PL system. Since the precipitators are not a megawatt producing piece of equipment, historically they have received less attention than other equipment. We are reviewing the impact of operating parameters and maintenance on the performance of the precipitators with our plant personnel.

8. Additional Collector Capacity

At the conclusion in early 1977, should the efforts in the seven previously listed investigational areas fail to bring Brunner Island 1 and 3 and Montour 1 and 2 into compliance (Martins Creek 1 and 2 are in compliance) with air quality regulation, additional collector capacity will be installed. The ground work in this area is being done at present to allow for the shortest lead time in purchasing and constructing any additional capacity that may be necessary. The alternatives that are being studied are hot precipitators, cold precipitators, fabric filters, and particulate scrubbers.

PAPER 2

SULFUR TRIOXIDE INJECTION AT STATE LINE STATION

Ronald Cook and Michael Trykoski
Commonwealth Edison Co.

INTRODUCTION

The passage of regulations in the late 1960's and early 70's regulating sulfur dioxide (SO_2) emission caused many utilities including Commonwealth Edison to switch to low sulfur fuel as a means of compliance. The burning of low sulfur (approximately 0.2 - 0.5%) coal in boilers designed for medium sulfur (approximately 3 - 4½%) coal created a host of problems, the most severe ones being boiler slagging and fouling, carbon carryover with its resultant ash hopper and air heater fire hazard, and electrostatic precipitator degradation. This paper describes Commonwealth Edison's efforts to overcome the last of these problem areas, electrostatic precipitator degradation, through the use of sulfur trioxide (SO_3) flue gas conditioning.

THE PROBLEM

Electrostatic precipitator operation depends on the flow of an electric current between the electrodes of the precipitator. This flow, in the form of ionized particles, must pass through the layers of fly ash which are normally present on the electrodes. For high sulfur coal, the fly ash has a resistivity of approximately 10^{10} ohm-cm, while for the low sulfur, low sodium western coals presently being used by Edison, the value is 10^{13} ohm-cm. An analysis of a typical low sulfur coal being burned in Edison boilers is shown in Table 1. Thus it can be seen that low sulfur coal fly ash, with its higher resistivity, will reduce the current flow between the electrodes, and therefore the precipitator performance, when compared to operation on high sulfur coal.

TABLE 1. TYPICAL COAL AND ASH ANALYSIS
ARCH MINERAL NO. 1

"AS RECEIVED" COAL ANALYSIS (% BY WEIGHT)	
Moisture	10.8 - 12.3
Sulfur	0.52 - 0.86
Ash	10.94 - 14.43
Gram-cal/g	5,358 - 5,654
(Btu/lb)	(9,644 - 10,176)

ASH ANALYSIS (% BY WEIGHT)	
Silica	31.6 - 39.7
Alumina	16.9 - 19.0
Iron oxide	10.6 - 18.8
Titanium oxide	0.5 - 0.7
Calcium oxide	15.3 - 18.8
Magnesium oxide	3.0 - 3.6
Potassium oxide	1.0 - 1.6
Sodium oxide	0.64 - 0.74

Evaluation of the Edison generating system showed that a total of 22 precipitators on ten generating units ranging in size from 120 to 620 MW would suffer degradation while burning low sulfur coal to the point where they could no longer meet particulate emission standards while operating at full load. A program was therefore begun to evaluate flue gas conditioning as a means of restoring precipitator efficiency through the lowering of fly ash resistivity.

SELECTION OF APPROACH

Various flue gas conditioning agents have demonstrated the ability to reduce the resistivity of fly ash. In the early 1970's the most promising appeared to be the use of SO_3 produced by one of the following methods:

1. Evaporation of liquid SO_3
2. Catalytic conversion of SO_2 to SO_3
3. Vaporization of sulfuric acid
4. Burning of elemental sulfur followed by the catalytic conversion of SO_2 to SO_3

After evaluating the available methods using criteria such as installation and operating cost, reliability, safety, and current generating station work practices, Edison elected to install, for further investigation, a pilot sulfur burner at its State Line generating station in Hammond, Indiana, and a full scale liquid SO_3 system at its Waukegan Station in Waukegan, Illinois.

The State Line system went into service in May, 1973, and is shown schematically in Figure 1. The system consisted of a liquid sulfur feed to a pan type burner where sulfur dioxide is formed by combustion. The sulfur dioxide is then passed through an electric heater and a two-pass catalytic converter with interstage cooling which converts over 90% of the SO_2 to SO_3. The SO_3-air mixture of about 10% SO_3 is then piped through an insulated manifold to the probe and nozzle system located internally in the ducts leading to the electrostatic precipitator.

It was obvious soon after startup that the burner portion of the system was undersized and did not have the capacity to adequately condition the fly ash from the low sulfur Wyoming coal which was currently being burned at State Line. Therefore, when extensive testing of the system was performed in November, 1973, additional SO_2 from an external source was added at a point prior to the electric heater.

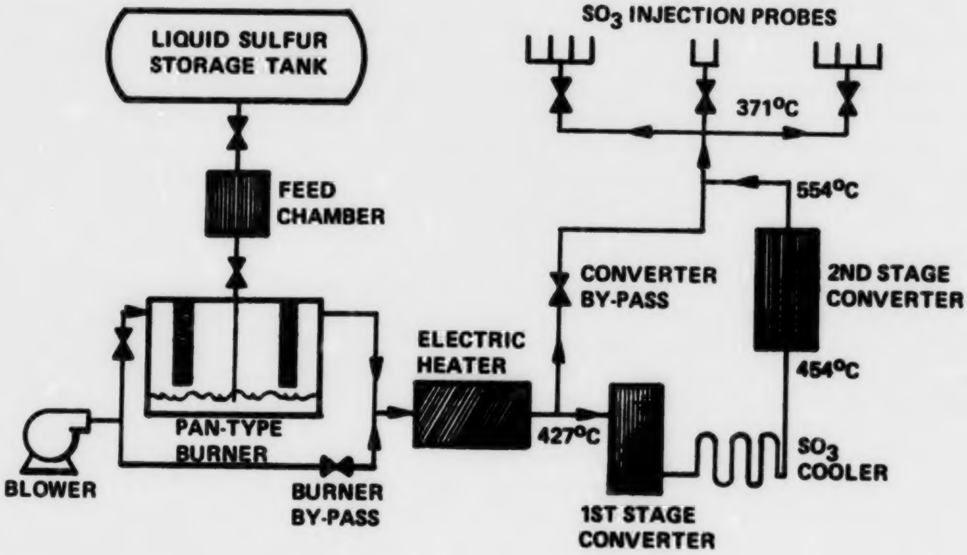
SO3 INJECTION PROBES
LIQUID SULFUR STORAGE TANK
371°C
FEED CHAMBER
554°C
CONVERTER BY-PASS
2ND STAGE CONVERTER
ELECTRIC HEATER
454°C
PAN-TYPE BURNER
427°C
SO3 COOLER
BLOWER
BURNER BY-PASS
1ST STAGE CONVERTER

Figure 1. Sulfur burning flue gas conditioning, System State Line Unit 3

Test results showed a dramatic improvement in precipitator performance with flue gas conditioning. Precipitator efficiency, shown in Figure 2, increased from approximately 85% to 96% with an SO_3 injection rate of about 40 ppm, while corona power input, shown in Figure 3, increased ten-fold from about 25 watts/1000 acfm to about 250 watts/1000 acfm.

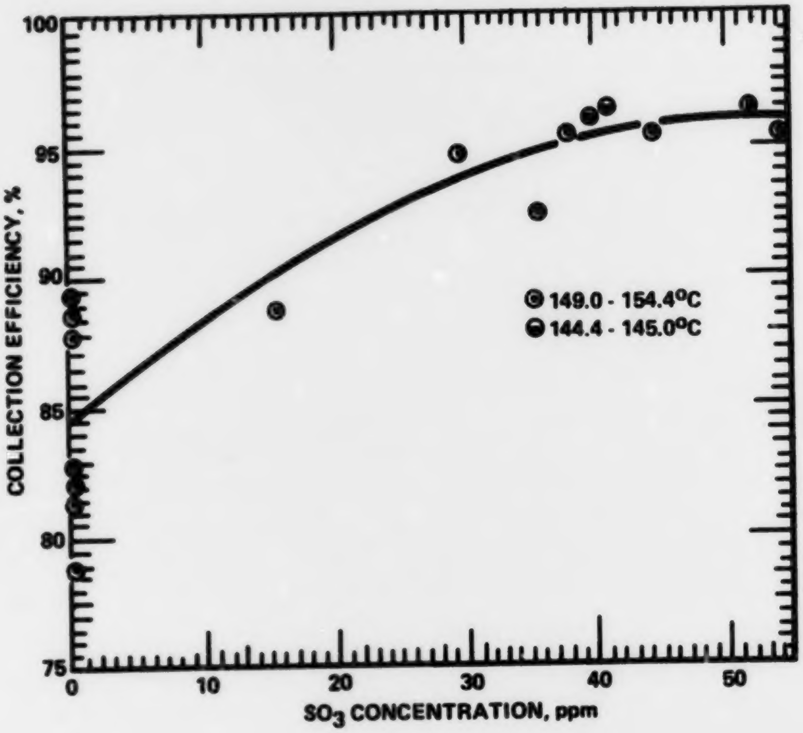

Figure 2. Effect of conditioning level on collection efficiency, State Line Unit 3

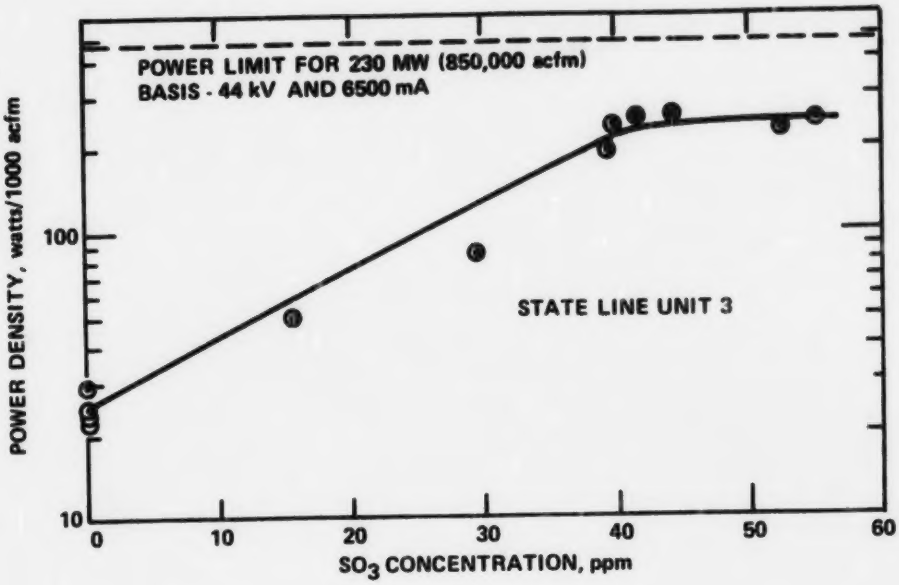

Figure 3. Corona power input as a function of SO_3 addition

The second SO_3 conditioning system, utilizing liquid SO_3, went into service on March 7, 1974, after several construction and startup delays. After approximately 200 hours of intermittent operation, it was discovered that the injection probes were experiencing severe chemical attack. Subsequent replacement of the nozzles with a different design failed to satisfactorily resolve the problem. Because of this and other assorted problems, the system was ultimately abandoned. Prior to the abandonment, however, an engineering and economic study of the performance of both systems had concluded that a sulfur burner type SO_3 system would be the best choice. Some of the factors considered in arriving at this decision were:

1. Installation and operating costs
2. Availability of chemical supply
3. Material storage and handling problems
4. Simplicity of operation

PROCUREMENT OF FULL SIZE SYSTEMS

Edison's Station Mechanical Engineering Department conducted an evaluation of available systems and vendor capability and selected Wahlco, Inc., of California to build the first 11 systems required. These were installed at the State Line Station, located in Hammond, Indiana, which had the earliest compliance date. Table 2 lists the State Line generating units involved and sizes.

TABLE 2. STATE LINE STATION GENERATING UNITS

Unit	MW (net)	No. Of Boilers/Precipitators
1	171	6
2	140	3
3	190	1
4	318	1

The Wahlco system, shown schematically in Figure 4, consists of a sulfur burner followed by a single-pass catalytic converter. Incoming combustion air is preheated by electric heaters, which are cycled to maintain proper combustion temperature. From the converter, the SO_3 is piped in insulated lines to injection probes located in ductwork as far ahead of the precipitator as practical to allow maximum time for mixing. Unfortunately, with some of the older units, sufficient space was barely available and considerable "shoe-horning" had to be done.

The system will follow boiler load and automatically modulate the liquid sulfur feed rate. The system is essentially "fail-safe" with a malfunction indication tripping the sulfur feed which results in system shut down as soon as residual sulfur already in the burner is consumed, which takes approximately 10 minutes, depending on what the burning rate had been. The system is designed to operate without an operator except for startup and normal shut down. Parallel sets of status lights, temperature recorders, and trip buttons are installed in each boiler control room and associated burner location.

The sulfur burner systems themselves were located throughout the generating station in as close proximity to the point of injection as possible to minimize heat loss in the piping and to limit the exposure of SO_3 piping from a safety standpoint. One of the greatest problems with any SO_3 injection system is maintaining proper gas temperature to avoid corrosion problems; as a precaution, thermocouples were attached to the probes themselves.

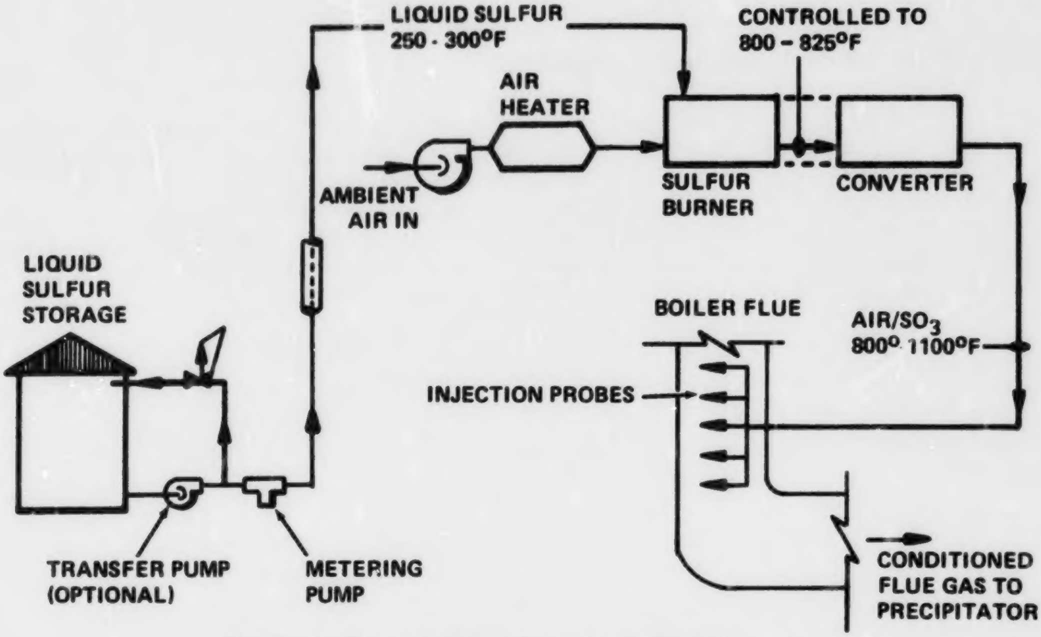
LIQUID SULFUR
250 - 300°F
CONTROLLED TO
800 – 825°F
AIR
HEATER
AMBIENT
AIR IN
SULFUR
BURNER
CONVERTER
LIQUID
SULFUR
STORAGE
BOILER FLUE
AIR/SO3
800° 1100°F
INJECTION PROBES
TRANSFER PUMP
(OPTIONAL)
METERING
PUMP
CONDITIONED
FLUE GAS TO
PRECIPITATOR

Figure 4. Flow diagram, flue gas conditioning unit

The two liquid sulfur storage tanks of 190 tons capacity for units 1 and 2 and 140 tons capacity for units 3 and 4 are located at grade level outside the building. The tanks are steam heated and the liquid sulfur lines to the various burner locations are steam traced. The sulfur feed pumps are located adjacent to the tanks with additional metering pumps installed at each burner on the multiple boiler installations for units 1 and 2. The separation of the sulfur burner from the storage tank presented somewhat of an engineering challenge in the case of unit 4, where the burner skid was located on the roof approximately 250 feet above grade.

STARTUP PROBLEMS

As with any new system, a certain number of problems can be expected during startup and de-bugging. The SO_3 systems at State Line were no exception; however, the supplier has made every effort to solve and correct the problems associated with his equipment.

Most of the initial problems were with the sulfur pumping system. Liquid sulfur is a touchy thing; below 246° F it solidifies and above 310° F it becomes extremely viscous. When thawing "frozen" sulfur lines, an allowance must be made for the expansion of the material - this was discovered after several pump diaphragms were ruptured while bringing the system into operation on several occasions. The unique temperature properties of sulfur also made it necessary to change from electrically heated to steam jacketed pumps for better temperature control; to add additional steam tracing and insulation on pump piping and valving; and to establish specific startup and shut down procedures to insure that the sulfur was in the liquid state before starting the pumps. Problems were also encountered with the pump hydraulic oil breaking down under the 290° F operating temperatures and with the air bleed system on the hydraulic circuit.

As the pumping system problems were being resolved and the burners began accumulating operating hours, several new problems appeared. Numerous failures were occurring in the electric air preheater elements without apparent reason. It was eventually determined by modeling studies that the U-shaped calrod type heater elements were developing hot spots under certain air flow conditions which resulted in premature failure. Turning vanes and baffles were installed in the ductwork to keep temperatures within limits. It was also necessary to install additional air flow sensors and interlocks to insure that the heaters were de-energized when a no air flow condition occurred. The need for these was discovered after 300 kW of heaters were burned out by a failure to de-energize following a unit shut down.

It was also necessary to revise the steam supply to the sulfur tank heaters and steam tracing system. The initial design for the steam supply utilized a manifold arrangement so that steam could be obtained from either one of the newer units, 3 and 4, or an older unit, 2. Unit 1 was not included because it was generally shut down every night. An unexpected long term outage of Unit 2 last fall, coincident with a planned overhaul outage of Unit 4, placed the burden of steam supply on Unit 3. Several tripouts of Unit 3 during this period therefore resulted in a shutdown of the sulfur burners on Unit 1 which then required a load reduction because of excessive particulate emissions. Unit 1 has been subsequently interconnected to the steam supply manifold.

It was recently discovered that the insulation on the injection probes was being eroded by the fly ash particles in certain locations. This was detected by changes in the readings from the thermocouples on the probes, which were described earlier. The insulation has been replaced and baffles installed to protect the probes. Since this modification was only recently completed, we are unable to say whether it will resolve the problem.

Generally, the sulfur burner and catalytic converter portion of the system have proved to be very reliable. The systems have followed boiler loads well and have demonstrated turn down ratios of 10 to 1, except on the smaller Unit 1 burners, which are still experiencing some sulfur metering pump problems.

TESTING

To demonstrate to the Hammond, Indiana, Air Pollution Control Department that the flue gas conditioning systems were effective, an extensive particulate emission testing program was undertaken. First, it was agreed that testing was only to be done while burning the low sulfur coal which appeared to cause the most severe precipitator degradation of all the low sulfur coals which were being shipped to the station. This required special coal shipments and stockpiling of the coal on station property. It also caused some delay to the testing program while supplies were being accumulated. It did, however, demonstrate performance of the systems under worst case conditions.

Second, the Hammond Agency required three tests at the same load to demonstrate compliance at that point. Because of the physical layout of the ductwork at State Line, it was not feasible to use EPA Method 5 for particulate testing. Approval was given to use a modified ASME method utilizing a 0.3 μm Gelman in-stack filter as a substitute only after concurrence was obtained from the Indiana Air Pollution Control Department and the U. S. EPA Region V office. In addition, because velocities could not be measured while sampling, it was necessary to conduct extensive pre-test velocity studies to verify that flow rates and patterns did not change materially with time.

After completing a satisfactory series of particulate emission tests on a given unit, the SO_3 system was then shut off and the precipitator allowed to de-condition for about three days. Particulate emission tests were again performed to accurately assess the improvement in performance due to the conditioning system and to determine what unit de-rating would be necessary during outages of the conditioning system in order to maintain compliance with particulate emission standards.

To date, seven of the 11 boilers at State Line have been tested. It has not been possible to complete testing of the remainder due to boiler-turbine related problems. For example, Unit 2 has been out of service for turbine repairs since September, 1975. Of the seven boilers tested, only one, Unit 3, was unable to meet emission standards and has had to be de-rated from approximately 244 to 226 MW (gross). This is through no fault of the SO_3 system, but due primarily to the fact that Unit 3's precipitator and control package were constructed in 1955 and were not designed to meet the current strict emission limits. The test results to date are summarized in Table 3. In addition, during the particulate emission testing, flue gas analysis for SO_3 showed no significant difference in SO_3 levels between the precipitator outlet and a point prior to the SO_3 injection probes.

TABLE 3. SUMMARY OF STATE LINE TEST RESULTS

Boiler	Emission Limit ($lb/10^6Btu$)	Actual Emissions At Full Load With FGC ($lb/10^6Btu$)	Efficiency, % With FGC	Efficiency, % Without FGC
1-1	0.24	0.09	97.9	-
1-2	0.24	0.10	97.1	86.9
1-3	0.24	0.14	96.5	-
1-5	0.24	0.13	96.5	43.8
1-6	0.24	0.10	97.0	-
3	0.26	0.26*	95.1*	85.9
4	0.24	0.06	97.0	88.4

* Unit 3 had to be derated from 244 MW to 226 MW (gross) to meet the emission limit.

CONCLUSIONS

The total cost of the 21 flue gas conditioning systems being installed on the Edison system is approximately $11.5 million, of which the State Line installation represents $3.8 million. Installation of the flue gas conditioning systems will be complete on all units by July 1, 1976. Testing has begun on some of the other completed units and preliminary results show improvements in precipitator performance similar to that obtained at State Line.

While the flue gas conditioning systems have not alleviated the other operating problems associated with the burning of low sulfur coal which still plague Edison's generating units, they are enabling these units to meet particulate emission standards with minimal de-rating at a cost far less than that of the only other feasible alternatives - major precipitator rebuild or a new precipitator.

PAPER 3

DISCUSSION AND COMPARISON OF CLINCH RIVER AND GLEN LYN PLANT ELECTROSTATIC PRECIPITATORS

W. J. Buchanan
American Electric Power Service Corporation

ABSTRACT

This paper reviews some of the factors that could affect precipitator performance and discusses how several differences may account for the ease on one hand and the difficulty on the other in achieving satisfactory performance. To demonstrate this, a comparison is made between the Clinch River and Glen Lyn 6 precipitators.

INTRODUCTION

The principal point of interest in regard to these two Virginia precipitator installations is that in using low sulfur coal at both plants, Glen Lyn 6 has performed well, with ease, while at Clinch River considerable effort has been required in order to meet performance requirements.

Glen Lyn 6 is a 225 MW pulverized-fuel fired dry-bottom steam generator, while at Clinch River there are three comparable 225 MW units. Gas flow and temperature conditions are comparable, i.e., 815-860,000 acfm at about 250-300° F to the precipitators at Clinch River and 800-850,000 acfm at 270-305° F for Glen Lyn.

Both the Glen Lyn and Clinch River precipitators were conservatively designed. They have a specific collecting area of 800 ft^2/1000 cfm and a design gas velocity of approximately four feet per second at 900,000 acfm.

DESIGN - COMPARISON

A comparison of the Glen Lyn 6 and Clinch River precipitator designs shows differences which favor the Clinch River installation (Table 1).

TABLE 1. PRECIPITATOR DESIGN PARAMETERS

		Glen Lyn	Clinch River
1.	Design Efficiency*, %	99.8	99.7
2.	Collecting Surface, ft^2	725,760	722,250
3.	Collecting Rappers	384	504
4.	Collecting Surface per Rapper, ft^2	1,890	1,433
5.	Corona Electrodes	15,552	15,840
6.	Corona Electrode Rappers	96	192
7.	Corona Wire Length per Rapper, ft	4,860	2,475
8.	Fields in Series	8-9 ft 4 in.	2-6 ft, 6-9ft Total - 8
9.	Transformer Rectifiers	48	48
10.	Collecting Surface per TR Set, ft^2	15,120	1st two fields, 10,938 3rd through 8th fields, 16,413
11.	Collecting Electrode Height, ft	30	30

* With any one field out of service

PERFORMANCE EXPERIENCE AND IMPROVEMENT PLAN

The Glen Lyn precipitator has required only normal attention since its initial start-up. After fine-tuning the power supplies and rapping system, there has usually been no visible emission.

On the other hand, the Clinch River precipitators experienced marked deterioration in performance six weeks after a promising start-up. Only one of the three units is on a stack by itself—this unit had no visible emission when first started.

In attempting to solve the performance problem at Clinch River, which is related to the high resistivity ash, there has been a continuing effort to increase the applied voltage and/or corona current. Two approaches have been taken——they are:

1. improve rapping,
2. optimize the electrical energization.

Reliability problems with some ash handling system components are being corrected. Their effect on precipitator performance is not known.

REVERSE IONIZATION, SYMPTOMS, ALLEVIATION

There were symptoms at Clinch River which indicated that reverse ionization, as associated with high resistivity ash and a thin deposited layer, was an important factor in this case of performance difficulty.

First of all, the corona electrodes were experiencing abnormal ash buildup, which is frequently a result of reverse ionization. This symptom has been largely eliminated by replacing all of the magnetic vibrators with heavier, more reliable, pulsating pneumatic rappers. However, back corona continues to have an adverse effect when the current density is above the acceptable limit.

In addition, console indications suggested reverse ionization. To confirm the presence of back corona, several transformer rectifier sets were monitored by making temporary provision for measuring the secondary voltage. Corona voltage-current curves plotted for these sections revealed severe reverse ionization. By improving the match between transformer rectifiers and load, the back corona has been reduced.

Although it was known that the Clinch River ash was of high resistivity even before the precipitator was designed, its *in-situ* resistivity was not determined until April, 1976. Southern Research Institute was then asked to make the necessary tests. As suspected, the values were high, being 10^{12} ohm-cm at 290° F, 10^{11} ohm-cm at 235° F and having a peak resistivity of slightly over 10^{12} ohm-cm at 300° F. This resistivity data, together with previous dew point test results, confirmed the ability to operate safely at temperatures as low as 250° F to the precipitator. A reduction in flue gas temperature, according to the temperature-resistivity curve determined by Southern Research Institute, should result in a reduction in ash resistivity as well as stack heat loss.

According to Figure 18 in an EPA report on a mathematical model of electrostatic precipitation[1], it should be expected that average corona current density must be limited to approximately 10-20 $\mu A/ft^2$, or less, to prevent back corona. To operate above this limit would most likely mean no practical gain in performance. It seems very likely that average current densities of 30 to 40 $\mu A/ft^2$, which occur at times in some fields, are only indications of stable back corona which affects performance adversely.

Based on our experience at Clinch River and other plants, not including Glen Lyn, when high resistivity ash is likely to be collected, it is of considerable value to install complete secondary voltage and current monitoring and not simply current indication. To be able to plot secondary voltage-current curves for any field at any time is of great practical importance when trying to analyze performance.

COAL SULFUR COMPARED

For the first three months of 1976, coal deliveries to these two plants reflect that Glen Lyn normally received a higher sulfur content coal (Table 2).

TABLE 2. PERCENT OF TOTAL COAL TONNAGE
DELIVERED IN TWO SULFUR RANGES

Sulfur,%	Glen Lyn,%	Clinch River,%
0.60 - 0.80	42	82
+ 0.90 - 1.0	58	13

Also, the largest deliveries of coal to Clinch River have lower than the overall average of 0.71% sulfur coupled with an ash content of 17.3%. Thus, the combination of low sulfur and high ash at Clinch River aggravates the performance problem.

ASH CHEMISTRY COMPARED

At both Glen Lyn and Clinch River, the coal sulfur averages less than 1% and the other elements, which affect resistivity are shown in Table 3.

TABLE 3. FLY ASH ANALYSIS

	Clinch River,%	Glen Lyn,%
Si	50.0	56.9
Al + Ti	28.5	30.9
Fe	6.5	6.7
Ca	9.8	0.6
Mg	1.2	1.6
K	1.5	2.0
Na	0.6	0.3
Free Lime	4.64	0

Note the significant difference in values of calcium and free lime.

FLY ASH CARBON CONTENT CONTRASTED

Although the exact effect is not known, there is probably some advantage at Glen Lyn, as far as precipitator performance is concerned, in having about 10% carbon uniformly distributed and combined with the fly ash, while the ash at Clinch River has a very low carbon content.

GAS VELOCITY DISTRIBUTION COMPARED

Another factor that may be of significance is the gas velocity distribution. The usual pre-operational tests were conducted with the result that at Glen Lyn the RMS deviation was 13.67% and at Clinch River the RMS deviation was 16.80%.

At Glen Lyn the velocity distribution standard used was for 85% of the velocity readings to be within plus or minus 10% of average velocity and no readings to be outside of plus or minus 25%. At Clinch River the standard used was an earlier one calling for 85% within plus or minus 25% of average and none outside of plus or minus 40%.

INLET DUCT ASH FALLOUT

After a relatively short time in service, all of the Clinch River inlet plenum turning vanes became filled with ash. This plenum on each precipitator is a box approximately 70 ft wide, 28 ft high and 14 ft deep. It serves to turn the gas from a downward vertical flow to horizontal while expanding about five times.

The turning vanes have vertical and horizontal sides with an eight-inch radius corner between. When the inlet turning vanes build up with ash they then present a flat surface which slopes downward toward the single diffusion baffle at the precipitator entrance by 30 or more degrees.

The problem of ash fallout in the inlet turning vanes is not unique to Clinch River. Glen Lyn is experiencing it, too, but the ash has accumulated at a lower rate. The point being made here is that this condition has a detrimental effect on performance and could be expected to reduce any margin of operating reserve.

EMISSION TEST AND SUMMARY

Even though all planned improvements have not been completed, preliminary tests have confirmed that at Clinch River a level of performance has been reached that satisfies the state's emission regulation.

At these two installations, i.e., Glen Lyn and Clinch River, we see relatively minor differences in several areas which add up to a difficult situation requiring an unusual effort to correct.

REFERENCE

1. Gooch, J.P., J.R. McDonald, and S. Oglesby, Jr. A Mathematical Model of Electrostatic Precipitation. EPA-650/2-75-037, NTIS PB 246188/AS, U.S. Environmental Protection Agency, Washington, D.C., 1975.

PAPER 4

THE MCCS COAL CLEANING PLANT AT HOMER CITY STATION

Willard A. Crandall
GPU Service Corporation

ABSTRACT

The MCCS coal cleaning plant, now under construction at Homer City Station, represents the implementation of several unique concepts in coal cleaning technology - providing the means to utilize available coal supplies in the generation of electric power in compliance with currently applicable emission control regulations for both SO_2 and particulate matter.

This paper discusses the process design and its application to other installations where other fuel supply and environmental considerations prevail. Concurrent with the basic process development is the adoption and/or development of the latest state-of-the-art technology in analytical instrumentation and process control—required for successful operation of the plant. Also concurrent are studies on the effect of coal cleaning, both the MCCS and other advanced processes, on the coal properties in respect to furnace combustion, electrostatic precipitation of fly ash, etc. These studies are also discussed.

INTRODUCTION

The Homer City generating station, located near Indiana, Pennsylvania, is operated by the Pennsylvania Electric Company (PENELEC), which is part of the General Public Utilities System. Ownership of the station is shared with the New York State Electric and Gas Company.

The expansion of the Homer City generating plant by the addition of a new 650 MW coal fired unit necessitated an in-depth study of the technology and feasibility of the various options available for complying with the SO_2 and particulate matter emission control regulations, both State and Federal, for the new Unit 3 and for the existing Units 1 and 2 (also 650 MW each).

An obvious option was flue gas desulfurization (FGD) by lime/limestone scrubbing. While engineering design work was commenced for such a system for Unit 3, concurrent studies were made to seek a viable alternative to the adverse aspects of utilizing FGD. Major emphasis was directed toward fuel beneficiation by employing the best coal cleaning technology possible to the coal supply for the Homer City Station. The results of this study indicated that this route, utilizing various innovations developed by GPU and associated organizations, was the most desirable on an economic, operational, and environmental basis. The coal cleaning process conceived (termed the "Multi-Stream Coal Cleaning Strategy") would yield three coal product streams from treatment of the Homer City mine-mouth coal supply. These would be:

— a low-sulfur, low-ash coal for use in Unit 3 to meet Federal EPA "New Source" emission regulations of "less than 1.2 lb $SO_2/10^6$ Btu",

— a coal of medium ash and sulfur content for use in Units 1 and 2 to meet State emission regulations of "less than 4.0 lb $SO_2/10^6$ Btu".

— and a small refuse stream of high-sulfur, high-ash material which would be stored on site.

As a result of this study, work was stopped on the FGD program and engineering design and construction was begun on the MCCS plant which is now due to start up in late 1977.

This project involves the joint efforts of many organizations and individuals — not only in respect to actual plant design and construction, but also in the conducting of pertinent studies on the technology involved and its ramifications. Table 1 lists the major participants in the project.

PROCESS TECHNOLOGY

Let us take a brief look at the technology involved in the process design for this coal cleaning concept.

Multi-stream coal cleaning, per se, is not a new idea. Nor does the Homer City project involve new discoveries, special hardware, exotic reagents, and "black boxes". The GPU-PENELEC MCCS system, as the Homer City Station owners and operators are applying it, instead includes a number of innovative applications and extensions of multi-stream coal cleaning technology which will be pointed out as we proceed.

Let us consider a piece of coal—typical of the coal available at Homer City, mined from the upper and lower Freeport seams. This piece of coal is not a homogeneous compound of carbon, hydrogen, sulfur, mineral matter, etc. Instead, when it is

TABLE 1. PARTICIPANTS IN HOMER CITY MCCS PROJECT

OWNERS AND OPERATOR OF HOMER CITY STATION

General Public Utilities Corporation
  GPU Service Corporation
  Pennsylvania Electric Co. (Operator, 50% Ownership)

New York State Electric & Gas Corp. (50% Ownership)

OPERATOR OF MCCS COAL CLEANING PLANT

Rochester & Pittsburgh Coal Co.

ENGINEERING DESIGN AND CONSTRUCTION

Heyl & Patterson, Inc.

CONSULTANTS

Australian Coal Industries Research Laboratories, Ltd.

Mr. J.W. Leonard	Mr. A.C. Gilbert
Mr. E.A. Zawadzki	Others

COOPERATING ORGANIZATIONS

Electric Power Research Institute
U.S. Environmental Protection Agency
Energy Research and Development Agency
U.S. Bureau of Mines
Babcock & Wilcox Co.
Research-Cottrell, Inc.
Southern Research Institute
Others

crushed down to small size particles, each individual particle contains varying amounts of the volatile and "hydrocarbonaceous" material (which provides the Btu "heating value") and the mineral matter (which provides the "ash content").

Chemical analysis of this coal has shown that the sulfur content totals about 2.9% and exists in three general forms:

- about 2.3% as pyritic sulfur (FeS_2)
- about 0.6% as organic sulfur
- and less than 0.01% as sulfate (SO_4^{-2})

The heating value of this coal was determined to be about 11,900 Btu/lb.

The specific gravity of the individual particles will vary over a wide range, depending upon the size and composition of each particle. For example, the following are the specific gravities of a few pertinent mineral components of coal in their pure crystalline form:

Silica (SiO_2),	sp. gr. 2.3	Hematite (Fe_2O_3),	sp. gr. 5.2
Alumina (Al_2O_3),	sp. gr. 4.0	Magnetite (Fe_3O_4),	sp. gr. 5.2
Pyrite (FeS_2),	sp. gr. 4.9		

The specific gravity of the combustible carbon-hydrocarbon portion of coal is approximately 1.2.

- Conventional coal cleaning practice involves size reduction to create heterogeneous particles, followed by separation procedures based upon specific gravity. Over the years, a large variety of hardware for this purpose has been developed to meet the then-existing needs of the industry.
- Specific gravity separations made on large particle size material obviously limits the working range of the specific gravity cuts which can be applied and the composition of the material which can be removed.
- Specific gravity separation at high specific gravity would remove only a portion of the ash and pyritic sulfur present. Separation at low specific gravity would remove more ash and pyritic sulfur, but also would remove combustible matter. Imprecise separation procedures would reduce the efficiency of the cleaning operation.

It can be said that coal cleaning technology, as generally practiced, has been limited by the prevailing economic and fuel quality criteria rather than by potentially available technology. Now, however, the situation is different. The sulfur and ash contents of available coal supplies are a matter of critical concern as all fuels have become more costly, emission control requirements have become more severe, and emission control technology available today is both costly and uncertain in respect to performance and reliability.

With this background, let us consider the composition of this piece of coal and the SO_2 emission control requirements for the Homer City Station.

The emission control requirements are as follows:

Units 1 and 2	- SO_2 less than 4.0 $lb/10^6$ Btu heat input. Particulate matter less than 0.1 $lb/10^6$ Btu heat input.
Unit 3	- SO_2 less than 1.2 $lb/10^6$ Btu heat input. Particulate matter less than 0.1 $lb/10^6$ Btu heat input.

This can be translated into the need of a coal for Units 1 and 2 having a sulfur content less than 2.0 $lb/10^6$ Btu and a coal for Unit 3 having a sulfur content less than 0.6 $lb/10^6$ Btu. Minimum ash content is obviously necessary to insure the attainment of the low particulate matter emission levels by the use of the electrostatic precipitators on each unit. It should be noted that the electrostatic precipitators to be installed on Unit 3 (furnished by Research-Cottrell) represent what we believe to be the best state-of-the-art in conventional precipitator design.

The analysis of the Homer City coal, as typified above, translates into approximately 2.4 lb sulfur per 10^6 Btu.

The coal cleaning strategy evolved by GPU and PENELEC is shown in the flowsheet of Figure 1. Multiple stream coal cleaning circuitry is employed to both remove the maximum amount of sulfur from the raw coal and to redistribute the remaining sulfur and ash contents of the cleaned coal to produce the two product streams of the desired quality.

As is well known, both particle size and specific gravity are interrelated as factors affecting the efficiency of coal cleaning operations. While crushing and size classification of the raw coal, followed by a gravity separation at Sp. Gr. 1.80 can remove a major portion of the sulfur and ash content, further treatment is necessary to produce the desired quality coal. This consists of gravity separations of selected particle size coal at a lower specific gravity to distribute the sulfur and ash content of the initially cleaned coal in the proper proportion between the two desired product streams. Such gravity separations, both at Sp. Gr. 1.80 and at a lower value, can be accomplished in heavy-media cyclones, using suspensions of fine sized magnetite as the "heavy-media" for the separations.

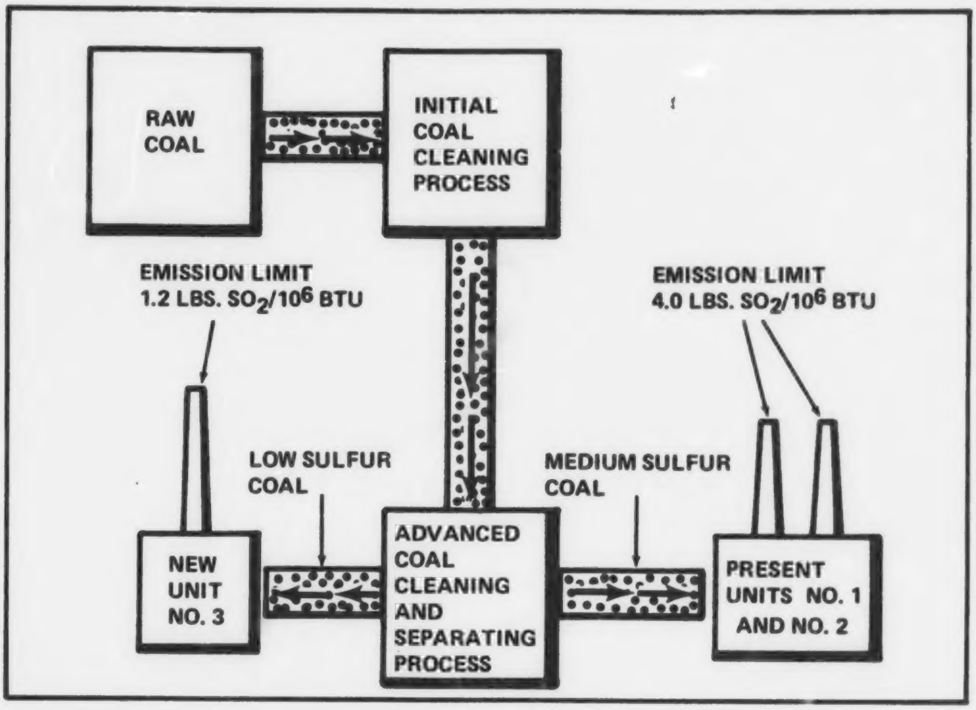
RAW COAL
INITIAL COAL CLEANING PROCESS
EMISSION LIMIT 1.2 LBS. $SO_2/10^6$ BTU
EMISSION LIMIT 4.0 LBS. $SO_2/10^6$ BTU
LOW SULFUR COAL
MEDIUM SULFUR COAL
NEW UNIT NO. 3
ADVANCED COAL CLEANING AND SEPARATING PROCESS
PRESENT UNITS NO. 1 AND NO. 2

Figure 1. New multi-stream coal cleaning process, Homer City Electric Generating Station

How is this accomplished? The theoretical basis for the plant design is illustrated in Figures 2 and 3.

Figure 2 shows the effect of the particle size of the processed coal on the sulfur content of the "float product" of a float/sink specific gravity separation made at a Sp. Gr. of 1.30. The two curves are for the coals from two different mines. As can be seen, decreasing the particle size leads to a decrease in sulfur content. However, the nature of actual gravity separation process equipment limits the practical extent to which the particle size can be reduced to achieve lower product sulfur contents.

Figure 3 shows the effect of the specific gravity of separation on the sulfur content of the "float/sink" products when making a gravity separation on a coal of a given particle size - e.g., 1/4 × 100 mesh. As can be seen, in this particular case, a gravity separation at Sp. Gr. 1.3 produces the desired sulfur distribution.

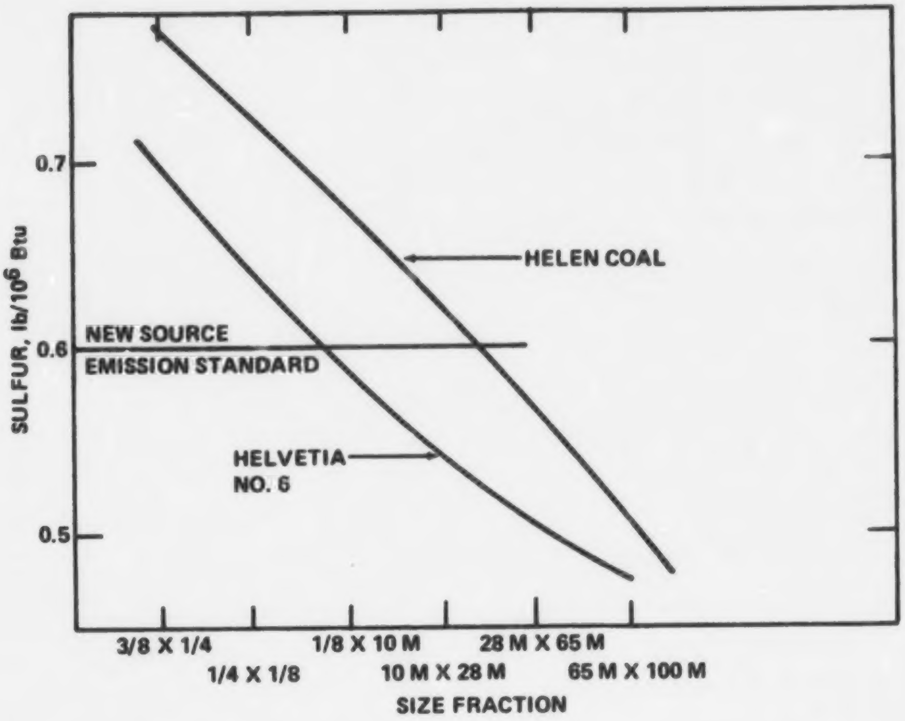

Figure 2. Effect of size on quality of 1.3 sp. gr. float product

Now to tie this all together, the Homer City Multi-Stream Coal Cleaning Strategy is based on the following assumptions which have been implemented into the process design:

1. By removal of most of the pyritic sulfur and very little of the combustible material from the coal available for use at Homer City, the overall/composite 3.0 lb $SO_2/10^6$ Btu quality fuel required can be created. Then, by redistributing the sulfur content of this coal, two product coal streams can be created.

   - one, $\leq$ 0.6 lb $S/10^6$ Btu, low ash, for Unit 3,

   - the second, $\leq$ 2.0 lb $S/10^6$ Btu for Units 1 and 2.

2. With the proper selection of existing types of coal cleaning hardware incorporated into a multi-stream coal cleaning process design tailored for the available coal, the desired product coals could be obtained if —

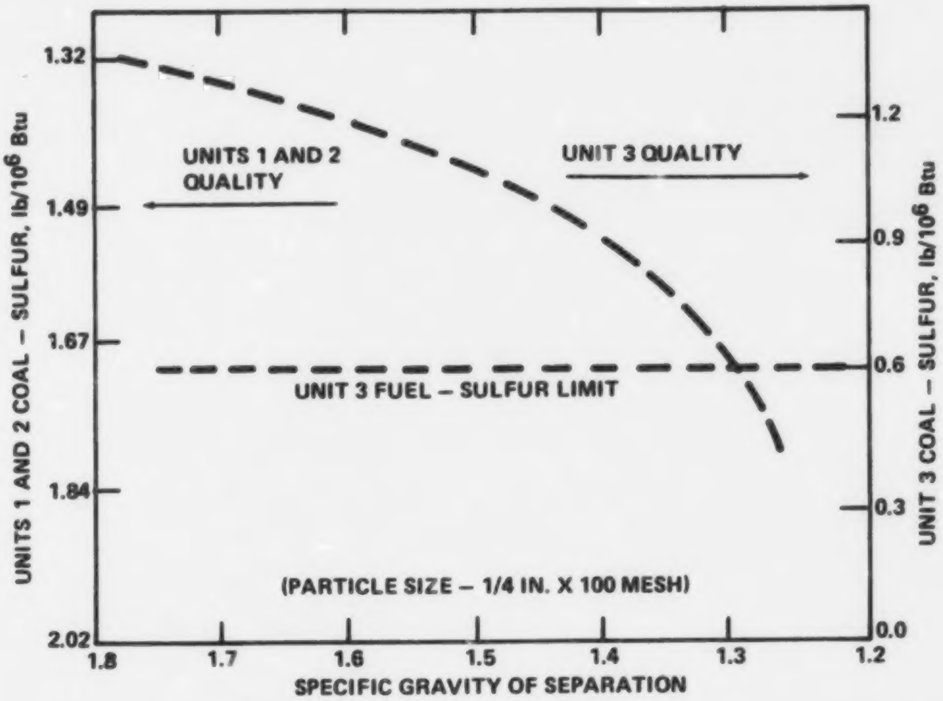

Figure 3. Effect of specific gravity of separation on sulfur content of cleaned coal

- precise control was maintained in respect to particle size of coal
- precise control was maintained in respect to the specific gravity of separation
- supporting operations were conducted as effectively as possible

The MCCS process design, to accomplish the above, incorporates the following features:

1. Using heavy media cyclones, with magnetite as the media, for specific gravity separation - extending the range of application of heavy media cyclone equipment to smaller sized coal fractions (100 mesh from the usual 28 mesh bottom size).
2. Substitution of full stream electromagnetic separators for drain and rinse screens in the 2 mm × 100 mesh coal circuit for recovering magnetite.
3. Extending the range of operating specific gravity of heavy media cyclones to 1.8 at the upper end and to 1.3 at the lower end.

4. Development of a novel control system for tighter control of the specific gravity of operation in the nominal 1.3 specific gravity circuit operating on fine size coal.

THE HOMER CITY MCCS COAL CLEANING PLANT

Figure 4 is a simplified process flow diagram for the Homer City MCCS coal cleaning plant. It shows the basic circuits and the major items of process equipment.

Figure 5 shows the overall process with boundary markings added to segregate the coal cleaning circuits on the basis of the coal particle size. Now, let's look at each circuit separately.

Circuit A - Crushing and Classification

A portion of the cleaning plant is dedicated to crushing and size classification. Provision is made to selectively crush all major sources of supply to the cleaning plant in variable speed cage crushers to control the production of plus 1/4 inch and minus 100 mesh material while optimizing the release of pyrite and ash.

Circuit B - Fine Coal, Deep Cleaning

The fine coal cleaning circuit cleans 2 mm × 100 mesh coal in heavy media cyclones at 1.3 specific gravity. In this circuit, underflow from the classifying and desliming screens is pumped to 14-inch classifying cyclones. Underflow, containing mostly 2 mm × 100 mesh coal, is cleaned at 1.3 specific gravity in heavy media cyclones. Overflow product is partially dewatered and washed of fines in spiral classifiers. Product makes up the major portion of intensively cleaned coal for Unit 3.

Circuit C - Medium Coal Cleaning

The medium coal cleaning circuit cleans 1/4 × 2 mm coal in two stages of heavy media cyclones. The first stage cleans at 1.3 specific gravity. The clean coal overflow product of this circuit is available as intensively cleaned coal for use in Unit 3. Surplus 1.3 float product from this stage is blended into the moderately cleaned middling coal. Underflow from the first stage is recleaned in the second stage of heavy media cyclones at 1.8 specific gravity. Underflow from this stage is refuse coal; overflow is 1.8 float -1.3 sink and is blended into middling coal.

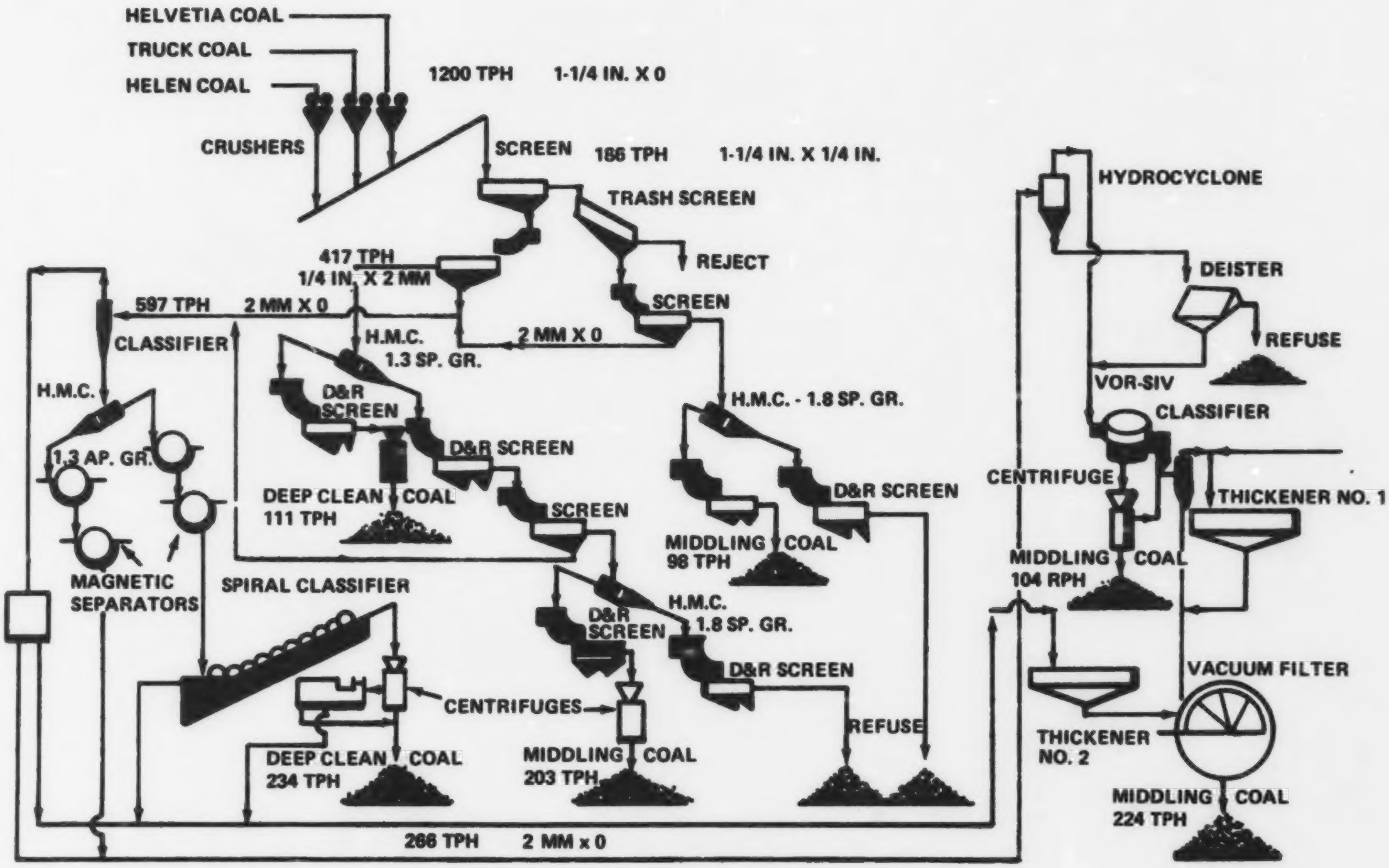
HELVETIA COAL
TRUCK COAL
HELEN COAL
CRUSHERS
1200 TPH
1-1/4 IN. X 0
SCREEN
186 TPH
1-1/4 IN. X 1/4 IN.
TRASH SCREEN
REJECT
SCREEN
417 TPH
1/4 IN. X 2 MM
597 TPH
2 MM X 0
2 MM X 0
CLASSIFIER
H.M.C.
H.M.C.
1.3 SP. GR.
D&R SCREEN
D&R SCREEN
DEEP CLEAN
COAL
111 TPH
SCREEN
H.M.C. - 1.8 SP. GR.
D&R SCREEN
MIDDLING
COAL
98 TPH
1.3 AP. GR.
MAGNETIC SEPARATORS
SPIRAL CLASSIFIER
D&R SCREEN
H.M.C.
1.8 SP. GR.
D&R SCREEN
CENTRIFUGES
DEEP CLEAN
COAL
234 TPH
MIDDLING
COAL
203 TPH
REFUSE
266 TPH
2 MM x 0
HYDROCYCLONE
DEISTER
REFUSE
VOR-SIV
CLASSIFIER
CENTRIFUGE
THICKENER NO. 1
MIDDLING
COAL
104 RPH
VACUUM FILTER
THICKENER NO. 2
MIDDLING
COAL
224 TPH

Figure 4. Homer City—MCCS simplified diagram

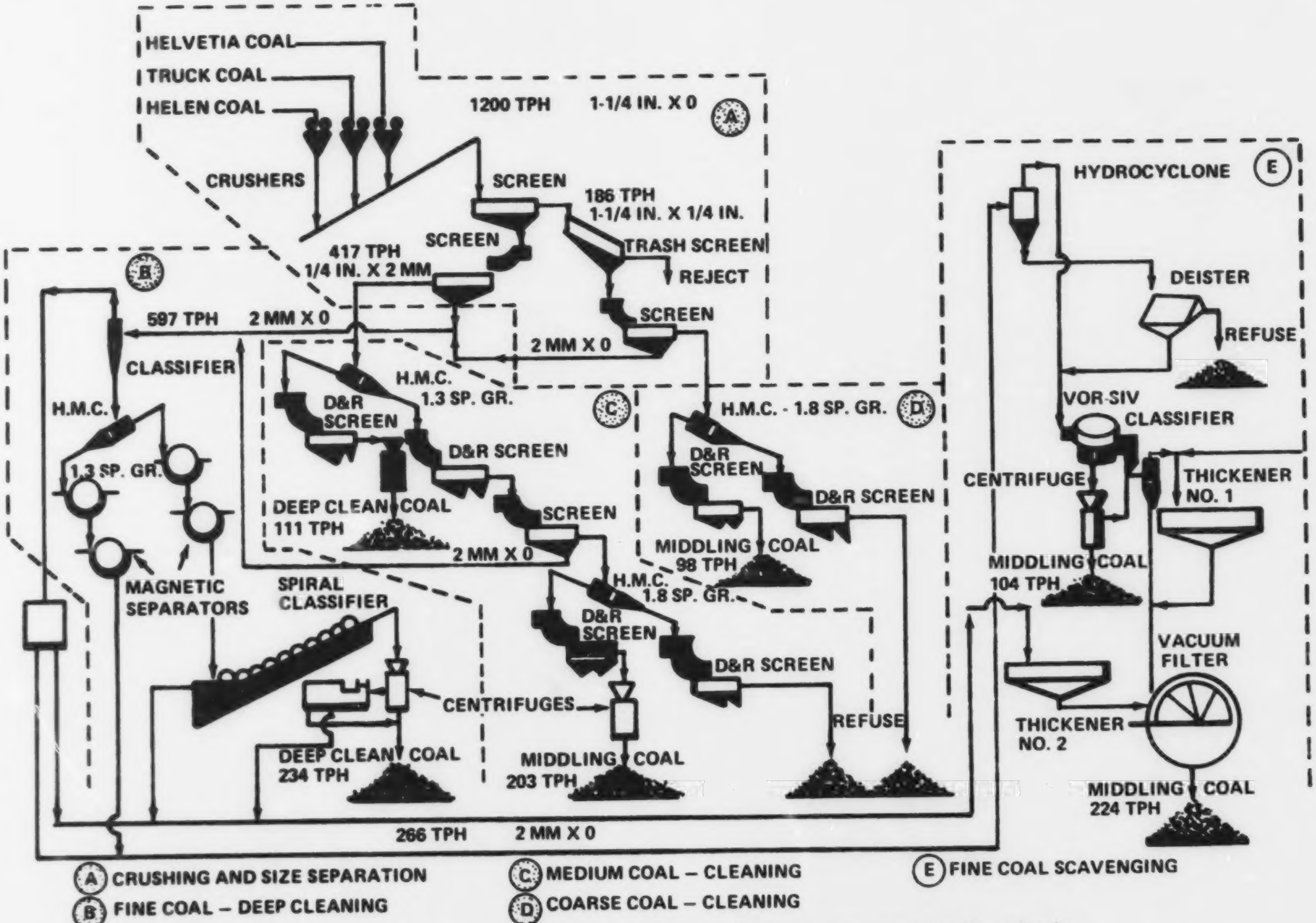
HELVETIA COAL
TRUCK COAL
HELEN COAL
CRUSHERS
1200 TPH
1-1/4 IN. X 0
A
SCREEN
186 TPH
1-1/4 IN. X 1/4 IN.
TRASH SCREEN
REJECT
SCREEN
417 TPH
1/4 IN. X 2 MM
SCREEN
2 MM X 0
B
597 TPH
2 MM X 0
CLASSIFIER
H.M.C.
1.3 SP. GR.
MAGNETIC SEPARATORS
SPIRAL CLASSIFIER
CENTRIFUGES
DEEP CLEAN COAL
234 TPH
C
H.M.C.
1.3 SP. GR.
D&R SCREEN
D&R SCREEN
DEEP CLEAN COAL
111 TPH
SCREEN
2 MM X 0
H.M.C.
1.8 SP. GR.
D&R SCREEN
D&R SCREEN
MIDDLING COAL
203 TPH
REFUSE
H.M.C. - 1.8 SP. GR.
D
D&R SCREEN
D&R SCREEN
MIDDLING COAL
98 TPH
266 TPH
2 MM X 0
HYDROCYCLONE
E
DEISTER
REFUSE
VOR-SIV CLASSIFIER
CENTRIFUGE
THICKENER NO. 1
MIDDLING COAL
104 TPH
VACUUM FILTER
THICKENER NO. 2
MIDDLING COAL
224 TPH
A CRUSHING AND SIZE SEPARATION
B FINE COAL – DEEP CLEANING
C MEDIUM COAL – CLEANING
D COARSE COAL – CLEANING
E FINE COAL SCAVENGING

Figure 5. Homer City–MCCS simplified diagram, coal cleaning circuits

Circuit D - Coarse Coal Cleaning

The coarse coal cleaning circuit cleans plus 1/4 inch coal in heavy media cyclones at 1.8 specific gravity. Cleaned plus 1/4 inch coal becomes part of the moderately cleaned middling coal blend.

Circuit E - Fine Coal Scavenging

The fine coal scavenging circuit deals with 2 mm × 100 mesh, 1.3 specific gravity sink coal and minus 100 mesh coal. Coal prepared in this circuit is used as moderately cleaned middling coal. Coarser material is cleaned in hydro-cyclones. Hydro-cyclone underflow is sent over deister tables for pyrite removal.

Now, after the local coal gets beaten, battered, screened, swirled, and scrubbed in this coal cleaning plant, what is the expected nature of the coals produced for use in our Homer City Station?

Table 2 shows the expected typical analyses of the raw and product coals. These data are based upon analyses made on coal samples prepared by laboratory simulation of the coal cleaning processes.

As the route of coal cleaning, rather than the route of flue gas desulfurization, was chosen as the means to meet the SO_2 emission control requirements for Homer City Station, a few comparisons of MCCS vs. FGD should be of interest.

Table 3 is an economic comparison of the two options considered for SO_2 emission control, based upon the most realistic cost estimates available.

Table 4 is a comparison of the two options based upon process material requirements.

Table 5 is a comparison of the effluents produced in operating each of these options.

Table 6 represents a comparison of the environmental effects of each option, based upon predicted ambient air quality. In addition to the ambient air quality, a major environmental aspect to be considered is the solid and liquid waste situation associated with each process. The problem of disposing of vast quantities of FGD sludge was a major factor in our choice between the two options.

Figures 6 and 7 illustrate the predicted sulfur and energy balances for the Homer City MCCS facility. As can be seen, the energy loss is low in comparison with the reduction in sulfur and ash.

TABLE 2. TYPICAL COAL ANALYSES

(Data Based On Laboratory Simulation of MCCS Process)

ANALYSIS	Raw coal (Helen & Helvetia)	MCCS PRODUCTS Deep-clean coal (Unit 3)	Middling coal (Units 1&2)	Refuse
Sulfur Content				
Pyritic, %	2.28	0.27	1.48	-
Organic, %	0.58	0.57	0.50	-
Sulfate, %	0.007	0.018	0.006	-
Total %	2.87	0.86	1.99	6.97
Ash Content, %	22.02	3.06	16.35	71.19
Heating Value, Btu/lb	11,923	15,299	12,880	-
Yield, %		27.1	53.7	19.2
Lb $SO_2/10^6$ Btu	4.81	1.12	3.09	-

TABLE 3. HOMER CITY GENERATING STATION ALTERNATIVE SO_2 CONTROL STRATEGIES

Cost Comparison - Coal Preparation vs FGD

CAPITAL INVESTMENT - $ × 10^6	FGD	MCCS
Coal Preparation Facilities		
Original Plant (for use with FGD)	18	18
MCCS Addition		32
FGD	59	0
Subtotal	77	50
ANNUAL REVENUE REQUIREMENTS - $ × 10^6		
Fixed Charges	11.6	7.5
Operating and Maintenance Expenses		
FGD	10.6	0
Coal Preparation	3.2	7.6
Subtotal	25.4	15.1

TABLE 4. HOMER CITY GENERATING STATION ALTERNATIVE SO_2 CONTROL STRATEGIES

Estimated Materials Consumed - Coal Preparation vs FGD

Materials Consumed	FGD	MCCS
Coal, ton/yr @ 1200 Btu/lb		
Boilers	4,800,000	4,800,000
Coal Dryers	17,200	46,400
Lime Kilns (Off Site)	17,000	0
Limestone, ton/yr	144,000	0

TABLE 5. HOMER CITY GENERATING STATION ALTERNATIVE SO_2 CONTROL STRATEGIES

Estimated Effluent Comparison - Coal Preparation vs FGD

Effluents - Tons Per Year	FGD	MCCS
SO_2		
Boilers	176,000	176,000
Coal Dryers	600	2,100
Lime Kilns (Off Site)	700	0
Subtotal	177,300	178,100
Sludge (50% Solids)	334,000	0
Fly Ash and Bottom Ash	1,057,000	577,000
Coal Refuse	552,000	1,032,000

TABLE 6. AMBIENT AIR QUALITY SO_2 CONCENTRATIONS (FORECAST)

	24 hr av	3 hr av
FGD	0.0771 ppm	0.2475 ppm
MCCS	0.0713 ppm	0.2289 ppm

Homer City Generating Station Site

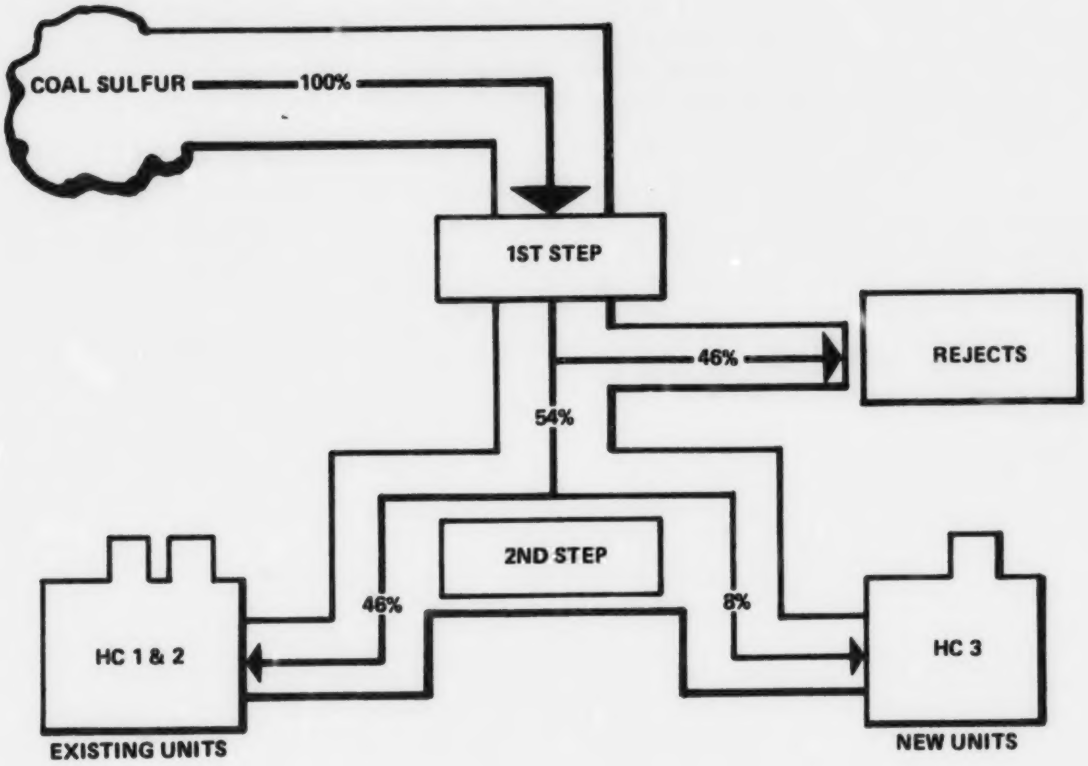

Figure 6. MCCS coal sulfur balance

RAMIFICATIONS OF MCCS

This paper is being presented at an EPA-sponsored conference which is concerned with the particulate collection problems associated with conversion to low-sulfur coals. Therefore, it is appropriate that we discuss the ramifications of the MCCS project with respect to particulate emission control and other related areas of concern.

First, this concept of a coal cleaning process is not restricted to its application at Homer City. Multi-stream coal cleaning processes, based upon Homer City MCCS design technology and operating experience, provide a means for both reducing and redistributing the sulfur content of coal - producing several product streams tailored to the individual fuel requirements of multiple-unit power generation complexes. This is illustrated in Figures 8 and 9.

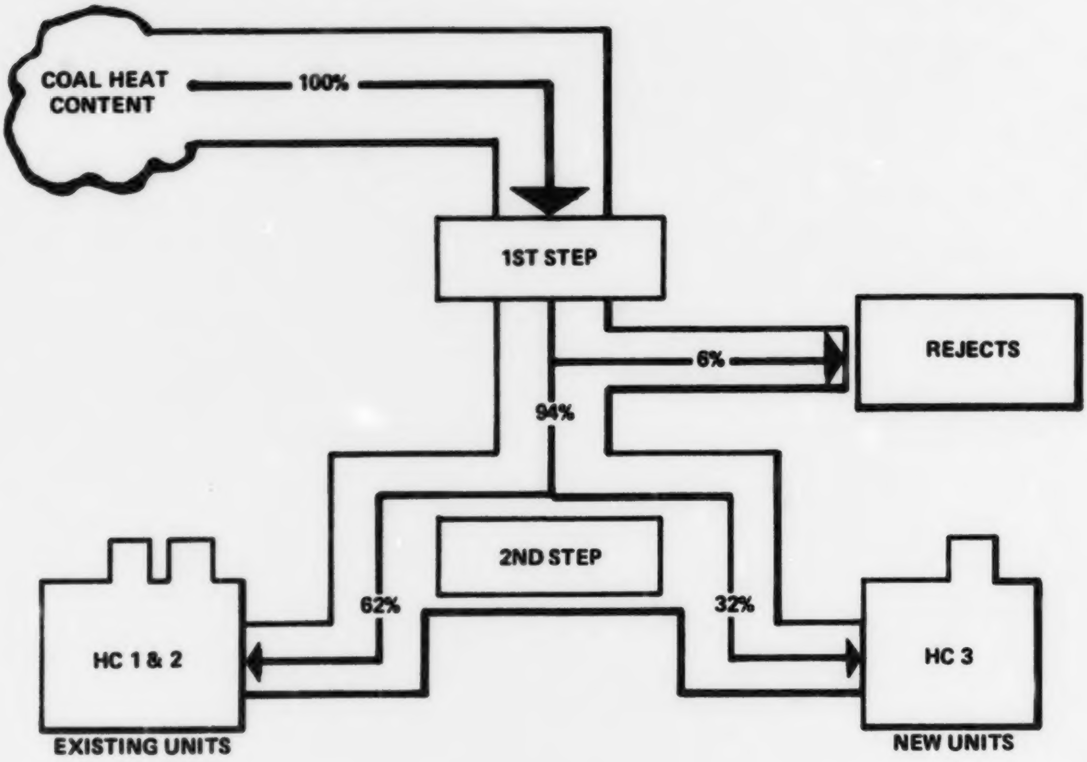
COAL HEAT CONTENT
100%
1ST STEP
6%
REJECTS
94%
2ND STEP
62%
32%
HC 1 & 2
HC 3
EXISTING UNITS
NEW UNITS

Figure 7. MCCS coal heat content balance

When the proper factors exist with respect to the nature of the coal supply available and the SO_2 emission requirements of existing and new generating units at some station or combination of stations, this concept, with appropriate modifications, may be a viable alternative to flue gas desulfurization.

Therefore, one must seriously consider what are the other properties (beside lower sulfur content) of the coals produced by such processes. Laboratory studies have verified the fact that intensive coal cleaning operations alter the composition of the fly ash which will be produced during combustion. Ash fusion temperatures, slagging and caking characteristics, etc., may also be altered.

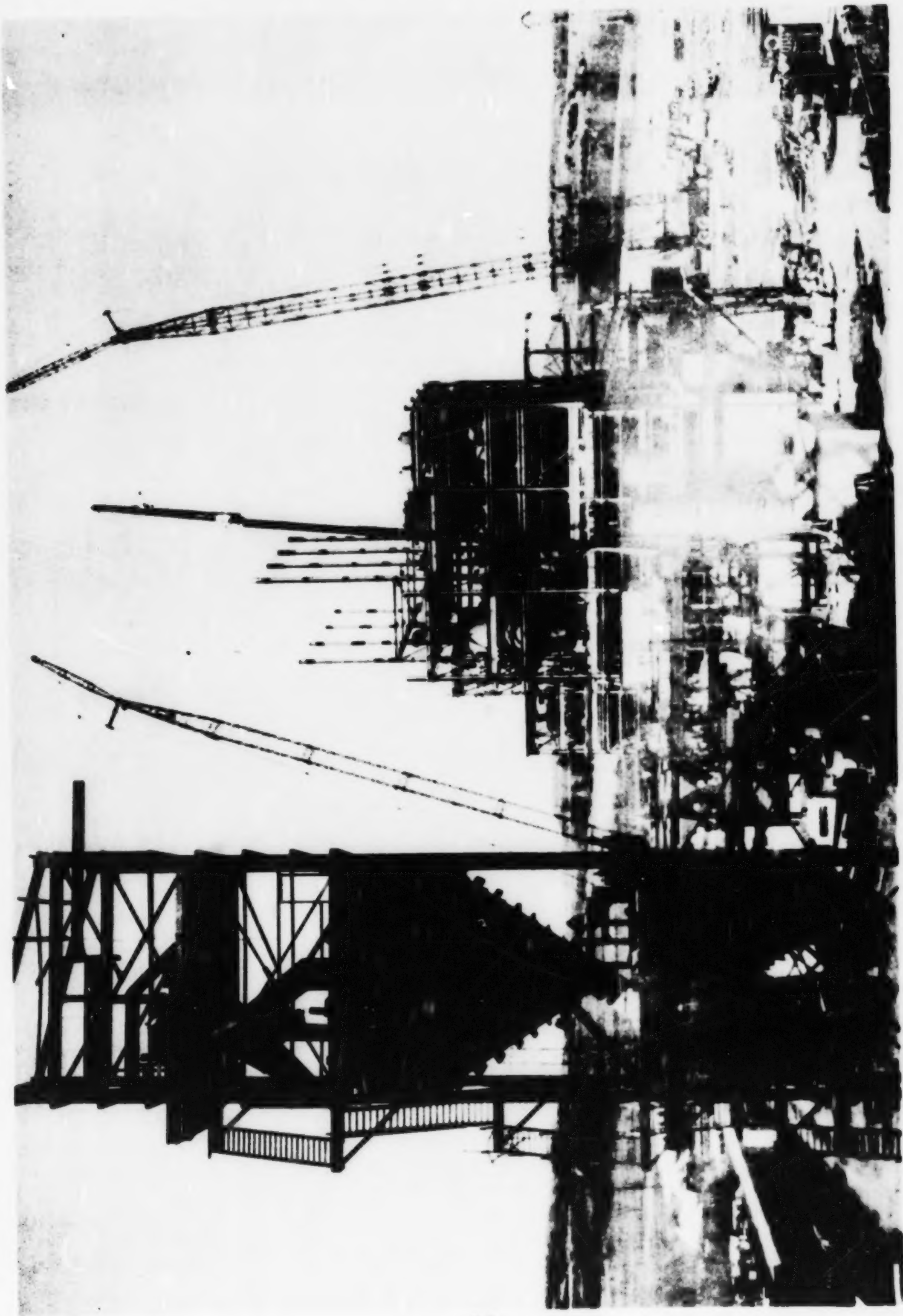

Figure 8. Photo of Homer City MCCS plant during construction

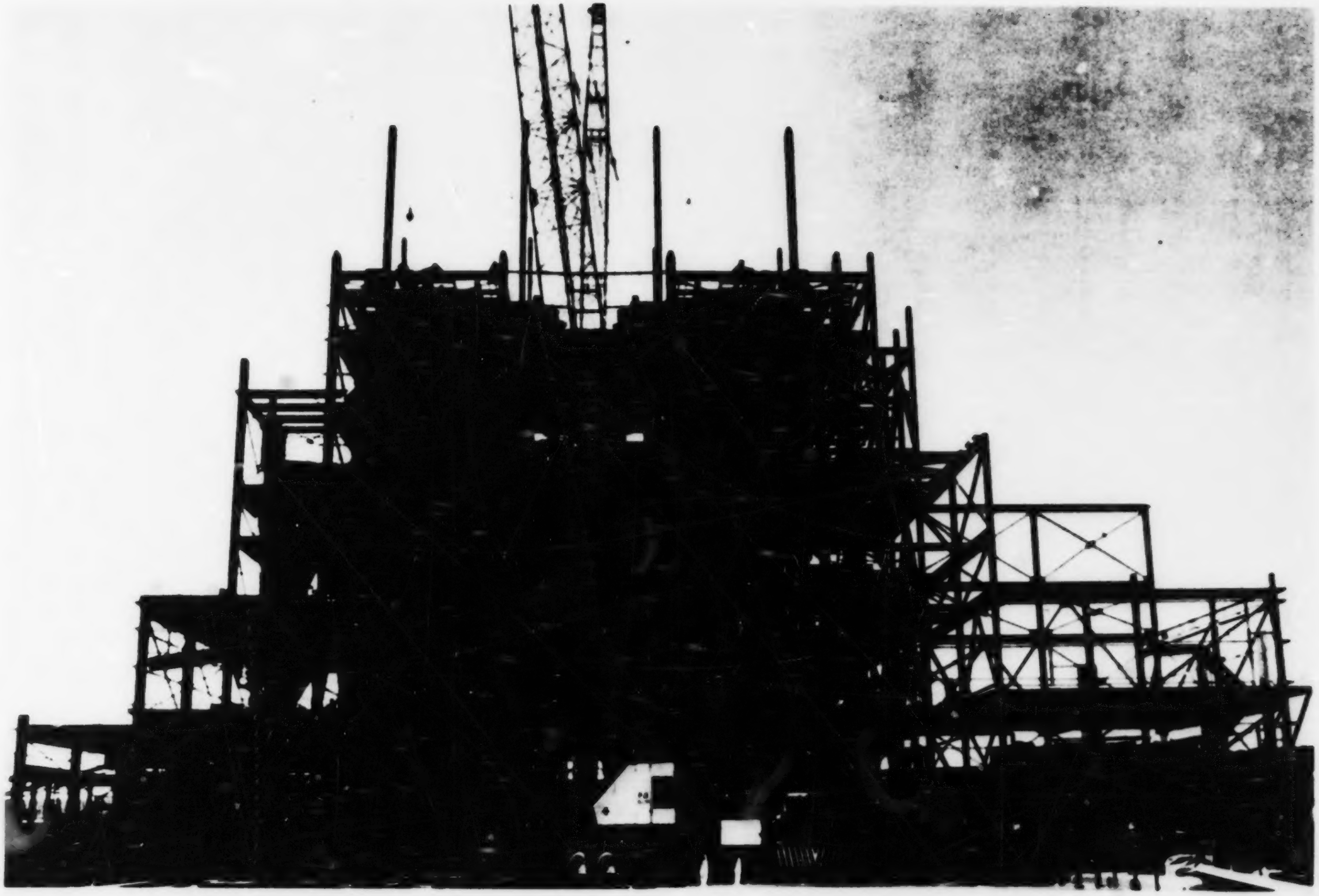

Figure 9. Photo of Homer City MCCS plant during construction

Table 7 lists the various research activities being conducted concurrently with the design, installation, and operation of the MCCS facility at Homer City Station. Item 4 on this list is an item of major concern to us.

TABLE 7. CONCURRENT RESEARCH & DEVELOPMENT PROGRAMS

1. Development of design and operating criteria for maximizing the performance of coal cleaning equipment with the coal available for use in the Homer City Generating Station.
2. Development and evaluation of process control instrumentation systems for the precise control of heavy-media cyclone coal washing operations.
3. Development of "on-line" analytical instrumentation for the measurement of sulfur content, ash content, and heating value of the coal being processed.
4. Prediction and evaluation of the combustion properties of low-sulfur cleaned coal in respect to furnace firing, boiler operation, and electrostatic precipitator performance and collection efficiency.
5. Development of assessment techniques for evaluating potential coal supplies.

What kind of particulate matter, and how much, will be in the combustion product gases when coals from our coal cleaning plant and other intensive cleaning processes are burned in existing and new utility boilers?

What will be the effects on furnace combustion and fly ash collector performance as a result of changing the ash composition, the coal particle size distribution, and the sulfur oxide concentrations in the flue gases?

Means for both measuring and predicting these phenomena with reasonable accuracy must be developed now so that the combustion and emission control equipment is compatibly designed and properly operated to accommodate them.

We are currently working with the Australian Coal Industry Research Laboratories, Southern Research Institute, Research-Cottrell, Babcock and Wilcox, and others on this problem, as well as conducting our own internal research program.

This research is now taking the form of determining the physical nature and the chemical composition, including complete "ash analysis", of the Homer City MCCS product coals - then, using both the classically accepted and the currently developing correlation techniques, predicting their combustion characteristics in respect to large utility boilers and their fly ash characteristics in respect to electrostatic precipitator performance. This requires the preparation of coal samples which resemble, as closely as possible, the low sulfur (Unit 3) and medium sulfur (Units 1 and 2) coals which will be produced in the Homer City MCCS facility when completed. This was done by taking samples of the raw Homer City coal that will be the input to the MCCS plant and subjecting them to size reduction/classification and specific gravity separation procedures in the laboratory in a manner which simulates the various processing steps incorporated in the MCCS plant.

In addition to the analyses made in our laboratories, portions of these samples were sent to other cooperating laboratories for analyses and study. Samples of the low sulfur (Unit 3) coal have been sent to Southern Research Institute and to the Australian Coal Industry Research Laboratories. The tests in Australia include the combustion of the coal in a laboratory combustion train under conditions simulating those for Unit 3 and the collection of the ash/fly ash produced to determine furnace ash properties, slagging characteristics, etc., and to determine the bulk electrical resistivity and other properties of the fly ash which would affect electrostatic precipitator performance.

Following the startup of the MCCS facility in 1977, these test results and the predictions made therefrom will be compared with analyses of the actual product coals and with the boiler/precipitator performance data as these coals are burned in the Homer City Station.

Items 2 and 3 in Table 7, concerning analytical and process control instrumentation, also merit some discussion.

Item 3 is concerned with an anomalous situation in the current state of development and availability of analytical instrumentation. While sophisticated instruments have been developed and utilized to measure everything of interest contained in stack gases, including quite possibly the "Hay Fever Index for Elderly Asthma Sufferers", we are still forced to use crude sampling and slow analytical procedures to determine the sulfur and ash contents of the solid and liquid fuels we burn.

This can give us a good handle on what happened yesterday or last week—why we had an opacity problem or our SO_2 emissions were out of line. It can also tell us that we had received and burned a coal that didn't meet specifications for sulfur and ash content.

The present state of coal sampling and analysis technology provides no on-stream capability for fuel quality assessment or process control.

Such a capability, if developed, could be of infinite value in the field of air pollution emission control. Therefore, we are promoting and supporting various research efforts to develop practical analytical instrumentation systems of this type—instrumentation which can be utilized for improved process control in the Homer City MCCS facility and which can be used in the many applications of coal processing and utilization where on-stream evaluation of coal quality is of concern. It is hoped that through the cooperative efforts of the Electric Power Research Institute, the U.S. Environmental Protection Agency, and other organizations working with us, we can achieve some measure of success in this project.

Item 2 in Table 7 concerns another area in the field of process control instrumentation where efforts conducted to satisfy the needs of the MCCS program may result in technological advancements which can be usefully applied elsewhere. The need for accurately measuring and controlling the density of multi-phase mixtures of such heterogeneous materials as water, pulverized coal of varying size and consistency, finely-sized magnetite particles, etc., requires the use of analytical and process control instrumentation which is currently not available "off-the-shelf". The further development of the design and application of currently available instrumentation components is a major activity within the MCCS program.

To further this effort, a major part of the MCCS process development program is the installation and operation of a pilot plant scale "test circuit" at the Bruceton Laboratory of the Bureau of Mines where both the performance of process control system concepts and component performance as well as the performance characteristics of other items of process equipment will be determined and evaluated.

CONCLUSIONS

The development and implementation of the MCCS coal cleaning program for the Homer City Station is not merely an activity of interest to those concerned with coal cleaning technology. The successful completion of this program has many ramifications with respect to the future utilization of our nation's available coal resources. Among these are those which are of an internal nature—concerned with the combustion and emission control problems which may be involved with the utilization of the "cleaned coals" produced in such facilities. This paper, while providing a brief description of the MCCS process, is primarily intended to acquaint those persons not intimately involved with coal cleaning technology with the implications and ramifications of this MCCS program in the related areas of boiler design and operation, electrostatic precipitator design and performance, etc. While this has not been done in depth due to the complexities of the subject and the length of the paper, it is hoped that an interest will be aroused in those who hear or read this paper to pursue this matter further in their various areas of expertise and concern.

The following references from which much of the material in this paper was taken, provide more information on the background and process design of the Homer City multi-stream coal cleaning plant.

REFERENCES

1. McConnell, James F., and Charles W. Statler. Multi-stream Coal Cleaning Strategy for the Control of Sulfur. Presented at Fall Meeting, Society of Mining Engineers, Salt Lake City, Utah, Sept. 10-12, 1975.

2. Statler, Charles W. Multi-stream Coal Washing—A Systems Approach for the Control of Sulfur. Presented at Conference on Air Quality Management in Electric Power Industry, Austin, Texas, Jan. 28-30, 1976.

3. McConnell, James F. Multi-stream Coal Cleaning Strategy for Control of Sulfur Oxide Emissions at the Homer City Generating Station. Presented at Coal Processing and Conversion Symposium '76, West Virginia Geological and Economic Survey, Morgantown, West Virginia, June 2-3, 1976.

PAPER 5

ELECTROSTATIC PRECIPITATOR OPTIONS FOR COLLECTION OF HIGH RESISTIVITY FLY ASH

L. E. Sparks
Industrial Environmental Research Laboratory
Environmental Protection Agency

ABSTRACT

An analysis of the technical options for collecting high resistivity fly ash is presented. The options are a large specific collector area electrostatic precipitator operating at normal temperatures (about 150°C), a wet electrostatic precipitator, a moderate to large specific collector area electrostatic precipitator operating at either high (about 370°C) or low temperature (about 110°C), or a moderate specific collector area at normal temperature for an electrostatic precipitator plus fly ash conditioning. The advantages and disadvantages of each option are discussed. The potential for adverse environmental impact of the conditioning option is also discussed.

INTRODUCTION

Combustion of low sulfur coal generally produces fly ash with higher resistivity at 150°C than does combustion of high sulfur coal. Thus, fly ash from low sulfur coal is more difficult to collect in electrostatic precipitators than is fly ash from high sulfur coal.

There are several methods of overcoming the influence of high resistivity caused by low sulfur coal. The options are:

1. Provide additional precipitator capacity; *i.e.*, add collector plate area to overcome the poorer performance.
2. Use a wet electrostatic precipitator.
3. Change the flue gas temperature to achieve a more favorable resistivity.
4. Add fly ash conditioning agents to change the resistivity or otherwise modify electrical conditions in the precipitator.

In deciding which of these options is optimum for a given situation, one must recognize that coals, even from the same mine, vary. This means that the design coal will not be burned all the time. The variation in coal composition, especially of the sodium, iron and potassium content of the coal (Bickelhaupt[1]) will result in variations in fly ash resistivity with resultant variations in electrostatic precipitator performance. Available data indicate that coal composition variations can easily result in day to day resistivity variations of plus or minus a factor of two. The fact that coal composition and thus fly ash resistivity will vary from day to day must be considered in selecting ESP options. The method and costs of dealing with the variation must be considered. Questions such as, "Will plate area be added to handle the expected resistivity extremes?" or "Will the boiler be operated at reduced load?", must be answered. Regardless of which option is picked, it is essential that the precipitator be well designed, built, operated and maintained. Gas flow distribution must be good to excellent; sneakage and rapping reentrainment losses must be minimized; wire alignment must be good; ash handling must be properly designed; etc.

COLD SIDE ELECTROSTATIC PRECIPITATORS

Cold side electrostatic precipitators (operating at ∿ 150°C) can collect fly ash from low sulfur coal if sufficient collector plate area is provided. The required collector plate area depends on the resistivity of the fly ash and can be as high as 200 $m^2/am^3/sec$ (∿1015 $ft^2/akcfm$). Specific collector areas in the range of 80 $m^2/am^3/sec$ to 120 $m^2/am^3/sec$ (400 $ft^2/akcfm$ to 600 $ft^2/akcfm$ are common) (am^3 is actual cubic meters; akcfm is actual thousand cubic feet per minute). High efficiency precipitators with specific collector areas in this range have been built for low sulfur applications.

If the required specific collector area is near the low end of the range cited above, a normal cold side precipitator is likely to be the most economical method of collecting high resistivity fly ash. Some designers feel that in general cold side units are less expensive than hot side units for collection of fly ash from low sulfur coal (Matts[2]). Other designers believe the opposite (Walker and Frisch[3]).

The disadvantages of cold side electrostatic precipitators for collecting high resistivity fly ash all center around the sensitivity of precipitator performance to small changes in resistivity. This sensitivity to resistivity makes initial design of the precipitator somewhat uncertain, since fly ash resistivity is likely to vary somewhat during the life of the boiler. Once the precipitator is built, normal variations in resistivity can result in performance degradation such that violations of air pollution regulations occur. If the resistivity variation is of a short term nature, emission limits can be met by reducing boiler load. However, if the resistivity change is of long term, such as might be expected if a new coal supply is used to fuel the boiler, long term de-rating of the boiler or retrofit of additional particulate collection equipment may be required.

WET ELECTROSTATIC PRECIPITATORS

Because the dust layer is continuously washed from the electrodes and the gas is saturated with water vapor, dust resistivity is not a factor in the performance of wet electrostatic precipitators. Thus, wet electrostatic precipitators may be an economically attractive method of collecting high resistivity fly ash.

Whether or not wet precipitators are economically feasible for fly ash collection depends on the cost of purchasing and operating the precipitators. Because wet precipitators must be built of corrosion-resistant materials, they cost more per square meter of plate area than do dry precipitators. Presently available information indicates that for utility boiler applications wet precipitators are likely to cost 2½ times or more per square meter of collection plate area. If the total collection plate area of the wet precipitator is small enough, the added cost per unit of collector area can be overcome. Performance data (Gooch and McCain[4]), on large plate-type wet electrostatic precipitators indicate that a specific collection plate area of about 60 $m^2/am^3/sec$ may be required for high efficiency fly ash collection.

Wet electrostatic precipitators have all the potential water pollution problems that wet scrubbers have. The problems associated with meeting water pollution requirements are likely to increase the cost of wet electrostatic precipitators.

RESISTIVITY MODIFICATION

As discussed in the Cold Side ESP section, precipitator performance becomes extremely sensitive to slight changes in resistivity when the resistivity is high. Under such conditions a relatively small change in ash resistivity can lead to excessive particulate emission. Compliance with emission standards can require operation at reduced boiler load with consequent loss of power generation. Therefore, at some point it becomes necessary to consider steps to reduce the resistivity to a more acceptable level.

Resistivity can be changed by operating the precipitator at a higher or lower temperature or by adding chemical agents either to the fuel or to the flue gas to condition the fly ash and reduce its resistivity. Although resistivity modification may appear to be more expensive than living with the problem, the advantages of improved confidence in design and lessened sensitivity to small changes in resistivity must also be considered.

HIGH TEMPERATURE OPERATION

Location of the electrostatic precipitator before the air heater allows operation at about 370°C. At this temperature resistivity of most fly ash is in the range 2-4 × 10^{10} ohm-cm or lower. Thus, except for rare problem ashes, hot side precipitators can be designed for relatively high current densities and with confidence that changes in fuel chemical composition are unlikely to affect performance.

Calculations based on the electrostatic precipitator performance model described by Gooch, et al[5] and data reported by Walker and Frisch[4] indicate that a specific collector area of at least 67 $m^2/am^3/sec$ is required for 99.5% particle collection efficiency in a hot side precipitator.

The primary disadvantage of hot side operation is the increase in gas volume due to elevated temperatures. Thus the reduction in SCA for high temperature operation is somewhat offset by the increased gas flow. Table 1 compares calculated collector plate areas for 99.5% particulate removal for various current densities at 150°C with collector plate area required at 370°C on the basis of $m^2/am^3/sec$ and $m^2/nm^3/sec$. Note that the hot side precipitator requires a specific collector area of 158 $m^2/nm^3/sec$.

TABLE 1. ELECTROSTATIC PRECIPITATOR SPECIFIC COLLECTOR AREA REQUIRED FOR 99.5% PARTICLE COLLECTION FOR VARIOUS CURRENT DENSITIES

Current Density, nA/cm²	Temperature, °C	Specific Collector Area $m^2/am^3/sec$	 $m^2/nm^3/sec$
5	150	122	189
20	150	53.1	82.3
40	150	39.4	61
30	370	67	158

Normal conditions 0°C at 1 atmosphere pressure
Calculations based on Gooch, et al[5]

Problems associated with thermal expansion must be given special attention during the design and construction of hot side precipitators. There have been cases where sufficient care was not taken in dealing with thermal expansion which resulted in poor electrostatic precipitator performance.

Hot side precipitators must be well insulated to reduce heat losses. Insulation and unavoidable heat losses are likely to increase the cost of hot side operation. Walker and Frisch[3] present a lucid discussion of design, construction, and operation of hot side electrostatic precipitators.

LOW TEMPERATURE ELECTROSTATIC PRECIPITATORS

For some cases a 20-50°C reduction in electrostatic precipitator operating temperature may result in resistivities in the acceptable range. The exact nature of the resistivity versus temperature curve at low temperatures is variable and depends on the particular situation. A tenfold or greater variation in low temperature resistivity is common. Thus the option of reducing gas temperature is subject to verification that the resistivity does indeed decrease with decreasing temperature to a satisfactory level at achievable temperatures. This option is also subject to verification that the rate of corrosion is acceptable; this verification may be possible if the corrosive effect of SO_3 is minimized by the CaO content of the ash. Several precipitator installations have performed satisfactorily at temperatures in the 95-120°C range without undue problems, when sufficient attention was given to the ash-removal system to keep the collected ash hot and to maintain the insulators free of condensed acid.

Achieving a flue gas temperature low enough to overcome the resistivity problem presents problems that must be dealt with on an individual plant basis. If there is sufficient capacity in the air heater, the problem can be handled simply; however, this is not often the case. Whitehead[6] reported that 120°C is about the minimum temperature that can be achieved even if the air heater has sufficient capacity. An alternative approach to reaching low flue gas temperatures in an existing boiler with insufficient capacity in the air heater, or if temperatures below 120°C are required, is to increase the flow of secondary air through the air heater and by-pass some of the excess air to the stack. This approach requires additional fan capacity and imposes an energy penalty due to reduction in boiler efficiency, and therefore in most cases is not too attractive.

Berube presents an excellent discussion of low temperature operation at one plant[7]. For this plant a 0.8% reduction in boiler efficiency was necessary to obtain the required temperature.

In general, low temperature operation is sensitive to coal composition. In a situation where coal composition varies over a wide range, low temperature may not be practical.

CONDITIONING

The addition of a chemical agent to the fuel or to the flue gas to reduce fly ash resistivity has been successful in some cases. Whitehead[6] and others report that flue gas conditioning should be considered as an option for most high resistivity applications.

A partial list of presently available or proposed conditioning agents is shown in Table 2.

TABLE 2. PARTIAL LIST OF CONDITIONING AGENTS

- Aluminum sulfate
- Ammonia
- Ammonium bisulfate
- Ammonium sulfate
- Hydrogen chloride
- Iron oxide
- Iron sulfate
- Organic amines
- Sodium carbonate
- Sulfamic acid
- Sulfur trioxide
- Sulfuric acid
- Vanadium oxide

The most commonly used conditioning agent is sulfur trioxide, SO_3. It is injected into the flue gas either as SO_3 or as sulfuric acid, H_2SO_4. Many of the other agents shown in Table 2 are sold as proprietary agents which may be blends of several of the compounds listed. At the temperatures existing in the flue gas many of the compounds in Table 2, for example, ammonia and sulfur trioxide, dissociate into other compounds. Except for SO_3 there is little industrial experience with these conditioning agents, some of which have not been demonstrated as being effective.

With the exception of sodium and SO_3 conditioning, the mechanisms by which many of the conditioning agents work are unclear. Both sodium conditioning and SO_3 conditioning reduce the resistivity of the fly ash, as shown by Bickelhaupt[8] and Dismukes[9]. Some of the sulfate conditioning agents appear to reduce resistivity probably because SO_3 is one of the products of dissociation (Dismukes[10]). Vanadium and iron oxides are claimed to catalyze the reaction of SO_2 and O_2 to SO_3 and thus increase the quantity of SO_3 present in the flue gas.

The effectiveness of conditioning with some of the agents listed in Table 2 is summarized in Table 3. Based on the available data it appears that properly engineered, operated, and maintained conditioning systems using SO_3 as the active agent can improve resistivity-limited performance of electrostatic precipitators. The data on most other agents are insufficient to make a general judgment of the effectiveness possible.

TABLE 3. EFFECT OF CONDITIONING ON EFFICIENCY

	ESP Efficiency for Particulate Emissions	
Agent	**Without Injection**	**With Injection**
SO_3	94%	95.2% (Dismukes[9])
SO_3	37.5%	51.4% (Dismukes[9])
SO_3	67.3%	77.3% (Dismukes[9])
SO_3	69.7%	93.5% (Dismukes[9])
Sulfamic acid	No statistically significant difference, (Dismukes[10])	
Apollo LPA40	$0.34 g/10^6 J$	$0.13 g/10^6 J$, (McMinch[12])
Apollo LPA40	90%	97% (Harris[13])
SO_3	80-88%	95-96% (Klipstein[14])
SO_3	85%	94-95% (Cook[15])

There are few data on the fate of conditioning agents after they are injected into the flue gas. It is generally assumed that all the conditioning agent is deposited on the fly ash and then collected in the precipitator (Hall[11]). The available data, although limited, cast doubt on this assumption.

There are more data on the effects of SO_3 than other conditioning agents. Whitehead[6] reported that in Great Britain conditioning with up to 50 ppm SO_3 resulted in no increase in SO_3 emissions. Dismukes[9] reported data for two plants that showed that from 28 to 80% of the injected conditioning agent was emitted. Published data on SO_3 emissions with and without conditioning for many plants with conditioning systems are lacking. Hall attributes any increase in SO_3 to poor system design and operation[11].

Because SO_3 emitted due to conditioning will form particulate sulfuric acid or particulate sulfates essentially instantaneously upon reaching the atmosphere, it seems reasonable to count the excess SO_3 as particulate sulfuric acid. Since 1 ppm of sulfuric acid is 5.3 mg/nm^3 (0.0023 gr/scf) of particulate, it is clear that the amount of SO_3 that can escape the stack, if SO_3 is counted as particulate, must be kept at a minimum in order to reduce ambient particulate loading.

Except for data taken by Harris[13], there are no published data on emissions from other agents. Harris reported that the injection of Apollo Chemical's proprietary conditioning agent LPA40 appeared to result in increased emissions of SO_3, ammonia, surface active agent, and other organic compounds. Many of the other proprietary conditioning agents and proposed conditioning agents probably dissociate at flue gas temperatures to produce SO_3 and/or NH_3 - some of which may be emitted to the atmosphere.

The agents that are claimed to catalyze the oxidation of SO_2 to SO_3 are likely to catalyze SO_2 to SO_3 in the plume as well as in the boiler. Thus, the emission of such an agent to the ambient air may increase the ambient particulate concentration above acceptable limits due to formation of sulfates.

It should be noted that many of the conditioning agents listed in Table 2 are known to be toxic. Thus, an appreciable increase in the emission of these substances may result in adverse health effects - at least near the power plant.

As stated above there are few data to support or contradict the discussion above. It is clear, however, that toxic substances are being used as conditioning agents and at least some of these agents are emitted to the atmosphere. The impact of these emissions on ambient air quality is unclear.

Conditioning does appear to be an acceptable option for collecting high resistivity fly ash in electrostatic precipitators under some conditions and with some agents. Whenever conditioning is used, careful measurements of all emissions are required to ensure that emissions of toxic substances are not increased. EPA is presently conducting research to determine the overall environmental impact of conditioning agents.

Dismukes reviewed the capital and operating cost of SO_3 conditioning[9]. His data show that the cost of SO_3 conditioning is sensitive to the method used to produce the SO_3 and the concentration of SO_3 injected.

McNinch reports data on costs of Apollo conditioning agent[12]. Dismukes presents some data on costs of sulfamic acid conditioning[10].

CONCLUSIONS

The ideal general solution to the problems associated with collecting high resistivity fly ash from combustion of low sulfur coals does not exist. Utilities that design plants initially for operation using low sulfur coal have several options, one of which is likely to be best for their application. In situations where fuel source and chemical composition are uncertain, hot side electrostatic precipitators should certainly be considered. In cases where coal supply is certain and coal chemical composition is well defined, large cold side electrostatic precipitators may be attractive.

Conditioning is likely to be the least expensive retrofit solution. However, extreme care must be taken in all steps of design, construction, and operation of conditioning systems to avoid unacceptable emissions due to the conditioning agents.

REFERENCES

1. Bickelhaupt, R.E. Effect of Chemical Composition on Surface Resistivity of Fly Ash. EPA-600/2-75-017, NTIS PB244885/AS, U.S. Environmental Protection Agency, Washington, D.C., 1975. 50 pp.

2. Matts, S. "Cold Side" Electric Precipitators for High-Resistivity Fly Ash Require Different Design Philosophy. In: Proceedings of Symposium on Electrostatic Precipitators for Control of Fine Particles. EPA-650/2-75-016, NTIS PB 240440/AS, U.S. Environmental Protection Agency, Washington, D.C., 1975. pp 229-236.

3. Walker, A.B., and N.W. Frisch. U.S. Design and Operating Experience with Hot Electrostatic Precipitators on Coal-Fired Utility Boilers. Paper presented at Joint US/USSR Symposium on Control of Particulate Emissions and Related Problems, 1976.

4. Gooch, J.P., and J.D. McCain. Particulate Collection Efficiency Measurements on a Wet Electrostatic Precipitator. EPA-650/2-75-033, NTIS PB 244173/AS, U.S. Environmental Protection Agency, Washington, D.C., 1975. 60 pp.

5. Gooch, J.P., J.R. McDonald, and S. Oglesby. A Mathematical Model of Electrostatic Precipitation. EPA-650/2-75-037, NTIS PB 246188/AS, U.S. Environmental Protection Agency, Washington, D.C., 1975. 162 pp.

6. Whitehead, C. Gas Conditioning. In: Proceedings of the Electrostatic Precipitator Symposium. Birmingham, Alabama, 1971. pp 177-222.

7. Berube, D.T. Low Gas Temperature Solution to High Resistivity Ash Problems. In: Proceedings of the Electrostatic Precipitator Symposium. Birmingham, Alabama, 1971. pp 223-280.

8. Bickelhaupt, R.E. Sodium Conditioning to Reduce Fly Ash Resistivity. EPA-650/2-74-092, NTIS PB 236922/AS, U.S. Environmental Protection Agency, Washington, D.C., 1974. 9 pp.

9. Dismukes, E.B. Conditioning of Fly Ash with Sulfur Trioxide and Ammonia. EPA-600/2-75-015, NTIS PB 247231/AS, U.S. Environmental Protection Agency, Washington, D.C., 1974. 155 pp.

10. Dismukes, E.B. Conditioning of Fly Ash with Sulfamic Acid, Ammonium Sulfate, and Ammonium Bisulfate. EPA-650/2-74-114, NTIS PB 238922/AS, U.S. Environmental Protection Agency, Washington, D.C., 1974. 50 pp.

11. Hall, H.J. SO_3/H_2SO_4 Gas Conditioning for Control of High Resistivity Ash Problems in Electrostatic Precipitators. Technical Report HAR 73-35, 1973.

12. McNinch, M.O. Chemotherapy Tames Fly Ash from Low Sulfur Coal. Electrical World:32, January 15, 1976.

13. Harris, D.B. Personal communication, 1976.

14. Klipstein, D.H. Improved Precipitator Performance by Gas Conditioning. Combustion:43, October, 1975.

15. Cook, R.E. Sulfur Trioxide Conditioning. In: Proceedings of Symposium on Electrostatic Precipitators for Control of Fine Particles. EPA-650/2-75-016, NTIS PB 240440/AS, U.S. Environmental Protection Agency, Washington, D.C., 1975. pp 315-326.

PAPER 6

MATHEMATICAL MODELLING OF FINE PARTICLE COLLECTION BY ELECTROSTATIC PRECIPITATION

John P. Gooch and Jack R. McDonald
Southern Research Institute

ABSTRACT

A mathematical model is described which calculates collection efficiency in an electrostatic precipitator as a function of particle size and operating conditions. The model takes into account the dynamics of particle collection by determining the electric field, particle charge, and removal efficiency as functions of position along the length of the precipitator. The model contains procedures for estimating collection efficiency losses caused by non-uniform gas velocity distributions, gas bypassing the electrified regions, and particle reentrainment. Comparisons of the model predictions with experimental data obtained under essentially idealized conditions in a laboratory scale precipitator indicate that the model provides a reasonable basis for describing the precipitation process. Model predictions are compared with field data obtained from precipitators used to collect fly ash and the results are discussed.

INTRODUCTION

The techniques used in the sizing of electrostatic precipitators for various applications differ with the manufacturer and the application area. These techniques may be classified into two general categories:

1. The development of statistically-based relationships between precipitator performance and the properties of the dust or fuel, or the operating parameters of the precipitator. Usually this approach involves a correlation of a precipitation rate parameter which is used as an empirical factor in the Deutsch-Anderson equation.

2. The use of a pilot plant and prior experience for determining the collection area required for the design efficiency at a given application.

Although these techniques can be effective, they can also result in serious design errors if improperly used. Furthermore, in order to design a precipitator for a new installation, it is necessary either to have extensive data for similar applications, or to conduct a test program with a pilot unit. A preferable approach is to develop theoretical relationships to the point that precipitator design can be performed by calculation from theoretical principles and the properties of the dust to be collected. This approach offers the potential for increased confidence in design and in cost savings by preventing under-sizing on the one hand and over-sizing on the other. The reliability of predictions obtained from such an approach is subject to the extent to which certain fundamental parameters are known, the degree to which the theoretical relationships describe precipitator operation, and the accuracy with which the factors that correct for non-ideal conditions can be modelled and determined. At present, efficiency losses due to non-ideal conditions are accounted for only by estimation procedures in which assumed values of the descriptive parameters are normally used.

In order to model particulate collection by the electrostatic precipitation process from first principles, it is necessary to (1) calculate electric fields as a function of position and operating conditions, (2) calculate particle charge as a function of time, electrical conditions, and particle size, and (3) mathematically represent the process by which charged particles are transported from the bulk gas stream to the collection electrode. The mathematical model described in this paper includes these operations and predicts collection efficiency as a function of particle size and operating conditions in electrostatic precipitators.

Comparisons of the model predictions with experimental fractional collection efficiency data obtained in a laboratory precipitator indicate that the model provides a reasonable basis for describing the precipitation process. Application of the model to simulate conditions existing in full-scale and pilot-scale precipitators used to collect fly ash leads to results which are in reasonable agreement with experimental field measurements. In certain cases, however, part of the ideally calculated fractional collection efficiency curve lies below the measured curve. This type of discrepancy can be attributed in part to certain unmodelled and approximately modelled processes which are important under certain conditions in precipitators.

DESCRIPTION OF THE MATHEMATICAL MODEL

Ideal Calculation of Particle Collection Efficiency

The details of a mathematical model for electrostatic precipitation and a computer program which performs the various operations are described elsewhere in the literature.[1,2,3] In the following, a brief description of the physical processes is given, and the mathematical framework of the model is developed.

The first fundamental step in the model is to determine the electric field existing in the precipitator. An accurate calculation of the electric field is important because of its influence on particle charging and particle collection. Although the electric field in a precipitator is a function of position, the value of the electric field used in the particle charging calculations is approximated by the average value between the discharge and collection electrodes. In order to calculate the velocity of charged particles near the collecting electrode, however, it is necessary to compute the local electric field values in this region of space.

In the model the electric field is determined as a function of position by the numerical relaxation technique suggested by Leutert and Böhlen.[4] Using this technique, Poisson's equation and the current continuity equation are solved simultaneously and subject to the existing boundary conditions. These two equations can be written in two dimensions in discrete form as:

$$\frac{\Delta^2 V}{\Delta x^2} + \frac{\Delta^2 V}{\Delta y^2} = -\frac{\rho}{\varepsilon_0} \qquad (1)$$

and

$$\rho^2 = \varepsilon_0 \left(\frac{\Delta V}{\Delta x} \frac{\Delta \rho}{\Delta x} + \frac{\Delta V}{\Delta y} \frac{\Delta \rho}{\Delta y} \right) \quad , \qquad (2)$$

where

V = potential, volts

ρ = space charge, coul/m^3

x = distance perpendicular to gas flow from wire to plate, m

y = distance parallel to gas flow from wire to wire, m.

The numerical solutions to Equations (1) and (2) are obtained by iterating on a grid of potential and space charge density until convergence is obtained. In the iteration procedure, the space charge density at the wire is adjusted until solutions are found that satisfy experimentally measured boundary conditions of applied voltage and average current density at the plate. The major approximation in the method is the assumption that the motion of all charge carriers can, on the average, be described by a single "effective mobility". In addition, the "effective mobility" is assumed to be independent of position in formulating Equation (2). In previous work,[3] it has been shown that this technique yields theoretical electric field distributions which agree well with existing experimental data in the literature.

The introduction of a significant number of fine dust particles or a heavy concentration of large particles into an electrostatic precipitator significantly influences the voltage-current characteristics of the interelectrode space. Qualitatively, the effect is seen by an increased voltage for a given current compared to the dust-free situation. The increased voltage results from the lowered "effective mobility" of the charge carriers which occurs as the highly mobile gas ions are bound to the relatively slow dust particles, thus creating a "space charge". It is desirable to determine the space charge resulting from dust particles because this quantity influences the electric field distribution, especially near the collecting plate where, for the same current, it is raised above the dust free situation. Also, the "space charge" is a function of position along the length of the precipitator.

It has been shown[3] that the effect of "space charge" on the electrical conditions can be estimated by using an "effective mobility" given by:

$$b_e = b_i \left(\frac{j_T}{200\, j_p + j_T} \right) , \tag{3}$$

where

b_e = effective mobility, m^2/(volt-sec)

b_i = ionic mobility, m^2/(volt-sec)

j_T = total current density at the plate, amp/m^2

j_p = particulate current density at the plate, amp/m^2.

The derivation of Equation (3) is based on the assumptions that (1) free electron current can be ignored, (2) the current carried by the particulate is insignificant, (3) particle mobility can be treated as independent of size and on the average, $b_i = 200\, b_p$, and (4) the particles instantaneously acquire a limiting charge given by the "saturation charge" from field charging theory. The quantity j_T is measured experimentally and j_p can be determined for a given incremental length of the precipitator from an estimated or calculated overall mass efficiency.

In a given incremental length of the precipitator, the effect of "space charge" on the electrical conditions can be determined by solving Equations (1) and (2) subject to the condition that:

$$j_T = b_e \rho_p E_p , \tag{4}$$

where $\rho_p E_p$ is the product of the space charge density and electric field at the plate averaged over the number of grid points used in the direction of gas flow.

The second fundamental step in the model involves the calculation of particle charge as a function of particle size, residence time, and precipitator operating conditions. Accurate values of particle charge are necessary because the electrical force which causes the particle to migrate towards the collection electrode is directly proportional to the charge on the particle. In the model particle charge is calculated using the charging rate equation developed by Smith and McDonald[5] and given by:

$$\frac{dq}{dt} = \frac{N_0 ebq_s}{4\varepsilon_0}\left(1 - \frac{q}{q_s}\right)^2 + \frac{\pi a^2 e\tilde{v}N_0}{2}\int_{\theta_0}^{\pi/2} \exp - \left[\left(\frac{qe(r_0-a)}{4\pi\varepsilon_0 ar_0 kT}\right.\right.$$

$$\left.\left. + \frac{[3ar_0^2 - r_0^3\ (K+2) + a^3\ (K-1)]}{kTr_0^2\ (K+2)}\right)\right] \sin\theta d\theta$$

$$+ \frac{\pi a^2 e\tilde{v}N_0}{2} \exp\left(- \frac{qe}{4\pi\varepsilon_0 akT}\right), \tag{5}$$

where

$$q_s = 4\pi\varepsilon_0 E_0 a^2 \left(1+2\,\frac{K-1}{K+2}\right),$$

$$\theta_0 = \arccos\left(\frac{q}{qs}\right),$$

and

q = instantaneous charge on the particle, coul

q_s = saturation charge, coul

θ = azimuthal angle in a spherical coordinate system with origin at the center of the particle, radians

θ_0 = maximum azimuthal angle for which electric field lines enter the particle, radians

N_0 = free ion density, number/m^3

e = electronic charge, coul

ε_0 = permittivity of free space, $coul^2/(Nm^2)$

E_0 = average electric field between the electrodes, volt/m

b = ion mobility, $m^2/(\text{volt-sec})$

$\tilde{v}$ = mean thermal speed of ions, m/sec

a = particle radius, m

k = Boltzmann's constant, J/°K

T = absolute temperature, °K

t = time, sec

K = dielectric constant of the particle

r_0 = radial distance along θ at which the radial component of the total electric field is zero, m.

Equation (5) represents the sum of three charging rates corresponding to three different charging regions on the particle surface. The first term corresponds to a region of the particle surface where field charging occurs; the second, to a region where field-enhanced diffusion occurs; and the third, to a region where diffusion occurs with the effects of the applied electric field neglected as an approximation. The charging rate given by Equation (5) approaches the results obtained from the classical field charging equation for large particles and high electric fields and reduces to the classical diffusion charging equation in the absence of an applied electric field.

The agreement between the results predicted by Equation (5) and Hewitt's[6] experimental data for dioctyl phthalate droplets is within 25% over the entire range of data that is available and is within 15% for practical charging times in precipitators. The agreement between the theory and the experiment over the particle size range 0.1-1.3 μm and a wide range of electric field strengths indicates that Equation (5) should predict closely particle charge as a function of time in the precipitator model.

The third fundamental step is the calculation of particle collection efficiency. Once the particle charge and the electric field adjacent to the collecting electrode are calculated, the electrical drift velocity, or migration velocity, resulting from the coulomb and viscous drag forces acting upon a suspended particle can be obtained. For particle sizes in the size range of interest, the time required for the particle to achieve the steady-state value of velocity is negligible, and the migration velocity is given by:

$$w = \frac{qE_pC}{6\pi a\mu} \quad , \tag{6}$$

where

w = migration velocity of a particle of radius a, m/sec

E_p = electric field adjacent to the collecting electrode, volt/m

C = Cunningham correction factor

μ = gas viscosity, kg/(m-sec).

Gas flow velocities in most cases of practical interest are between 0.60 and 1.8 m/sec, while theoretical migration velocities for particles smaller than 6.0 μm are usually less than 0.3 m/sec. The path of these smaller particles therefore tends to be dominated by the turbulent motion of the gas stream in the interelectrode region. The classical equation for describing particle collection in electrostatic precipitators under turbulent flow conditions was derived by Deutsch[7] and gives collection efficiency as a function of gas volume flow, collection area, and migration velocity in the form:

$$\eta = 100\ [1 - \exp\ (-A_p w/Q)] \quad , \tag{7}$$

where

η = collection efficiency of a particle of radius a, %

A_p = collecting area, m^2

Q = gas volume flow, m^3/sec.

The assumptions on which the derivation of Equation (7) is based are discussed in detail elsewhere in the literature and will not be restated here.[1,8] Of greatest concern in the modelling of the precipitation process is the assumption that gas turbulence provides sufficient mixing to establish a uniform particle concentration at any cross section of the precipitator. The validity of this assumption is most important in determining theoretical collection efficiencies for fine particles.

The mathematical model uses the Deutsch equation to predict the collection fraction, $\eta_{i,j}$, for the i-th particle size in the j-th incremental length of the precipitator. Thus, the Deutsch equation is applied in the form:

$$\eta_{i,j} = 1 - e^{-W_{i,j} A_j/Q} \quad , \tag{8}$$

where $W_{i,j}$ (m/sec) is the migration velocity of the i-th particle size in the j-th increment, and A_j (m^2) is the collection plate area in the j-th increment. Since the Deutsch equation is based on the assumption that the migration velocity is constant over the collection area of the precipitator, it is necessary to make the incremental lengths sufficiently small that the electric field at the plate and the charge accumulated by a given particle size remain essentially constant over the increment.

The collection fraction (fractional efficiency) η_i for a given particle size over the entire length of the precipitator is determined from:

$$\eta_i = \frac{\sum_j \eta_{i,j} N_{i,j}}{N_{i,1}} , \tag{9}$$

where $N_{i,j}$ is the number of particles of the i-th particle size per cubic meter of gas entering the j-th increment. The quantity $N_{i,j}$ can be written in the form:

$$N_{i,j} = N_{i,j-1} e^{-W_{i,j-1} A_{j-1}/Q} , \tag{10}$$

where $N_{i,1} = N_{i,0}$, the number of particles of the i-th particle size per cubic meter of gas in the inlet size distribution.

The overall mass collection efficiency η for the entire polydisperse aerosol is obtained from:

$$\eta = \sum_i \eta_i P_i , \tag{11}$$

where P_i is the percentage by mass of the i-th particle size in the inlet size distribution.

Methods for Representing Non-Ideal Effects

In the preceding section, a basis for calculating ideal collection efficiencies has been developed. This section will discuss the non-idealities which exist in full-scale electrostatic precipitators and describe calculational procedures for estimating the effects on predicted collection efficiencies. The factors of major importance are: (1) gas velocity distribution, (2) gas sneakage, and (3) particle reentrainment due to rapping.

Non-idealities will reduce the collection efficiency that may be achieved for a precipitator operating with a given specific collecting area. Since the model is structured around the Deutsch equation for individual particle sizes, it is convenient to represent the effect of the non-idealities in the model as correction factors which apply to the exponential argument of the Deutsch equation. In the subsequent discussions, these correction factors will be used as divisors for the theoretical migration velocities. The resulting "apparent" migration velocities are empirical quantities only and should not be thought of as an actual reduction in the migration velocity in the region of space adjacent to the collecting electrode.

Although it is widely known that a poor velocity distribution gives a lower than anticipated efficiency, it is difficult to apply a numerical description for gas flow quality. White[8] discusses non-uniform gas flow and suggests corrective actions. Preszler and Lajos[9] assign a figure-of-merit based upon the relative kinetic energy of the actual velocity distribution compared to the kinetic energy of a uniform velocity. This figure-of-merit will be a measure of how difficult it may be to rectify the velocity distribution but not necessarily a measure of how much the precipitator performance would be degraded.

It is possible to develop an approach to estimating the degradation of performance due to a non-uniform velocity distribution based upon the velocity distribution, the ideal collection efficiencies, and the Deutsch equation.[1,2] It will be assumed that the Deutsch equation applies to each particle size with a known migration velocity and that the specific collection area and size of the precipitator are fixed. A constant k can be determined from the Deutsch equation such that:

$$k = \frac{A_p w}{A_1} = u_a \ln \left(\frac{1}{1-\eta} \right) , \qquad (12)$$

where A_1 is the total inlet cross-sectional area (m^2) and u_a is the average inlet velocity (m/sec). Now, the mean corrected penetration p for a given particle size can be written as:

$$p = \frac{1}{N u_a} \sum_{i=1}^{N} u_i \, e^{-\frac{k}{u_i}} , \qquad (13)$$

where N is the number of points in a velocity traverse and u_i are the point values of velocity (m/sec).

For any practical velocity distribution and efficiency, the mean penetration obtained by summation over the velocity traverse will be higher than the calculated penetration based on an average velocity. If an apparent migration velocity for a given particle size is computed based upon the mean penetration and the Deutsch equation, the result will be a value lower than the value used for calculation of the single point values of penetration. The ratio of the original migration velocity to the reduced migration velocity is a numerical measure of the performance degradation caused by a non-uniform velocity distribution. An expression for this ratio may be obtained by setting the penetration based on the average velocity equal to the corrected penetration obtained from a summation of the point values of penetration, and solving for the required correction factor, which will be a divisor for the migration velocity.

The correction factor "F" may be obtained from:

$$\exp\left(-\frac{k}{F}\cdot\frac{1}{u_a}\right)=\frac{1}{Nu_a}\sum_{i=1}^{N}u_i\exp\left(-k/u_i\right)=p\quad. \tag{14}$$

Therefore,

$$F=-\frac{k}{u_a(\ln p)}\quad. \tag{15}$$

Whether the quantity F correlates reasonably well with statistical measures of velocity non-uniformity is yet to be established. A limited number of traverse calculations seem to indicate a correlation between the factor F and the normalized standard deviation of the velocity traverse. Figure 1 shows F as a function of the ideal efficiency for several values of gas velocity standard deviation. These curves were obtained by computer evaluation of Equation 15, and the data on which the calculations are based were obtained from Preszler and Lajos.[9] The standard deviations have been normalized to represent a fraction of the mean. The overlapping of the curves for standard deviations of 1.01 and 0.98 indicates that the standard deviation alone does not completely determine the relationship between F and collection efficiency.

The data in Figure 1 were used to obtain the following empirical relationship between F, the normalized standard deviation of the gas velocity distribution, and the ideal collection predicted for the particle size under consideration:

$$F=1+0.766\,\eta\sigma_g^{1.786}+0.0755\,\sigma_g\ln\left(\frac{1}{1-\eta}\right)\ , \tag{16}$$

where

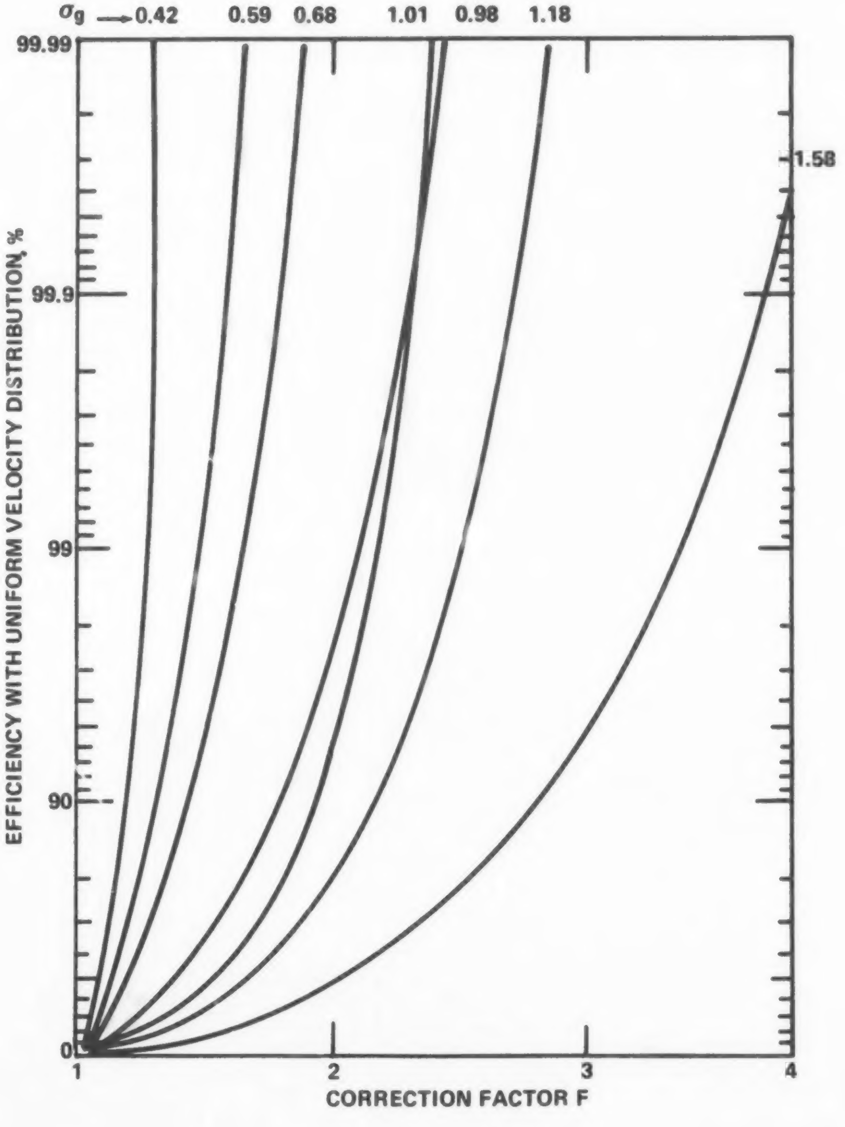

Figure 1. "F" as a function of ideal efficiency and gas flow standard deviation

$$\sigma_g = \frac{\sqrt{\frac{1}{N}\sum_{i=1}^{N}(u_a-u_i)^2}}{u_a} \quad . \tag{17}$$

This relationship is based on a pilot plant study, and should be regarded as an estimating technique only. If it is desirable to simulate the performance of a specific precipitator, the preferred procedure would be to obtain the relationship between F, η, and σ_g for the conditions to be simulated from a velocity traverse at the entrance to the unit.

Gas sneakage occurs when gas bypasses the electrified areas of an electrostatic precipitator by flowing through the hoppers or through the high voltage insulation space. Sneakage can be reduced by frequent baffles which force the gas to return to the main gas passages between the collection plates. If there were no baffles, the percent sneakage would establish the minimum possible penetration because it would be the percent volume having zero collection efficiency. With baffles, the sneakage re-mixes with part of the main flow and then re-bypasses in the next unbaffled area. The limiting penetration due to sneakage will therefore depend on the amount of sneakage gas per section, the degree of re-mixing, and the number of sections.

If the simplifying assumption is made that perfect mixing occurs following each baffled section, an expression for the effect of gas sneakage may be derived. Let:

S = fractional amount of gas sneakage per section,

η = collection fraction of a given size particle obtained with no sneakage for total collection area,

η_j = collection fraction per section of a given particle size $= 1 - (1 - \eta)^{1/N_s}$,

N_s = number of baffled sections, and

p_j = penetration from section j.

Then the penetration from section one is given by:

$$p_1 = S + (1 - \eta_j)\ (1 - S)$$

and from section two,

$$
\begin{aligned}
p_2 &= Sp_1 + (1 - \eta_j)\ (1 - S)p_1 \\
&= p_1\ [S + (1 - \eta_j)\ (1 - S)] \\
&= [S + (1 - \eta_j)\ (1 - S)]^2
\end{aligned}
$$

and from section N_s (the last section),

$$
\begin{aligned}
p_{N_s} &= [S + (1 - \eta_j)\ (1 - S)]^{N_s} \\
&= [S + (1 - S)\ (1 - \eta)^{1/N_s}]^{N_s} \quad . \qquad (18)
\end{aligned}
$$

Figure 2 shows a plot of the degradation of efficiency from 99.9% design efficiency versus percent sneakage with number of baffled sections as a parameter. For high efficiencies, the number of baffled sections should be at least four and the amount of sneakage should be held to a low percentage. With a high percentage of sneakage, even a large number of baffled sections fails to help significantly.

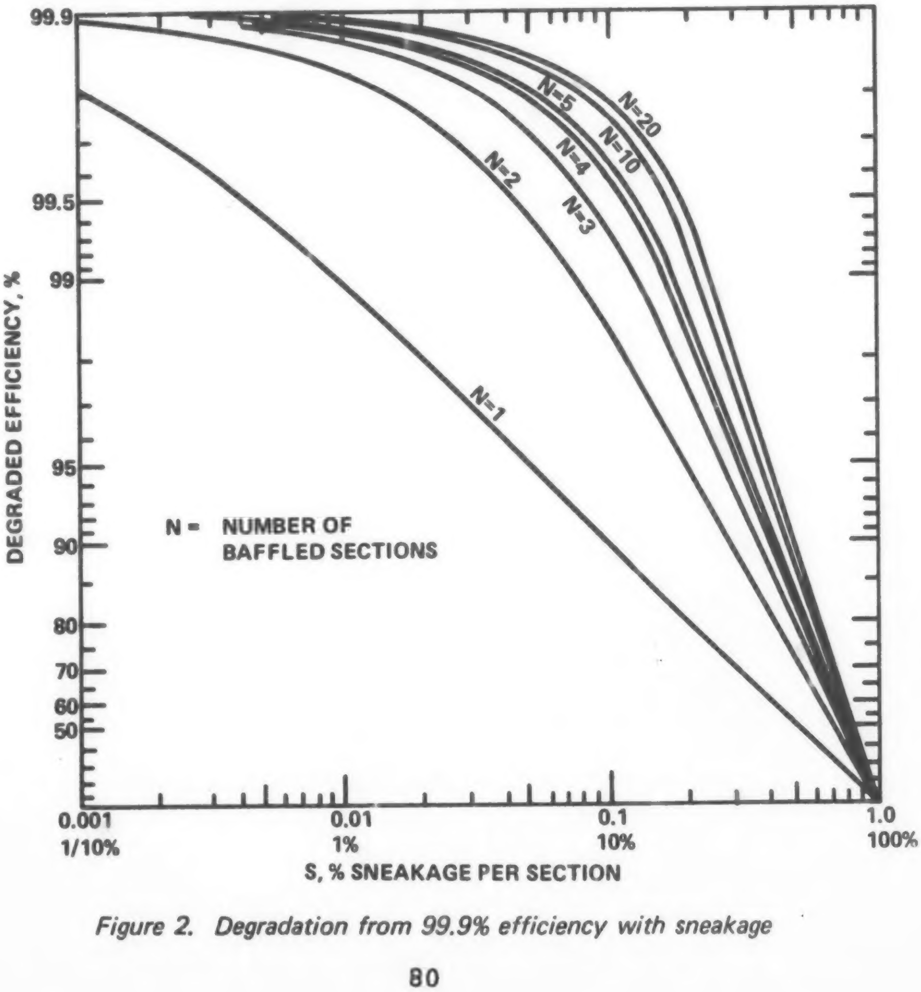

Figure 2. Degradation from 99.9% efficiency with sneakage

A gas bypass or sneakage factor B can be defined in the form of a divisor for the effective, or length averaged, migration velocity in the exponential argument of the Deutsch equation. The factor B is obtained by taking the ratio of the effective migration velocity w_e under ideal conditions to the apparent value of the effective migration velocity w_e' under conditions of gas sneakage so that

$$B = \frac{w_e}{w_e'} = \frac{\ln(1-\eta)}{\ln P_{N_s}} = \frac{\ln(1-\eta)}{N_s \ln [S + (1-S)(1-\eta)^{1/N_s}]} \quad . \qquad (19)$$

Figure 3 shows a plot of the factor B versus sneakage for a family of ideal efficiency curves for five baffled sections. Similar curves can easily be constructed for different numbers of sections.

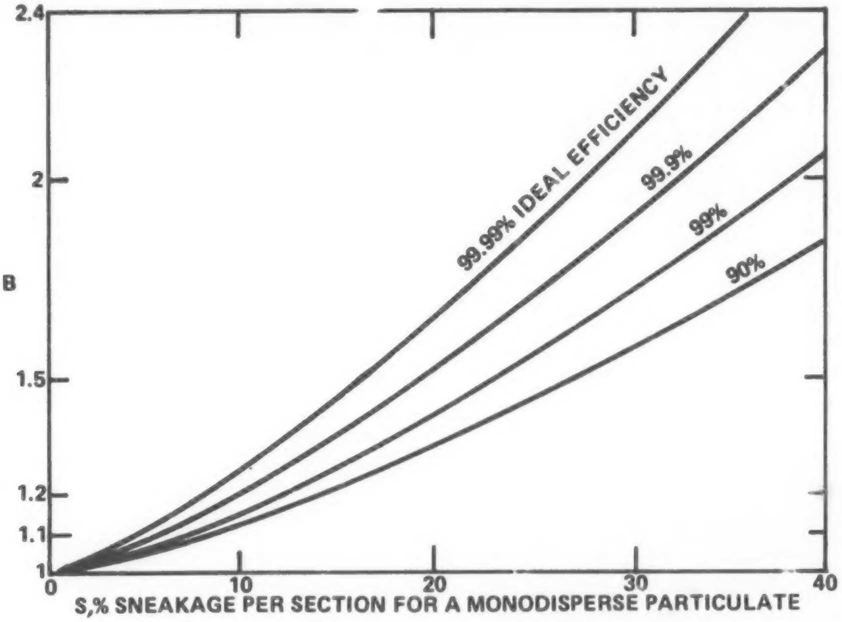

Figure 3. Correction factor for by-pass sneakage when $N_S = 5$

The foregoing estimation of the effects of sneakage is a simplification in that the sneakage air passing the baffles will not necessarily mix perfectly with the main gas flow, and the flow pattern of the air in the bypass zone will not be uniform and constant. The formula is derived to help in designing and analyzing precipitators by establishing the order of magnitude of the problem. Considerable experimental data will be required to evaluate the method and establish numerical values of actual sneakage rates.

Rapping reentrainment is defined as the amount of material that is recaptured by the gas stream after being knocked from the collection plates by rapping or vibration. With perfect rapping, the sheet of collected material would not be reentrained, but would migrate down the collection plate in a stick-slip mode, sticking by the electrical holding forces and slipping when released by the rapping forces. However, the rapping forces are necessarily large to overcome adhesion forces, and much of the material is released into the gas stream as sheets, agglomerates, and individual particles. Most of the material is recharged and recollected at a later stage in the precipitator.

Based upon the simplifying assumptions that a fixed fraction of the collected material of a given particle size is reentrained, and that the fraction does not vary with length through the precipitator, an expression can be derived identical in form to that obtained for gas sneakage:[1,2]

$$p_R = [R + (1-R)\ (1-\eta)^{1/N_R}]^{N_R} \qquad (20)$$

where

p_R = penetration corrected for reentrainment

R = fraction of material reentrained

N_R = number of stages over which reentrainment is assumed to occur

η = collection fraction of a given particle size obtained with no reentrainment.

Since Equations (18) and (20) are of the same form, the effect of reentrainment can be expected to be similar to the effect of sneakage, provided that a constant fraction of the material is always reentrained. It is doubtful that such a condition exists, since precipitators frequently use different rapping programs on different sections, agglomeration occurs during collection, and different holding forces exist in different sections. However, until sufficient data on rapping losses per section as a function of particle size can be accumulated, the relationship may be used to estimate the effect of rapping reentrainment on precipitator performance.

Figure 4 shows the effect on resultant efficiency for a given size particle of various degrees of reentrainment for a four-section precipitator with the indicated values of no-reentrainment efficiency.

Since reentrainment and sneakage effects are estimated with identical mathematical expressions, a combined correction factor B' is used in the mathematical model. From input values of the

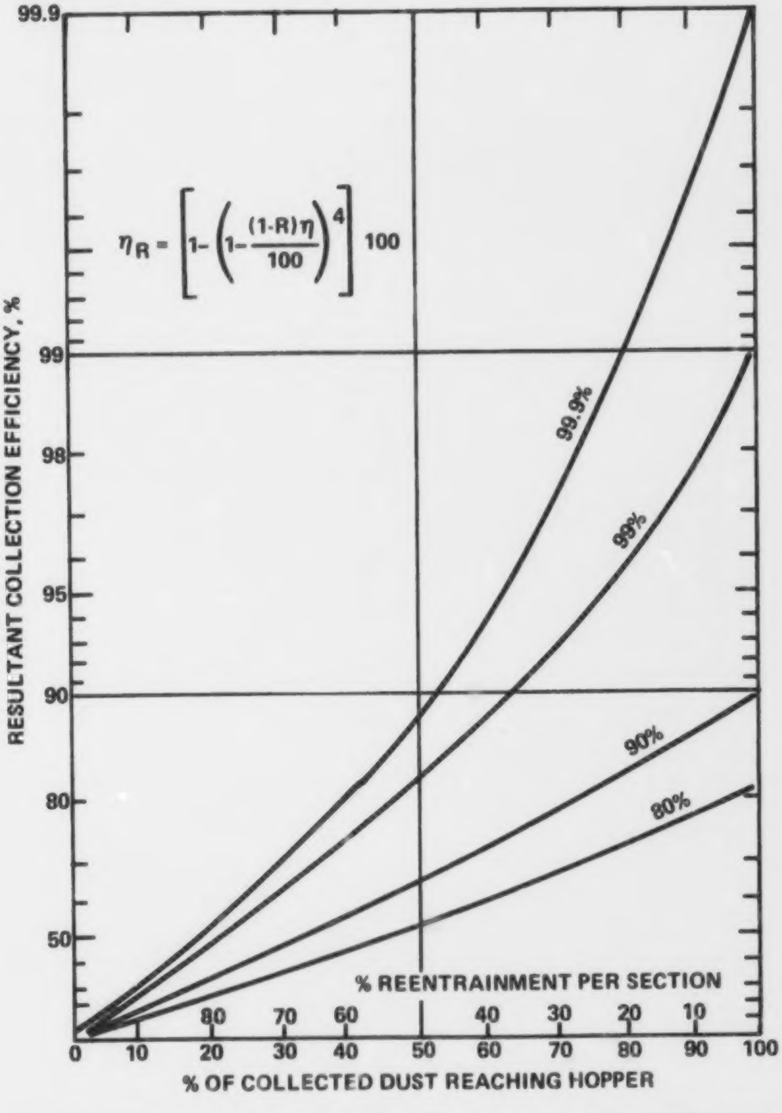

Figure 4. Effect of reentrainment on the efficiency of a four-section precipitator designed for a no-reentrainment efficiency as indicated for a monodisperse particulate

fraction of material assumed to be lost by reentrainment and sneakage, and the number of stages over which losses are assumed to occur, B' is determined from the ideal collection fraction for each particle size.

In summary, the mathematical model takes into account the non-ideal effects of non-uniform gas velocity distribution, gas sneakage, and rapping reentrainment by reducing the ideally calculated migration velocities w_e by the correction factors F and B'. An "apparent" migration velocity w_e' is determined for each particle size from:

$$w_e' = \frac{w_e}{F \cdot B'} \quad . \tag{21}$$

Using w_e', the corrected fractional collection efficiencies are calculated.

EXPERIMENTAL LABORATORY MEASUREMENTS AND COMPARISON WITH MODEL PREDICTIONS

Laboratory-Scale Precipitator

A laboratory-scale precipitator was constructed for the purpose of studying collection of fine particulate under idealized conditions. The test unit has an electrode irrigation capability and provisions for humidifying flue gas produced from a gas-fired burner. For the experiments described here, however, the carrier gas was ambient air, and the particulate source was an atomizer which produced a polydisperse aerosol of dioctyl phthalate (DOP). Electrode irrigation and humidification were not used, and the collected oil droplets drained from the collection electrodes by gravity.

Figure 5 is a schematic drawing of the laboratory precipitator assembly. Wire-plate geometry is employed, with plate-to-plate spacing and wire-to-wire spacing of 12.7 cm (5 in.). Discharge electrodes consist of 0.269 cm (0.106 in.) diameter wires. The collecting plate area is 2.32 m^2 (25 ft^2) which results in a specific collecting area of 35.0 $m^2/(m^3/sec)$ (178 $ft^2/1000$ cfm) at a gas velocity of 1.37 m/sec (4.5 ft/sec). The precipitator is divided into four equal-length sections separated by baffles to limit bypassage, or sneakage, through the hoppers and the region above the collecting electrode. Three power supplies are used, the first two of which each energize a 76.2 cm (30 in.) length section. The third power supply is connected to the last two sections.

Gas bypassage was estimated by measuring gas velocity with a thermal anemometer in the hoppers and in the region above the collection electrodes. The estimated amount of bypassage, expressed as a fraction of the total gas flow through the unit, was

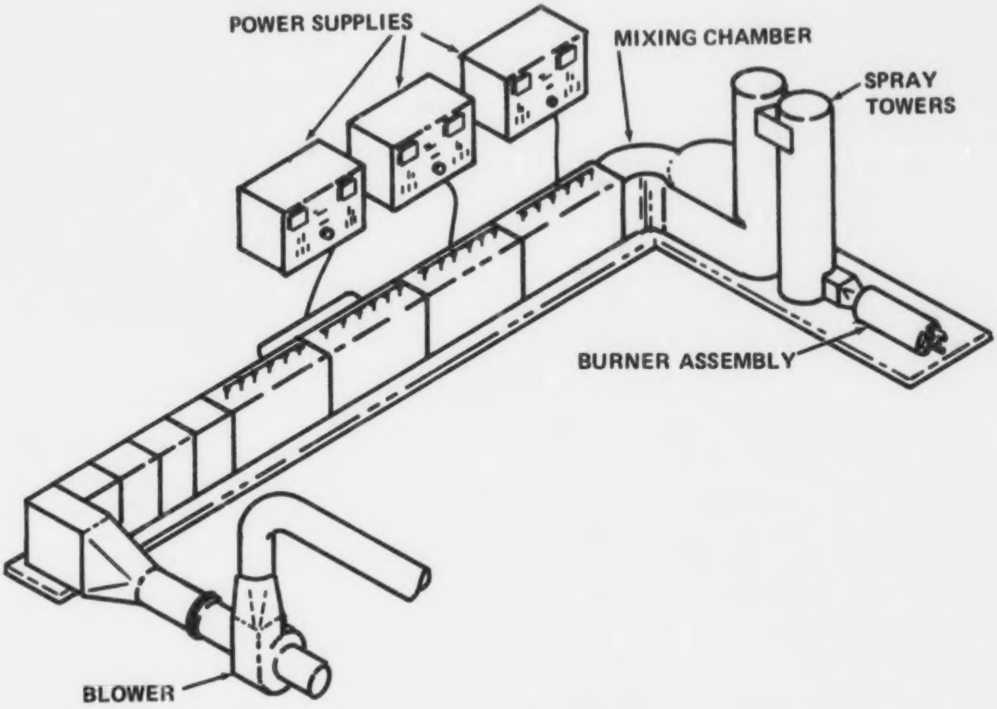

Figure 5. Schematic drawing of the laboratory precipitator

between 8% and 10% for the two values of gas flow reported here. Gas flow uniformity was determined by conducting a traverse with the thermal anemometer at the precipitator inlet. The standard deviation of the velocity distribution, expressed as a percentage of the average velocity, was 11.2% for an average gas velocity of 1.09 m/sec.

Measurement Technique

Fractional efficiency measurements were conducted using a five-stage Brink impactor at the precipitator inlet and outlet. Aluminum foil substrates were used to facilitate weighing of the small masses collected on the individual stages. The mass determinations were made with a Cahn Electrobalance. For the experiments conducted at the lower gas velocity, a sampling time of six hours was required at the precipitator outlet to obtain weighable quantities on the impactor substrates. Six and four point traverses were conducted with the impactor at the inlet and outlet, respectively, in order to insure that a representative size distribution was obtained at each location.

Since the particulate exiting from an electrostatic precipitator will have an electrical charge, it was necessary to employ a charge neutralizer at the inlet of the sampling line for all measurements at the precipitator outlet. Measurements with an optical particle counter indicated that, if metal substrates were used in the impactor, the charge acquired by the particulate substantially influenced the size distribution obtained with the impactor. Since the impactor was calibrated with an uncharged aerosol, the use of the charge neutralizer minimized sizing errors due to electrostatic attraction.

Table 1 gives a typical set of inlet and outlet data obtained from duplicate experiments at the indicated conditions. Good reproducibility was obtained for all stages at the inlet, and for stages 2 through 5 at the outlet. Isokinetic sampling was not employed, since the effect of anisokinetic conditions on particles with diameters less than 2 μm is expected to be negligible. The effect of changing the gas flow rate through the impactor on the indicated size distribution was checked by reducing the flow rate from 56.6 cm^3/sec to 28.3 cm^3/sec. The higher flow rate, which was used for all of the fractional efficiency determinations, resulted in a gas velocity of 0.76 m/sec at the sample point. Figure 6 shows the inlet size distributions from Table 1 and the distribution obtained at the

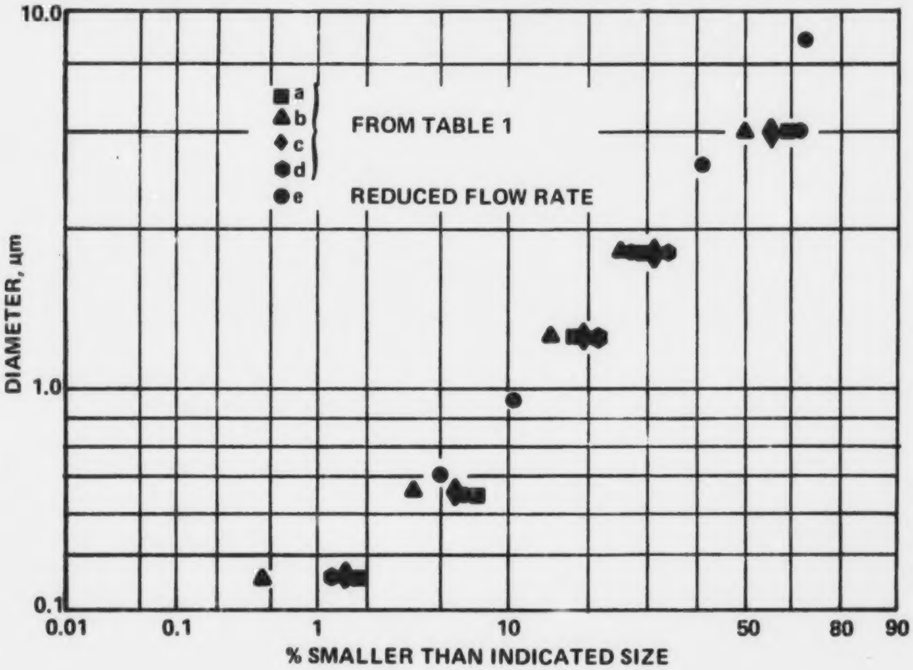

Figure 6. Inlet particle size distributions from Brink data

TABLE 1. TYPICAL INLET AND OUTLET PARTICLE SIZE DATA FOR WET ESP EXPERIMENTS
(DOP Sprayer, Gas Velocity = 1.37 m/sec, Current Density = 55 nA/cm^2)

Test No.		Mass Loading, mg/am^3								Geometric Mean Diameter, µm	Collection Efficiency, %
		Inlet					Outlet				
		2ai	2bi	2ci	2di	Average	2ao	2bo	Average		
Stage	Lower Size Limit, µm										
1	3.04	26.341	28.956	24.596	24.088	25.995	0.0414	~0	0.207	-	-
2	1.80	18.659	13.526	14.128	15.226	15.385	0.1494	0.1103	0.1299	2.34	99.16
3	1.24	7.249	6.285	7.238	8.226	7.250	0.2575	0.2115	0.2345	1.49	96.77
4	0.65	7.448	6.984	6.743	7.419	7.148	0.5724	0.4782	0.5253	0.90	92.65
5	0.46	2.954	1.775	2.514	2.654	2.474	0.3862	0.3770	0.3816	0.55	84.58

same location with the reduced impactor flow rate. These data indicate that the same size distribution is obtained at either flow rate. The higher flow rate is more desirable because of the smaller cut points and the increased amount of gas that may be sampled per unit time.

Experimental and Theoretical Results

Fractional efficiency measurements were performed with the Brink impactor and DOP aerosol at current densities of 26.9, 53.8, and 107.5 nA/cm^2 at a gas velocity of 1.37 m/sec, and at current densities of 26.9 and 53.8 nA/cm^2 at a gas velocity of 0.72 m/sec. The results obtained from these experiments, expressed as collection efficiency as a function of particle size, are presented in Figures 7, 8, and 9. Computed collection efficiencies obtained with the mathematical model are also shown. In view of the difficulties in making these types of measurements, the agreement between measured and calculated efficiencies shown

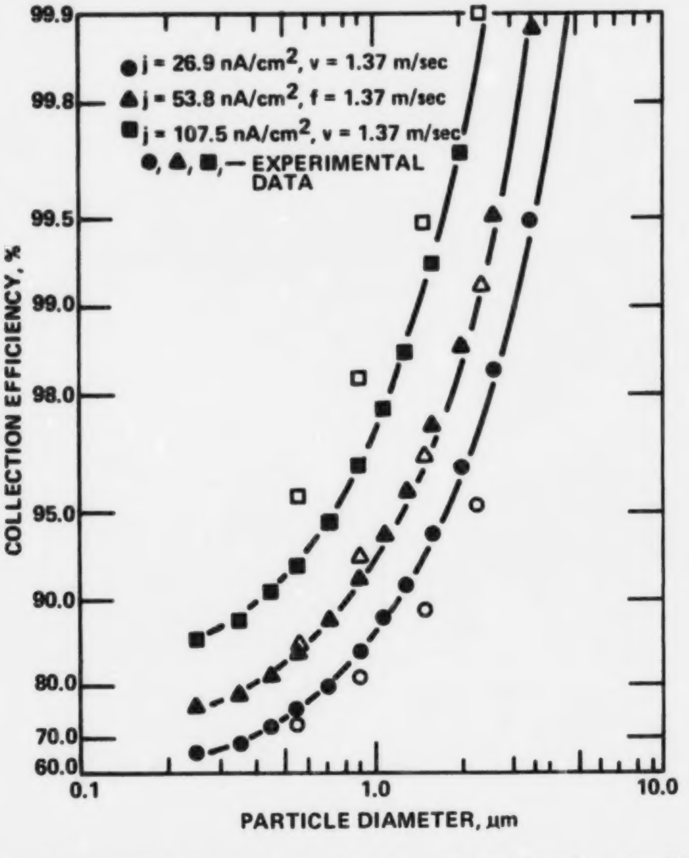

Figure 7. Experimentally measured and ideal calculated fractional collection efficiencies in the laboratory precipitator

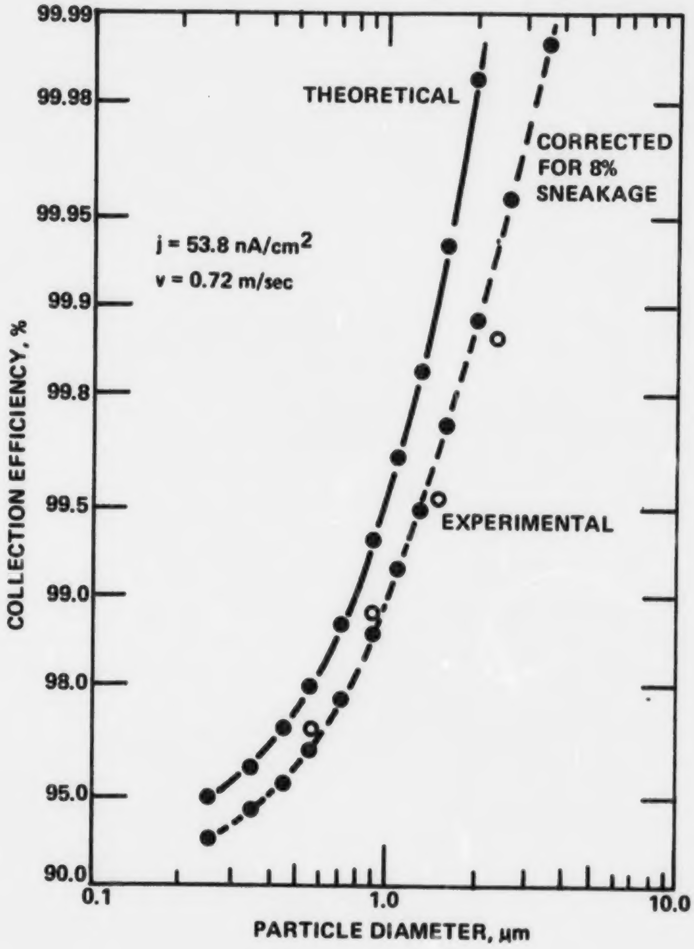

Figure 8. Experimentally measured, ideal calculated, and sneakage-corrected fractional collection efficiencies for a current density of 53.8 nA/cm^2 and a gas velocity of 0.72 m/sec in the laboratory precipitator

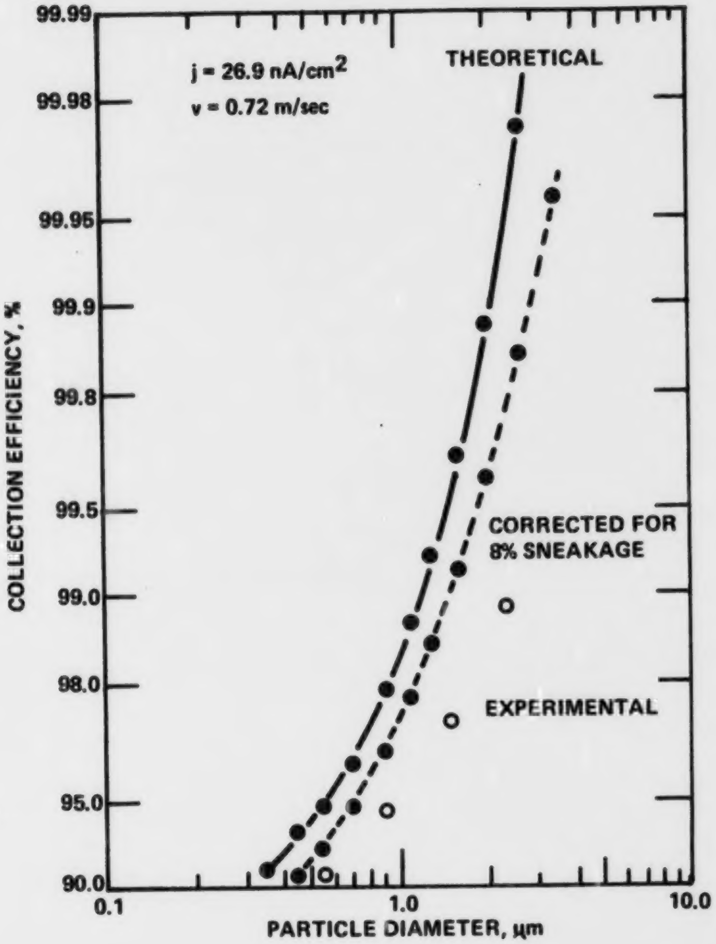

Figure 9. Experimentally measured, ideal calculated, and sneakage-corrected fractional collection efficiencies for a current density of 26.9 nA/cm² and a gas velocity of 0.72 m/sec in the laboratory precipitator

in Figure 7 is considered good. Figures 8 and 9 suggest that the agreement obtained between computed and measured results decreases with decreasing gas velocity and current density. The assumption of 8% gas sneakage over four stages improves agreement between computed and measured results at a gas velocity of 0.72 m/sec. However, the data obtained at this lower gas velocity with 26.9 nA/cm^2 are considerably below the computer projections. Possible causes of this lack of agreement are unmodelled effects such as non-uniform current density and electric field, and particle concentration gradients in the inter-electrode space.

Another series of experiments is being conducted at the present time in which fractional efficiencies are being measured for different wire-to-plate spacings and wire sizes. Figure 10 shows experimental and theoretical fractional collection efficiencies and migration velocities for a plate-to-plate spacing of 19.05 cm (3.75 in.), wire radius of 0.1588 cm (0.125 in.), and gas velocity of 1.46 m/sec (4.79 ft/sec). These results indicate that the model predictions give good agreement with experimental data for current densities of 26.9 nA/cm^2 or less. However, for current densities greater than 26.9 nA/cm^2 it appears that the agreement worsens and, in fact, the ideal calculated fractional

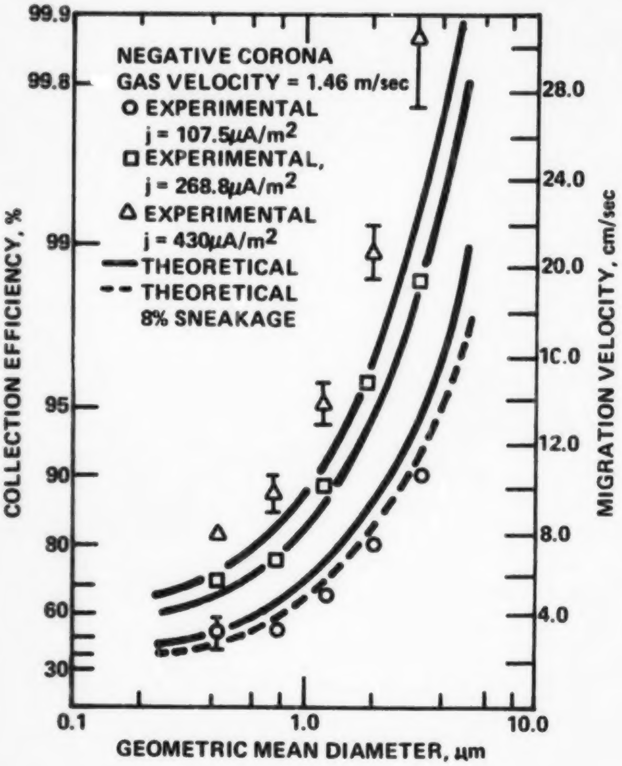

Figure 10. Experimental and theoretical data for a wire of radius 1.488 x 10^{-3}*m*

efficiency curve lies below the measured curve.

The disagreement in Figure 10 between theory and experiment for current densities greater than 26.9 nA/cm^2 occurs at a plate spacing and gas velocity which are not too different from those encountered in the field. Since space charge effects are not significant in these experiments, it might be suspected that particle concentration gradients exist under certain conditions and that in these cases the collection mechanism in the model is not strictly applicable.

Measurements have been made at the outlet of the laboratory scale precipitator under several operating conditions to determine whether or not concentration gradients existed. A "Climet" optical particle counter was used to count 1.0, 0.5, and 0.3 μm diameter particle sizes at several positions located between the collecting plate and the wire. The measurements at the 12.7-cm plate spacing under all conditions presented here showed no build-up of particles near the collecting electrode. These results are consistent with the fact that the model yields good agreement with experiment under all conditions at the 12.7-cm plate spacing. The measurements at the 19.05-cm plate spacing showed definite concentration gradients existing for all three particle sizes under several conditions. In these cases, the concentration was greatest near the collecting plate and decreased towards the discharge electrode. This type of behavior might be expected due to the directed coulomb motion of a particle which is superimposed on the turbulent motion of the gas stream. The ratios of the concentration near the collecting plate to that near the wire for 1.0, 0.5 and 0.3 μm diameter particles were 1.7, 1.3, and 1.3, respectively, at approximately 43.0 nA/cm^2. The causes for such gradients, the conditions under which they would exist, and their effects on predicted collection efficiency of fine particles need further investigation.

FIELD MEASUREMENTS AND COMPARISON WITH MODEL PREDICTIONS

In this section the predictions of the mathematical model are compared with experimental field data for several different precipitators. These precipitators were involved in the collection of coal fly ash under various operating conditions. Also, "typical" performance curves are generated using the model for "cold" precipitators with operating current densities from 5 to 40 nA/cm^2 and for a "hot" precipitator operating at a current density of 30 nA/cm^2.

Figure 11 gives a comparison of fractional effective migration velocities obtained from the model with those obtained from inertially-determined fractional efficiency measurements on a coal-fired power boiler. This "cold" full-scale precipitator has a low specific collection area (SCA) and moderate current density. The particulate under collection had a mass median

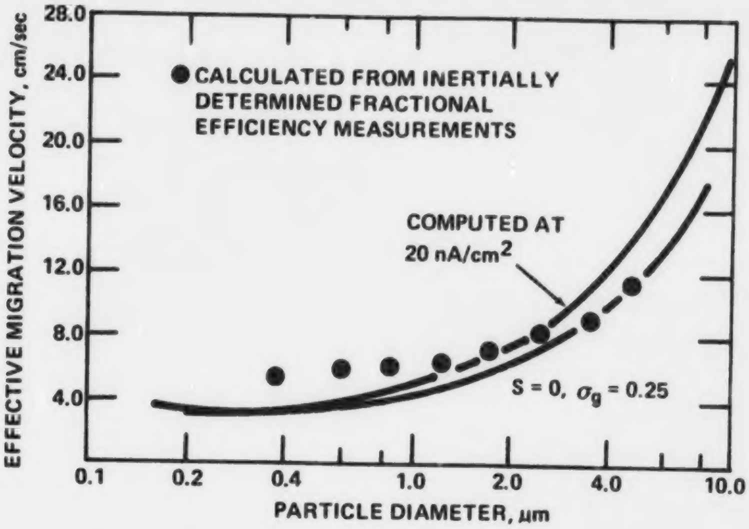

Figure 11. Effective migration velocities for a full-scale precipitator on a coal-fired boiler, SCA = 55.7 $m^2/(m^3/sec)$

diameter (MMD) of approximately 25 μm and a low value of resistivity. In addition to the ideal predictions, Figure 11 shows the effect of correcting for a gas velocity standard deviation (σ_g) of 0.25. A comparison of the w_e values in Figure 11 indicates that the theoretical predictions are low for the particle diameters below 2.0 μm and high for larger particles. Due to limitations in the measurement technique, no data are available for particle diameters larger than 5.0 μm. Figure 12 shows the fractional efficiency data from which the w_e values of Figure 11 were calculated. The overall mass efficiency predicted by the model was 99.8%, as compared to a measured value of 99.6%.

Figures 13 through 18 give results predicted by the model in terms of overall mass efficiency as a function of SCA for current densities of 5, 10, 15, 20, and 40 nA/cm^2 at 150°C, and for a current density of 30 nA/cm^2 at 370°C. The relationships presented in these figures are based on a 22.86-cm (9-in.) plate spacing, and secondary volt-amp curves and particle size distribution (MMD = 25 μm) considered to be typical for a coal-fired power boiler. Also given are test results obtained under conditions approximating the electrical conditions represented by the given values of current density. A comparison of the limited amount of applicable test data with the computed results indicates that the ideal predicted overall mass efficiencies are generally higher than those obtained from the field measurements. The measurements were taken with sampling techniques which insured that essentially all of the mass for particles larger than 0.3 μm in diameter was captured by the sampling device.

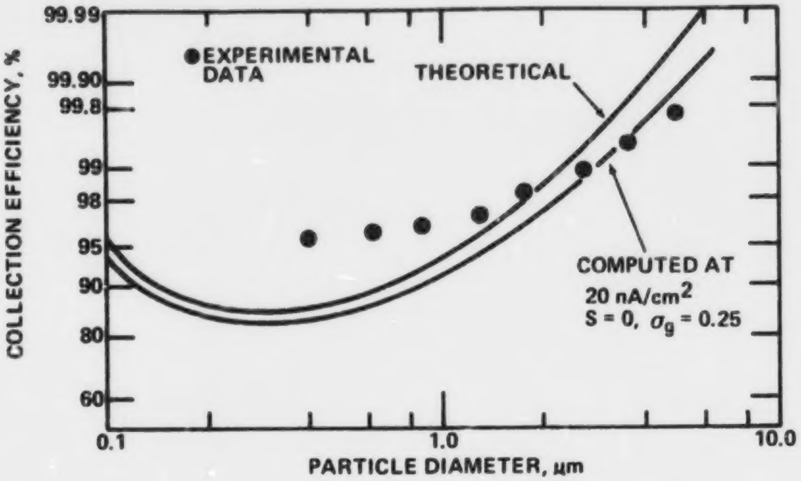

Figure 12. Fractional collection efficiencies for a full-scale precipitator on a coal-fired power boiler

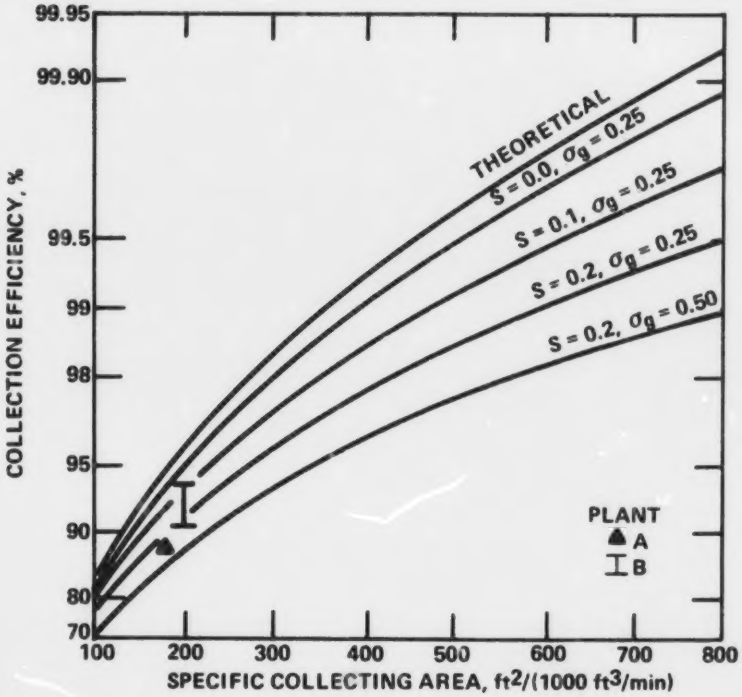

Figure 13. Computed performance curves at 5 nA/cm^2

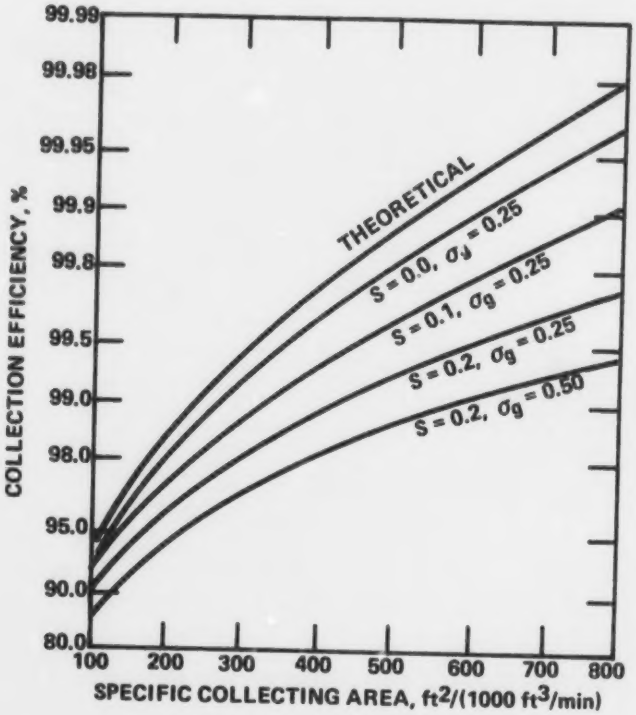

Figure 14. Computed performance curves at 10 nA/cm^2

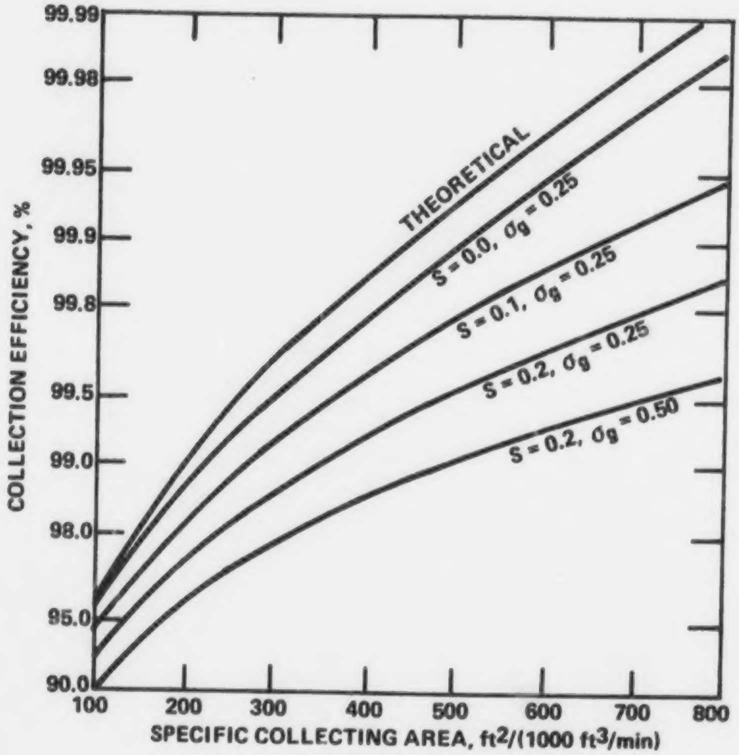

Figure 15. Computed performance curves at 15 nA/cm^2

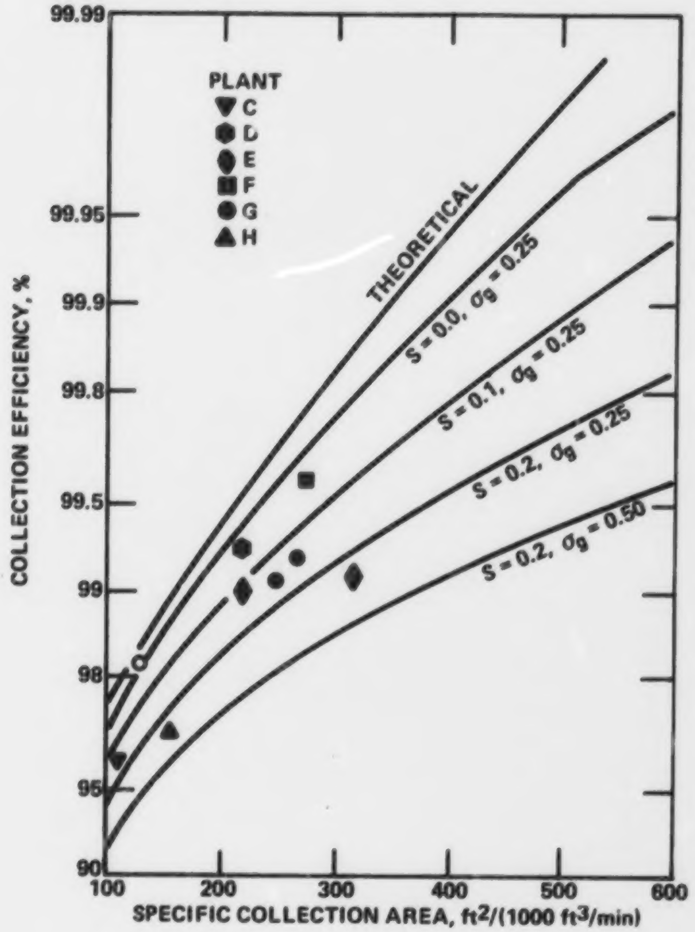

Figure 16. Computed performance curves at 20 nA/cm^2

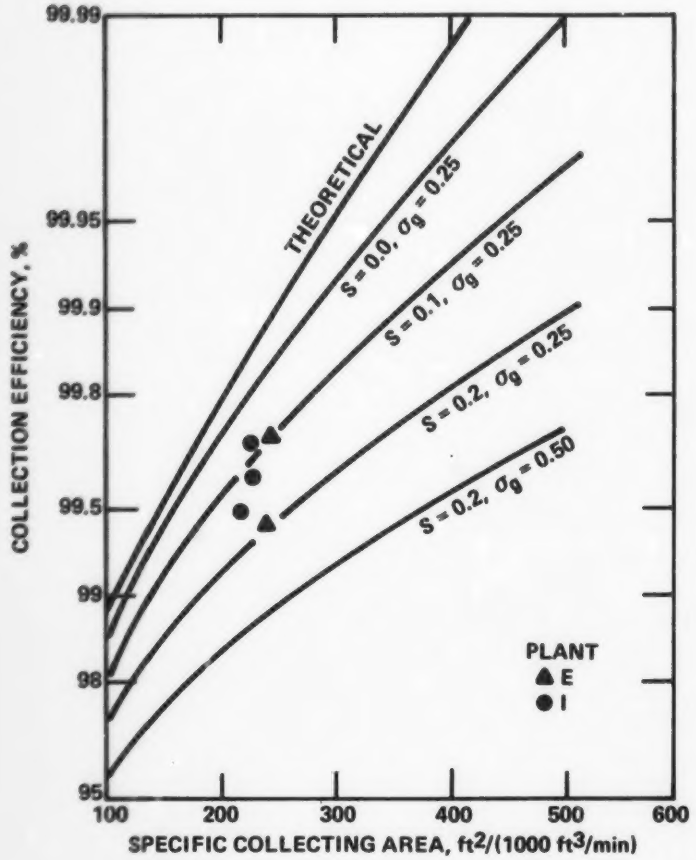

Figure 17. Computed performance curves at 40 nA/cm^2

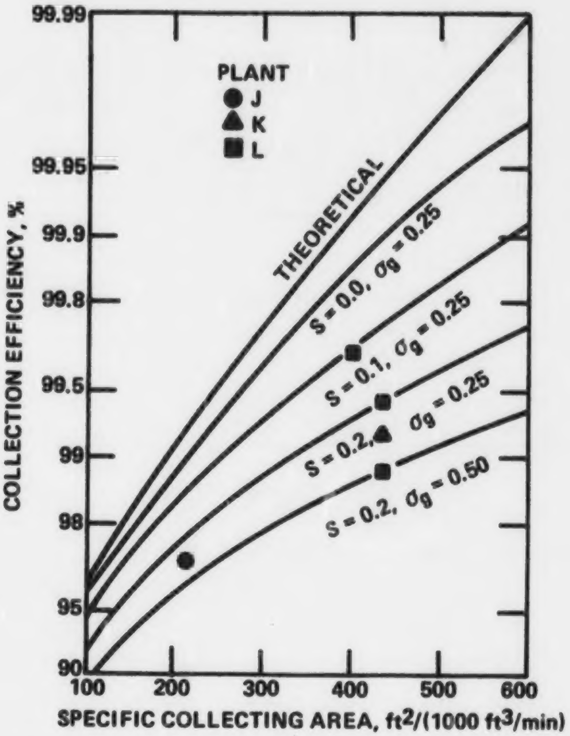

Figure 18. Computed performance curves for "hot" precipitator

The use of the empirical correction factors reduces the computed values of overall mass collection efficiency to the range of values obtained from the field measurements. Reentrainment and sneakage effects were combined by assuming that the indicated fractional losses per stage occurred over four effective stages. Note that high efficiency (>99.5%) precipitators operating on the low-temperature side of the air heater fall reasonably close to the computed line obtained with σ_g = 0.25 and S = 0.1. A gas velocity distribution with a standard deviation of 0.25 is generally considered to be a good distribution for a full-scale unit. The computed results show that a poor distribution (σ_g = 0.5) seriously degrades performance. The detrimental effects of sneakage and reentrainment are also indicated in the decrease of computed performance resulting from variations in the parameter S.

Figures 19 and 20 show results obtained from the analysis of a "cold" full-scale precipitator having a large SCA [560 ft^2/(1000 ft^3/min)] and low current density (12 nA/cm^2). The experimental results were obtained from inlet and outlet size distribution measurements obtained using inertial, optical, and electrical sizing techniques. The precipitator is preceded by

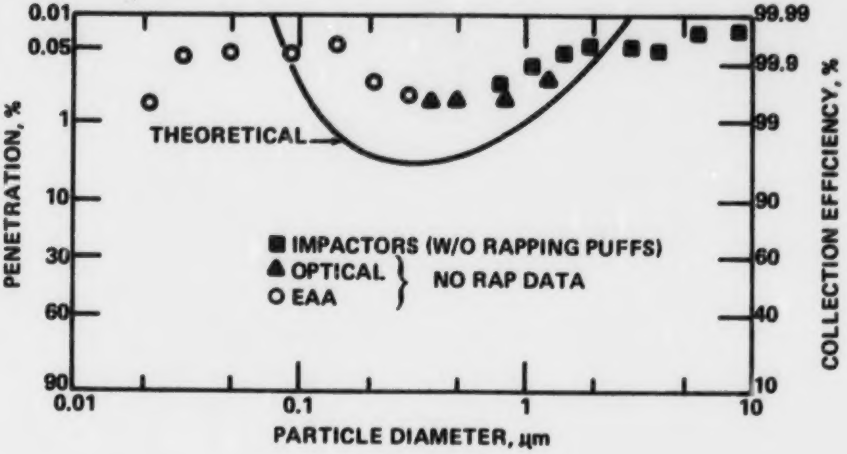

Figure 19. Measured and theoretical fractional efficiency

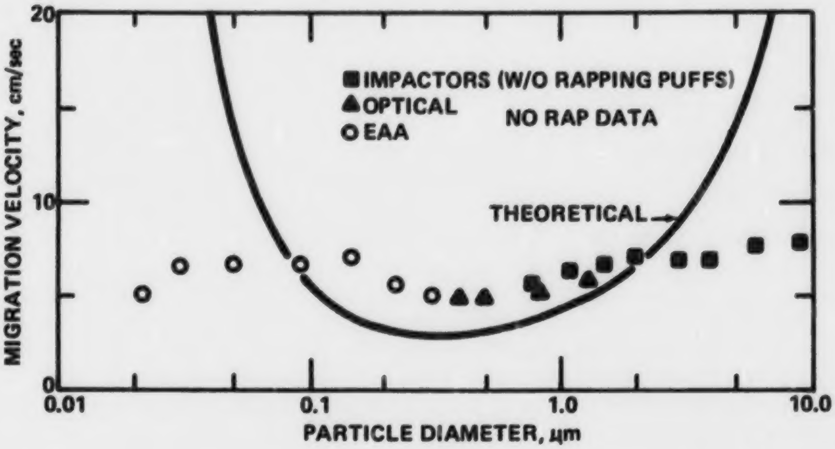

Figure 20. Effective migration velocity vs particle diameter

a mechanical collector so that the inlet size distribution consisted of finer particles with an MMD of approximately 3 μm. The fly ash under collection had a high resistivity resulting in limitations on the current density. The measurements were performed with no rapping so that reentrainment should be minimized. The ideally predicted fractional efficiency and migration velocity curves lie below the experimental data for particle sizes in the 0.06-2.5 μm range. Over this size range the theoretical curve has the same shape as the experimental data with the minimum occurring at about 0.4 μm in both cases. The overall mass efficiency predicted by the model is 99.7% as compared to the measured value of 99.9+%.

Figures 21 and 22 show results obtained from a study of a "cold" pilot precipitator operating at various SCA values and current densities ranging from 7 to 40 nA/ft^2. The experimental results were obtained from inlet and outlet measurements with mass trains using in-stack filters. Particle size distribution measurements made at the pilot precipitator inlet with inertial impactors indicated that a typical fly ash distribution was obtained and that for particle diameters below about 5 μm, the cumulative mass loadings obtained in the main duct were within the range of those obtained at the pilot plant inlet.

Both Figures 21 and 22 indicate that in order to match the test data with the predicted model results at comparable current densities, it is necessary to either assume a poor gas velocity distribution ($\sigma = 0.50$) or relatively large losses due to reentrainment and gas bypassage. The bypassage and reentrainment losses are assumed to occur over three effective stages, since the pilot unit consisted of three sections. Gas flow measurements with a thermal anemometer indicated that at this installation gas flow quality was poor ($\sigma \geq 0.46$), and that gas sneakage was estimated to be no smaller than 8% and no greater than 30% of the total gas flow. Resistivity data from in-situ measurements and voltage-current curves from the pilot unit power supplies indicated that the current densities of 11 and 32 nA/cm^2 could be sustained without experiencing electrical breakdown of the dust layer deposited on the collection electrodes under the test conditions.

Figure 23 shows results obtained from the analysis of a "hot" full-scale precipitator having an SCA of 430 ft^2/(1000 ft^3/min) and current density of 35 nA/cm^2. The experimental results were obtained from inlet and outlet size distribution measurements obtained using inertial, optical, and diffusional sizing techniques. For this installation, the fractional efficiency curve obtained from the measurements is lower than the theoretical curve obtained from the mathematical model. Although the average electrical operating conditions for this unit are used in the model, some of the electrical readings for individual sets were characterized by anomalously low current and voltage levels,

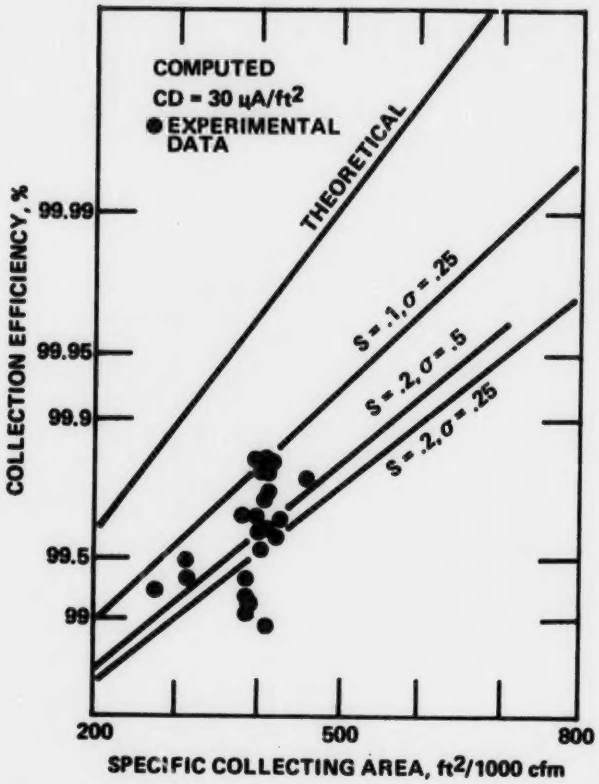

Figure 21. Computed and measured data from pilot precipitator

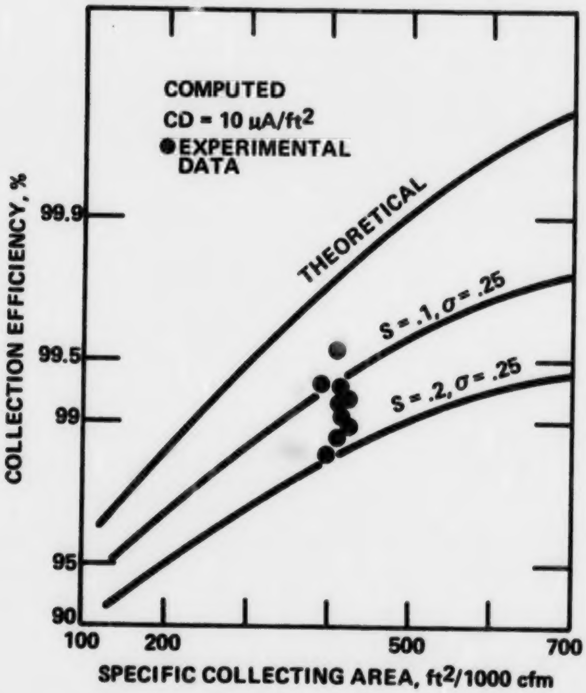

Figure 22. Computed and measured data from pilot precipitator

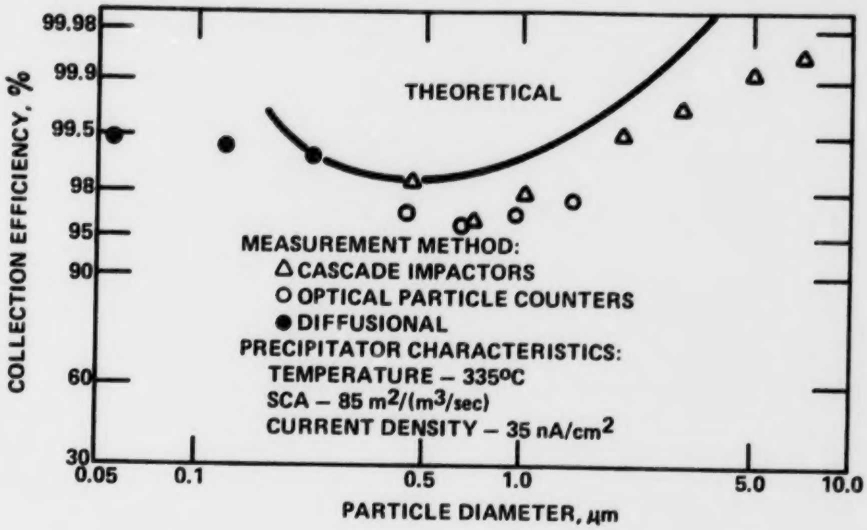

Figure 23. Comparison of measured and computed fractional collection efficiencies

suggesting the possibility of electrode misalignment. This is a contributing factor in the disagreement between theoretical and measured results, since the average electrical conditions will not adequately represent the effects of low voltages and current in individual sets on collection efficiency. The theoretically predicted overall mass efficiency was 99.9% at the indicated condition, and the average measured collection efficiency was 99.3%. If a gas velocity distribution standard deviation of 0.25 is assumed, sneakage and reentrainment losses of 10 to 20% over three stages are required to reconcile the computed and measured mass efficiency.

CONCLUSIONS

Comparisons of theoretically calculated collection efficiencies with laboratory data obtained under essentially idealized conditions indicate that the mathematical model gives good agreement with experiments for particle sizes from 0.55 to 2.5 µm in diameter over a wide range of current densities at gas velocities of 0.72 and 1.37 m/sec, with a 12.7-cm plate spacing. For a 19.05-cm plate spacing and gas velocity of 1.46 m/sec, the model predicts ideal fractional efficiency curves which lie below the measured data for current densities greater than 25 nA/cm^2. This discrepancy may at the present be attributed to unmodelled concentration gradients which were measured for 0.3, 0.5, and 1.0 µm diameter particles under these conditions.

Comparisons of model predictions with field data obtained from full-scale and pilot precipitators indicate that the theory generally gives a good prediction of overall mass collection efficiency although, in certain cases, the fine portion of the fractional efficiency curve lies below the measured data. The laboratory measurements obtained to date indicate that the cases in which the model underpredicts fine particle collection may be due to concentration gradients which exist under certain conditions.

Considering the broad range of laboratory and field data with which the theory has been compared, it can be concluded that the mathematical model provides a basis for indicating performance trends caused by changes in specific collecting area, electrical conditions, and particle size distribution, provided that back corona does not exist. Current density, applied voltage, and the particle size distribution are the most important variables in the calculation of overall mass collection efficiency for a given specific collection area. The theoretical calculation of ideal overall collection efficiency of polydisperse particulate in an electrostatic precipitator generally gives results higher than those obtained from performance measurements on coal-fired power boilers. Corrections to the idealized or theoretical collection efficiency to estimate the effects of non-uniform gas flow, rapping reentrainment, and gas bypassing the electrified sections reduce the overall values of calculated efficiency to the range of values obtained from field measurements. These calculations suggest that the theoretical model may be used as a basis for quantifying performance under field conditions if sufficient data on the major nonidealities become available.

ACKNOWLEDGEMENTS

The work described in this paper was supported under contracts with the Environmental Protection Agency, the Electric Power Research Institute, and the Tennessee Valley Authority.

REFERENCES

1. Gooch, J. P., and N. L. Francis. A Theoretically Based Mathematical Model for Calculation of Electrostatic Precipitator Performance. J. Air Pollution Control Assoc. 25 (2):108-113, 1975.

2. Gooch, J. P., J. R. McDonald, and S. Oglesby, Jr. A Mathematical Model of Electrostatic Precipitation. EPA-650/2-75-037. NTIS PB 246188/AS, U.S. Environmental Protection Agency, Washington, D.C., 1975. 162 pp.

3. Gooch, J. P., and J. R. McDonald. Mathematical Modelling of Fine Particle Collection by Electrostatic Precipitation. 1975 Air Symposium (in press) Amer. Inst. Chem. Eng.

4. Leutert, G., and B. Böhlen. The Spatial Trend of Electric Field Strength and Space Charge Density in Plate-Type Electrostatic Precipitators. Staub 32 (7):27, 1972.

5. Smith, W. B., and J. R. McDonald. Calculation of the Charging Rate of Fine Particles by Unipolar Ions. J. Air Pollution Control Assoc. 25 (2):168-172, 1975.

6. Hewitt, G. H. The Charging of Small Particles for Electrostatic Precipitation. Trans. Amer. Inst. Elec. Eng. 76, Part I:300-306, 1957.

7. Deutsch, W. Ann. Phys. (Leipzig) 68:335, 1922.

8. White, H. J. Industrial Electrostatic Precipitation. Addison-Wesley, Reading, Mass., 1963.

9. Preszler, L., and T. Lajos. Uniformity of the Velocity Distribution upon Entry into an Electrostatic Precipitator of a Flowing Gas. Staub 32 (11):1-7, 1972.

PAPER 7

TECHNIQUES FOR CONDITIONING FLY ASH

Edward B. Dismukes
Southern Research Institute

ABSTRACT

Conditioning of fly ash is discussed in connection with electrostatic precipitators from several points of view: the purposes served, the types of chemicals used, and their mechanisms of action. Major emphasis is given to resistivity modification with sulfur trioxide and other agents. Comments are also made on alternative conditioning mechanisms: increasing the cohesiveness of deposited fly ash to minimize reentrainment and improving the electrical properties of flue gas to increase the efficiency of collection.

INTRODUCTION

Conditioning of fly ash usually involves the injection of a chemical (most often sulfur trioxide) into flue gas to control the electrical resistivity of the ash and improve its collection in an electrostatic precipitator. Currently, however, the term is assuming a much broader meaning, for conditioning involves processes other than resistivity modification. This paper discusses conditioning to achieve resistivity modification, but it also deals with two other purposes of conditioning: to increase the cohesiveness of fly ash particles deposited in a precipitator and to improve the electrical properties of the gas stream flowing between discharge wires and collection electrodes.

RESISTIVITY MODIFICATION: TREATMENT OF ASH FROM LOW - SULFUR COAL

Conditioning By Sulfur Trioxide

Origin of High Resistivity. The production of fly ash with a high electrical resistivity is the usual—but not inevitable—consequence of the combustion of a low-sulfur coal. The problem of high electrical resistivity is clearly associated with the combustion of Western coals containing around 0.5% of sulfur. It is widely assumed to occur when Western coals of relatively low-sulfur content (often around 1%) are substituted for the more prevalent Eastern coals containing 3 to 4% sulfur. However, in terms of the frequently quoted upper limit of acceptable resistivity values (about 1 x 10^{10} ohm-cm), ash from Eastern coals presents less of a difficulty than ash from Western coals. There are at least two factors that control resistivity: one is the sulfur content of the coal, and the other is the overall elemental composition of the fly ash.

Sulfur occurs in coal as organic compounds and as inorganic compounds—notably pyrite and sulfate salts. Regardless of the distribution of the sulfur in these different forms, however, the predominant product of combustion in the boiler is sulfur dioxide. From a thermodynamic point of view, sulfur dioxide would be the only product found in the boiler, and sulfur trioxide (or, more exactly, sulfuric acid) would be the only product present when the flue gas reaches a temperature around 150° C where electrostatic precipitators normally operate,[1] as shown in Table 1. Thermodynamics evidently is the process-limiting factor in the boiler but not toward the end of the flue-gas train, for the kinetics of oxidation does not allow more than a small fraction of the sulfur oxides to appear as sulfur trioxide.

TABLE 1. EQUILIBRIUM DISTRIBUTION OF OXIDIZED FORMS OF SULFUR AT VARIOUS GAS TEMPERATURES [a]

Temperature, °C	Relative concentrations, %, of sulfur compounds		
	SO_2	SO_3	H_2SO_4 [b]
1400	99.7	0.3	0.0
1000	97.6	2.4	0.0
800	88.7	11.3	0.0
600	42.2	57.7	0.1
500	12.3	87.3	0.4
400	1.6	94.8	3.6
300	0.1	59.3	40.6
200	0.0	6.5	93.5
100	0.0	0.0	100.0

a. Calculated from the data in JANAF Tables,[1] assuming concentrations of oxygen and water vapor equal to 4% and 10% by volume, respectively.

b. The maximum absolute concentration of each compound is sharply limited below 300° C as a result of the condensation of the predominant compound, H_2SO_4, in a binary H_2SO_4-H_2O liquid mixture.

Even so, the small fraction of the total of sulfur oxides occurring as sulfur trioxide at 150° C can be sufficient to lower the resistivity of ash to an acceptable range. Obvious factors of importance are the available concentration of sulfur dioxide (roughly proportional to the amount of sulfur in the coal) and the extent of oxidation to sulfur trioxide. A less obvious factor is the nature of the interaction of sulfur trioxide with the fly ash. We are only beginning to gain answers to this last question, but this much seems clear: sulfur trioxide and water vapor are jointly adsorbed or condensed on the surfaces of fly ash particles, and either vapor assists in the deposition of the other. The resulting acid may remain essentially intact in a chemical sense, producing a conductive surface layer on an otherwise poorly conducting substrate. The acid may, however, react with basic constituents of the ash and thus undergo conversion to a nonconducting layer of sulfate salts. Calcium oxide, a fairly abundant component of ash from Western coals, is a probable cause of acid neutralization and its nullification as a conductor. Thus, two coals similar in sulfur content may ultimately produce similar concentrations of sulfur trioxide, but the one producing a more alkaline ash is likely to have a substantially higher resistivity.

Conditioning by Naturally Occurring Sulfur Trioxide. Some of the concepts outlined above were verified[2] in a study of the natural conditioning of fly ash in a plant burning an Eastern coal containing about 2% of sulfur and producing an ash in which the total percentage of alkaline oxides was low, about 7% by weight (4.2% as the alkali metal oxides Li_2O, Na_2O, and K_2O, and 2.4% as the alkaline earth oxides MgO and CaO). Experimental data showing fly ash resistivity in a range of temperatures at the precipitator inlet are shown in Figure 1. The upper curve shows the expected maximum—in this instance, around 175° C—that occurs as the result of the transition between volume conduction at high temperatures and surface conduction at low temperatures. The lower segment of a different curve indicates the effect produced by injecting water vapor in an amount sufficient to double the normal level—i.e., increasing the concentration of water vapor from 7% to 14% by volume.

Other experimental data of value in explaining the observed changes in resistivity are given in Figures 2 and 3. Measured concentrations of sulfur trioxide in gas samples taken upstream and downstream from the air preheater indicate the occurrence of two effects: (1) the thermodynamically predicted increase in the oxidation of sulfur dioxide to sulfur trioxide as the gas temperature falls across the air heater (but short of the extent predicted for equilibrium) and (2) the loss of sulfur trioxide from the gas phase, a phenomenon aided by either the lowering of temperature or the injection of water vapor. Measurements of slurries of fly ash in water show corresponding increases in the acidity of the ash (decreases in pH) and in the sulfate content of the ash.

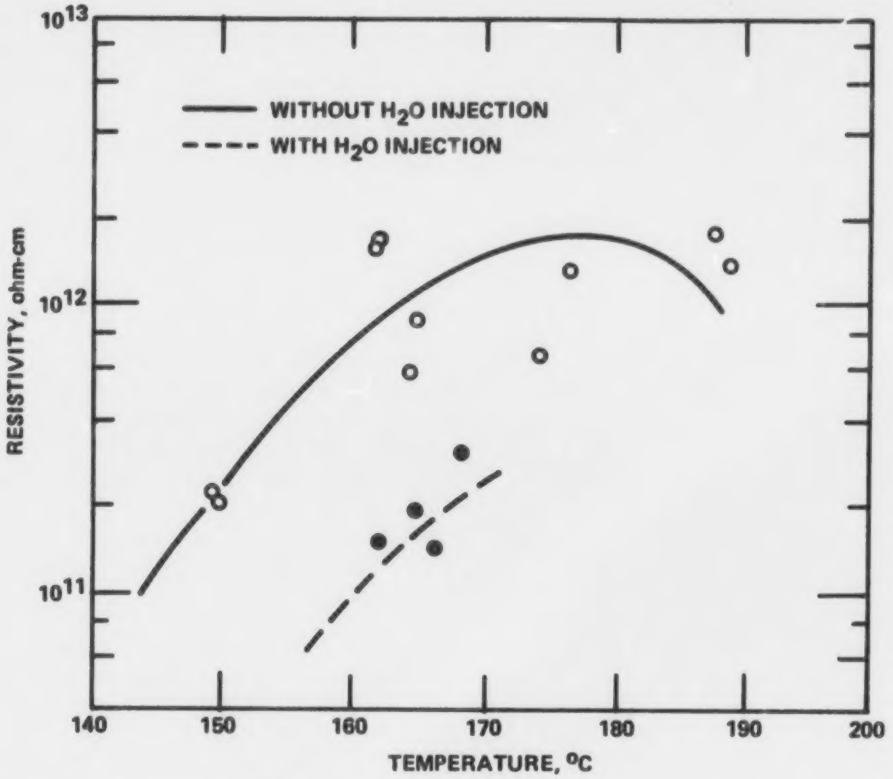

Figure 1. Electrical resistivity of fly ash as a function of temperature or water vapor concentration

Conditioning by Injected Sulfur Trioxide. In plants where the naturally available concentration of sulfur trioxide is too low—in an absolute sense, as the result of a low sulfur concentration in the coal or, in a relative sense, as the result of reaction with a highly alkaline ash—the conditioning agent can be introduced by an artificial process. Sources of sulfur trioxide are vapor generated by vaporizing the liquid form of this compound, by vaporizing sulfuric acid, or by oxidizing sulfur dioxide gas on a vanadium pentoxide catalyst. In the last-mentioned type of process, sulfur dioxide may be purchased as the liquid compound under pressure and evaporated prior to conversion, or it may be generated at the site in a burner for elemental sulfur. The molecular composition of vapors injected in the various systems depends not only on the source material but on the temperature and water vapor concentration in the dilution air. The vapor may be sulfur trioxide per se, or it may be sulfuric acid. It is of little consequence which substance is injected for, once injected, either compound will occur only as sulfuric acid vapor in the gas stream. This statement stems from the rapid rate of the gas phase reaction $SO_3 + H_2O \longrightarrow H_2SO_4$ under typical flue-gas conditions (temperatures around 150° C and water-vapor concentrations around 7% to 10% by volume), to approach equilibrium conditions as indicated in Table 1.

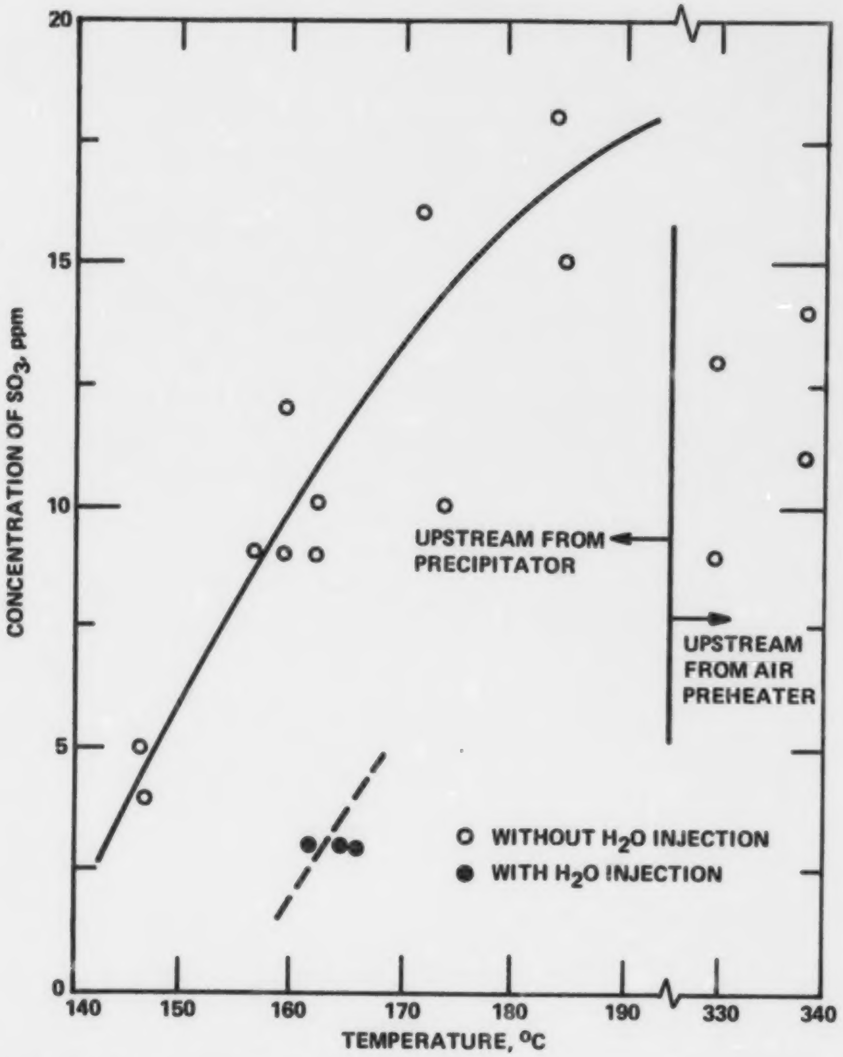

Figure 2. Concentration of sulfur trioxide as a function of sampling location or temperature

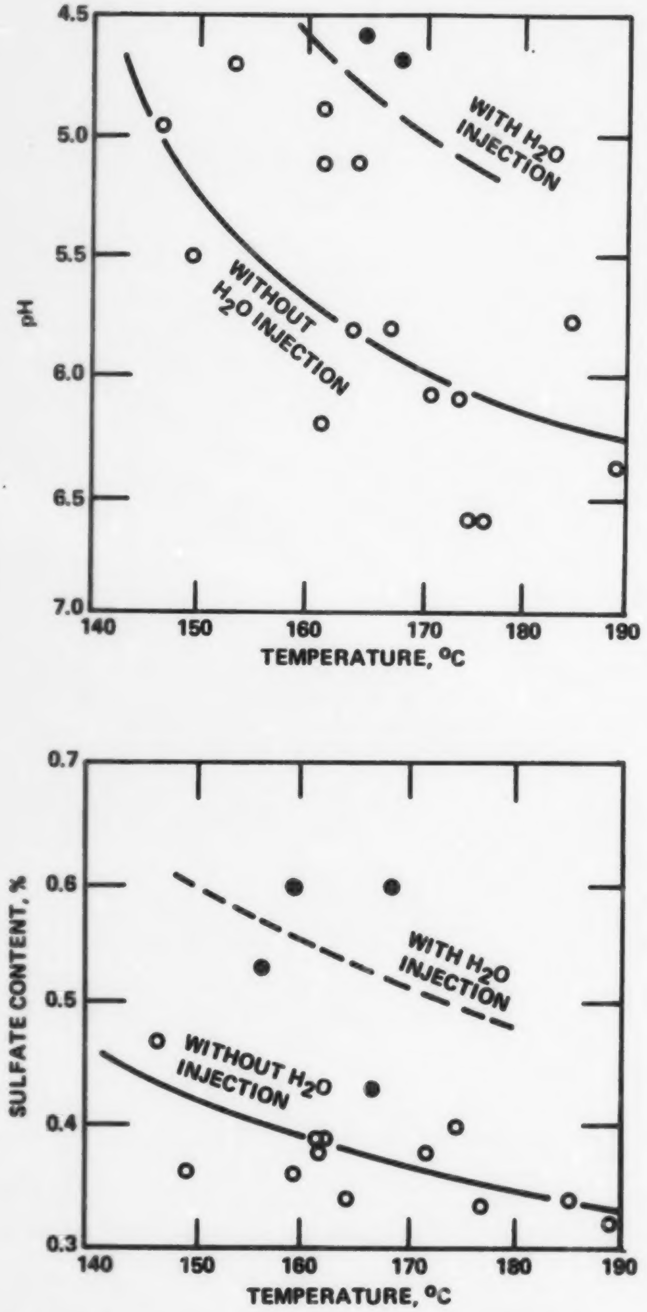

Figure 3. Acidity and sulfate content of fly ash as functions of temperature and water vapor concentration

Investigators at the Institute have studied the results achieved by the injection of sulfuric trioxide or sulfuric acid in a number of full-scale power plants.[2] We have considered both practical and theoretical questions and obtained answers that, to us, seem generally satisfactory, subject to the limitations imposed by the characteristics of plants available for study.

One question considered is whether there is any high resistivity ash that cannot be suitably conditioned with sulfur trioxide. We believe that the answer is no, but we do recognize that the quantity of conditioning agent required varies with such factors as the chemical composition of the ash and the gas temperature. The importance of these factors is illustrated in Figure 4, which gives the results obtained with ashes characterized broadly as acidic, neutral, or alkaline at temperatures varying from 110 to 160° C. If a resistivity of about 1 x 10^{10} ohm-cm is required, more sulfur trioxide is required if the ash is alkaline or if the gas temperature is high.

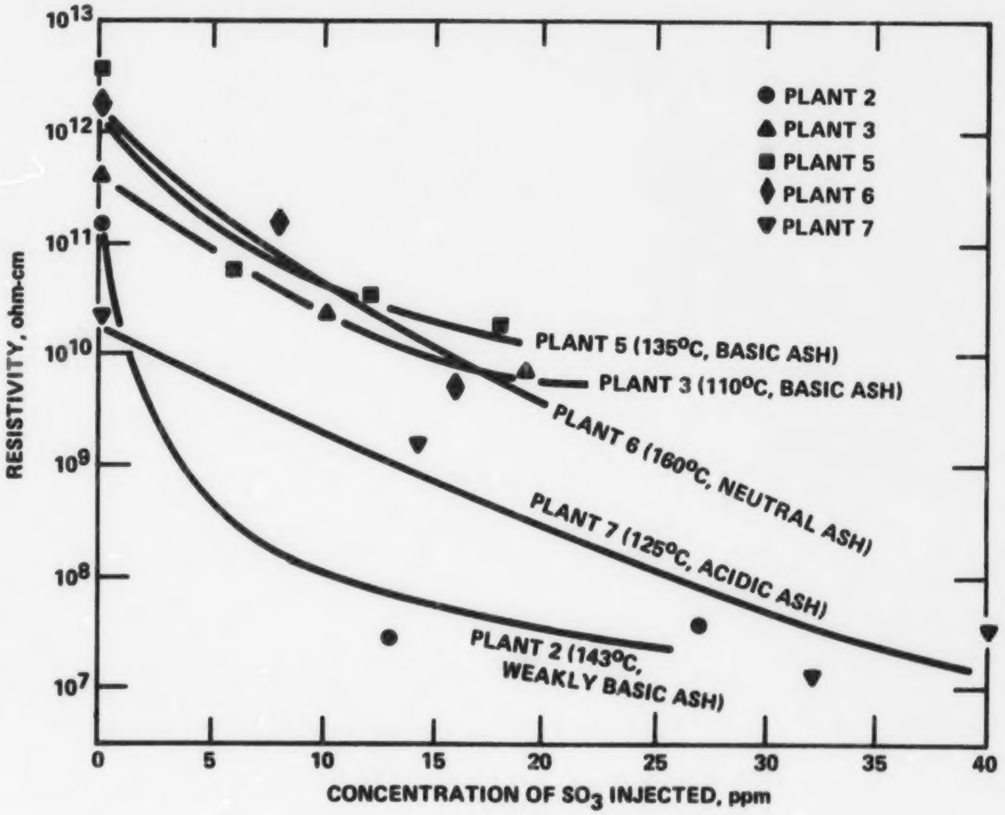

Figure 4. Resistivity as a function of the concentration of injected sulfur trioxide

Another question considered is whether the efficiency of conditioning is markedly affected by the choice of location in the flue-gas train where the agent is added. Our studies have included plants with and without mechanical collectors to aid precipitators in the collection of fly ash; they have included plants with injection ahead of the mechanical collectors, between the mechanical and electrostatic collectors, and ahead of precipitators operating without mechanical collectors. No important change in the efficiency of conditioning can be attributed to these variations in plant operation. We have not had experience with injection ahead of the air preheater, which would be attractive from the point of view of ensuring uniform introduction of sulfur trioxide or sulfuric acid as a vapor.

Another question was whether a choice is to be made among the different types of injection systems (based on injection of sulfur trioxide directly, as catalytically oxidized sulfur dioxide, or as sulfuric acid). We have not recognized any change in the efficiency of conditioning that we believe to be fundamentally attributable to the type of system. We did have experience with one acid-injection system that was inefficient as the apparent result of excessive condensation near the point of injection.

A fourth matter of practical interest was whether a significant fraction of the injected sulfur trioxide is lost through the stack. A close examination of this point was made in only one plant where conditions favored a stack loss, as the result of the acidic character of the ash and incomplete removal of the conditioning agent. Figure 5 compares the measured concentrations of sulfur trioxide with and without injection as a function of distance across the outlet duct at the precipitator or, in other words, as a function of the gas temperature (a variable across the duct as a result of the influence of the Ljungstrom air heater). The difference in the areas under the two concentration curves corresponds to an average concentration of 5 ppm, about 30% of the 14 ppm injected. An increase in the sulfur trioxide concentration by 5 ppm would produce a concentration of condensed sulfuric acid of 20 $\mu g/m^3$ (about 0.01 gr/ft^3) in the relatively cool plume from the stack—a significant level in terms of "clear stack" concentration levels for fly ash. We recognize that, under typical conditions with an alkaline ash from low-sulfur Western coals, the stack loss of sulfur trioxide will be lower and perhaps insignificant. But it is not a matter that can be ignored.

A theoretical question of some importance is: What is the mechanism of conditioning? One facet of this question is whether deposition of the agent into ash occurs by adsorption or condensation. Our conclusion is that adsorption of vapor above the acid dew point can certainly occur, although condensation may also occur if the gas is below the dew point. This conclusion is based on a prediction of dew points from thermodynamic data that are applicable only if the condensed vapor occurs as a binary liquid mixture of sulfuric acid and water. The possibility that reaction of vapors with alkaline fly ash constituents may take precedence over condensation makes prediction of dew points on this basis uncertain; if such a reaction occurs, however, the deposition of vapors would be even more likely to occur as an adsorption process.

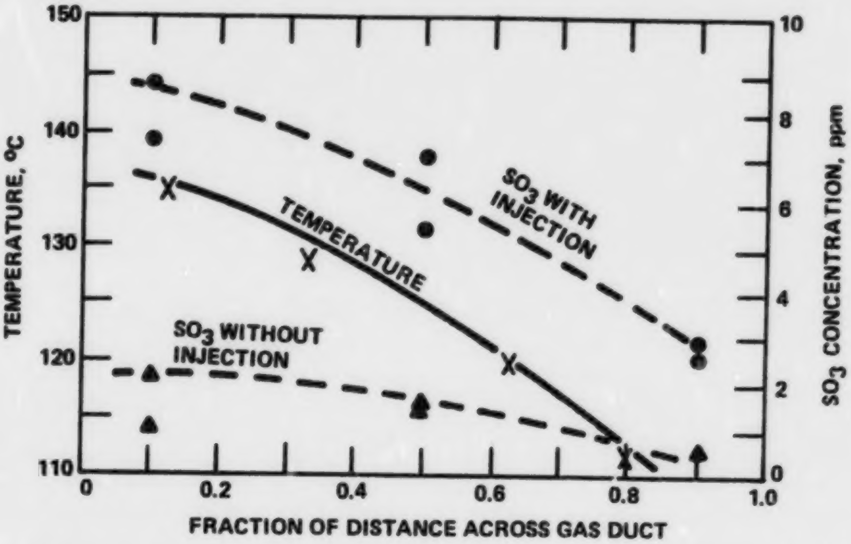

Figure 5. Concentration of sulfur trioxide as a function of gas temperature at the outlet of a precipitator

Conditioning By Other Agents

No discussion of conditioning of high-resistivity fly ash would be complete without mention of the role of ammonia, although the subject must be approached with caution. It appears that this agent sometimes is effective by other mechanisms of conditioning, as discussed subsequently, and that its ability to alter resistivity is not clear-cut.

The value of ammonia as a conditioning agent for one type of suspended particulate matter—catalyst dust in a petroleum refinery, rather than fly ash from a coal-burning boiler—has been known for many years. J. F. Chittum of the former Western Precipitation Company was one of the pioneers in the use of ammonia. He believed that ammonia was of greater value than sulfur trioxide in treating an acidic dust, such as the catalyst material in a refinery.[3]

We may very well ask: What can be expected of ammonia as a conditioning agent for fly ash? Suppose we accept Chittum's premise that the use of ammonia and not sulfur trioxide is indicated if the ash is acidic. We would then have to imagine a fly ash that is at once acidic and high in resistivity. The experience and interpretation of ash chemistry leads to the viewpoint that these may be mutually exclusive factors. None of the constituents of fly ash except adsorbed sulfur trioxide is sufficiently acidic to have a strong affinity for ammonia, which is a rather weakly basic compound. But, if adsorbed sulfur trioxide is present, how can resistivity be high?

These are ideas that will have to change if enough clear-cut evidence of a resistivity effect by ammonia becomes available. There are data available either directly indicating that ammonia lowers resistivity or indirectly indicating that ammonia has this effect, such as changes in precipitator voltages and currents that are most easily explained as a result of lowered resistivity. It does not appear, however, that conclusive evidence of lowered resistivity with ammonia conditioning is now in existence.

What about other agents? Sodium is an example that we believe to have clear-cut significance in lowering resistivity. The importance of sodium first became evident in a comparison of resistivity values of ashes varying naturally in percentages of sodium oxide. It was later confirmed in trials of various sodium compounds (notably the carbonate) as additives to coal being fed to the boiler of a power plant. Our experience on the use of sodium is entirely restricted to boiler additions (not flue gas treatment),[4] but others have reported the use of sodium as a flue gas additive.[5]

What about some of the proprietary agents now on the market? For some of these agents, the claim is made that they function as resistivity modifiers, but the data upon which such claims are made are not often, if ever, given. From what is known about the compounds present in the proprietary agents and what has been published from laboratory studies of the compounds, their functioning as resistivity modifiers is not an unreasonable assumption.[6] One of the compounds identified is sulfamic acid; another is ammonium sulfate. It is perhaps noteworthy that each of these compounds is, in theory at least, derived from sulfur trioxide and ammonia. From a constitutional point of view, sulfamic acid is equivalent to these constituents in a 1:1 mole ratio ($HO\text{-}SO_2\text{-}NH_2 = SO_3 + NH_3$). Similarly, ammonium sulfate or $(NH_4)_2SO_4$ is equivalent to sulfur trioxide, ammonia, and water in the molar proportions $SO_3:NH_3:H_2O = 1:2:1$. Thermal decomposition of either compound can thus produce both sulfur trioxide and ammonia as gases along with further breakdown products, such as SO_2 and N_2.

RESISTIVITY MODIFICATION OF ANOTHER TYPE: TREATMENT OF ASH FROM HIGH-SULFUR COAL

It is important to realize that the problem of excessively low resistivity occasionally exists, although it is less widely recognized than the problem of high resistivity. It occurs in the burning of a high-sulfur coal, and it conceivably may occur if ash from a low-sulfur coal is overtreated with sulfur trioxide. If resistivity is low—below 1×10^7 ohm-cm—the practical consequence may be excessive reentrainment, owing to the inadequacy of the electrical force across the ash deposit for maintaining the physical integrity of the deposit under the influence of scouring or electrode rapping.

In view of the likelihood that low resistivity can be attributed to an excessive amount of sulfur trioxide, it is reasonable to try ammonia as an agent for chemically neutralizing the acid. From a theoretical point of view, one must be troubled over the prospects of increasing resistivity sufficiently by simply converting sulfuric acid to ammonium sulfate. The conductivity of ammonium sulfate in water is lower than that of sulfuric acid, but the ratio of conductivities is roughly 1:4 and thus not as great as one order of magnitude. A study of the mechanism of ammonia conditioning under circumstances where it apparently gave the desired resistivity change failed to confirm the mechanism assumed.

REENTRAINMENT CONTROL: INCREASING THE COHESIVENESS OF PRECIPITATED ASH

If, as just discussed, the resistivity of ash from a high-sulfur coal can be increased, one has a means for minimizing reentrainment. If one is unable to make any significant change in the resistivity and thus in the electrical force needed to maintain physical integrity of deposited ash, he has the option of increasing mechanical forces that bind individual particles together.

Dalmon and Tidy[7] recognized the value of sulfur trioxide as an agent for increasing the binding forces between particles of fly ash and unburned carbon. Carbon is a highly conductive material (relatively speaking) and is especially difficult to retain after it is electrostatically precipitated, except by means of cohesive forces. The method used by Dalmon and Tidy for demonstrating the reported activity of sulfur trioxide involved packing a bed of ash and carbon in a bed with one end detachable from the other and determining the mechanical force needed to rupture the bed of particles.

Investigators at the Institute[2] obtained evidence in one plant for a similar effect of sulfur trioxide, although in this instance there was no indication of excessive carbon being the cause of excessive reentrainment. In this plant, conditioning by sulfur trioxide had been adopted as a measure for restoring the original efficiency of a precipitator after a change had been made to burn coal with a lower sulfur content. Our data failed to indicate that resistivity was a problem; the resistivity of untreated ash was found to be about 1 x 10^{10} ohm-cm, and the value with 14 ppm of sulfur trioxide injected was about 1 x 10^{9} ohm-cm. One might have expected increased reentrainment as a result of the change in resistivity. In actuality, however, we found that injection of sulfur trioxide increased the precipitator efficiency markedly. Data in Table 2 show a parallel between the effects achieved by injecting sulfur trioxide and by discontinuing electrode rapping. Our conclusion, therefore, is that the principal mechanism of conditioning in the circumstances investigated was increased cohesiveness of the fly ash and decreased rapping reentrainment.

TABLE 2. REDUCTION OF RAPPING REENTRAINMENT BY SULFUR TRIOXIDE

SO_3 injected, ppm	Rapping	Precipitator efficiency, %
0	Normal	69.7
	Off	82.0
14	Normal	93.5
	Off	96.8

We also found evidence that ammonia injection suppressed rapping losses in plants burning high-sulfur coal.[2] A reproduction of a chart recording the signal from a transmissometer at the precipitator outlet in one of these plants is given in Figure 6. After ammonia injection was started, the intensity of rapping puffs was slowly suppressed. After ammonia injection was discontinued, the intensity of rapping puffs gradually increased again. The findings at the plant in question would not be complete without mention of other experimental results: no measurable effect of ammonia on the resistivity of the ash (about 1 x 10^{9} ohm-cm) was evident, but significant effects of ammonia on the electrical properties of the gas stream were discerned, as discussed later.

It appears that triethylamine, which has recently been found a promising agent in Australia,[8] may act in the manner described for ammonia but even more effectively. Both agents are basic, but the basic strength of triethylamine is greater and the reported stronger effect of triethylamine seems logical. It must be recognized that the Australian workers have concluded that triethylamine acts as an "agglomerating" agent, which we interpret to mean an agent that increases particle size before precipitation occurs. However, if this mechanism of conditioning does occur, specific evidence for the process does not appear to have been obtained.

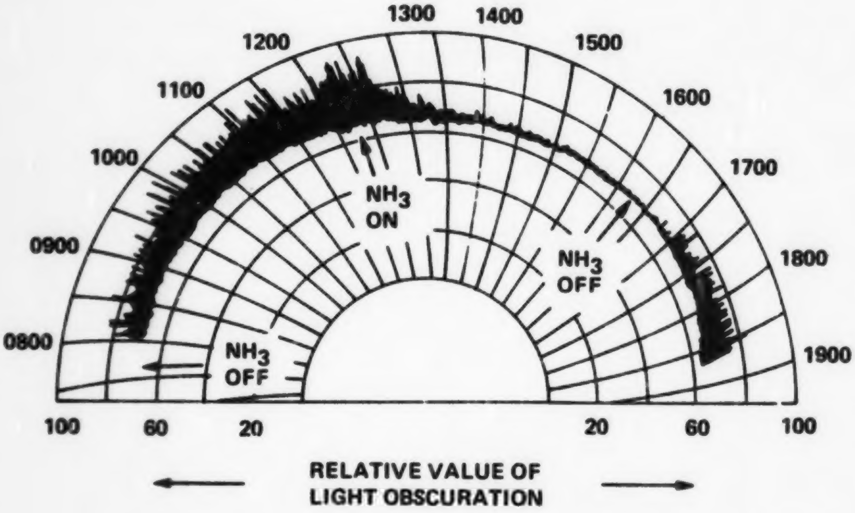

Figure 6. Reduction of rapping reentrainment by ammonia

ALTERATION OF ELECTRICAL PROPERTIES OF THE GAS STREAM: THE SPACE-CHARGE EFFECT

Conditioning through this mechanism has been observed in several power plants where ammonia was used for conditioning fly ash.[2,9] Two of the plants investigated burned high-sulfur coals and produced fly ash with resistivities around 1 x 10^8 to 1 x 10^9 ohm-cm. Another two plants burned so-called low-sulfur coals from Eastern mines, but in these instances the sulfur level was around 1.0% and measured resistivities were about 1 x 10^{11} ohm-cm. Moreover, significant concentrations of sulfur trioxide were found in the flue gas—around 2 to 5 ppm, in contrast to usually undetectable levels (less than 1 ppm) in plants burning 0.5%-sulfur Western coals.

No measurable effect of ammonia on resistivity could be detected. However, the gradual change in the intensity of rapping puffs, indicating an increase in the cohesiveness of deposited ash, was detected clearly in one plant. Moreover, there were other changes that were virtually instantaneous. One effect was a change in the precipitator electrical conditions in the direction consistent with a decrease in the mobility of charge carriers in the gas phase, as shown in Figure 7. Another phenomenon that occurred rapidly was a marked enhancement in the concentration of suspended fine particles at the precipitator inlet. Coupled with these effects were pronounced decreases in the concentration of sulfur trioxide as a constituent of the gas stream.

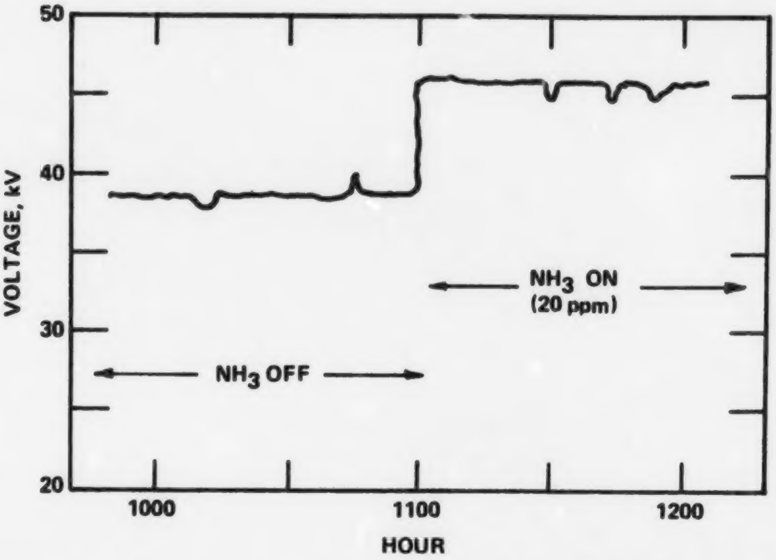

Figure 7. Rapidity of the effect of ammonia on the voltage of a precipitator

Taken together, the observations suggested a chemical reaction between the injected ammonia and the normally present sulfur trioxide (actually, the vapor of sulfuric acid) to produce a fume of fine particles of ammonium sulfate or perhaps the bisulfate, as shown by the following equations:

$$2NH_3(\text{gas}) + H_2SO_4(\text{gas}) \longrightarrow (NH_4)_2SO_4(\text{solid})$$

$$NH_3(\text{gas}) + H_2SO_4(\text{gas}) \longrightarrow NH_4HSO_4(\text{solid or liquid})$$

The bisulfate in the second equation is shown as either solid or liquid; the transition point is about 144° C.

What is the likelihood of a similar space-charge effect in a plant burning a typical low-sulfur Western coal, and what would be the value of such an effect? The reaction of injected ammonia with normally occurring sulfur trioxide would generally be less likely to occur in such a plant because of the insignificant quantity of sulfur trioxide present. However, much higher concentrations of ammonia than are generally used for conditioning—say, 100 to 200 ppm—could react with trace concentrations of sulfur trioxide (less than 1 ppm). Concentrations of ammonia in this range, it may be noted, are used to advantage with high resistivity Australian ashes. Such concentrations of ammonia may also react with sulfur dioxide to produce fine particles of ammonium sulfite, although this does not appear likely from the thermodynamic data now available.

What about the possible value of the space-charge effect if it does occur? Possibly this effect could suppress the abnormal currents that are encountered in instances of back corona. Data published by Watson and Blecher in Australia some years ago[10] gave evidence of back corona suppression by ammonia, at a rate rapid enough to be attributed to a space-charge effect.

PERSPECTIVE ON THE FUTURE OF CONDITIONING

Chemical conditioning is only one of the alternatives open to the power industry in dealing with difficult fly ash. The technology of conditioning has been tried far more often on an experimental basis than it has been adopted for full-time continuous use. When permanent installations for conditioning have been made, usually they have been intended to upgrade the performance of an existing precipitator, not to ensure adequate performance by a new collector.

A major factor leading to this policy has been the unpopularity of conditioning with sulfur trioxide, mainly as a result of operating difficulties with injection systems for this agent and hazards associated with the compound. Another factor has been the frequent lack of success with ammonia and other flue gas additives as alternative agents and the absence of an understanding of the mechanisms by which they operate.

Some of the needs that must be met if conditioning is to have a continuing or expanding application are: (1) development of new agents that are attractive on the basis of cost and convenience and (2) research on the mechanisms of action by various agents that will give a more dependable basis for predicting performance. Coupled with these developments, there must be a careful diagnosis of the specific problems in individual power plants that cause inefficient precipitation and a recognition of the fact that conditioning cannot rectify all difficulties. In other words, chemical companies, equipment vendors, and utility companies must all accept their responsibilities if, in the long range, conditioning is to serve the immediate interests of all concerned.

One final point to be made is that research must be done to ensure that conditioning has a favorable overall impact on the environment. Regulatory agencies will not, in the long run, tolerate conditioning as a means of reducing fly ash emissions if it leads to other undesirable effects that can be avoided through the adoption of some other corrective measure.

REFERENCES

1. Stull, D.R., and H. Prophet (ed.). JANAF Thermochemical Tables. Washington, National Bureau of Standards, 1971. Unnumbered pages listed in this alphabetical order: H_2O, H_2O_4S, O_2S, and O_3S.

2. Dismukes, E. B. Conditioning of Fly Ash with Sulfur Trioxide and Ammonia. EPA-600/2-75-015, NTIS PB 238922/AS, U. S. Environmental Protection Agency, Washington, D.C., 1975. 50 pp.

3. Chittum, J.F. Western Precipitation Corporation, Los Angeles, California. Unpublished data from studies in 1942-1945.

4. Bickelhaupt, R.E. Electrical Volume Conduction in Fly Ash. J. Air Pollution Control Assoc. 24 (3): 251-255, 1974.

5. Selle, S.J., and L.L. Hess. Factors Affecting ESP Performance on Western Coals and Experience with North Dakota Lignites. Symposium on Particulate Control in Energy Processes. San Francisco, May 11-13, 1976.

6. Dismukes, E.B. Conditioning of Fly Ash with Sulfamic Acid, Ammonium Sulfate, and Ammonium Bisulfate. EPA-650/2-74-114, U. S. Environmental Protection Agency, Washington, D.C., 1974. 51 pp.

7. Dalmon, J., and D. Tidy. The Cohesive Properties of Fly Ash in Electrostatic Precipitation. Atmos. Environ. (Oxford, England) 6 (2): 81-92, 1972.

8. Potter, E.C., and C.A.J. Paulson. Improvement of Electrostatic Precipitator Performance by Carrier Gas Additives. Chem. Ind. (London) 1974: 532-533, July 6, 1974.

9. Dismukes, E.B. Conditioning of Fly Ash with Ammonia. J. Air Pollution Control Assoc. 25 (2): 152-156, 1975.

10. Watson, K.S., and K.J. Blecher. Further Investigation of Electrostatic Precipitators for Large Pulverized Fuel-Fired Boilers. Air Water Pollution Int. J. (Oxford, England) 10 (9): 573-583, 1966.

PAPER 8

RAPPING REENTRAINMENT STUDIES

Herbert W. Spencer, III
Southern Research Institute

ABSTRACT

The results of experimental investigations of rapping reentrainment in four electrostatic precipitators connected to coal-fired boilers and in a large pilot electrostatic precipitator are reported. The objective of the studies was quantification of rapping reentrainment in terms of the percentage and particle size distribution of the reentrained particulate.

Impactors and mass trains were used to measure separately rap and nonrap emissions. An extraction real time optical particle sizing system was also used to determine the percentage of rapping emissions in five particle size bands. This system also supplied data on the temporal variations of the emissions due to rapping. During the pilot-scale test and during one of the field tests, the rapping emissions were observed to depend on the time interval between raps. Rapping emissions decreased from 53% to 18% of total emissions for the pilot test as the time interval between raps was increased. The percentage contribution of rapping reentrainment to total emissions for all tests ranged from a high of 53% to a low of 6.5%. Data on the particle-size distribution of the rapping puffs indicated that the mass median diameters of the particles were on the order of 10-20 μm. The large particles emitted during the rapping puffs appeared to be agglomerates. Rapping emissions were observed during the pilot-scale test to have a significantly higher concentration in the lower half of the precipitator. One of the major causes for this appeared to be hopper "boil-up". It was photographically observed that most of the particulate dropped into the hoppers; then a portion rebounded and slowly escaped over the hopper baffles to exit the precipitator.

INTRODUCTION

Rapping reentrainment accounts for significant losses from many electrostatic precipitators. The losses occur when the collected dust is removed from precipitator collection plates by rapping or shaking. The dust is lost by direct reentrainment in the gas stream and by dispersion when the dust falls into the collection hoppers.

The rapping losses are in addition to losses from uncollected material and to losses from other sources of reentrainment. Other sources of reentrainment can include the direct scouring action of the gas on the collected dust, scouring during sparking, and sweepage of dust directly from the hoppers, caused by poor gas-flow conditions or by air leakage into the hoppers.[1]

This paper discusses the results of experimental investigations of rapping reentrainment of fly ash in four electrostatic precipitators connected to coal-fired boilers,[2,3] and the results of an experimental investigation of rapping reentrainment of fly ash in a large pilot precipitator at FluiDyne Engineering Corporation's Rosemount Laboratory.[4]

The main objective of the studies was quantification of rapping reentrainment in terms of the percentage of total emissions and in terms of the particle size distribution of the reentrained particulate with the intent of providing data for inclusion of losses due to rapping reentrainment in a systems model of electrostatic precipitation. In addition, during the studies using the pilot precipitator, the basic mechanics of removal of dry dust by rapping and the variations in the removal mechanisms with changes in dust properties were investigated.

BACKGROUND

The removal of particulate from a gas stream by a dry electrostatic precipitator involves four separate processes. The first is the precipitation of the particulate from the gas stream onto the collection plate. A Southern Research Institute report discusses the physical mechanisms involved and describes a computer model for the dust collection from the gas stream.[5] The second process is the removal of the particulate from the collection plate, and the third is the transfer of this particulate to a hopper. The fourth process is the removal of the collected particulate from the hopper to a disposal area.

In present-day precipitator applications, two approaches are prevalent with regard to the removal and transfer of the particulate from the collecting plates. One approach is to rap often and to provide maximum rapping acceleration to these plates during each rap in an attempt to minimize the thickness of the residual dust layer. The other approach is to vary the intensity and frequency of rapping in an attempt to minimize the quantity of material reentrained. A determination of the best rapping technique for a specific application depends on an understanding of the method by which dust is actually removed and transferred from the collection plates during a rapping sequence and of the effects of residual dust layers.

The mechanics of the dust removal process vary with the properties of the dust, precipitator operating conditions, and rapping parameters. Dust properties and precipitator operating conditions affect the adhesion and cohesion of the dust layer. The adhesion and cohesion of dust layers depend upon particle-to-particle forces. According to Tassicker,[6] the component forces are: London-van der Waals, triboelectric, capillary, surface dipole, and electric-field corona forces. These component forces are influenced by the following: particle diameter, porosity and compaction of the layer, complex dielectric constant, humidity in the gas, adsorbed surface dipolar molecules, work-function interfaces on the material, and the electric field and current density in the dust layer.

Theory of the Mechanics of Dust Removal. An elementary theory of dust removal which considers only the tensile strength (P) of the dust layer and the acceleration (a) normal to the plate has been developed by Tassicker.[7] The theory predicts that the dust layer is removed only when

$$a > \frac{P}{\delta \ell} = \frac{P}{M/A} \qquad (1)$$

where δ is the bulk density, ℓ is the dust layer thickness, and M/A the mass per unit area. According to this equation, for a given dust thickness, the rapping intensity must be of sufficient magnitude to produce an acceleration greater than the ratio of the tensile strength of the ash layer and the mass per unit area. For a given acceleration, dust is removed only when

$$M/A > P/a; \qquad (2)$$

that is, when the mass per unit area (dust surface density) is greater than the ratio of dust layer tensile strength to the normal plate acceleration. Since the mass per unit area depends on the dust layer thickness, which in turn is related to collection time between raps, the time interval between the raps is directly related to the efficiency of dust removal from the plates.

Experimental data obtained by Sproull[8] and by Penney and Klingler[9] show that the requirements for removal of a precipitated dust layer are in basic agreement with Tassicker's elementary theory for dust removal.

Emissions Due to Rapping. Emissions due to rapping and their dependence on rapping parameters have been reported previously by Sproull,[10] Plato,[11] Sanayev and Reshidov,[12] Schwartz and Lieberstein,[13] and Nichols, Spencer, and McCain.[2] Sproull found that reducing the intensities of the raps lead to a reduction in rapping emissions. He also observed a vertical stratification of the emissions during rapping, with higher concentrations in the lower portion of the precipitator. The work by the others showed improvements in performance of full-scale precipitators when the time intervals between raps were increased.

Although these previous studies have added to our understanding of rapping reentrainment, they have not provided quantitative data on the amounts of emissions due to rapping reentrainment.

EXPERIMENTAL PROCEDURES

A complete characterization of rapping reentrainment requires the measurement of a large variety of variables. A block diagram of an experimental layout for our pilot rapping reentrainment study is shown in Figure 1. In addition to the data that is obtained with this arrangement, a complete characterization utilizes the precipitator design data.

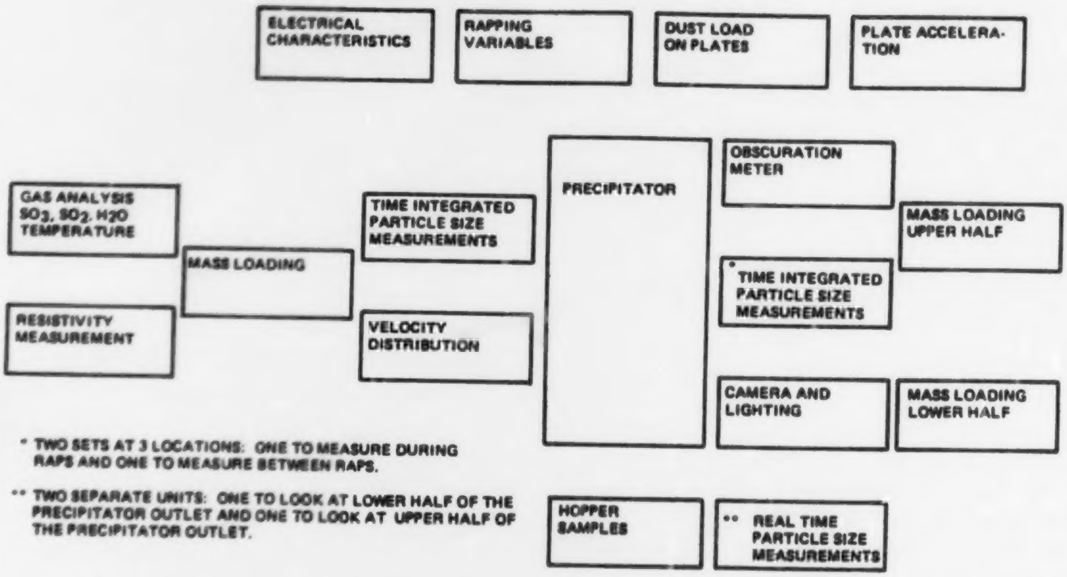
ELECTRICAL CHARACTERISTICS
RAPPING VARIABLES
DUST LOAD ON PLATES
PLATE ACCELERATION
GAS ANALYSIS SO_3, SO_2, H_2O TEMPERATURE
RESISTIVITY MEASUREMENT
MASS LOADING
TIME INTEGRATED PARTICLE SIZE MEASUREMENTS
VELOCITY DISTRIBUTION
PRECIPITATOR
OBSCURATION METER
* TIME INTEGRATED PARTICLE SIZE MEASUREMENTS
CAMERA AND LIGHTING
MASS LOADING UPPER HALF
MASS LOADING LOWER HALF
HOPPER SAMPLES
** REAL TIME PARTICLE SIZE MEASUREMENTS
* TWO SETS AT 3 LOCATIONS: ONE TO MEASURE DURING RAPS AND ONE TO MEASURE BETWEEN RAPS.
** TWO SEPARATE UNITS: ONE TO LOOK AT LOWER HALF OF THE PRECIPITATOR OUTLET AND ONE TO LOOK AT UPPER HALF OF THE PRECIPITATOR OUTLET.

Figure 1. Block diagram of experimental layout for a rapping reentrainment study

The field experiments included a similar set of measurements to those made during the pilot studies. However, sampling view ports for photographing rapping emissions and for determining the vertical stratification of the rapping emissions were not available in the full scale units nor were load cells for measuring the quantity of fly ash collected on the collection plates. Hence these measurements were not included in the field tests.

The adhesion and cohesion properties of the collected dust layers were also not determined during each test since suitable field test equipment was not available. However, some information about the tensile strength of the collected ash layers was obtained during the pilot studies by using the elementary theory of adhesion given in the introduction, the load cell data, and plate acceleration data.

Quantification of rapping reentrainment in terms of the percentage of total emissions and in terms of the particle size distribution of the reentrained particulate required determining the amount of emissions with and without rapping reentrainment. To define the mechanisms by which the rapping losses occurred required time-resolved data on the particulate concentrations and size distributions across typical portions of the precipitator exit plane.

During the investigations the above requirements were met by using real-time systems and integrating systems. A real-time system based on an optical single-particle counter was developed which included a five-channel analog ratemeter, which provided parallel monitoring of the instantaneous concentrations of particles in five pre-selected size intervals ranging from 0.6 to 20 µm.

To conform to instrumental limitations on the total concentration of aerosol particles in the sample gas stream arriving at the sensor, the aerosol sample from the flue was diluted before measurement. Because of the very steep gradient in the size distribution, on a number basis, at the exit of a precipitator on a power boiler, the diluter was made as a size-selective device which, under ideal conditions, dilutes the concentration of small particles in the sample gas stream by fairly large factors while passing a relatively confined and undiluted stream of the lower concentrations of large particles directly to the particle sensor. Figure 2 illustrates the operating system for the particle dilution train. Because of the potentially large probe losses that can result from impaction and settling in the probe, the system was intended to be used only from below a duct with a minimum number of bends (one) between the sampling point and the particle sensing volume. The probe was oriented in the vertical direction so that settling was in the direction of the probe axis and consequently did not result in a loss of particles.

For those circumstances in which it was not possible to sample from below the duct, a second sample extraction system was constructed. These samples were removed at high flow rates, 0.002-0.02 m^3/sec (5-40 cfm), through a large bore probe (4 cm diameter) and conveyed to a suitable location beside or on the top of the duct, at which point a secondary sample was extracted into the diluter and counter as illustrated in Figure 3. This sampling method provided information on relative concentrations of particles of various sizes during and between puffs, but did not provide quantitative concentration data because of the uncertainties in the probe losses and in the degree to which the secondary sample represents the average concentration in the high flow rate probe.

Integrated measurements of rapping emissions were made with separate sets of inertial impactors and mass trains during the pilot studies to independently quantify rapping reentrainment losses and non-rapping reentrainment losses. One set of impactors and mass trains measured losses between raps and the other set measured rapping losses. The dust feed was turned off during rapping. During two of the field tests, losses were measured with separate sets of impactors and mass trains during alternating periods with rapping and without rapping. The weighted time average of the measurements was compared with data obtained during normal operation to determine if losses were affected by use of the non-rapping intervals. During the other two field tests, measurements were made during non-rapping periods and compared with measurements during either normal operation or operation with a modified rapping frequency.

RESULTS OF EXPERIMENTAL STUDIES

In the tests on the five electrostatic precipitators, the following data were obtained: the percent of total emissions due to rapping reentrainment, the percent of emissions for a given particle size due to rapping, the particle size distribution of the particulate emitted due to rapping, and the effects of rapping reentrainment on fractional collection efficiencies. Selected examples of the test results are contained in this paper.

The percentage contributions of rapping reentrainment to total emissions at each of the test locations and for various test conditions are tabulated in Table 1. The percentage contributions ranged from a high of 53% to a low of 6.5%.

The percentage of emissions for a specific particle size that are due to rapping are given in Figure 4. This data indicates that rapping reentrainment accounts for only 2-5% of the emissions of 1 μm diameter particles, and that the percentage of emissions due to rapping increases significantly with increasing particle size, ranging from 24% to 48% for 4 μm diameter particles and from 50% to 88% for 12 μm diameter particles.

Averaged particle size distributions for rapping puffs are plotted in Figures 5 and 6. The particle size distribution data shows that the rapping puffs consisted of relatively large particles when compared with non-rapping emissions.

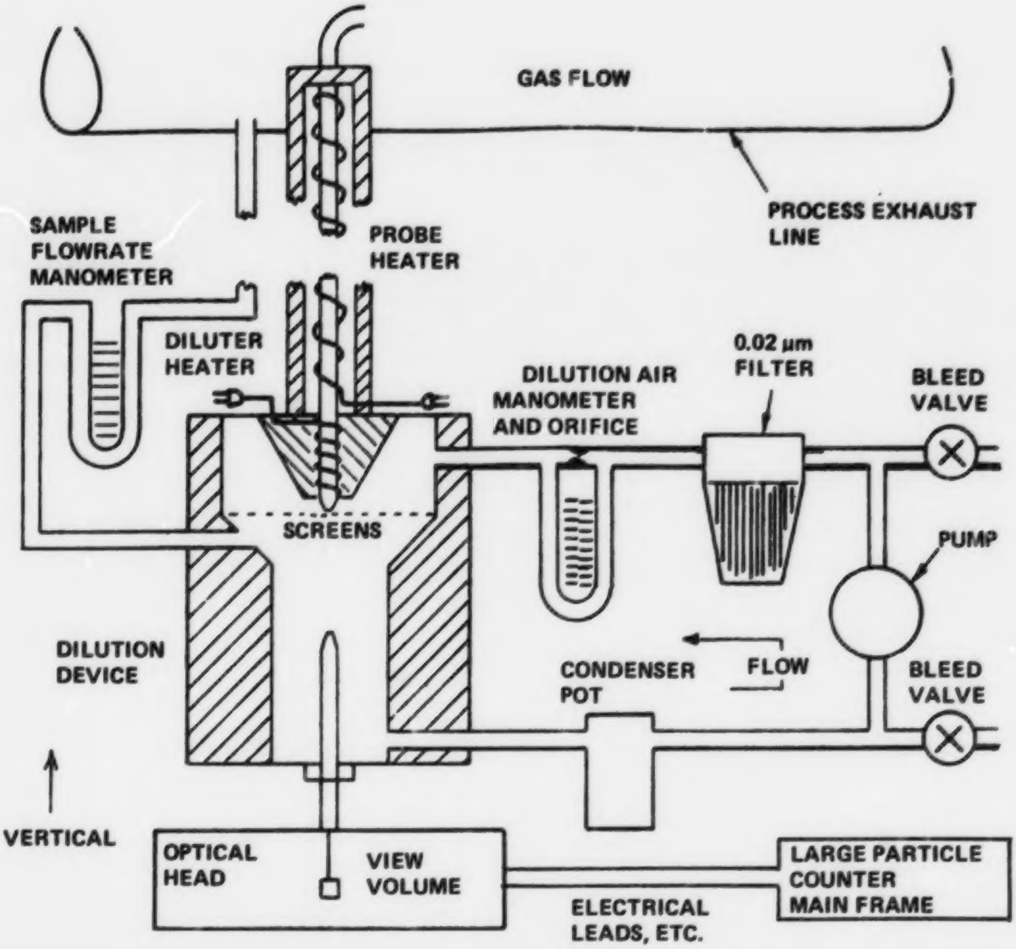
GAS FLOW
PROCESS EXHAUST LINE
SAMPLE FLOWRATE MANOMETER
PROBE HEATER
DILUTER HEATER
DILUTION AIR MANOMETER AND ORIFICE
0.02 µm FILTER
BLEED VALVE
SCREENS
PUMP
DILUTION DEVICE
CONDENSER POT
FLOW
BLEED VALVE
VERTICAL
OPTICAL HEAD
VIEW VOLUME
ELECTRICAL LEADS, ETC.
LARGE PARTICLE COUNTER MAIN FRAME

Figure 2. Schematic of diluter for real time particle sizing system

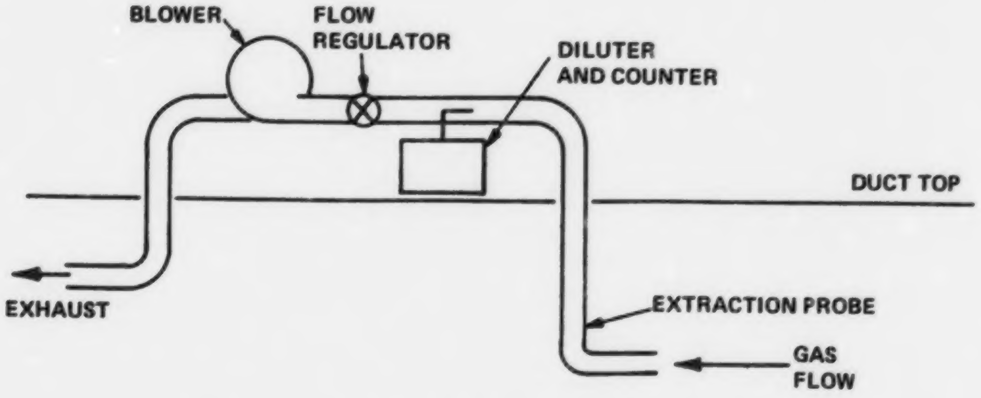
BLOWER
FLOW REGULATOR
DILUTER AND COUNTER
DUCT TOP
EXHAUST
EXTRACTION PROBE
GAS FLOW

Figure 3. Extractive sampling system for real time system

Table 1. PERCENTAGE CONTRIBUTION OF RAPPING REENTRAINMENT TO TOTAL EMISSIONS

Test Location	Comments	Type Rapper	Plate Acceleration G's	Rap Intervals Min.	Gas Velocity m/sec	Avg. Plate Current Densities** mA/cm^2	Gas Temp °C	SCA*, $\frac{m^2}{m^3/sec}$	Total Penetration %	Penetration Due to Rapping Reentrainment, %
			x,y,x axis							
1		Vibrator	3.7, 1.6, 2.9	4, 6.5, 6.5		7.6, 10.4, 15.3, 13.9	137		32.1	46
		Vibrator	3.5, 1.8, 2.6	8, 13, 13		11.2, 11.2, 16.7, 12.5	137		25.8	33
	SO_3 injection	Vibrator		4, 6.5, 6.5		11.2, 11.2, 16.7, 12.5	132		6.2	48
		no rap							17.4	
	SO_3 injection	no rap							3.2	
2	pilot test	Drop hammer	11, 16, 15	12	0.87	23.3	122	33	11.4	53
	pilot test	Drop hammer		32					7.6	32
	pilot test	Drop hammer		52					6.1	18
	pilot test	Drop hammer		150					6.9	25
	pilot test	no rap							5.2	
3		Drop hammer two plates		10, 10, 20, 20 60, 60	1.52	8.4, 9.1, 13.2 15.1, 12.3	154	110	0.85	30
4		Drop hammer		10, 20, 60	1.25	11.1, 17.6, 22.7	157	48	0.40	35
		two plates				4.6, 7.8, 11.3	157		0.95	38
5		Rotating Drop hammer		6, 6, 12, 12	1.83	14, 24.6, 33.0, 47.7	162	52	0.19	6.5

*SCA - specific collection area
**for each electrical field

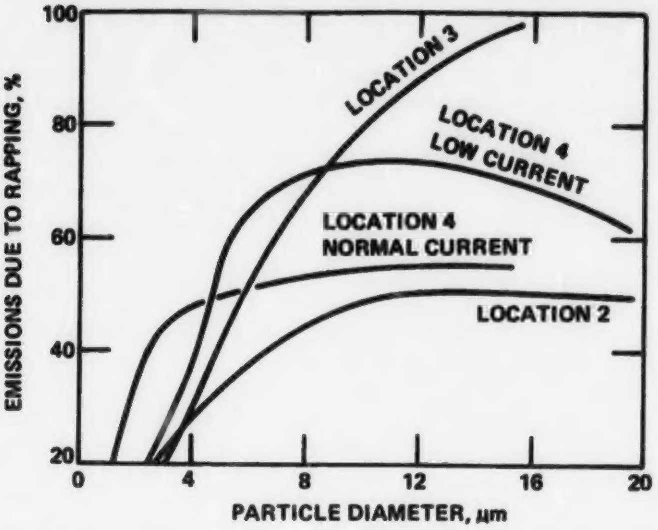

Figure 4. Percent emissions due to rapping for particles with diameters of 1 to 20 µm

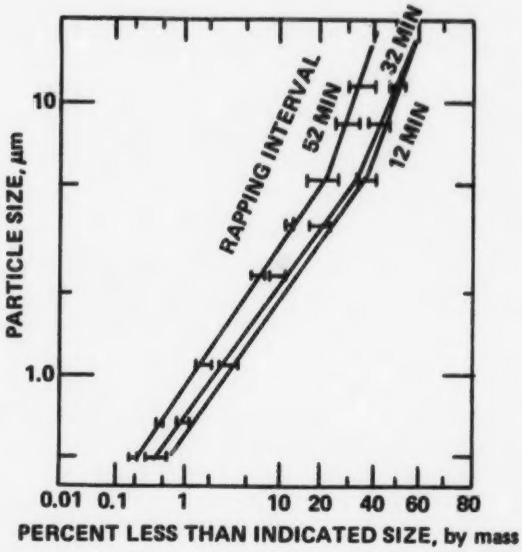

Figure 5. Cumulative percent distribution for rapping puffs, rapping intervals of 12, 32, and 52 minutes, pilot test

A selected example of the effect of rapping reentrainment on precipitator fractional efficiency is shown in Figure 7. Fractional efficiencies for alternating periods with the rappers off and with the rappers on are given along with fractional efficiencies determined during normal rapper operation. These data show that collection efficiency is relatively independent of rapper operation for particles with diameters from 0.1 μm to 2 μm with the possible exception in the region of 0.3 to 8 μm in which there is some ambiguity in the data. Above 2 μm, rapping significantly reduced collection efficiency.

Discussion of Experimental Results

The percentage contribution of rapping reentrainment to total emissions varied significantly for changes in test conditions at the same location and for the different precipitators. The lowest rapping emissions were apparently obtained for a precipitator with high plate accelerations, i.e., accelerations greater than 150 Gs (1.5 × 10^5 cm/sec^2) and with a rap interval of 30 minutes. There are several possibilities for the apparent low rapping emissions at this location that are of interest and which merit further investigation. One is the use of large and relatively deep hoppers (depth 6 meters). It is suspected that these aided in reducing hopper "boil-up", which is discussed in the section on reentrainment mechanisms. Another possibility is the effect of having a relatively fine inlet dust. There also is the possibility that other sources of reentrainment may have contributed to non-rap emissions, resulting in the apparently low rapping emissions.

The highest percentage rapping emissions were obtained during the pilot studies with a rapping interval of 12 minutes and with normal plate accelerations on the order of 11 Gs (1 × 10^{11} cm/sec^2). The rapping emissions during the pilot study (test location number 2) decreased with increasing time between raps. The effect on overall efficiency is shown in Figure 8. The percentage of the collected dust removed from the precipitator plates also increased with increased time between raps, as shown in Figure 9.

The collecting of a larger mass per unit area (dust surface density) produces the two effects mentioned above. According to the elementary theory of dust removal, the product of the normal plate acceleration and dust surface density has to be greater than the tensile strength of the layer, typically 0.5 × 10^3 to 3 × 10^3 dynes/cm^2, if the dust layer is to be removed. This theory indicates that dust removal efficiency should increase with increased time between raps, as illustrated by the data shown in Figure 9. Laboratory measurements by Sproull[8] produced similar data. Figure 9 also illustrates the build-up of a residual dust layer that was not removed with normal plate accelerations on the order of 11 Gs. There are several possible causes for the

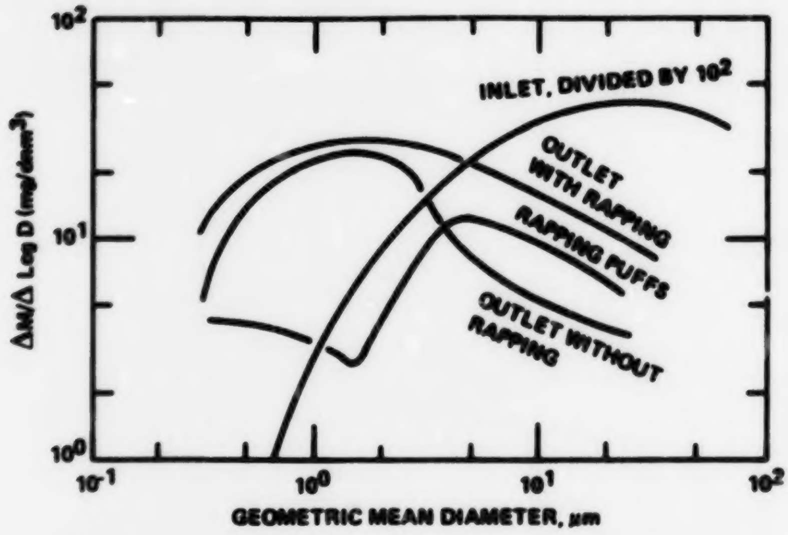

Figure 6. Particle size distributions for inlet particulate, outlet particulate with rapping, outlet particulate without rapping, and average effective distribution for rapping puffs

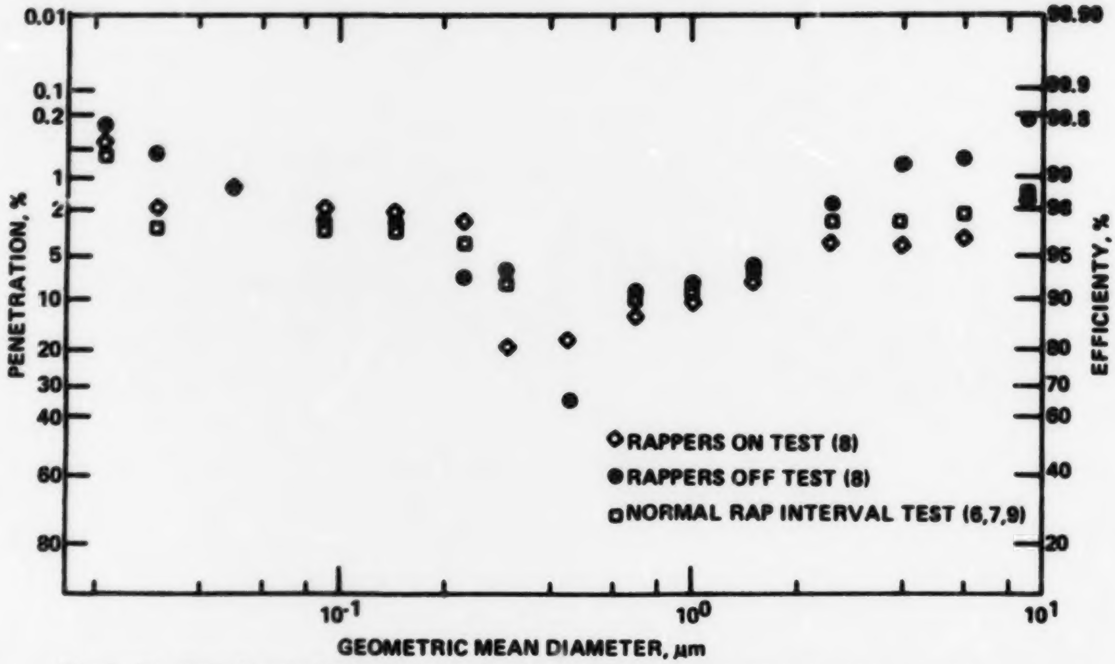

Figure 7. Fractional efficiencies as function of particle diameter for half normal current density test. Test location Number 3

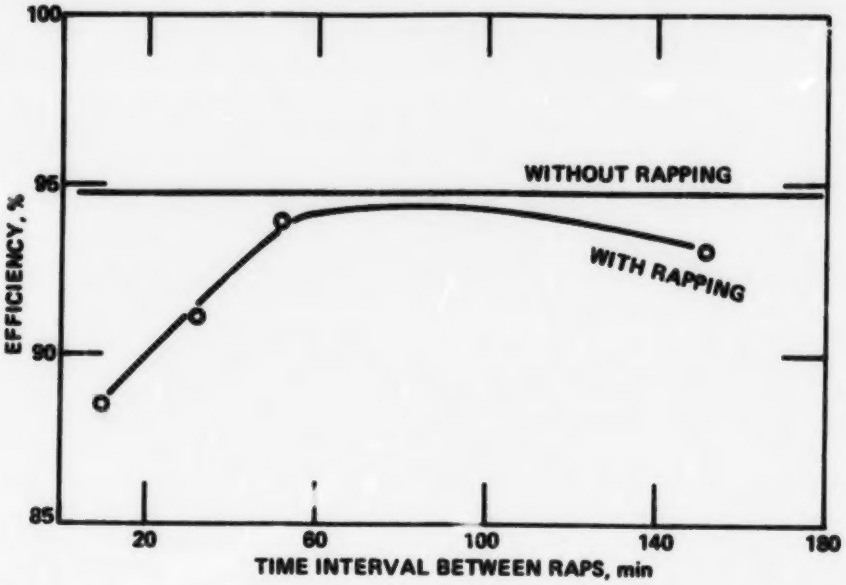

Figure 8. Average efficiencies for FluiDyne pilot precipitator for various rapping intervals

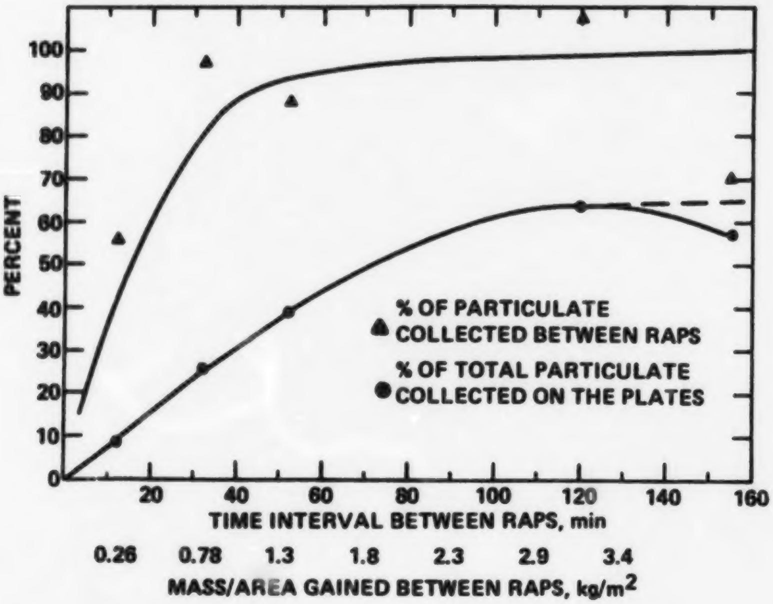

Figure 9. Dust removal efficiency versus time interval between raps

development of the residual layer. For one, the dust layer directly in contact with the collection plates has a much higher tensile strength than the remainder of the layer. Estimates for removal of the layer called for accelerations greater than 10^3 Gs (9.8×10^5 cm/sec^2).[7] Consolidation of the dust that remains on the plate after a rap also aids in producing residual layers. The vibrations during a rap can have the effect of compacting the dust layer if it is not removed making it more difficult to remove. A third possible cause of the residual layer is the removal of patches of dust only from selected locations on the collection plates where the removal criteria are met. Dust can be removed from one location during one rap and from another location on the next rap due to changes in distribution of the dust surface density. This results in a nonuniform dust layer and the presence of a residual layer. This is often the result of nonuniform plate accelerations. At one location where plate accelerations are on the order of only 4 to 5 Gs (3.4-4.9×10^3 cm/sec^2), residual dust layers as thick as 2 cm were observed in the vicinity of plate baffles where the plate accelerations are dampened. Between the baffles, the residual layers were only 1 to 2 mm thick.

The decrease in rapping emissions observed during some of the tests with an increase in the time between raps or, correspondingly, an increase in dust surface density appears to be the result of a shift in the size distribution of the reentrained particulate to larger particle sizes. Thicker dust layers appear to produce larger particles. In this case the large particles that are emitted are not the primary particles that entered the precipitator but agglomerates consisting of smaller particles. Inspection of impactor substrates after collecting dust at the outlet of test locations number 2 and 3 indicated that the majority of the large particles in the rapping puffs were agglomerates. The shift to larger particles in the rapping puffs observed during the pilot studies as the time between raps was increased is illustrated by the shift of the cumulative percent particle size distribution of the rapping puffs shown in Figure 5.

This effect was previously observed by Plato,[11] who found that with a dust layer surface density greater than 1 kg/m^2, dust was removed in cakes and for values less than this it formed clouds. Producing agglomerates instead of individual particles when the plates are rapped reduces the quantity of material that escapes from the precipitator due to rapping. This is because the large agglomerates are recollected faster by gravitational settling and by electrostatic precipitation than discrete single particles or smaller agglomerates.

The above provides an explanation for the results that are given in Figures 8 and 10. Sanayev and Reshidov have also used the above explanation for the decrease in the percentage of dust collected on the plates that is emitted due to rapping with an increase in dust surface density. A comparison of results obtained during the pilot studies[4] and by Sanayev and Reshidov[12] is shown in Figure 11.

Both sets of data indicate that for the conditions used during the tests, minimum reentrainment loss occurred with a dust surface density on the order of 1 kg/m^2 or larger. The Sanayev and Reshidov data also show the expected dependence on gas velocity. The results given in Figure 11 do not include the effects of collecting thicker layers on overall performance.

The 50 to 88% emissions due to rapping reentrainment observed for large particles (>10 μm) which are shown in Figure 4 can be explained either by a continuing transfer of collected large particles from the inlet to the outlet by rapping or by the above mentioned agglomeration of the collected particles. Both effects probably occur, with agglomeration being the dominant effect, as indicated by the agglomerates observed on the upper stage of inertial impactors.

During collection by an electrostatic precipitator, the mass median diameter of the fly ash from a coal-fired boiler typically decreases from the inlet of the precipitator to the outlet. This is illustrated by a shift in the particle size distributions of the inlet and outlet dust concentrations. In Figure 6, the dm/dlogD particle size distributions are plotted for the inlet dust at test location number 4 and for the outlet dust with the rappers off and with the rappers on. The expected shift in particle size which can be theoretically predicted for the inlet and outlet dust concentrations with the rappers off is clearly evident. When the plate rappers are on, the mass median diameter of the particle size distribution shifts back towards larger size particles as shown by the dm/dlogD plot in Figure 6 with the rappers on and by the effective average dm/dlogD for the rapping puffs. The large particle size of the particulate in the rapping puffs is also illustrated by the data given in Figure 5. The rapping emission percentages in Figure 4 reflect the shift in the outlet particle size distribution produced by plate rapping. At locations such as at test location number 3, where the precipitator is very large and preceded by a mechanical collector, almost all of the large particles ($\gtrsim$10 μm) are collected before reaching the outlet. Thus the percentage of emission due to rapping can approach 100% for the large particles.

Rapping reentrainment has the effect of transferring particles from particle size intervals consisting of small single particles to particle size intervals consisting of larger particles.

At test location number 4, data were obtained at normal operating current densities (see Table 1) and at one-half the normal operating current density. This resulted not only in a

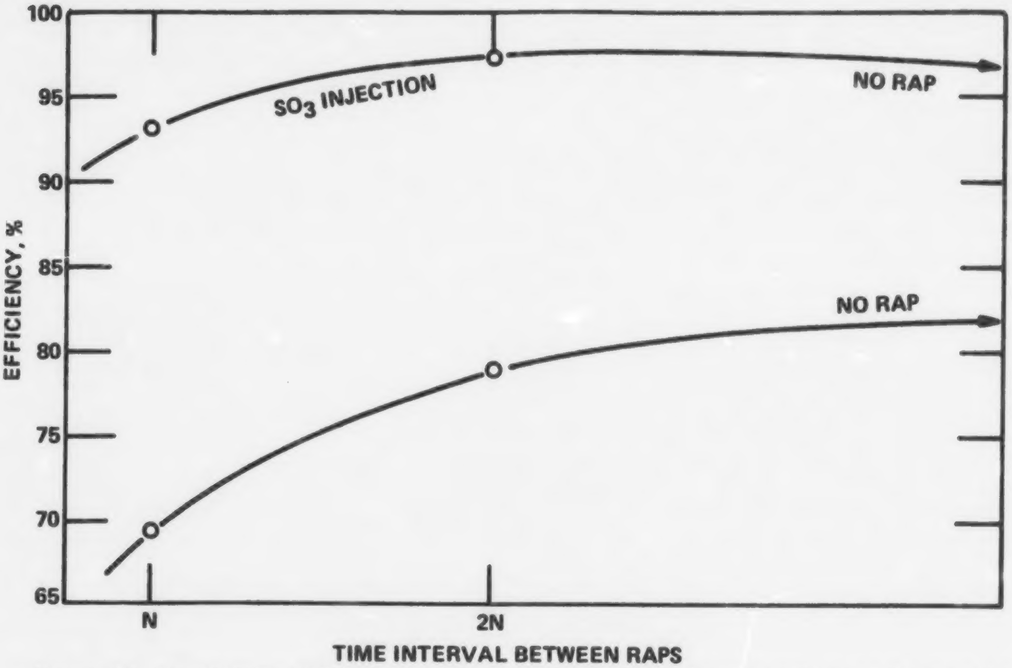

Figure 10. Precipitator efficiency at Test location Number 1 as a function of the rapping interval

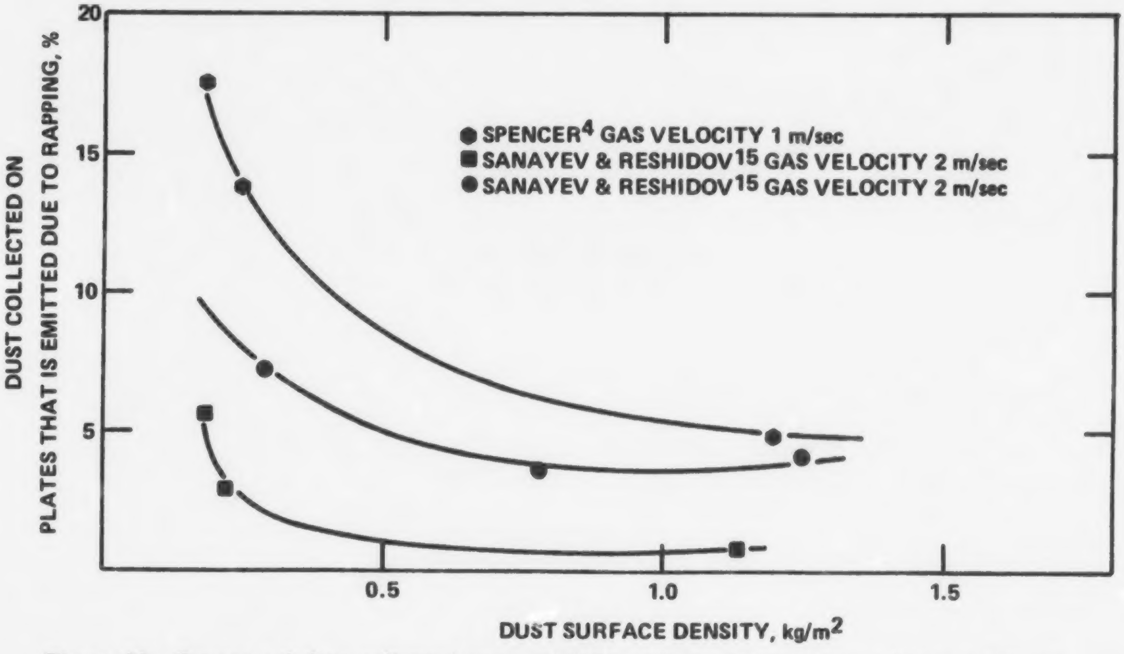

Figure 11. Percent of dust collected on precipitator plates emitted from pilot precipitator due to rapping

decrease in efficiency between raps but also, as shown by the data given in Figure 4, in an increase in the percentage contribution of rapping reentrainment for large particles. This implies that a change in particulate properties such as an increase in resistivity that reduces operating current density can result not only in a decrease in efficiency between raps but also in an increase in the percentage emissions due to rapping reentrainment. However, since the forces holding the dust layer together theoretically increase with resistivity, the effects may not be the same as those obtained during the test at location number 4, where dust resistivity was held constant.

REENTRAINMENT MECHANISMS

The amount of rapping reentrainment that occurs depends on the processes by which the dust is reentrained into the gas stream. Sproull[10] has suggested that the rapping processes occur in a sequence in which the collected dust is removed by what is termed a slip-stick process. The concept is that the dust layer builds up to a sufficient thickness that the acceleration of the plate causes a shearing force between the dust layer and the plate. The dust then slides along the surface of the plate until it is recollected on the plate. The process is repeated with each successive rap until the dust finally falls into the hopper.

Another concept of rapping is that the collected dust is dislodged in large agglomerates or clumps and falls directly into the hopper without being recollected.

Neither concept adequately explains the rapping process as observed in the FluiDyne pilot precipitator or in the Southern Research Institute small-scale precipitator. Motion pictures (32 frames/sec) of the removal of a dust layer (2-3 mm thick) by rapping in the SRI pilot unit show the dust layer fracturing along lines of discontinuity in the dust surface. The resulting fractured sheet of dust starts to fall as separate sheets which break up as they encounter other falling sheets and patches of unremoved dust. The dust appears to fall without being recollected and to become turbulently mixed as it falls. The motion pictures show the majority of the dust dropping into the hoppers from which a portion boils up and becomes reentrained into the gas stream. Motion pictures taken in the large pilot precipitator at the FluiDyne Engineering Rosemount Laboratory showed similar behavior.

Measurements of the vertical distribution of the rapping loss at the exit of the FluiDyne unit indicated that 82% of the rapping emissions occurred in the lower 32% of the precipitator. This effect, evidently due to hopper "boil-up" combined with gravitational settling of the reentrained particulate, produced a significant vertical stratification of the reentrained emissions from the large pilot precipitator as shown in Figure 12.

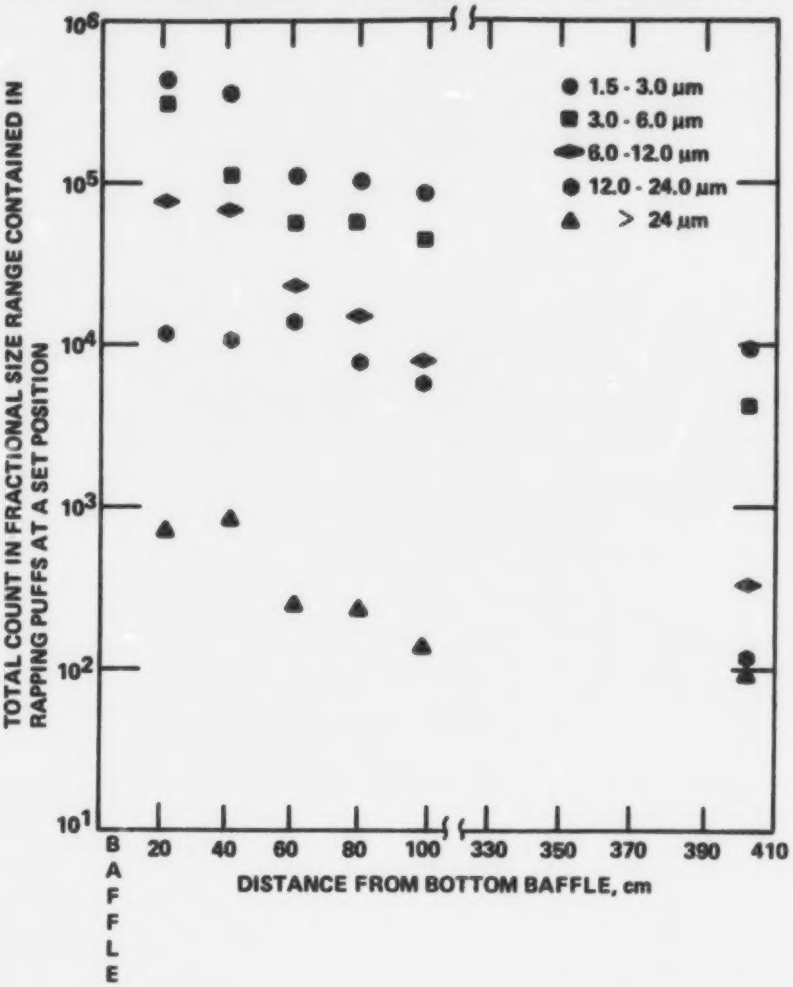

Figure 12. Spatial distribution of particles in rapping puff

Rapping puffs observed in the lower portion of the precipitator occurred in two bursts for both upstream and downstream raps as shown in Figure 13. The first burst lasted 2-4 seconds. This burst was interpreted as being the result of particulate reentrained directly in the gas stream and being carried out of the precipitator at the velocity of the gas through the unit. The longer lasting second burst, which for the larger particles was a series of puffs, can be interpreted as resulting from hopper "boil-up". These data indicate that hopper "boil-up" contributes significantly to rapping reentrainment emissions.

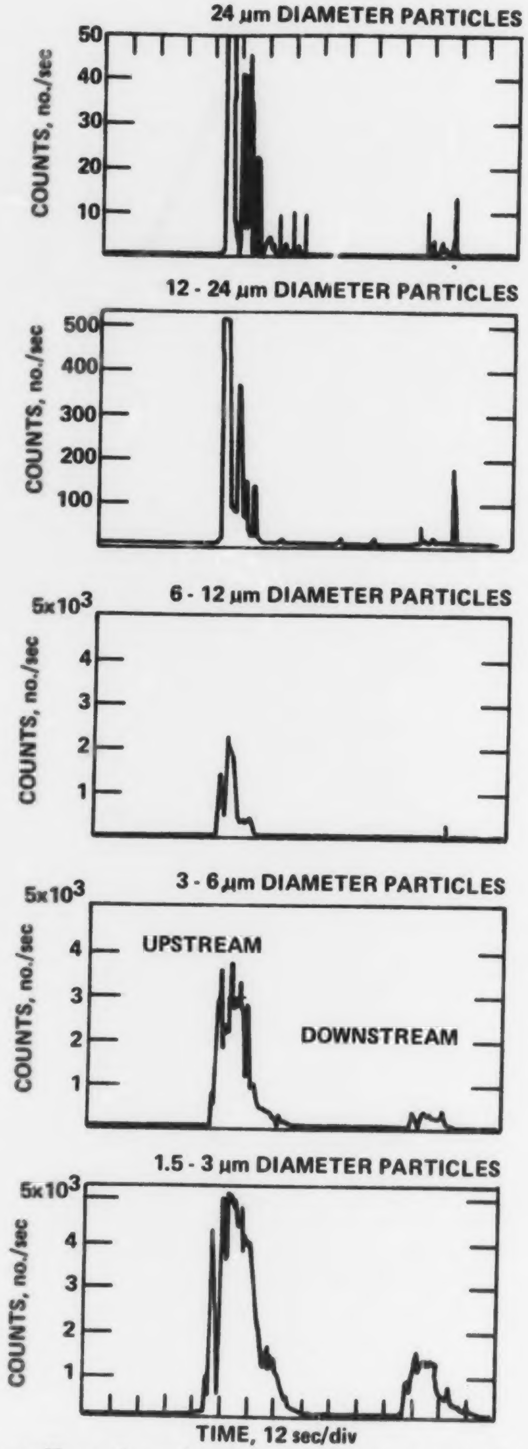

Figure 13. Rapping puffs at the exit plane of the pilot precipitator, upstream and downstream raps

EFFECT OF RAPPING REENTRAINMENT ON COLLECTION EFFICIENCY, PENETRATION, AND SIZING OF ELECTROSTATIC PRECIPITATORS

Rapping reentrainment can have a considerable effect on collection efficiency, penetration, and sizing of electrostatic precipitators. In this section two approaches to estimating the effects of rapping reentrainment are discussed. The examples are based on the results of the FluiDyne pilot tests and computer calculations by Gooch et al.[5] The results of the example calculations are tabulated in Tables 2 and 3.

These examples show that the percentage increase in collection efficiency obtained with no rapping reentrainment decreases with increasing efficiency of the precipitator. However, due to the exponential dependence of precipitator efficiency on particle migration velocity, plate collection area, and gas volume flow rate, the effect of rapping reentrainment on the size of a precipitator required for a given collection efficiency is substantial. Estimates of the effect of rapping reentrainment on precipitator size are tabulated in Tables 2 and 3 for various conditions. Two approaches were used to generate the tabulated values. One approach was to assume that the percentage penetration due to rapping was independent of the size of the unit. This assumption, although not strictly true, may fairly represent real situations. According to the data obtained during the pilot experiments, the rapping puff concentration has a significant vertical gradient and the rapping puff consists of large particles. Thus, in a multi-section precipitator the rapping puffs from upstream sections may be recollected in the lower portion of a downstream section and later transferred from this lower position into the hoppers without making any significant contribution to outlet emissions. In this case, outlet fields would contribute the largest portion of the rapping emission, and the percentage emission due to rapping should be relatively independent of the size of the unit. Estimates based on this approach are tabulated in Table 2.

The second procedure was developed by Francis.[14] This approach assumes that the fraction of collected dust per section reentrained and emitted is the same for every section, that the between-rap sectional collection efficiency is constant from one section to another, and that the recollection efficiency for the rapping puffs is the same as the between-rap sectional collection efficiency. According to Francis' procedure, the penetration of any downstream section is equal to the penetration of the first section (P_1) raised to the power of the number of preceding sections plus one. Thus, the penetration of the Nth section (P_N) is given by:

$$P_N = (P_1)^N \qquad (3)$$

Table 2. EFFECT OF RAPPING REENTRAINMENT ON EFFICIENCY FOR RAPPING LOSSES ACCOUNTING FOR 20%, 30%, 40% AND 50% OF EMISSIONS FOR VARIOUS OVERALL EFFICIENCIES (first approach)

Assumed percent of total penetration due to rapping reentrainment	Penetration			Assumed Overall Efficiency η %	Efficiency without rapping reentrainment, η_R, %	Increase in η without rapping reentrainment, %	SCA* required				Additional SCA required because of reentrainment		Additional SCA, %
	Due to rapping reentrainment, %	Without rapping reentrainment, %	Total %				For η without rapping reentrainment, $m^2/m^3/sec$	($ft^2/1000\ ft^3/sec$)	For η_R or for η with rapping reentrainment, $m^2/m^3/sec$	($ft^2/1000\ ft^3/sec$)	$m^2/m^3/sec$	($ft^2/1000\ ft^3/sec$)	
	3.75	3.75	7.50	92.50	96.25	3.90			16.2	(82)			
	2.25	2.25	4.50	95.50	97.75	2.31			21.3	(108)			
50	0.75	0.75	1.50	98.50	99.25	0.76	26.2	(133)	35.5	(180)	9.3	(47)	35.3
	0.25	0.25	0.50	99.50	99.75	0.25	41.8	(212)	53.2	(270)	11.4	(58)	27.4
	0.05	0.05	0.10	99.90	99.95	0.05	68.9	(350)	81.7	(415)	12.8	(65)	18.6
	3.00	4.50	7.50	92.50	95.50	3.24							
	1.80	2.70	4.50	95.50	97.30	1.88			18.7	(95)			
40	0.60	0.90	1.50	98.50	99.10	0.61	26.2	(133)	32.9	(167)	6.7	(34)	25.6
	0.20	0.60	0.50	99.50	99.70	0.20	41.8	(212)	50.2	(255)	8.5	(43)	20.3
	0.04	0.06	0.10	99.90	99.94	0.04	68.9	(350)	78.8	(400)	9.8	(50)	14.3
	2.25	5.25	7.50	92.50	94.75	2.43							
	1.35	3.15	4.50	95.50	96.85	1.41							
30	0.45	1.05	1.50	98.50	98.95	0.46	26.2	(133)	30.5	(155)	4.5	(23)	16.5
	0.15	0.35	0.50	99.50	99.65	0.15	41.8	(212)	47.3	(240)	5.5	(28)	13.2
	0.03	0.07	0.10	99.90	99.93	0.03	68.9	(350)	75.8	(385)	6.9	(35)	10.0
	1.50	6.00	7.50	92.50	94.00	1.62							
	0.90	4.60	4.50	95.50	96.40	0.94							
20	0.30	1.20	1.50	98.50	98.80	0.30	26.2	(133)	29.2	(148)	3.0	(15)	11.3
	0.40	0.10	0.50	99.50	99.90	0.10	41.8	(212)	68.9	(350)	3.5	(18)	8.5
	0.08	0.02	0.10	99.90	99.92	0.02	68.9	(350)	73.3	(372)	4.3	(22)	6.3

*Specific Collection Area (SCA) based on data given by Gooch, et al.[5] (Figure 26 computed performance curves at 20 nA/cm^2).

Table 3. EFFECT OF RAPPING REENTRAINMENT ON PERFORMANCE FOR VARIOUS REENTRAINMENT PERCENTAGES AS A FUNCTION OF NUMBER OF SECTIONS AND A CONSTANT COLLECTION EFFICIENCY PER SECTION.

Assumed percent of collected material per section reentrained	Number of Sections	Penetration			Percent of penetration due to rapping reentrainment, %	Efficiency η, %	Assumed efficiency η_R without rapping reentrainment, %	Increase in η with no rapping reentrainment, %	SCA* Needed				Additional SCA		Additional SCA, %
		Due to rapping reentrainment, %	Without rapping reentrainment, %	Total %					Without rapping reentrainment to obtain η		With rapping reentrainment				
									m^2/m^3/sec	(ft^2/1000 ft^3/sec)	m^2/m^3/sec	(ft^2/1000 ft^3/sec)	m^2/m^3/sec	(ft^2/1000 ft^3/sec)	
5.9	1	6.2	5.2	11.4	52	88.6	94.8	6.54							
	2	1.02	0.27	1.29	79	98.7	99.73	1.03	28.0	(142)	51.6	(262)	23.6	(120)	84
	3	0.136	0.014	0.150	91	99.85	99.986	0.14	62.1	(315)	105.4	(535)	43.3	(220)	69
	4	0.0193	0.0007	0.020	97	99.98	99.9993	0.02	98.5	(500)	108.3	(550)			
2.3	1	2.23	5.20	7.43	30	92.57	94.80	2.35							
	2	0.28	0.27	0.55	51	99.45	99.73	0.28	40.4	(205)	51.6	(262)	11.2	(57)	28
	3	0.027	0.014	0.041	66	99.959	99.986	0.03	83.7	(425)	105.4	(535)	21.7	(110)	25
	4	0.0023	0.0007	0.0030	77	99.997	99.9993	0.002	108.5	(550)	108.3	(550)			
0.97	1	0.90	5.20	6.1	15	93.9	94.8	0.95							
	2	0.10	0.27	0.37	27	99.63	99.73	0.10	46.3	(235)	51.6	(262)	5.3	(27)	11
	3	0.009	0.014	0.023	39	99.97	99.986	0.016	91.0	(462)	105.4	(535)	14.4	(73)	16
	4	0.0007	0.0007	0.0014	50	99.9986	99.9993	0.001	108.3	(550)	108.3	(550)			

*Specific Collection Area (SCA) based on data given by Gooch, et al.[5] (Figure 26 computed performance curves at 20 nA/cm^2).

Using this equation, the collection efficiencies of a precipitator having 1, 2, 3, or 4 sections with a between-rap sectional collection efficiency of 94.8% were calculated for percent penetrations of the first section due to rapping reentrainments of 52%, 30%, and 15%. These percentages correspond to 5.9%, 2.3%, and 0.97%, respectively, of the collected material per section being reentrained and emitted from a section. These values were chosen to correspond approximately to those obtained during the FluiDyne experiments. The results of the calculations based on this procedure are tabulated in Table 3. According to this procedure, for the conditions corresponding to the worst rapping reentrainment case at FluiDyne, the contribution of rapping reentrainment to total emissions would be greater than 90% for a three or four section precipitator with 94.8% sectional collection efficiency. For a case in which reentrainment accounts for only 15% of the emissions for the first section, a situation slightly better than the best obtained during the FluiDyne experiments, rapping reentrainment, according to Francis' procedure, would account for 39% of emissions for a 3-section precipitator and 50% of emissions for a 4-section precipitator, if the precipitator had a sectional efficiency of 94.8%. These calculations indicate that, as the size of the precipitator increases, the percentage contribution of rapping reentrainment to total emissions increases. As previously discussed, this may not happen. Investigations of rapping reentrainment in multi-section precipitators do not appear to show a general increase in the percentage contribution of rapping reentrainment to total emissions with precipitator size except for large particles. To obtain an indication of the effect of rapping reentrainment on the sizing of a precipitator, estimates of the theoretical specific collection area needed to obtain a given collection efficiency for a particular set of conditions were obtained from the model developed by Gooch, et al.[5] For the example chosen, a typical particle size distribution for an ash from a coal-fired boiler plant was selected and a precipitator operating current density of 20 nA/cm^2 was assumed (see the report of Gooch, et al.,[5] for further details).

The theoretical specific collection area (SCA) required to obtain a desired collection efficiency with rapping reentrainment was compared with a theoretical SCA that would give the same efficiency if there were no rapping emissions. This gave an estimate of the increase in SCA needed to counterbalance the rapping reentrainment emissions. The theoretical SCA needed to obtain the desired collection efficiency with rapping reentrainment was determined by first computing the collection efficiency that would be obtained if there were no rapping reentrainment, by assuming that either the percentage of emissions due to rapping reentrainment or the fraction of collected dust reentrained and emitted from a section due to rapping were known. Once this collection efficiency was calculated and assuming that there were no other nonidealities beside rapping reentrainment, the required theoretical SCA was obtained from data given by Gooch, et al. Then, again using the data given by Gooch, et al., the SCA was determined that would give the desired efficiency if there were no nonidealities such as rapping reentrainment. For the particular cases considered, the increase in required SCA due to the rapping reentrainment ranged from 6% to 84% (see Tables 2 and 3). Thus, although the percentage decrease in collection efficiency due to rapping reentrainment is relatively small, the effect on the size required for a given collection efficiency can be significant. The data obtained from the Flui-Dyne pilot experiments indicates that even moderate changes in rapping parameters can significantly affect the size of a precipitator for a given collection efficiency.

SUMMARY

Experimental investigations of rapping reentrainment were conducted utilizing a large pilot electrostatic precipitator and several electrostatic precipitators installed at coal-fired power plants. The objectives of the experimental study included a fundamental study of the mechanics of removal of dry fly ash by rapping and the quantification of rapping reentrainment in terms of the percentage and particle size distribution of the reentrained fly ash.

During the experiments the percentage of fly ash removed from the plates was observed to depend on the mass per unit area of ash collected on the plates, as predicted by theory. The build-up of residual dust layers was also observed.

During the tests the contribution of rapping reentrainment to the total emissions ranged from 6.5 to 53%, depending on the rapping conditions and the precipitator design. A significant decrease in rapping emissions was obtained by increasing the time interval between raps. This decrease was due to the resulting larger mass per unit area collected on the plates when they were rapped. Particle size distribution measurements showed that the mass median diameter of the particles emitted during the raps increased with increased time between raps. As would be expected, this produced lower overall emissions. The increase in the size of the particles emitted during rapping was ascribed to an increase in the extent of agglomeration of the particulate removed from the precipitator plates with the corresponding increase in the mass per unit area collected on the plates (thicker dust layers) before the plates were rapped.

A major portion of the reentrained material was observed to result from hopper "boil-up". A small portion of the dust was observed to pass out a pilot precipitator in a short burst at the velocity of the gas passing through the unit, while the remaining portion of the material was observed to fall into the hoppers, then to rebound, and finally to escape slowly over the baffles and out of the precipitator. This produced a significant vertical gradient in the concentration of the dust emitted from the precipitator due to rapping reentrainment.

The fractional collection efficiencies of the precipitators both excluding and including rapping reentrainment emissions were determined. Rapping reentrainment decreased the fractional collection efficiencies for particles larger than 2 μm. Below 2 μm, rapping reentrainment did not appear to contribute significantly to overall emissions.

Two approaches using simplified assumptions were used to estimate the effect of rapping reentrainment on the size of a precipitator. The first assumed that a fixed percentage of emissions was emitted from a precipitator independent of the size of the unit, and the second assumed that the same percentage of collected material was reentrained and emitted from each section and that the recollection efficiency for the reentrained material for all sections was the same as the efficiency between raps, with all sections having the same efficiency. The estimates based on the above approaches showed that the increase in precipitator size needed to recover the rapping reentrainment emissions can account for 6% to greater than 80% of the size of the unit for the cases considered.

The parameters studied during the experiments were somewhat limited. A data bank for detailed modelling of rapping should include additional data on rapping emissions as a function of plate accelerations and gas velocity.

The pilot experiments also indicated a need for a study of the parameters affecting hopper "boil-up" and the development of methods for reducing it. Additional studies on the effects of residual dust layers for high resistivity dust and studies of dust cohesive properties are also needed to aid in determining optimum rapping conditions.

ACKNOWLEDGEMENTS

This work was conducted under various contracts with the Tennessee Valley Authority, the Environmental Protection Agency, and the Electric Power Research Institute.

REFERENCES

1. White, H. J. Industrial Electrostatic Precipitation. Addison-Wesley, Reading, Mass., 1963, p.331.

2. Nichols, G. B., H. W. Spencer, and J. D. McCain. Rapping Reentrainment Study. Report SORI-EAS-75-307 to Tennessee Valley Authority, TVA Agreement TV36921A, November 1975.

3. Gooch, J. P., H. W. Spencer, J. D. McCain, and G. H. Marchant. A Study of the Performance of a Full Scale Electrostatic Precipitator with a High Specific Collection Area. Report to Electric Power Research Institute, EPRI Project RP 413-1, December 1975.

4. Spencer, H. W. A Study of Rapping Reentrainment in a Nearly Full Scale Pilot Electrostatic Precipitator. EPA-600/2-76-140, U.S. Environmental Protection Agency, Washington, D.C., 1976. 1976.

5. Gooch, J. P., J. R. McDonald, and S. Oglesby, Jr. A Mathematical Model of Electrostatic Precipitation.EPA-650/2-75-016, U.S. Environmental Protection Agency, Washington, D.C., 1975.

6. Tassicker, O. J. Some Aspects of Electrostatic Precipitator Research in Australia. J. Air Pollution Control Assoc. 25(2):122-128, 1975.

7. Tassicker, O. J. Aspects of Forces on Charged Particles in Electrostatic Precipitators. Dissertation, Wollongong University College, University of New South Wales, Australia, 1972.

8. Sproull, W. T. Fundamentals of Electrode Rapping in Industrial Electrical Precipitators. J. Air Pollution Control Assoc. 15(2):50-55, 1965.

9. Penney, G. W., and E. H. Klingler. Contact Potentials and Adhesion of Dust. Trans. Amer. Inst. Elec. Eng. Part I 81:200-204, 1962.

10. Sproull, W. T. Minimizing Rapping Loss in Precipitators at a Megawatt Coal-Fired Power Station. Paper No. 71-125, Air Pollution Control Assoc. Meeting, Atlantic City, N.J., 1971.

11. Plato, H. Rapping of Collecting Plates in Electrostatic Precipitators. Staub-Reinhalt. Luft (in English) 29(8): 22-30, 1969.

12. Sanayev, Yu. I., and I. K. Reshidov. Study of Dust Reentrainment Phenomena and Their Influence on Efficiency of Industrial Electrostatic Precipitators. Promyshlennaya i Sanitarnaya Ochistka Gazov, (Moscow) 1974 (1):1-5.
(Moscow USSR) 1974(1):1-5.

13. Schwartz, L. B., and M. Lieberstein. Effect of Rapping Frequency on the Efficiency of an Electrostatic Precipitator at a Municipal Incinerator. Proceedings of the Fourth Annual Environmental Engineering and Science Conference, Louisville, Kentucky, March 4-5, 1975.

14. Gooch, J.P., and N. L. Francis. A Theoretically Based Mathematical Model for Calculation of Electrostatic Precipitator Performance. J. Air Pollution Control Assoc. 25(2):108-113, 1975.

PAPER 9

FABRIC FILTRATION PERFORMANCE MODEL

Douglas W. Cooper and Vladimir Hampl
GCA Corporation
GCA/Technology Division

ABSTRACT

The goals of this program were to formulate and develop mathematical methods for predicting and analyzing fabric filter drag (pressure drop per unit face velocity) and fabric filter collection efficiency as a function of particle size. The literature with respect to filtration is vast, but the efforts to model fabric filtration have been few. Most attempts have used a linear approximation to the increase of fabric drag with added weight per area, and those who attempted to model collection efficiency did so with models based upon arrays of cylinders. The woven fabric structure is much more like an array of pores (before the cake is formed) and this representation has given rise to a new, nonlinear model of fabric drag and a new model of fabric collection efficiency, both presented here. The nonlinear drag model fits the experimental data much better than does the linear. The efficiency model appears to give results which are both reasonable and informative. These models have been combined to form a preliminary computer program for an entire multi-bag filtration installation, and results of such modeling are presented for both flow and efficiency variables. Also presented are design equations which are readily adaptable for a programmable calculator. Finally, we indicate several areas in which further investigation seems warranted in analyzing cleaning and seepage.

INTRODUCTION

This presentation indicates our progress toward development of a predictive model for industrial fabric filtration, with special emphasis on the use of fabric filtration to control the particulate emissions of coal-fired power plants. Primary goals are the prediction of collection efficiency versus particle size and the relationship between the flow per unit area and the

---

Dr. Cooper is now at the Harvard School of Public Health, 665 Huntington Ave., Boston, MA.

pressure drop for a fabric filtration installation. The following factors can be expected to influence efficiency and the pressure/flow relationship:

1. Dust - chemical composition, particle size distribution, particle shape, particle phase, particle concentration.
2. Gas - chemical composition (especially moisture content), temperature, pressure.
3. Fabric - material, weave (including fill and warp counts), finish, history (especially accumulated dust).
4. Cleaning operations - cleaning type, intensity, frequency, duration.

Ideally, we would like to be able to predict fabric filter drag as well as efficiency for all combinations of the above, but this is a very ambitious task. In forming a useful model, one treads a narrow path between untractable complexity and impractical simplicity - this seems particularly difficult in modeling fabric filtration.

DESCRIPTION OF A FILTRATION SYSTEM

Figure 1 shows a very simple schematic of a fabric filter installation. A dust-laden flow of gas enters the filter installation with a volumetric flow rate Q and a concentration c. The flow is divided among n compartments, the bags within these compartments having average dust weight per unit area of fabric given by W_i. The pressure drop across the i^{th} compartment's bags is given by the equation

$$\Delta p_i = Q_i S_i / A_i , \tag{1}$$

in which Q_i is the volume flow rate, A_i is the cloth face area, and S_i is the drag caused by the fabric and any accumulated dust. The ratio S_i/A_i is analogous to electrical resistance (with Q_i analogous to current and Δp_i analogous to voltage). The total flow, Q, is the sum of the individual flows, Q_i (as long as temperature and pressure corrections are made). Usually the compartments are in parallel and so constructed that the pressure drop at any given time is the same across all of them, so that Δp_i just becomes Δp.

The relationship between the pressure drop and the volume flow for a particular installation will depend upon the locus of the intersections of the system fan curve and the system resistance curve,[1] each of which can be expressed as volume rate of flow versus pressure drop. Usually, one of the following conditions holds approximately for the installation:

1. The fan produces a constant volume of flow, and pressure drop changes with system resistance.
2. The fan produces a constant pressure drop, and the volume flow changes with system resistance.

OBJECTIVES

The cost of the installation will depend upon the fabric chosen and its total area, among other things, and one of the operating costs will be the power consumption due to the pressure drop across the system. Often the available choice of fabrics will be limited, so that the major question becomes the area of cloth needed to handle a volume flow rate of gas.

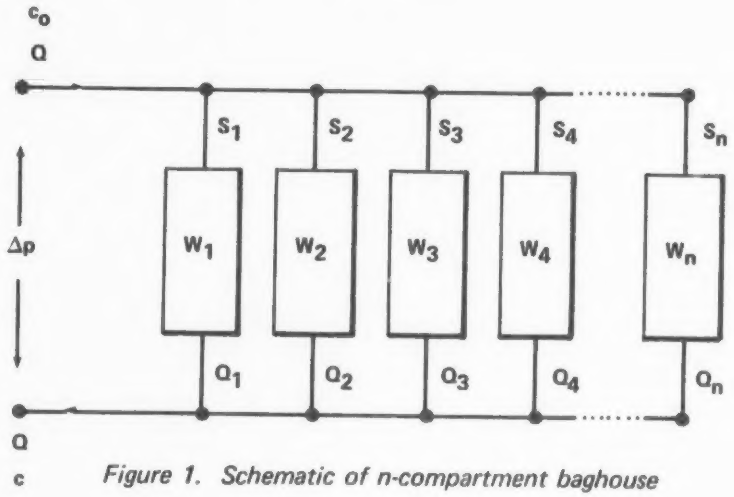

Figure 1. Schematic of n-compartment baghouse

The cloth area required has as its criterion "operation at an acceptable pressure drop across the cloth for a predetermined cycle".[2] One might add that this assumes that the collection efficiency is adequate under these conditions. Thus one important goal is to be able to predict the pressure drop for a particular dust and fabric combination at a given ratio of air flow to cloth area, the face velocity. The drag will depend upon how much dust is on the filter surface, how it is distributed, its geometrical nature in cake form, the geometry of the fabric, and the viscosity of the gas. A second goal is to predict the emissions from such a system.

OUTLINE OF MODEL

A procedure for calculating the pressure/flow relationship and the efficiency of an installation can be developed by subdividing the fabric area into smaller homogeneous sub-units (compartments, bags, or areas on bags) and then doing the following:

1. Calculate the drag (the pressure drop per unit face velocity) for the sub-unit.

2. Determine the flow from the drag and the instantaneous pressure drop.

3. Determine the penetration, the fraction of the particulate concentration reaching the sub-unit which then penetrates to the clean air side.

4. Calculate the emissions rate from the sub-unit (penetration times inlet concentration times volume flow rate).

5. Calculate the new dust loading of the sub-unit.

6. Determine the new pressure drop or the new total flow rate by combining the resistances of the sub-units according to the law for the addition of parallel resistances:

$$Q = \Delta p \frac{A}{S} = \Delta p \sum_{i=1}^{n} A_i / S_i \tag{2}$$

$$S = \left[\sum_{i=1}^{n} A_i / S_i \right]^{-1} A \tag{3}$$

To develop a time profile of the performance, this procedure must be done iteratively, with any cleaning taken into account as well.

Developing this kind of model was our goal. With such a model one should be able to predict the collection efficiency and the relationship between flow and pressure drop for fabric installations for reasonable combinations of variables relating to dust, gas, fabric, and cleaning. Another part of the work at GCA has been laboratory investigations by Dennis _et al._,[3] the results of which have influenced aspects of this model.

MODELS FOR DRAG – BACKGROUND

Much of the work in filtration has been done on systems other than fabric filters. Of the fabric filtration work, most of the predictive modeling has been directed at forecasting the pressure drop given a fabric and dust combination.

Robinson _et al._,[4] for example, produced a three-compartment model. For the increase of drag in any one compartment with increased weight per unit area on the filter, they used the linear drag expression:

$$\frac{\Delta p}{(Q/A)} = S = S_E + K_2 W \tag{4}$$

in which the term S_E is the effective drag, the drag on the fabric obtained by extrapolating the linear portion of the actual drag versus weight curve (S versus W) back to $W \doteq 0$. By solving the equations for the total drag at constant pressure drop for the three-bag system, Robinson _et al._[4] fit the flow rate of the i^{th} bag to:

$$Q_i = a_i t^{x_i} \tag{5}$$

where t_i is the time since last cleaning. They used this flow to obtain the loadings on each bag as a function of time. They combined the individual compartment drags to get the total drag for the system, developing a complicated approximate expression that is only appropriate for a three-compartment system, although the technique can clearly be extended to many-compartment systems.

Solbach[5] also used the linear drag versus weight model, Equation (4). For the case for which the pressure drop, Δp, is fixed but the flow is changing, Solbach[5] expressed the increase of drag due to the increase of the dust loading as

$$dS = K_2\ c\ V\ dt \tag{6}$$

and integrated this to give the velocity of the gas flowing through a single compartment at any time (t = 0 right after cleaning):

$$V = \Delta p / \left[2K_2 c \Delta p t + S_E^2\right]^{1/2} \qquad (7)$$

Solbach extended this to a multi-compartment system by averaging V to obtain the expression:

$$V_{av} = \left(\left[2K_2 c t_c \Delta p + S_E^2\right]^{1/2} - S_E\right) \Big/ K_2 c t_c \qquad (8)$$

This expression is derived assuming constant pressure drop and infinitely many compartments. It is approximately correct (assuming linear drag versus weight) for systems with much more than a few compartments and even for constant flow in such a system rather than for constant pressure drop. (The reason it is nearly correct for a many-compartment system is that the parallel flow arrangement tends to even out the pressure drop changes). One obtains the required total filter area from the total volume flow rate and the average face velocity

$$A = Q/V_{av} \qquad (9)$$

Dennis and Wilder[6] derived an equation for the average drag for a changing pressure drop:

$$S_{av} = (\Delta p)_{av}/V_{av} = S_E + K_2 W_c/2 \qquad (10)$$

$$W_c = c V_{av} t_c \qquad (11)$$

It can be shown that this result and Solbach's agree: in both cases, the average drag is just the drag at half the final cloth loading (W_c).

This is not an exhaustive list of the investigators who worked with linear models, but it is meant to present the linear drag multi-compartment model. We note that the linear models cannot describe the nonlinear part of the performance curves and there remains the problem of obtaining both parameters K_2 and S_E.

To predict K_2, one approach is to use the Kozeny-Carman equation (or variants), as did Williams et al.,[7] a version of which is[8]

$$K_2 = (25/6)\mu(1-\varepsilon)S_p^2/\rho_p\varepsilon^3 \qquad (12)$$

where K_2 = cake resistivity, sec^{-1}
μ = gas viscosity, poise
ε = filter cake porosity (fractional void volume)
S_p = surface-to-volume ratio of particulate material, cm^{-1}
ρ_p = particle density, g/cm^3.

K_2 is quite dependent upon particle size (increasing for smaller particles) and the porosity of the cake deposit (Unfortunately, K_2 is often measured in such English units as (inches WC/fpm)/(lb/ft^2)).

Fraser and Foley[9] took a somewhat different approach, keeping the K_2 particle size dependence (and integrating over the particle size distribution), while using correction factors for particle shape, gas velocity and fabric-surface interaction, following Billings and Wilder.[10]

The effective drag, S_E, is really just an extrapolated value, artificial in that such a drag does not occur at that ($W \doteq 0$) condition, so it is not surprising that there is no theory for predicting it, only correlations. Often one must measure it for the dust and fabric of immediate interest.

The only nonlinear model of drag versus weight of which we are aware was presented by Davis et al.[11] which we learned about after beginning our rather different approach. Davis et al.[11] fit equations of the form

$$S = a\ W^b \tag{13}$$

to data obtained for the nonlinear part of the drag versus weight curve. They found correlation coefficients of greater than 0.90 for 104 of 106 data sets. Davis et al.[11] evaluated this at a loading of 0.0244 g/cm^2 (0.05 lb/ft^2), where their drag data generally became linear with W, to obtain S_E. They found that both a and b could be correlated with K_2, but an analysis of variance did not show that K_2 was different for different fabrics for a given dust, which is as expected, even though contradicting the conclusion of Draemel.[12] The model for drag presented by Davis et al.[11] is useful because it includes the nonlinear, cake-repair zone. The model we present also has this feature, with the advantage that the parameters seem more amenable to theoretical prediction rather than just empirical correlation.

NONLINEAR DRAG MODEL

The linear models of drag versus weight are incorrect for the low dust loading portion of the filtration cycle, during which the flow and the emissions through the bag are the greatest. The new fabric drag is S_0. The conditioned, cleaned fabric drag is S_R at residual loading W_R. Typically, the drag of the filter increases with added weight per area at one rate, K_R, as the conditioned bag collects dust right after cleaning. This rate (which is the slope of S versus W) changes until it reaches a value K_2, after which the rate remains constant (the S versus W curve becomes linear). The linear part of the performance curve starts at loading W_I. An improvement on the linear model would be one that starts with S_R and K_R, approximates the transition to the linear zone, and matches the linear part of the drag curve.

Viewing the filter as an assemblage of pores (rather than cylinders), we assumed that pores which were unclogged ("open") had a different dust resistivity (K_0) than pores which were caked (closed), assumed to have resistivity K_2, as has the cake. We would expect K_0 and K_2 to be different because the velocity in the pores is much higher than through the cake but the particles in the "open" pores are not packed together the way they are in the cake. (Depending upon the magnitudes of such velocity gradient and dust packing effects, K_2 may be greater than K_0 or vice-versa.) By assuming that pores are either caked or open and that the decrease in the population of open pores is proportional to the number of pores still open and to the increase in fabric loading, dW, we obtained the expression:

$$dN = -(1/W^*)\ N\ dW \tag{14}$$

where N = number of open pores per face area of filter
W^* = fabric loading that is characteristic of pore-caking.

The fraction of pores still open at loading W becomes:

$$N/N_0 = e^{-W/W^*} \tag{15}$$

where N_0 is the number of pores per unit area in the fabric when $W = 0$.

If the caked pores and open pores contribute to the drag in proportion to their resistivities and their numbers, then it can be shown:

$$\frac{dS}{dW} = K_0\ f(W) + K_2\ g(W) \tag{16}$$

where $f(W) = \exp^{(-W/W^*)}$ (the fraction of pores which are open)

and $g(W) = 1 - f(W)$ (the fraction of pores which are caked).

By integrating Equation 16 we obtain:

$$S = S_0 + K_2 W + (K_0 - K_2)\, W^*\left(1 - e^{-W/W^*}\right) \tag{17a}$$

in which S_0 is measured new cloth drag; alternately

$$S = S_R + K_2 W' + (K_R - K_2)\, W^*\left(1 - e^{-W'/W^*}\right) \tag{17b}$$

where $W' = W - W_R$, the difference between the loading and the residual loading, W_R, at which $S = S_R$.

We hope to be able to predict K_R and W^* from dust and fabric characteristics, but thus far we too have had to rely on correlations. To show how well this form of equation can fit data from an actual fabric, we present Figure 2, for a glass fabric filtering mica dust and cleaned by shaking, and Figure 3, for Dacron filtering fly ash and cleaned by a combination of shaking and reverse air. Both are fabrics appropriate for high-temperature operations. The optimal choice of W^* produces excellent agreement with the measured values of drag versus weight. The three other such comparisons we made were similarly successful; Tables 1 and 2 give more information about the systems against which the model was compared in our Interim Report to EPA.[16]

To use this model for a variety of filtration systems, we need theoretical equations or predictive correlations for the parameters K_R, S_R, and W^* . . . assuming we have the usual information about the fabric (permeability, from which comes S_0) and dust (resistivity, K_2).

The value of K_R is expected to depend upon the dust, the fabric, and the cleaning, so we thought it might correlate with K_2 for the dust and S_0 for the fabric for cleaning by shaking. We calculated (K_2/K_R) for data on glass,[13,15] Dacron,[13,14,6] and Nomex[14] fabrics. (Aerosols of mica and fly ash were used with the glass and the Dacron filters; the Nomex tests were with fly ash). The correlation was

$$K_R = 515\, K_2\, S_0^{\,1.035} \tag{18}$$

where S_0 is in the units inches WC/fpm and K_R, K_2 are in inches WC-ft-min/lb. Similarly, correlations for the same five fabric-dust combinations gave:

$$S_R = 6.2\, S_0^{\,1.445} K_2^{\,0.747} \tag{19}$$

(residual drag increases with fabric drag and dust resistivity), and

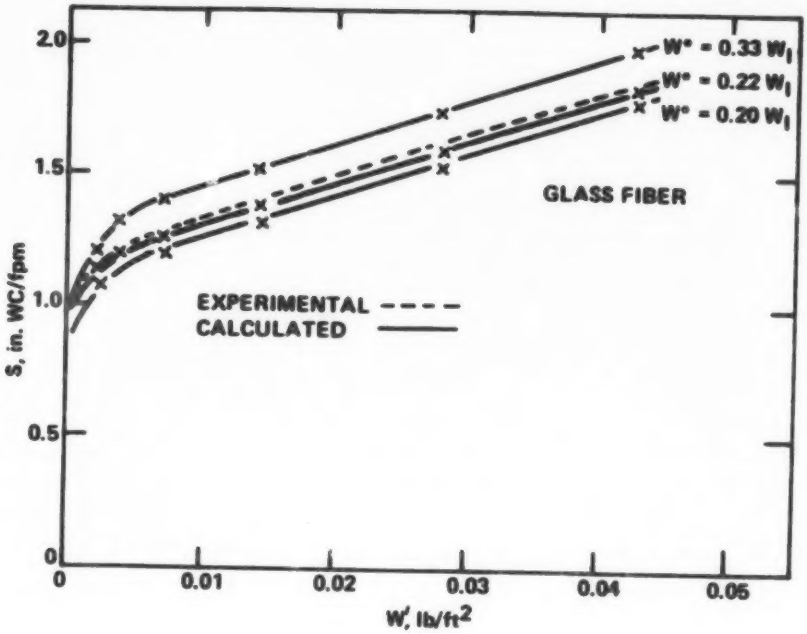

Figure 2. Theoretical and experimental curves of glass fiber filter

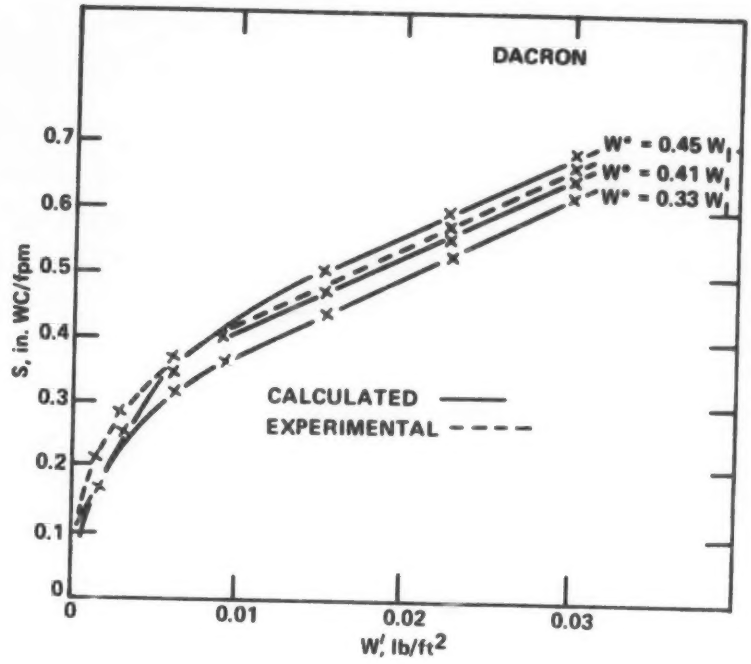

Figure 3. Theoretical and experimental curves of Dacron-type filter

TABLE 1. TECHNICAL DATA - FABRIC FILTERS SELECTED FOR VERIFICATION[16]

Type of Fabric	Weight, oz/yd^2	Weave and Yarn Count	Fraser Permeability, ft^3/min 0.5 in. H_2O	Reference
Glass fiber	9.06	3/1 crowfoot, filament 55 × 58	7.9	Spaite and Walsh[13]
Polypropylene	4.30	3 × 1 twill, filament 74 × 33	15.0	Durham[14]
Dacron	10.0	Plain, staple 30 × 28	55.0	Dennis and Wilder[6]
Cotton	10.0	Unnapped sateen 95 × 58	13.0	Dennis and Wilder[6]
Polyacrylester	9.8	2 × 2 twill, spun 39 × 35	60.0	Durham[14]

TABLE 2. EXPERIMENTAL DATA - FABRIC FILTERS SELECTED FOR VERIFICATION[14]

Fabric Type	K_2	K_R	S_R	W_1	Type of Cleaning	Dust Type	Remarks	Reference
	in. WC-ft-min/lb		in. WC/fpm	lb/ft^2				
Glass fiber	16.0	400.0	0.84	0.0036	Shaking	Wet ground mica	Conditioned, velocity 2 ft/min	Spaite and Walsh[13]
Polypropylene	6.1	135.4	0.35	0.0135	Shaking	Fly ash	Conditioned, velocity 4 ft/min	Durham[14]
Dacron	12.4	93.8	0.08	0.0066	Shaking and reverse air	Fly ash	Used fabric, velocity 3 ft/min	Dennis and Wilder[6]
Cotton	15.0	72.0	0.5	0.0075	Shaking and reverse air and shaking only	Fly ash	Velocity 3 ft/min	Dennis and Wilder[6]
Polyacrylester	4.6	26.3	0.05	0.030	Shaking	Fly ash	Conditioned, velocity 4 ft/min	Durham[14]

$$W^* = 7.68 \times 10^{-4}/K_2^{0.913}\ S_0^{0.945} \qquad (20)$$

(pore caking requires more material for rather open fabrics and more coarse dusts). Again, the parameters are in English units (W is in lb/ft^2 and K is in the units of S/W).

It should be mentioned, at least in passing, that data from the reported measurements of K_2 we used were better correlated with the inverse of particle mass median diameter than the inverse squared as might be expected from the Carman-Kozeny equation[16]) and showed a face velocity effect (as has been reported before[17]).

To sum up: the form of our nonlinear expression fits quite well that data for which we evaluated it. The parameters in the model should be theoretically predictable, a problem on which we are working, but until they are, one can use correlations such as those presented here. Such a model promises to be an improvement on the linear model because it can describe that part of the filter performance for which flow and emissions are greatest, the low-loading, nonlinear part.

EFFICIENCY MODELS – BACKGROUND

Before presenting our model for woven fabric filtration efficiency as a function of particle size, we will discuss several recent efforts in that direction.

A theory of particle collection by clean cylindrical fibers was adopted by Fraser and Foley[9] for the evaluation of the collection filter efficiency, expressed as a function of three collection mechanisms. They used an equation derived by Davies[18] for low gas velocity ($Re \sim 0.2$) and single cylinders, incorporating impaction, interception and diffusion. Then, they applied a correction factor to the single fiber efficiency γ to account for the effect of the neighboring fibers

$$\gamma_M = (1 + 4.5\beta) \qquad (21)$$

to obtain the total collection efficiency. The penetration for a fiber was expressed as:

$$Pn = \exp\left[\frac{-4\beta\ \gamma_M\ L}{\pi d_f (1-\beta)}\right] \qquad (22)$$

Due to the difficulties related to the precise measurement of the fiber diameter, they used an effective fiber diameter, derived by Davies:[18]

$$d_f = \left[\frac{70\ \eta_g \beta^{1.5} L(1 + 52\beta^{1.5})}{\Delta p}\right]^{\frac{1}{2}} \tag{23}$$

(The filter packing density is β, its thickness is L, and the gas viscosity is η_g.) That model of the penetration of the particles through the clean fiber filter was extended to the dusted fabric filter under the assumption that the main effect of the dust on the fabric itself is to change the effective fiber diameter. An equation for the change of the thickness of the filtering layer during the filtration cycle was developed by assuming that the dust fills up first the free volume of the filter (at the packing density of the dust) before building up the dust cake. The residual dust loading was expressed as a function of a cleaning parameter and permeability.

The collection efficiency used in that model was based on the calculation of particle trajectories around a single fiber, derived by Davies[18] for a clean fiber with a very small diameter. It is doubtful that the same equation will hold for fiber filters having fiber diameters $\sim 10^2$ μm. If we assume the average face velocity of 2 cm/sec (4 ft/min), with fly ash particles having a diameter of 10 μm, fiber diameters approximately 800 μm (which is an average yarn size) and filter packing density around 0.3, then the Stokes number equals 0.02, a lower value than the critical Stokes number, below which the impaction mechanism does not contribute to collection efficiency. (Also under such conditions the diffusion parameter is negligible.) Then the penetration for the particles would be 0.99, considering the interference effect of neighboring fibers to be $(1 + 4.5\ \beta)$. Modeling the fabric filter as an array of cylinders does not seem successful thus far.

Leith and First Model

By using tagged fly ash aerosols, Leith and First[19] were able to distinguish between those fly ash particles which, under laboratory conditions, penetrated a needled felt fabric filter immediately and those particles which exhibited a delay in their penetration. These researchers postulated three types of penetration mechanisms: direct penetration, gradual seepage of the dust, and the breakage and penetration of plugs of material in the vicinity of pinholes.

The experiments were done at face velocities from 5 cm/sec (10 fpm) to 15 cm/sec (30 fpm) for dust cakes up to 60 μm thick. These velocities are higher than those in normal use for the filtration of fly ash (~1 cm/sec) and these cake thicknesses are rather low. The efficiency as a function of particle size was such that the penetration was found to "remain relatively constant for particles from 0.3 to 4.0 micrometers in diameter". The penetration increased with face velocity. From their figures for mass flux versus time (at 10 cm/sec) we conclude:

1. Straight through mass flux seemed to decrease (roughly exponentially) with deposit thickness, but may have gone through a minimum near 20 μm thickness.

2. Seepage mass flux remained fairly constant with time and deposit thickness.

3. Pinhole plug mass flux decreased with increasing deposit thickness.

The fraction of the total penetration which was due to pinhole plugs and seepage was greater than the direct (straight through) contribution (at 60 μm thickness) for 15 cm/sec but substantially less than the direct for 10 cm/sec, which suggests the emissions due to seepage and pinhole plugs might be very much less than the direct at 1 cm/sec (2 fpm).

Leith and First[19] postulated the following functional forms for the three types of penetration:

1. Direct penetration proportional to e^{-aX^b}, where X is the deposit thickness.

2. Constant seepage mass flux versus thickness of deposit.

3. Pinhole plug mass flux proportional to Xe^{-cX} (in which a, b, c, are proportionality factors).

The correlations they found in using these equations ranged from 0.86 to 0.91 correlation coefficients, for mechanism-by-mechanism comparison, adding support for their proposed mechanisms.

Leith and First[19] found only a weak particle size dependence for efficiency, with the efficiency decreasing slightly as particle size increased. The particle size dependence, the velocity dependence, and their general appraisal of the filtration process led them to conclude:

> "Because media filtration theory does not describe the trends in penetration found in a fabric filter, and was not developed for the operational conditions found there, it should not be used to predict or interpret the penetration characteristics of fabric filters."

This conclusion underscored the need for a new approach to the prediction of fabric filter efficiencies, especially for woven fabrics.

A NEW MODEL FOR FABRIC FILTER COLLECTION EFFICIENCY

As indicated by our review of former models, most treatments of filter collection efficiency were not for fabric filters but for other kinds of filters. The synthesis attempted for fabric filters by Fraser and Foley[9] used as its basis formulas for collection on cylinders. Because of the overlapping caused by weaving and the closeness of the yarns, the flow in a fabric filter is very unlike that of a cylinder in a uniform flow stream, the starting point for models of filtration based on collection by cylinders. Rather, the fabric produces a flow which is directed through the interstices of the weave at and near the intersections of the yarns. This much more resembles flow to an array of apertures than it does flow around single or grouped cylinders. Because the nature of the flow has a strong bearing on the collection efficiency, one expects a pore model to be inherently better than models which start from a cylinder or an array of cylinders.

Our analysis fits into a baghouse simulation model outlined in the flow chart in Figure 4. Once the starting data are put into the simulation, the program calculates flow, pressure drop, fabric loading, penetration, and emissions as a function of time for the bags in the simulated baghouse. This section discusses the equations and analysis which went into calculating the emissions.

Collection Mechanisms

The model can calculate the fraction of incoming particles which are captured in the cake, in the fabric, and in the pinholes which go through cake and fabric. The collection mechanisms modelled are impaction, interception, and diffusion.

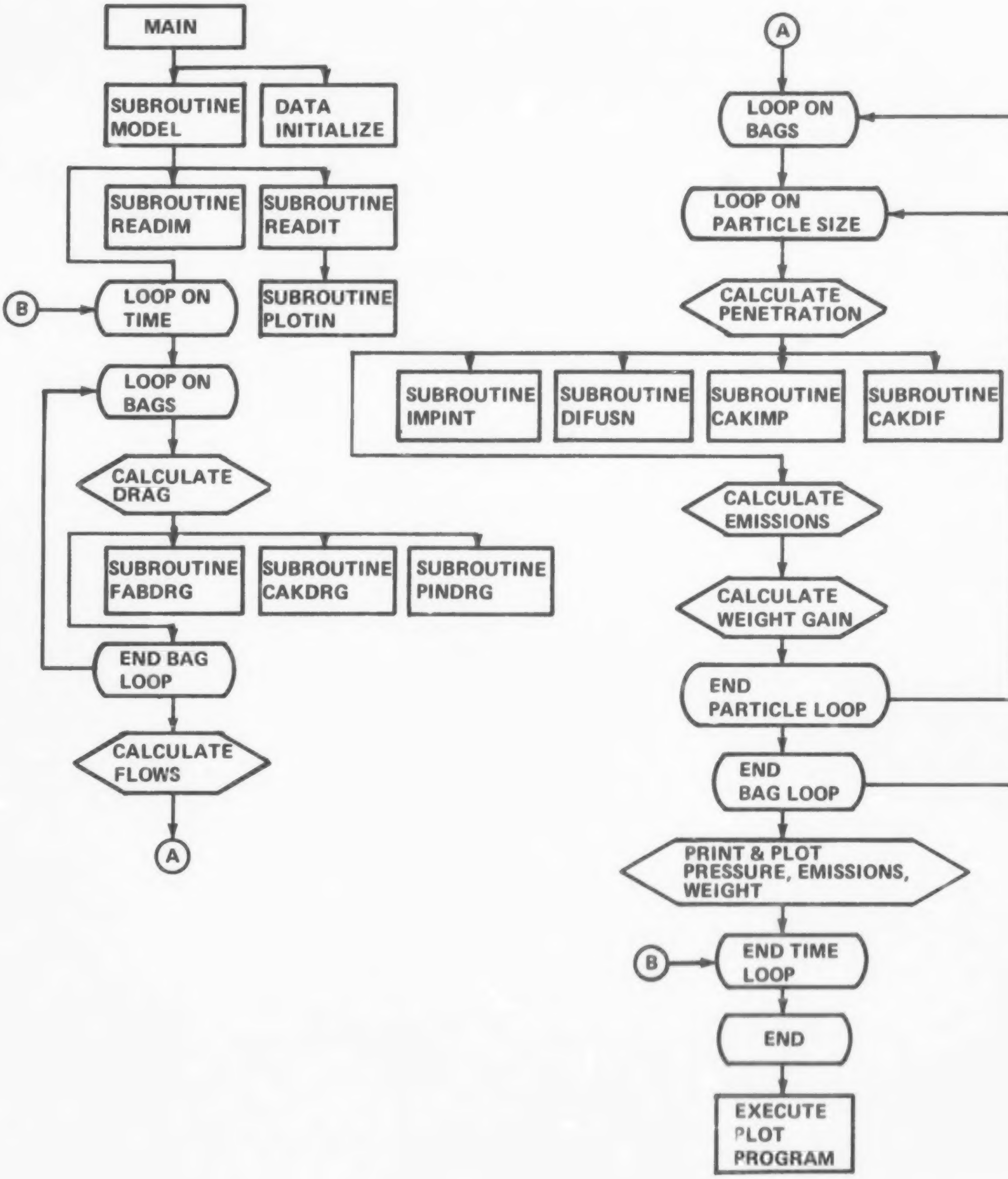
MAIN
SUBROUTINE MODEL
DATA INITIALIZE
SUBROUTINE READIM
SUBROUTINE READIT
SUBROUTINE PLOTIN
B
LOOP ON TIME
LOOP ON BAGS
CALCULATE DRAG
SUBROUTINE FABDRG
SUBROUTINE CAKDRG
SUBROUTINE PINDRG
END BAG LOOP
CALCULATE FLOWS
A
A
LOOP ON BAGS
LOOP ON PARTICLE SIZE
CALCULATE PENETRATION
SUBROUTINE IMPINT
SUBROUTINE DIFUSN
SUBROUTINE CAKIMP
SUBROUTINE CAKDIF
CALCULATE EMISSIONS
CALCULATE WEIGHT GAIN
END PARTICLE LOOP
END BAG LOOP
PRINT & PLOT PRESSURE, EMISSIONS, WEIGHT
B
END TIME LOOP
END
EXECUTE PLOT PROGRAM

Figure 4. Baghouse simulation program flow chart

Collection by Impaction, Interception, and Diffusion in the Cake. The particulate material collected by the fabric filter builds up first in the vicinity of the pores. As it builds, this deposit starts to form a cake through which a substantial portion of the flow passes, and particles are captured by the particulate matter of the cake. We seek to model the capture of particles by the filter cake. The geometry is quite complex where polydisperse aerosols are involved. The uncertainties are so great with regard to geometry that available information warrants only an approximate model. We have formed such a model on the basis of analysis of characteristic time scales, characteristic lengths, etc.

An idealized view of the filter cake is shown in Figure 5. The cake is viewed as a series of layers, with a total thickness L, in cm. The cake thickness is given by

$$L = W/\rho_p(1 - \varepsilon) \tag{24}$$

in which W = particle loading, g/cm^2
ρ_p = particle material density, g/cm^3
ε = void volume fraction, porosity.

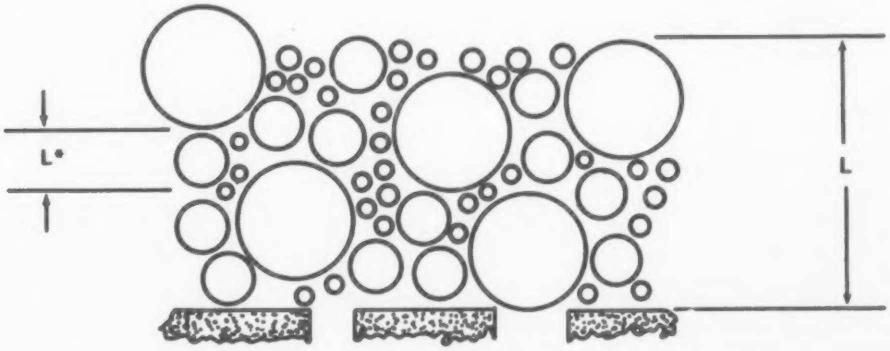

Figure 5. Fabric filter cake, resting on fabric

By taking the number of particles and dividing it into the volume of the cake, we can get the mean volume of cake per particle, thus the mean thickness of each layer:

$$L^* = \left[\pi/6(1 - \varepsilon)\right]^{1/3} \text{VMD} \tag{25}$$

in which VMD = particle volume mean diameter, cm.

Assuming that the number of void volumes in the cake is equal to the number of particles, we have the following void volume mean diameter, d_v:

$$d_v = \left[\varepsilon/(1 - \varepsilon)\right]^{1/3} \text{VMD} \tag{26}$$

The mean velocity in the open portions of the cake is given by:

$$\bar{U} = v_f/\varepsilon \tag{27}$$

in which v_f = face velocity, cm/sec.

A characteristic velocity for flow through the cake is the face velocity divided by the porosity, $\bar{U}$. A characteristic dimension over which the flow changes direction is the mean diameter of a void, d_v.

The inertial parameter (Stk, the Stokes number) can be defined from these equations as:

$$\text{Stk} = \bar{U}\tau/d_v \tag{28}$$

This parameter determines how large inertial impaction may be. We make the simple assumption (e.g., see Fuchs[20]) that the impaction efficiency of a single cake layer is approximately equal to the Stokes parameter at each void volume (up to Stk = 1):

$$E_{Ii} \doteq \text{Stk} \quad (E_{Ii} \leq 1) \tag{29}$$

The likelihood that a particle will penetrate through one void volume is just one minus the efficiency:

$$Pn_{Ii} = 1 - \bar{U}\tau/d_v \tag{30}$$

(τ is defined by Equation 46) and the likelihood of penetrating M such volumes (i.e., through M layers) is:

$$Pn_I = (1 - Pn_{Ii})^M. \tag{31}$$

(This assumes that the collection efficiency of each void volume in the cake through which the aerosol flows is independent of the earlier portions of the flow path.) The number of such layers is approximately the thickness of the cake, L, divided by the mean distance between particles forming the cake, L*, the mean layer thickness:

$$M \doteq L/L^*. \tag{32}$$

Interception is the collection contribution due solely to the size of the particles compared with the dimensions of the flow channels. Even if the particles follow the streamlines of the flow, those with centers on streamlines which come within a particle radius of an obstacle will strike the obstacle and be captured (it is assumed). We can approximate the likelihood of penetration in passing through the ith layer as that for passage through a cylindrical channel of diameter d_v:

$$Pn_{Ci} = (1 - d_p/d_v)^2 \tag{33}$$

and from this we derive an approximate expression for the penetration of a particle through the dust cake of thickness L by:

$$Pn_C = (1 - d_p/d_v)^{2\ L/L^*}. \tag{34}$$

The Brownian motion of particles causes them to diffuse in a concentration gradient so as to transport particles from higher concentration regions to lower. In the presence of a surface to which the particles adhere, there will be a net diffusive flux of particles to the surface due to this mechanism. The equation governing this diffusion for a flowing aerosol is given by:[8]

$$\frac{\partial n}{\partial t} + \vec{v} \cdot \vec{\nabla} n = D\, \vec{\nabla}^2 n \tag{35}$$

in which n = number concentration of particles of diameter d_p
$\vec{v}$ = flow velocity
D = particle diffusivity
$\vec{\nabla} n$ = gradient operator
$\vec{\nabla}^2$ = Laplacian operator

For systems of interest it is usually true that the convective term, $\vec{v} \cdot \vec{\nabla} n$, is negligible. Within a void volume this equation becomes approximately:

$$\Delta n/n \doteq D\Delta t/(0.5\ d_v)^2 \tag{36}$$

for the capture due to diffusion. The time, Δt, is the characteristic flow length divided by a characteristic flow:

$$\Delta t = d_v/\bar{U} \tag{37}$$

As before, for M (=L/L*) layers in the cake, the penetration becomes:

$$Pn_D = (1 - 4\ D/\bar{U}\ d_v)^{L/L^*}. \tag{38}$$

As Fuchs has noted,[20] there is no simple way for combining correctly the collection efficiency terms (or, equivalently, the penetration expressions). Commonly, the mechanisms are treated as operating independently, in which case the penetration becomes the product of the penetrations:

$$Pn = Pn_I \, Pn_C \, Pn_D \, . \tag{39}$$

We have used this approach in our model.

Impaction and Interception at a Pore or Pinhole. Near the intersections of the fabric yarns are openings which we call pores, the geometries for which are discussed in the Interim Report by Dennis et al.[3] and, to an extent, in Appendix A of our report.[16] It has been observed that often a fraction of such pores, and/or pores caused by other means, stay open during the filtration cycle. We denote them "pinholes". Our model simplifies both pores and pinholes into circular cylindrical channels in the fabric (and in the cake as well, for pinholes). The task then becomes to calculate the collection efficiency of such an array of channels.

Spurny et al.[21] presented calculations for a somewhat similar situation in their analysis of membrane and nuclepore filters, modeled as a highly porous array of parallel circular cylindrical channels. It can be shown that their equations for impaction do not go to the correct limits for low-porosity structures, which is our situation for fabric filters having a few percent or less free area.

Smith and Phillips[22] found numerical solutions to the problem of the collection efficiency of an aperture due to impaction and interception, but they included only capture at the face of the material having the orifice and not along the walls of the channel, which can be shown to be substantial in our context.

Thus, although we could use equations available in the literature for collection due to diffusion in a channel, we did not have applicable equations for impaction and interception of particles by the pores and pinholes and had to derive approximate expressions, discussed next.

Figure 6 shows the geometry of the model. The pore (channel, orifice, etc.) has a radius (or equivalent radius) R^* and a length L_p. The opening is one of several and the area $\pi R_0{}^2$ is the total face area divided by the number of pores, distributed approximately uniformly. The face velocity, v_f, far away from the pore, is just the flow through the pore, Q_p, divided by the area per pore:

$$v_f = Q_p/\pi R_0{}^2 \tag{40}$$

The flow is simplified by dividing it into three regions (see Figure 6):

I. In this region (radial distance, r, greater than R_0) there is a uniform face velocity toward the plane of the opening, and the face velocity is given by:

$$v_f = Q_p/\pi R_0{}^2 \tag{41}$$

II. In this region (radial distances: $R^* \leq r < R_0$) the flow is the same as it would be in potential flow to a point sink, being directed radially toward the center of the pore face, with the velocity at distance r governed by:

$$v(r) = v^*(R^{*2}/r^2) \tag{42}$$

in which

$$v^* = Q_p/2\pi R^{*2} \tag{43}$$

III. In the third region ($r < R^*$) and within the channel there is assumed a uniform flow profile.

Of course, this set of flow profile assumptions is somewhat different from what actually would take place. Still, far away from the pore opening the flow would generally be uniform; there would be an intermediate range for which the flow would be approximately that toward a point sink at the center of the orifice; and converging flow at the orifice would be expected to produce a rather uniform flow profile near the entrance before the typical parabolic flow was established for laminar flow conditions. Thus the flow model preserves many of the features of a more rigorous solution of the flow velocity field.

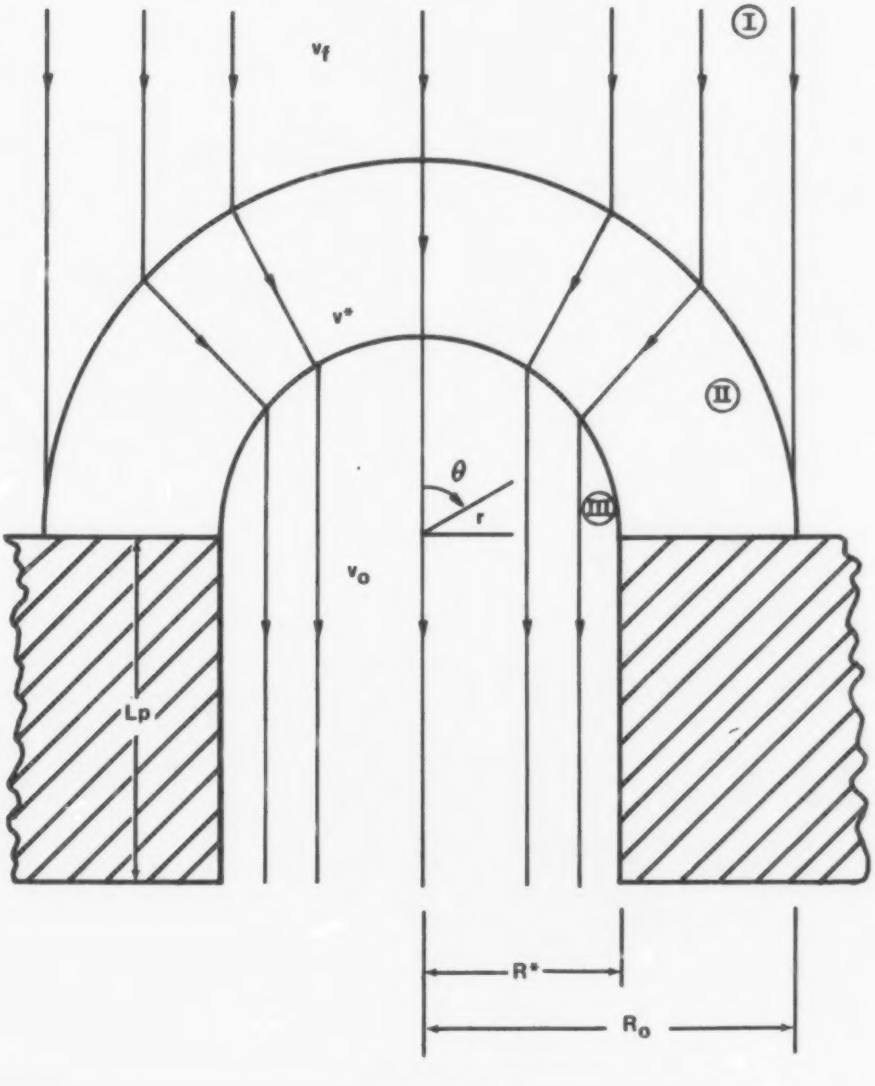

Ⓘ
v_f
v*
Ⓘⅰ
θ
r
Ⓘⅲ
v_o
Lp
R*
R_o

Figure 6. Schematic of flow model for analysis of impaction and interception

A particle with an initial velocity of v_f will travel a distance L'_{sI} in a stationary medium, with L'_{sI} given by:[20]

$$L'_{sI} = L_{sI}(1 - e^{-t/\tau}) \qquad (44)$$

where

$$L_{sI} = \tau v_f \qquad (45)$$

$$\tau = C\rho_p d_p^2/18\mu \qquad (46)$$

in which C is the Cunningham slip correction, ρ_p is the particle density, and d_p is the particle diameter. The variables L_{sI} and τ are the particle stopping distance and particle relaxation time,[20] and t is the time.

We will not give more details of the rather complex method used by us to obtain efficiency due to impaction. Essentially it involved comparing the stopping distances (L_s', including mean residence times in regions II and III) with the distance a particle would have to travel to strike the face of the pore or the inner wall, keeping track of particles which were captured in one region so as not to double-count them in capture in subsequent regions.

The other mechanism considered was diffusion to pore and pinhole walls. The formulas for the decrease in particle concentration in traversing a tube while diffusing have been presented by Fuchs.[20] The concentration decreases approximately exponentially with the parameter μ as the argument:

$$\mu = D L_p/V_0 R^{*2} \qquad (47)$$

in which the particle diffusivity is D. The approximate formula for μ much less than 1 is:[20]

$$Pn = 1 - E = 1 - 2.56 \mu^{2/3} + 1.2 \mu + 0.177 \mu^{4/3} \qquad (48)$$

Summary of Model Equations. The essential aspects are the collection mechanisms of impaction, interception, and diffusion as applied to the filter fabric, the cake, and pinholes in fabric and/or cake.

RESULTS OF MODELING OF FABRIC FILTRATION SYSTEMS

Introduction

This portion will present some of the results we have obtained in modeling fabric filtration systems with an initial emphasis on coal-fired power plants using fabric filtration, such as the Sunbury plant that was one of the subjects of the Interim Report by Dennis et al.[3] The order is as follows:

1. Q and Δp versus time for a 15-bag system, using a linear drag model.
2. Collection efficiency versus particle size and time for a single bag with linear drag.
3. Collection efficiency versus particle size and time for a single bag with nonlinear drag.
4. Collection efficiency versus particle size and time for a three-bag system, using nonlinear drag.

Flow Modeling

In Reference 16 we presented the computer program for our model. The drag equation used was linear:

$$S = S_E + K_2\ W \qquad (49)$$

$$W = cVT \qquad (50)$$

where S_E = 0.5 in. WC/fpm = 2.5 cm WC/(cm/sec) = 250 $(N/m^2)/(cm/sec)$
K_2 = 11 in. WC/fpm/lb/ft^2
= 1.1 $(N/m^2)/(cm/sec)\ (g/m^2)$
c = 5 gr/ft^3 = 11.5 g/m^3
t = time since cleaning, minutes.

Either V was constant (2 fpm = 1 cm/sec face velocity) or it was obtained from the pressure drop and the drag. Each bag was cleaned instantaneously (to the residual weight level) every 30 minutes, one bag cleaned per 2 minutes. The results are shown in Figures 7 and 8, where the information is plotted every minute so that we are getting an instantaneous reading at two points in the cycle, just after cleaning and midway between cleanings. From Figure 7, we see that after about two complete cycles (60 minutes), the pressure drop has come into dynamic equilibrium, with a minimum near 1.4, a midpoint about 1.45, and an (inferred) maximum about 1.5 in. WC (375 N/m^2). For 15 bags, the range of pressure drop values is much less than for one bag, as we expected.

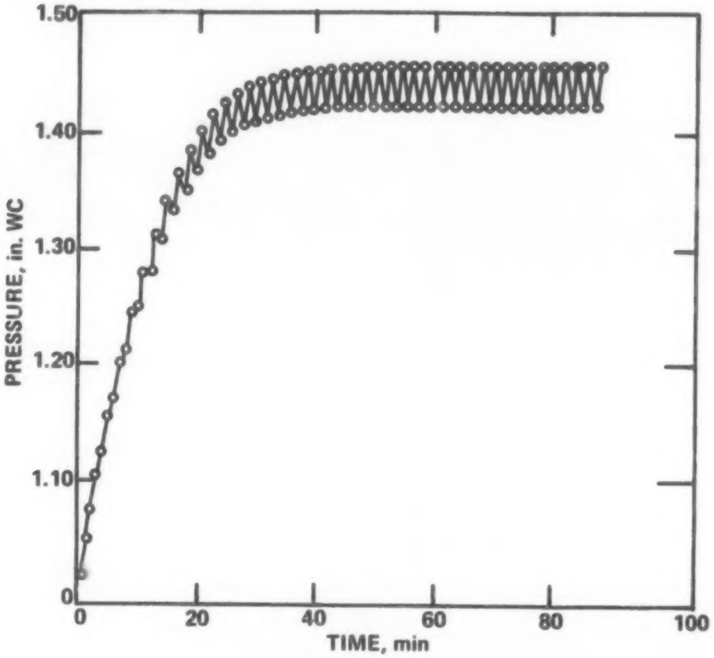

Figure 7. Test run No. 5: 15-bag simulation pressure versus time graph

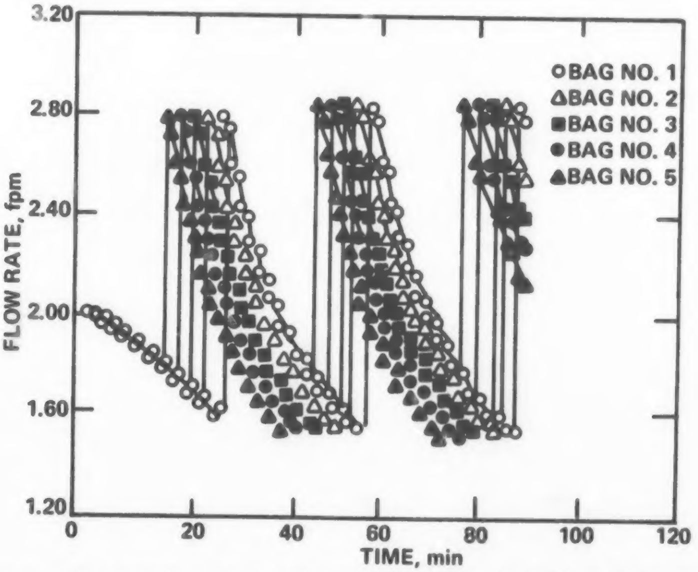

Figure 8. Test run No. 5: baghouse simulation individual flow rate graph

Because the many-bag system greatly reduces the pressure drop variations with time, we can approximate this new system as follows: even though the total system is one with a constant total flow, it behaves, bag-by-bag, almost as though each bag is kept at a constant pressure drop (and has a variable flow). This is significant, in turn, because we have available to us the general expression governing the relationship between drag and time (thus flow and time) for a bag with constant pressure drop and variable flow, which we presented as Equation 8, from Solbach.[5]

Figure 8 shows the flow rate for bags No. 5 to No. 1 (the cleaning order was from No. 15 to No. 1). The total flow rate remained constant, but the individual flow rates declined for these bags as they accumulated more weight than the other bags in the system, which were being cleaned before them. When it became the turn of bag No. 5 to be cleaned, its flow rate increased, while the others continued to drop. This process repeated itself with the other bags, and it is interesting to note that their flow rate versus time curves all look very much the same except for being displaced in time.

Efficiency Modeling

Figure 9 shows the results of modeling the collection efficiency of a single bag with the program discussed above and shown in Figure 4.

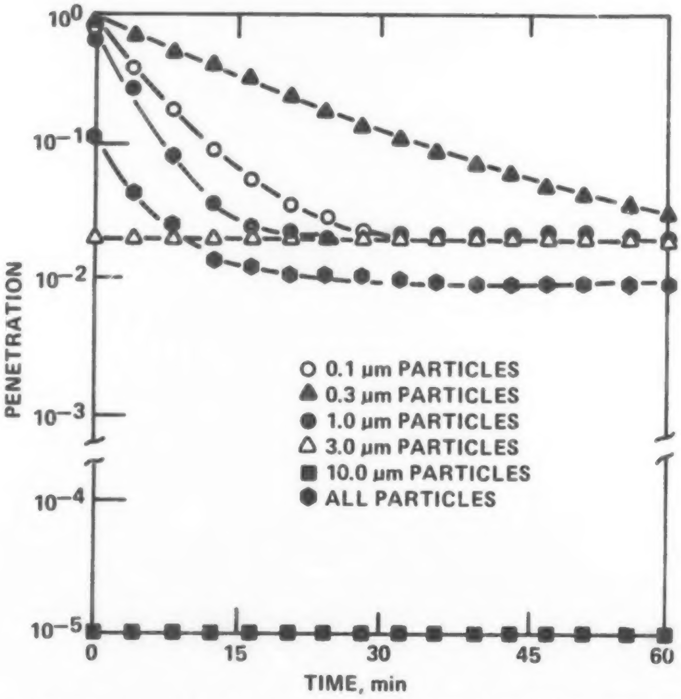

Figure 9. Test run No. 13a baghouse simulation penetration

The conditions for these results are listed as part of the program output, shown in Table 3. Volume flow rate per unit area was 2 fpm (1 cm/sec). The pore (fabric opening) sphere of influence radius is just the radius of a circle of area equal to the area per pore in the fabric. The pore radius is the equivalent open area radius of the pores. The pore length is the yarn thickness. Density is the particle density ρ_p, chosen to be one (the density of fly ash would have been a better choice). S_0 and K_0 were not used, but rather S_E and K_2 were the same values as above. Gas viscosity was that appropriate for temperature of 350°K (= 77°C = 171°F); a higher temperature would probably be more appropriate for coal-fired systems. The caked area (fraction of filter from which the cake is not removed by cleaning) was set to zero. The pinholes, which never close during the filtration cycle, were given the same radius of influence as the pores, with a radius estimated as twice the size of a typical pore, and with a number per unit area corresponding to about 2 per square inch (see Dennis *et al.*[3]) The cake dust was assumed to have a volume mean diameter of 5 μm and a porosity of 0.5. In Table 4 we give approximate size distribution for the Sunbury fly ash (Dennis *et al.*[3]) used to approximate the inlet particle size distribution; this is log normal with a mass median aerodynamic diameter of 6 μm and a geometric standard deviation of 3.0. The values 0.1, 0.3, 1.0, 3.0, 10, 30 μm have been used as the midpoints of equal logarithmic intervals (geometric means of the intervals) for the size distribution. The penetration results in Figure 9 are plotted on semilogarithmic scale. The penetrations are weighted by the mass fraction values in Table 4 to give the curve marked "all particles".

TABLE 3. TEST RUN NO. 13A BAGHOUSE SIMULATION INPUT DATA

Number of bags:	1 bag
Cycle time:	60 min
Number of increments per cycle:	15 increments
Velocity, Q/A:	1 cm/sec
Concentration:	1.142×10^{-5} g/cm^3
Initial drag resistance, S_E:	2.5×10^3 dyn/cm^2/cm/sec
Cake resistance coefficient, K:	1.12×10^5 dyn/cm^2/cm/sec/g/cm^2
Pore sphere of influence radius:	4.78×10^{-2} cm
Pore radius:	2.5×10^{-3} cm
Pore length:	4.0×10^{-2} cm
Yarn radius:	2.0×10^{-2} cm
Particle density:	1.0 g/cm^3

(continued)

TABLE 3. (continued)

Gas viscosity: 2.08×10^{-4} poise
Cake porosity: 0.5
Temperature: 350°K
Caked area (uncleaned fraction): 0.0
Pinhole radius of influence: 4.78×10^{-2} cm
Pinhole radius: 5.0×10^{-3} cm
Particle volume mean diameter: 5.0×10^{-4} cm
Number of pinholes per cm^2: 0.31

Particle information:

Diameter, cm	Mass Distribution	Slip Correction	Diffusion Constant, cm^2/sec	Relaxation time (τ), sec
1.0×10^{-5}	0.00	2.87	7.02×10^{-6}	7.79×10^{-8}
3.0×10^{-5}	0.01	1.56	1.27×10^{-6}	3.82×10^{-7}
1.0×10^{-4}	0.12	1.16	2.85×10^{-7}	3.16×10^{-6}
3.0×10^{-4}	0.32	1.05	8.51×10^{-8}	2.58×10^{-5}
1.0×10^{-3}	0.38	1.02	2.49×10^{-8}	2.75×10^{-4}
3.0×10^{-3}	0.17	1.01	8.21×10^{-9}	2.46×10^{-3}

TABLE 4. APPROXIMATE SUNBURY FLY ASH SIZE DISTRIBUTION
(mass median aerodynamic diameter = 6 μm, $\sigma_g \doteq 3$)

Size Interval, μm	Logarithmic Midpoint, Geometric Mean, μm	Aerosol Mass In Size Interval, %
17 -52	30	17
5.2 -17	10	38
1.7 -5.2	3.0	32
0.52 -1.7	1.0	12
0.17 -0.52	0.3	1
0.052-0.17	0.1	<<1

The particle size with the greatest penetration (of those tested) is 0.3 μm diameter, which is in accord with experimental results from many different fibrous filtration studies. The initially linear slope on this scale (semilogarithmic) is consistent with an exponential decay as the cake gets thicker (recall this is constant velocity, thus the rate of cake build-up is constant). Once the region is reached where much of the flow and virtually all of the penetration is that through the pinholes which do not cake, the penetration becomes nearly constant with cake thickness. A substantial fraction of the 0.3 and 1.0 μm particles penetrate the clean fabric, but then each of these decreases toward an asymptote as the pinhole penetration predominates. The 3 μm particles apparently penetrate only the pinholes and this penetration does not change appreciably during the cycle. The 10 and 30 μm particles do not even penetrate the fabric or the pinholes at all ($Pn < 10^{-5}$) so that the cake buildup does not affect them; they are caught by inertial impaction and by interception by fabric pores and by pinholes. The mass penetration, "all particles", starts at about 10% and rapidly declines to about 1%. The leveling off of the curve for total mass penetration indicates that this penetration is almost wholly due to pinholes, and it will thus be quite sensitive to the assumptions made about the pinhole population. (The pressure drop versus time, which follows the linear model, went from 2.5 cm WC (1 in. WC) to about 7 cm WC (about 2.7 in. WC), reasonable values.)

Figure 10 has penetration versus time curves for the same situation except that the nonlinear model of drag was used. We started with an initial drag which was roughly that of the Sunbury fabric (S_0 = 0.05 in. WC/fpm), then used the correlations developed above to get the ratio of K_2 to K_R from S_0, K_R/K_2 = 12.5, and to get $W^* = 0.004$ lb/ft^2 = 0.002 g/cm^2. The efficiency curves are very similar to those for the linear drag model, except that the initial rapid change in pressure drop somewhat changes the distribution of the flow between the fabric plus cake and the pinholes, shifting the flow more rapidly to the pinholes, thus producing a bit of increase in the penetration of the 3 μm particles initially, before their penetration becomes effectively independent of time. Again, major features include the maximum penetration by the 0.3 μm diameter particles, the initial exponential decrease for those particles being filtered out primarily by the cake, and the important role of the pinholes as the cake becomes thick.

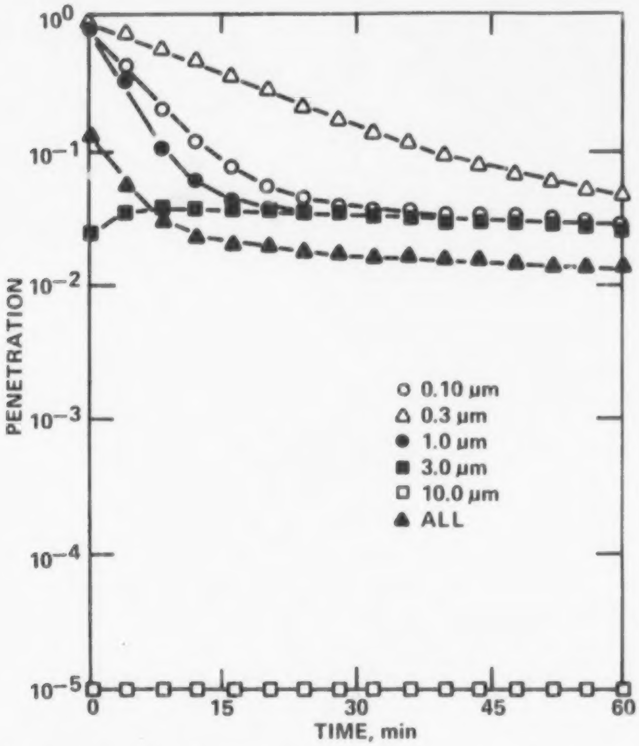

Figure 10. Test run No. 13b: baghouse simulation penetration versus time graph; single bag, nonlinear drag, with pinholes

To demonstrate further the impact of the pinholes, we repeated the last test (nonlinear drag, etc.) but removed the pinholes, so that all the flow is through fabric pores or cake only. Figure 11 is the penetration without pinholes. The most marked difference is that collection efficiency for all particle sizes now continues to decrease as the cake thickens, and this efficiency becomes better than 99% by mass for the particles within 10 minutes. The 0.3 μm penetration is still greatest. The 0.1, 0.3, and 1.0 μm particles all show an exponential decrease with cake thickness now. The 3 μm particles show more rapid changes in collection at the beginning part of the cycle, where pressure drop is changing most rapidly, and this is typical for other collectors where inertial impaction is the predominant mechanism, as it is for these 3 μm particles.

The final figure in this series is Figure 12. Here we have used three bags rather than one, the same nonlinear drag parameters as before, and we have restored the pinholes. First, the bags all have the same flow rate, then after one is cleaned, only two have the same flow rate, and the third is much higher in flow. Finally, all three have been cleaned once, and a pattern develops which will repeat itself.

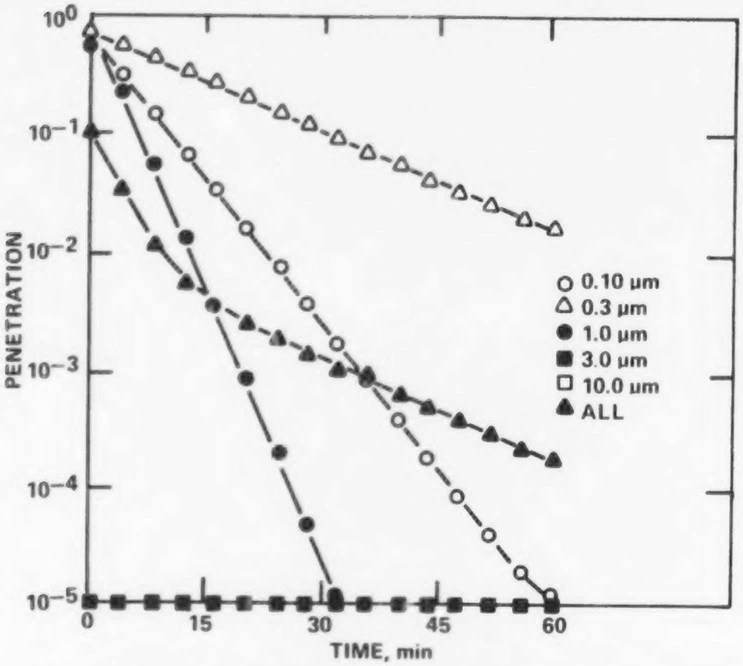

Figure 11. Test run No. 15 baghouse simulation penetration versus time graph; single bag, nonlinear drag, without pinholes

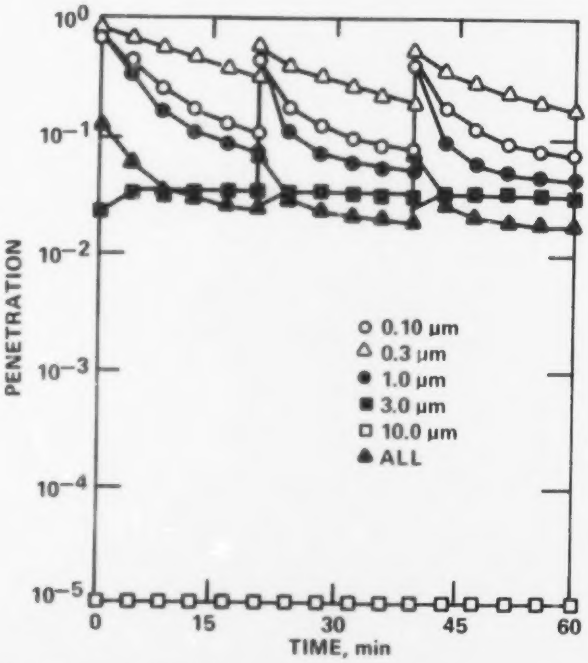

Figure 12. Test run No. 16 baghouse simulation penetration versus time graph; three bags, nonlinear drag, with pinholes

Figure 12 shows the changing pattern for particle penetration versus time with particle size as a parameter. The relative order of penetration with respect to size is the same, and we also still see the change of the penetration for the 3 μm particles as pressure drop changes. Finally, the asymptote provided by the pinhole mechanism is evident. The three-bag system with nonlinear drag produces nearly the same total mass penetration as the one-bag system after 15 minutes, but the cleaning process then returns one of the bags to low efficiency and high flow rate, producing a major increase in penetration for the total system.

Calculator Model for Drag

In some cases, a quick and approximate estimation of an average air-to-cloth ratio of a baghouse unit is necessary or satisfactory. Therefore, we tried to derive a simple equation for calculating an average air-to-cloth ratio. For our derivation we used an expression for the average face velocity (air-to-cloth ratio), $\bar{V}$, which was derived by Solbach[5] and independently also by Dennis and Wilder.[6] This expression is based on the linear drag model. The average face velocity is given by Equation (8):

$$\bar{V} = \frac{1}{K_2\ ct_c}\left[\sqrt{2K_2\ ct_c\Delta p + S_E{}^2} - S_E\right] \tag{51}$$

where K_2 = dust resistivity, in. WC-min-ft/lb

c = dust concentration, lb/ft^3

t_c = total filtration time, min

Δp = pressure drop across the baghouse, in. WC

S_E = effective drag, in. WC/fpm.

If we express the effective drag, S_E, as a function of the clean fabric drag, S_0, by[16]:

$$S_E = 7.4\ S_0{}^{0.672}\ , \tag{52}$$

and K_2 as a function of particle mass median diameter, d_p, by[16]:

$$K_2 = 142.4\ d_{p50}{}^{-1.06}\ . \tag{53}$$

the Equation (51) becomes:

$$\bar{V} = \frac{-7.4\, S_0^{\,0.672} + \sqrt{54.76\, S_0^{\,1.344} + 284.8\, d_{p50}^{\,-1.06}\, \Delta p\, c t_c}}{142.4\, d_{p50}^{\,-1.06}\, c t_c} \qquad (54)$$

Then, using industrial data for Δp, d_p, S_0, c and t_c, shown in Table 5, we calculated the face velocity (air-to-cloth ratio) for each baghouse. These values are shown in Table 5 along with the operating industrial values of the face velocity. (Sources of the data are listed elsewhere.[16]) The ratios of operating to predicted velocities are very close. The average of all values of that ratio was 2.29 so that we have a corrected estimate, $\bar{V}'$, of the average face velocity:

$$\bar{V}' = \bar{V}/2.29 \qquad (55)$$

The differences between corrected predicted and operating values were within ± 15%. More data would be needed to improve the reliability of our last equation, obviously.

FINAL COMMENTS

What is presented here seems the most detailed model yet of a fabric filtration system, and it has sufficient flexibility to have added to it a number of refinements as our information warrants.

The areas which seem most in need of further study are cleaning and seepage. Regarding cleaning, we would like to know the amount and spatial distribution of the residual dust as a function of cleaning type, intensity, duration, and frequency for several dust/fabric combinations, especially those of applicability to controlling fossil-fuel boiler emissions. Regarding seepage, we would like to know what variables affect the rate at which it occurs and what the relationships are. Of course, the application of fabric filtration does not require such information, but the optimization of fabric filtration does.

Accurate methods for prediction of fabric filter drag and collection efficiency would greatly aid the design of optimal fabric filter systems. By viewing the fabric as an array of apertures rather than an array of cylinders, we have been able to derive expressions describing the nonlinear dependence of filter drag on fabric dust loading and the collection efficiency of the fabric and the dust cake as functions of particle size. Much work remains to be done, especially regarding cleaning of fabrics, but we believe that this new approach can provide a useful framework for future development as well as yielding useful insights concerning the factors which determine drag and collection efficiency. As the model is improved and as more data from operating

TABLE 5. PARAMETERS FOR FIVE BOILERS USING FABRIC FILTRATION

Plant	Clean Cloth Fraser Permeability, fpm, 0.5 in. H_2O	Dust Concentration, gr/ft^3	Total Filtration Cycle Time, min	Pressure Drop, in. H_2O	Particle Mass Median diameter, μm	Operating Velocity, fpm	Velocity Predicted by Eq. 54 V, fpm
Pennsylvania Power and Light Co., Sunbury Station, Pa.	54.3	2.	33	2.5	8	1.92	3.90
Colorado UTE Electric Assoc., Nucla Power Station, Colo.	86.2	1.93	29.4	4.2	8	2.79	6.50
Sorg Paper Co., Middletown, Ohio	55.0	3.2	30	4 - 5	12	2.07	6.10
Crisp County Power Commission, Cordele, Georgia	55.	2.6	60	4.	12	2.2	4.69
Pennsylvania Power and Light Co., Holtwood Station, Pa.	45 - 65 (50)	7.7	33	6.5	10*	2.26	4.66

*Assumed values.

systems are incorporated, it is hoped we will have a method which will facilitate the application of fabric filtration to the problem of obtaining power economically with minimal environmental impact.

ACKNOWLEDGEMENTS

We appreciate the help we received from our colleagues at GCA, especially the computer programming done by Roger Stern and the comments and information given us by Richard Dennis. This program has been funded through EPA Contract No. 68-02-1438. The project officer is Dr. James H. Turner, Industrial Environmental Research Laboratory - Research Triangle Park, N.C.

REFERENCES

1. Jorgensen, R. Fan Engineering, 7th ed, Buffalo, N.Y., Buffalo Forge Co., 1970.

2. Snyder, C.A. Ind. Eng. Chem. Process Des. Dev. 47:960, 1955.

3. Dennis, R., R.W. Cass, and J.E. Langley. Development of Data Base and Fabric Filtration Models for Design of Particulate Control Systems. Environmental Protection Agency, Research Triangle Park, N.C. Contract No. 68-02-1438, Interim Report for Task 5.1, Dec 1975. 119 pp.

4. Robinson, J.W., R.E. Harrington, and P.W. Spaite. Atmos. Environ. 1:499-508, 1967.

5. Solbach, W. Staub (English) 29(1):28-33, 1969.

6. Dennis, R., and J. Wilder. Fabric Filter Cleaning Studies - Appendix J. EPA-650/2-75-009, U.S. Environmental Protection Agency, Washington, D.C., 1975.

7. Williams, C.E., T. Hatch, and L. Greenberg, Heating, Piping and Air Conditioning 12:259-263, 1940.

8. Bird, R.B., W.E. Stewart, and E.N. Lightfoot. Transport Phenomena, New York, Wiley, 1962.

9. Fraser, M.D., and G.J. Foley. A Predictive Performance Model for Fabric Filter Systems: I - Intermittently Cleaned Single-Compartment Systems. Presented at 67th Annual Meeting of APCA, Denver. 1974.

10. Billings, C.E., and J. Wilder. Handbook of Fabric Filter Technology. Vol. I. Fabric Filter Systems Study. NTIS PB 200648, USDHEW, Washington, D.C., 1970.

11. Davis, W.T., K.E. Noll, and P.J. LaRosa. A Predictive Performance Model for Fabric Filtration Based on Pilot Plant Studies. Proceedings of the User and Fabric Filtration Equipment II, Specialty Conference APCA, Niagara Falls, N.Y. 1975.

12. Draemel, D.C. Relationship Between Fabric Structure and Filtration Performance in Dust Filtration. EPA-R2-73-288, U.S. Environmental Protection Agency, Washington, D.C., 1973.

13. Spaite, P.W., and G.W. Walsh. Amer. Ind. Hyg. Assoc. J. 24:357-365, 1963.

14. Durham, J.R. Filtration Characteristics of Fabric Filter Media. NAPCA, PHS, USDHEW, Interim Report, 1969.

15. Dennis, R. Reported Experimental Measurements, GCA Tests, 1975.

16. Cooper, D.W., V. Hampl, and R. Stern. Development of Data Base and Fabric Filtration Models for Design of Particulate Control Systems. Environmental Protection Agency, Research Triangle Park, N.C. Contract No. 68-02-1438, Interim Report for Task 5.3, January 1976.

17. Borgwardt, R.H., R.E. Harrington, and P.W. Spaite. J. Air Pollution Control Assoc. 18(6):387-390, 1968.

18. Davies, C.N. Proc. Inst. Mech. Eng. 1B(5):185-213, 1952.

19. Leith, D., and M.W. First. Particle Collection by Pulse-Jet Fabric Filter. Presented at 68th Annual APCA Meeting. Boston. 1975.

20. Fuchs, N.A. Mechanics of Aerosols, New York, Pergamon, 1964.

21. Spurny, K.R., J.R. Lodge, Jr., E.R. Frank, and D.C. Sheesley. Environ. Sci. Technol. 3:453-469, 1969.

22. Smith, T.N., and C.R. Phillips. Environ. Sci. Technol. 9:564-568, 1975.

PAPER 10

OPERATING EXPERIENCE AND PERFORMANCE AT THE SUNBURY BAGHOUSE

Harry Spagnola
Pennsylvania Power & Light Company

James H. Turner
Environmental Protection Agency
Industrial Environmental Research Laboratory

PLANT – GENERAL DESCRIPTION

The Sunbury Steam Electric Station of Pennsylvania Power and Light Company is located on the west bank of the Susquehanna River in Shamokin Dam, Pennsylvania. It generates 402 MW of electricity from six pulverized-coal-fired steam generators and four turbine-generator sets. Turbines Nos. 1 and 2 are each rated at 87.5 MW. Steam is supplied to these turbines through a header system from Foster Wheeler anthracite-fired boilers. (A Foster Wheeler bituminous-fired boiler and a 110 MW turbine-generator set are also connected into this header system.) Each of the four boilers is rated at 415,000 lb/hour steam flow at 955°F and 1350 psig and was placed in commercial service in 1949. The boilers burn a mixture of anthracite (silt and No. 5 buckwheat), petroleum coke, and bituminous coal. (Typical analysis of the plant coal is given in Table 1.) The mixture varies considerably according to the availability and the quality of the fuel. The normal mix is 75% anthracite (consisting of 90% silt and 10% No. 5 buckwheat), 20% coke, and 5% bituminous coal. The normal fuel consumption is 25 tons per hour per boiler. No. 2 fuel oil is used for boiler fire-ups and to stabilize ignition.

TABLE 1. TYPICAL PLANT COAL ANALYSIS

	Anthracite	Bituminous	Petroleum Coke
Heating Value (wet basis) (Btu/lb)	8,680	12,159	14,054
% Ash	28.0	15.3	1.7
% Moisture	16.4	5.3	6.4
% Volatile Matter	8.4	27.1	13.3
% Sulfur	0.8	2.6	5.3

PARTICULATE REMOVAL EQUIPMENT

Original particulate removal equipment consisted of a mechanical-electrostatic precipitator set. Particulate removal efficiency with this equipment was 90%. In 1973 baghouses were installed on each of the four anthracite-fired boilers. The electrostatic precipitators were gutted due to a weight consideration. The weight reduction allowed utilizing some of the existing precipitator steel to support the baghouse. The mechanical collectors were modified by replacing the original vanes of the multicone collectors with new, less efficient vanes. The effect of this was a reduction of mechanical collector efficiency from 78% to 70%, while the pressure drop decreased from 4.5 in. VWC to 1.5 in. VWC. The mechanical collectors were left in to maintain a lower dust loading on the induced draft fans. It is not certain to what degree, if any, they improve baghouse performance.

The baghouses are installed in series with the mechanical collectors. The flue gas, after leaving the boiler economizer, passes through regenerative air heaters, mechanical collectors, the induced draft fans, and the baghouse. The then clean flue gases discharge to atmosphere through a stack, 300 feet above the ground. (Figure 1)

The baghouses were constructed by Western Precipitator Company. They were initially put into service on the following dates:

No. 1A Baghouse – February 10, 1973
No. 2B Baghouse – March 5, 1973
No. 2A Baghouse – April 14, 1973
No. 1B Baghouse – April 26, 1973

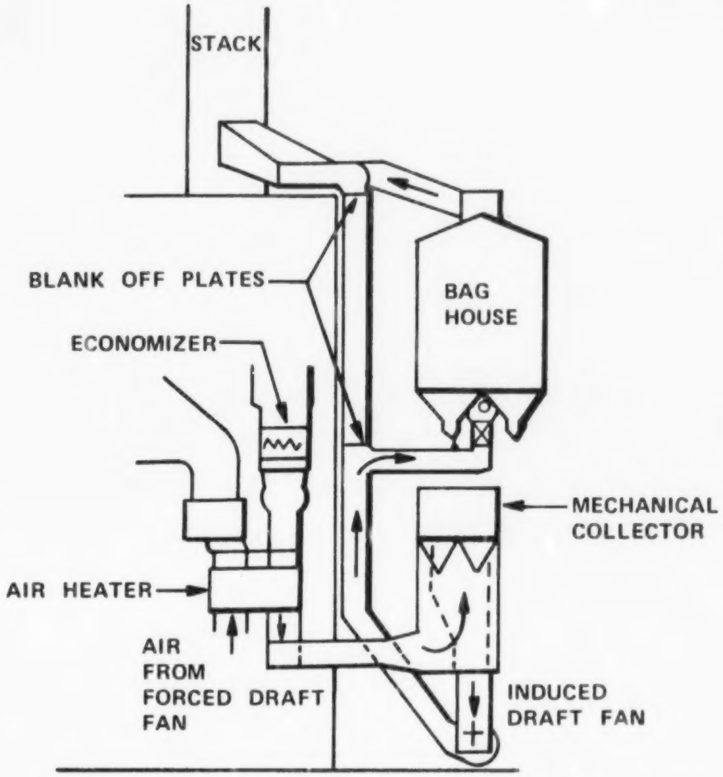
STACK
BLANK OFF PLATES
BAG HOUSE
ECONOMIZER
MECHANICAL COLLECTOR
AIR HEATER
AIR FROM FORCED DRAFT FAN
INDUCED DRAFT FAN

Figure 1. Location of dust removal equipment

BAGHOUSE – GENERAL DESCRIPTION

Each baghouse is approximately 80 feet long, 40 feet wide, and 62 feet high, including the dust hoppers. Each baghouse consists of 14 compartments arranged in two rows of seven compartments each. Each filter bag compartment is 19 ft, 9 in. wide × 10 ft, 1-3/4 in. long × 40 ft high. The baghouse enclosures, including the interior partitions, are constructed of 14-gauge mild steel and are of all welded construction. The 14-gauge partitions and welded construction were decided upon to insure gas tight construction to permit the safe entering of isolated compartments for routine inspections and minor maintenance while the baghouse is in service.

The entire baghouse including the hoppers, collapsing flues, and inlet/outlet flues up to the point of tie-in with the existing breeching are completely heat insulated and aluminum lagged. The bag filter dust hoppers, located below the thimble floor, are contained in an enclosure constructed of 0.032 in. thick aluminum siding over steel girts. The floor in the hopper enclosure is checker plate in order to contain any ash which may spill during maintenance periods or should malfunctions occur in the ash removal system.

Access for maintaining the filter bags is accomplished in the following manner. A 2-ft wide × 5-ft high insulated compartment access door is provided at the thimble floor elevation for each compartment. A checker plate walkway constructed of 3/16-in. steel plate is provided through the center of the filter bag rows (three rows of 15 filter bags each are located on each side of the walkway) to facilitate changing filter bags as well as to permit inspection to detect broken bags. A 2-ft wide × 5-ft high insulated compartment access door and grating walkway are provided in each compartment for access to the filter bags at the bag tensioning framework elevation.

An inlet flue and a collapse air flue run the length of each baghouse between the rows of hoppers. Side ducts from each flue to the individual compartments are provided to the upper portion of the compartment ash hoppers. The gas inlet damper and the collapse air damper, both timer-operated, are located in the gas inlet flue and the collapse flue, respectively, to permit cycling the compartments through the in-service and cleaning cycles. There is one main collapse fan for each baghouse and two spare collapse fans, each serving two baghouses.

The outlet flue surmounts the baghouse and ties into the existing stack breeching. Each compartment has a manually operated outlet flue damper which permits isolating a compartment during maintenance periods. (See Figure 2 for the baghouse's general arrangement.)

Vent stacks were installed on the top of each baghouse compartment in 1974 and 1975. Originally isolating a baghouse compartment was difficult. Since the gas inlet damper, a leaf type damper, does not provide a positive shut off, too much heat and gas leaked into the compartment. With a portable 7,000 cfm fan mounted on the vent stack, enough ventilation is provided to permit entry into the compartment for maintenance with the remainder of the baghouse in service. The vents are 2 ft × 2 ft × approximately 4 ft high, constructed of 10-gauge mild steel and are covered with 2-in. thick insulation and 0.032-in. thick aluminum siding. A spring clamped cover is mounted on top of each vent stack (Figure 3).

Filter Bags

The design filter ratio was 1.919:1 cfm/ft^2 of bag and the active filter ratio (based on one compartment being out of service at all times) was 2.067:1. Each baghouse compartment contains 90 bags for a total of 1,260 bags per baghouse, giving a total filter area of 115,668 ft^2.

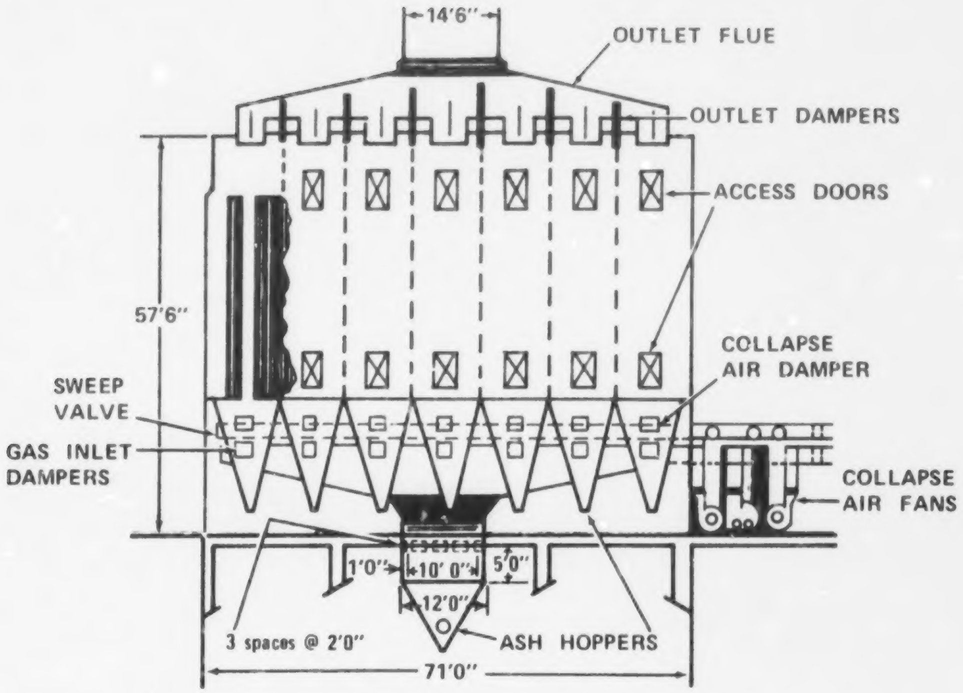
14'6"
OUTLET FLUE
OUTLET DAMPERS
ACCESS DOORS
57'6"
COLLAPSE AIR DAMPER
SWEEP VALVE
GAS INLET DAMPERS
COLLAPSE AIR FANS
1'0"
10' 0"
5'0"
12'0"
3 spaces @ 2'0"
ASH HOPPERS
71'0"

Figure 2. Baghouse general arrangement

Each filter bag is 11½ in. in diameter by 30 ft, 4 in. in length. The filter bags, Menardi Southern Company's style No. 601T, are made of glass fiber with Tuflex finish (Teflon base; specifications are listed in Table 2). The Teflon coating acts as a lubricant between the glass fiber filaments. It prevents the glass fiber filaments from abrading one another, and thus lengthens bag life. Each filter bag contains seven equally spaced anti-deflation rings. With the rings preventing the bag from collapsing completely during the cleaning cycle, the dust cake is released freely and drops to the hopper below. A metal band is sewn into the top and bottom of the bags for installing the bags. The bags are suspended from a framework in the top of each compartment housing and approximately 50 lb. tension is applied.

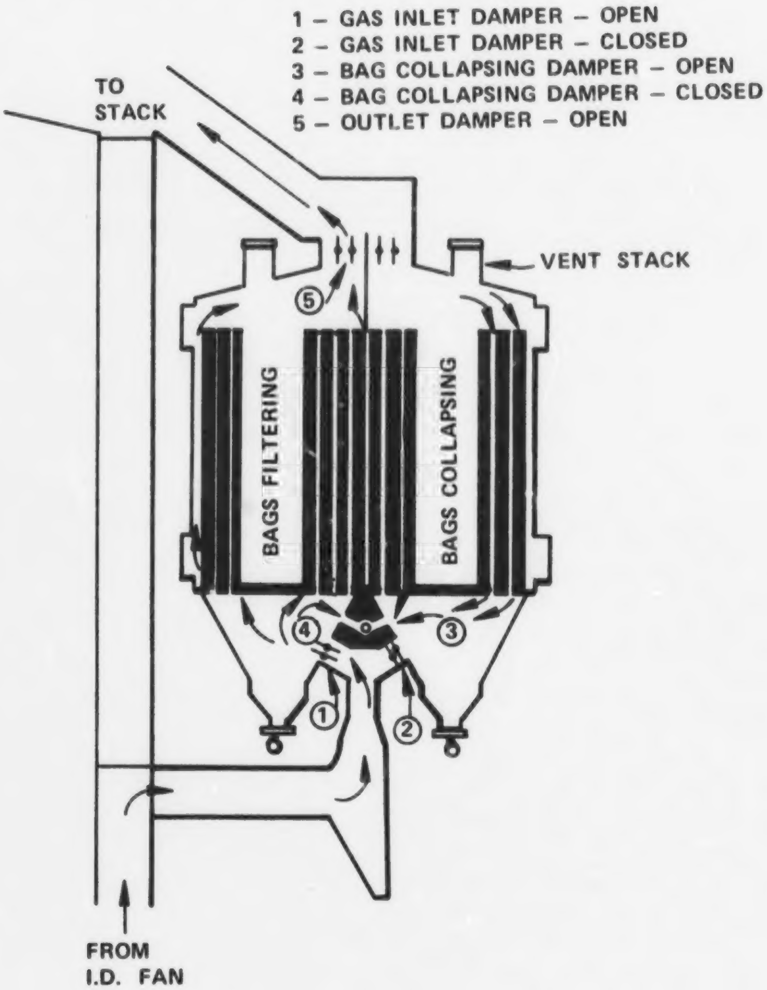

1 – GAS INLET DAMPER – OPEN
2 – GAS INLET DAMPER – CLOSED
3 – BAG COLLAPSING DAMPER – OPEN
4 – BAG COLLAPSING DAMPER – CLOSED
5 – OUTLET DAMPER – OPEN
TO STACK
VENT STACK
BAGS FILTERING
BAGS COLLAPSING
①
②
③
④
⑤
FROM I.D. FAN

Figure 3. Gas flow through baghouse compartments during normal operation and cleaning

TABLE 2. MENARDI FILTER BAG, STYLE NO. 601T

Fabric	Glass Fiber
Average Permeability	38.5
Mullen Burst Strength (av psi)	595
Weight (oz/yd^2)	10.0
Thread Count	54 × 30
Weave	3 × 1 Twill
Finish	Teflon 10% by weight
Warp Yarn	150's 1/2
Fill Yarn	Bulked 1/4

Cleaning Cycle

The bags are cleaned by reversing the gas flow through a compartment. This partially collapses the bags; some of the dust cake is then released and falls to the hopper below. A collapse fan (12,500 cfm @ 300°F and 10 in. VWC Buffalo Forge Company size 60, 1300 rpm) provides the force for the reverse gas flow. The collapse air flow is drawn through the collapse duct and into the collapse fan, and then is discharged into the baghouse inlet flue, where any entrained fly ash is filtered by the bags (Figure 2).

Each compartment is cleaned in the following manner:

1. The gas inlet damper to the compartment closes, shutting off the flow of "dirty" flue gas to this compartment.
2. The collapse damper opens, allowing a reverse flow of "clean" flue gas from the outlet flue to be pulled through the bags, which partially collapse, and thus are cleaned.
3. The collapse damper closes.
4. The gas inlet damper opens, returning the compartment to the filtering mode. (Figure 3 illustrates a compartment in the filtering mode and a compartment in the cleaning mode.)

This sequence is repeated on each of the 14 compartments. Twice during the 14-compartment cycle the collapse duct is swept clean. This is accomplished by opening a sweep valve located at the end of the collapse duct (Figure 2). This allows ambient air to be drawn through the collapse duct and fan, and thus purge any fly ash accumulation.

The time sequence of the cleaning and sweep cycles is detailed in Table 3. There are null periods between the operation of the gas inlet and collapse air damper. This is done to prevent reentrainment by allowing for some settling time for suspended fly ash; and also, to prevent a sudden reversal of air flow through the bags, which would put undue stress on the bags. The air-operated dampers are provided with a slow opening and closing device which also prevents any additional stress on the bags.

TABLE 3. CLEANING/SWEEP CYCLE TIME SEQUENCE

		Elapsed time, sec
I.	Clean compartments 1 through 7 one at a time	
	Gas Inlet Damper starts to close	0
	Gas Inlet Damper closed	2.0
	Collapse Air Damper starts to open	16.0
	Collapse Air Damper open	17.0
	Collapse Air Damper starts to close	68.0
	Collapse Air Damper closed	69.5
	Gas Inlet Damper starts to open	81.0
	Gas Inlet Damper open	83.0
	Next Gas Inlet Damper starts to close	122.0
II.	Sweep Collapse Air Duct	
	Last Compartment Gas Inlet Damper open	0
	Sweep Valve open	40
	Sweep Valve closed	120
	Next Compartment Gas Inlet Damper open	165
III.	Clean compartments 8 through 14 one at a time.	
	Repeat cycle shown under I	
IV.	Sweep Collapse Air Duct	
	Repeat cycle shown under II	

Instrumentation

Two instruments, a Bailey bolometer and a differential pressure recorder, are used to monitor baghouse performance continuously.

The bolometer consists of a light bulb and a receiver located in the breeching to the stack on each boiler. The receiver output varies as the light intensity striking it varies, and thus is an indication of smoke density. A 24-hour recorder located in the plant monitors this signal. A reading of zero of scale indicates no smoke and a reading of 100% of scale indicates 100% smoke. The bolometers are not calibrated and just give a relative indication of smoke density.

The differential pressure across each baghouse is recorded on a 24-hour recorder located in the plant control room. The taps are located in the baghouse inlet and outlet flues. An audible alarm is sounded if the differential pressure rises 1 in. VWC above its normal value, giving the operator time to take corrective action.

The differential pressure across each compartment is not monitored. It was decided that a continuous monitoring system would be too costly and of questionable value. There are taps across each compartment but no instruments were installed to indicate differential pressure.

Controls and Alarms

The four baghouse control panels are located in the plant mill room. Each control panel houses two cleaning cycle timers (one of which is a spare), a stepping switch, a cycle timer selector switch, a collapse fan selector switch, a control power "off-on" switch, and the compartment's status indicating lights.

The cleaning control timers and the stepping switch control the cleaning cycle, operating the air-operated baghouse gas inlet and collapse air dampers by activating the appropriate solenoid valves. The cleaning cycle control timers were originally electromechanical devices. Solid-state electronic timers were added in 1975 and 1976 to facilitate adjustment in the cycle time and increase the reliability.

The compartment status lights indicate the positions of the baghouse gas inlet and collapse air dampers. These indicate whether a compartment is in the filtering or the cleaning mode. Indication is accomplished through the use of limit switches on the dampers.

Adjacent to the baghouse control panels are alarm panels with alarms to indicate a collapse fan failure or a cleaning cycle timer failure.

Baghouse Vacuum Cleaning System

Individual vacuum cleaning systems are provided for each baghouse. Vacuum connections have been provided in each bag filter hopper enclosure as well as outside the compartment access doors at the thimble floor elevation.

Baghouse Ash Removal System

The two fly ash removal systems, one per unit, are United Conveyor Corp. vacuum type which pneumatically convey fly ash from the ash hoppers. Air flow required for conveying the ash is produced by an 8-ft Hydroveyor exhauster. The ash/air mixture is transported by the conveyor to the Hydroveyor exhauster, where the mixture is combined with water to form an ash slurry. This slurry is discharged into an air separator tank where the conveying air is vented to atmosphere while the ash slurry discharges by gravity into the Units Nos. 1-2 slurry tank.

High pressure (300 psi) water at a rate of 750 gpm is provided at the Hydroveyor for each system by one of three new raw water booster pumps. Plant ash disposal capabilities were increased by the duplication of the existing fly ash disposal system and also the installation of two new 2,000 gpm raw water pumps. The new fly ash disposal system is composed of one ash slurry tank, an ash slurry pump house, six slurry pumps (in series) 1600 gpm capacity and over 2 miles of 10-in. buried steel pipe through which the slurry is pumped to the fly ash settling basin.

OPERATION

The flue gas enters the baghouse at 350°F and leaves at 310°F. The flue gas temperature normally stays within this range, except during boiler startups and shutdowns, when the temperatures are in a lower range, anywhere from ambient air temperatures to normal operating temperature. Several times since 1973 the regenerative air heater drives have failed. This has caused the baghouse inlet temperature to rise as high as 510°F. The high temperatures were sustained for about 1 to 2 hours. There were no discernible effects on the bags.

The design pressure drop across the baghouse and baghouse duct work was not to exceed 6 in. VWC, which was dictated by the capacity of the existing induced draft fans. Average draft loss across the baghouses is as follows:

Baghouse No.	Av Draft Loss (in. VWC)	Bags Installed
1B	3.5	4/26/73
2A	3.5	11/20/74
2B	3.0	2/23/75
1A	2.5	3/20/75

The baghouses are on the discharge side of the induced draft fan and thus are under a positive pressure.

The gas flow through each baghouse is 222,000 acfm at a temperature of 325° F. Baghouse inlet grain loading is approximately 2 gr/ft^3.

There is no visible stack discharge from any of the baghouses, except for vapor condensation during the coldest days of the year (approximately 10° F or lower). When a large bag failure occurs (e.g., a 2 to 3-ft tear in a single bag) there will sometimes be a very faint stack discharge (approximately 5% opacity or less) depending on the location of the bag failure.

Boiler Start-Ups and Shutdowns

To prevent blinding of the bags with the oil used during boiler fire-ups, before a new set of bags is placed in service they are precoated with fly ash remaining in the boiler gas passes. The boiler is brought on the line and the baghouse cleaning cycle is not activated until one hour after coal is fired. This allows an additional coating to form on the bags.

Each boiler is shut down and fired-up several times a year. Other than the precoating of new bags, no special precautions are taken. During normal fire-ups, shutdowns, and outages, the cleaning cycle is left on. The continued cleaning during outages does not remove the initial fly ash coating but will prevent the formation of a thick cake, which can accumulate from moisture carryover while water lancing boiler slag deposits.

The number of fire-ups for each boiler is given below.

Boiler No.	1973	1974	1975
1A	6	3	2
1B	3	5	2
2A	3	3	5
2B	7	3	3

Operating Problems

The major operational problem has been occasional baghouse high differential pressure. An alarm sounds to warn the operator of the high differential. The usual causes are either collapse fan failure, cleaning cycle timer failure, or gas inlet or collapse air damper failure. Once the problem is corrected, the differential pressure returns to normal in a short time, approximately 30 minutes. Normally the problem is corrected without affecting boiler operation. However, if the differential increases to approximately 5 or 6 in. VWC, the boiler steam flow must be reduced due to the loading on the induced draft fans.

Baghouse problems infrequently (about 5 or 10 times per year for all baghouses) have required reductions in boiler load of about 20,000 to 40,000 lb/hr steam flow, but have never forced a boiler off the line.

At present there are no alarms for collapse fan failure. Flow switches were installed in the collapse fan duct to indicate fan failure, but the switches proved to be inoperative. It is planned to install other alarms. At present collapse fan failure is detected from increased differential pressure signals.

When a main collapse fan fails the spare collapse fan is put into service by opening blast gate (butterfly-type) dampers. The spare fan is normally filled with fly ash due to leakage past the blast gate dampers, and normally the fan must be cleaned out before it is put into service. This can take as much as 2 to 3 hours. Originally the spare fan was isolated by sliding gate dampers. These dampers provided a tight seal; however, they were difficult to open and close. It took four men with a chain hoist approximately 4 hours. There is a study underway to determine a method to prevent fly ash accumulation in the spare fan and still allow easy damper operation. As a temporary measure the spare fans are pressurized with compressed air to prevent in-leakage.

If a cleaning cycle timer fails, an alarm is sounded and the operator switches to the spare timer. Originally the timers failed frequently. This has been alleviated by adding more reliable, electronic timers.

Damper failures can sometimes be detected by observation of the differential pressure chart. As the dampers open and close the differential pressure swings. If a damper fails, the absence of this pressure swing leaves a "gap" on the differential pressure chart (Figure 4). If a high differential pressure alarms, the dampers are routinely checked for proper operation. The operator must go up to the baghouse and visually observe damper operation through the complete cycle (a total of 32 minutes).

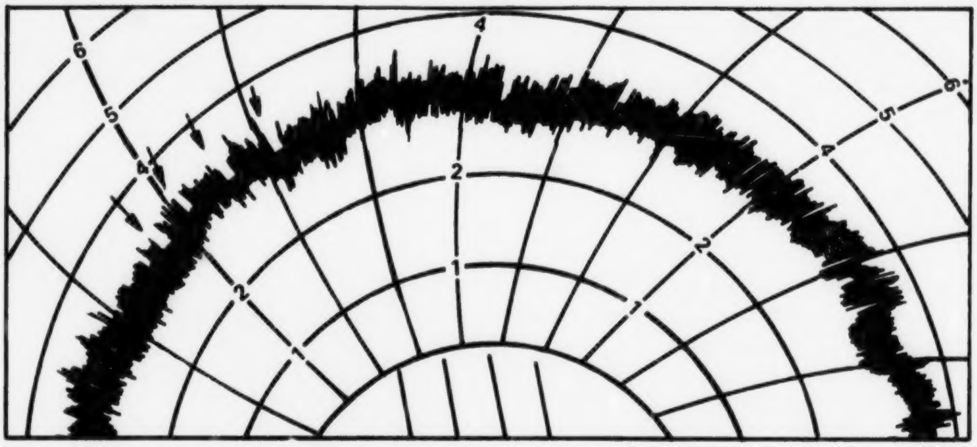

Figure 4. Differential pressure chart - indicating a damper malfunction on 2A baghouse (notice arrows). A normal differential pressure chart has no gaps.

When a baghouse hopper becomes plugged and fills with fly ash, a high pressure spike, in sequence with the 32-min cleaning cycle, is indicated on the differential pressure recorder. No operational problems are experienced. The operator must sledge-hammer and/or air-lance the hopper to free the blockage.

Since the number of bag failures has been small, they have not caused operational problems. Most failures are single-bag; no more than two bags have failed at any one time. Isolating a compartment increases the differential pressure by approximately 0.5 in. VWC. Two compartments have been taken out of service together with an increase of approximately 1.0 in. VWC in differential pressure and no reduction in boiler load was necessary. Any number of compartments may be taken out of service without affecting boiler load as long as the differential pressure remains below 6.0 in. VWC.

There have been two major baghouse pressure excursions. On Baghouse No. 2A in July 1975 after a boiler outage the draft loss increased from 3.0 in. to 6.0 in. VWC over a 3-week period. This was apparently due to moisture carry over to the bags from heavy water-lancing of boiler slag deposits during the outage. Several methods were tried to reduce the draft loss: two collapse fans were placed in service on the baghouse, the collapse dampers were opened and closed several times during each 2-minute compartment cleaning time (this was an attempt to dislodge any thick dust cake on the bags), all hoppers were inspected and any blockage was cleared, and the thimble floor was vibrated by pounding it with sledge hammers to dislodge any buildup on the thimbles. (This buildup, a fly ash deposit reducing the 12-in. diameter thimble size to 6 in. to 9 in. diameter, has been noted on all baghouses but never has had any noticeable effect on baghouse performance.) All of these methods proved unsuccessful. A compartment was isolated and the bags were inspected. The dust cake on the bags was very thick, from 1/2 in. to 3/4 in. It was decided to manually shake the bags. Each bag was grasped between the palm of each hand and vigorously shaken from side to side. The release of the dust cake could be felt as the dust fell to the hopper below. Alternately, all of the compartments were taken out of service and the bags were manually shaken. When all compartments were returned to service the pressure drop had decreased to 3.5 in. VWC and has remained stable since.

In the fall of 1975 the pressure drop on Boiler No. 1B increased from 3.5 to 5.0 in. VWC over a 3-month period. The bags were inspected during the boiler outage. The cake was at most about 1/4 in., so the bags were not manually shaken. All other methods used on No. 2A were tried with no success. With the new electronic timers it is possible to readily change the cleaning cycle time. On January 23, 1976, the time was reduced from the 30-minute cycle to a 15-minute cycle, doubling the number of collapses. In the last part of February the draft loss began to decrease until it reached 3.5 in. VWC at the end of February. The cleaning cycle was returned to the normal 30-minute cycle on March 16, 1976. The draft loss has remained stable at 3.5 in. VWC since. Because of the time frame it is uncertain whether the 15-minute cleaning cycle caused the draft loss reduction. Normally, when a change is made to reduce draft loss the effect is noticed in several hours. Additional background information on the Sunbury installation may be found in References 1, 2, and 3.

MAINTENANCE

Most maintenance hours have been spent on bag replacement, collapse fan repairs, and air-operated damper repairs.

Bag Replacement

The procedure for bag replacement is detailed in Figure 5.

During each annual boiler outage all baghouse compartments are inspected. If an accumulation of dust is found on the compartment floor, each bag in the compartment is inspected for possible failure and all failed bags are replaced.

To replace a bag with the boiler in service, the associated compartments must be isolated by closing the gas inlet and outlet dampers. The lower and upper doors of the compartment are opened to allow ambient air to circulate. The cover is removed from the vent stack, and a portable 7,000-cfm fan is set on the vent stack

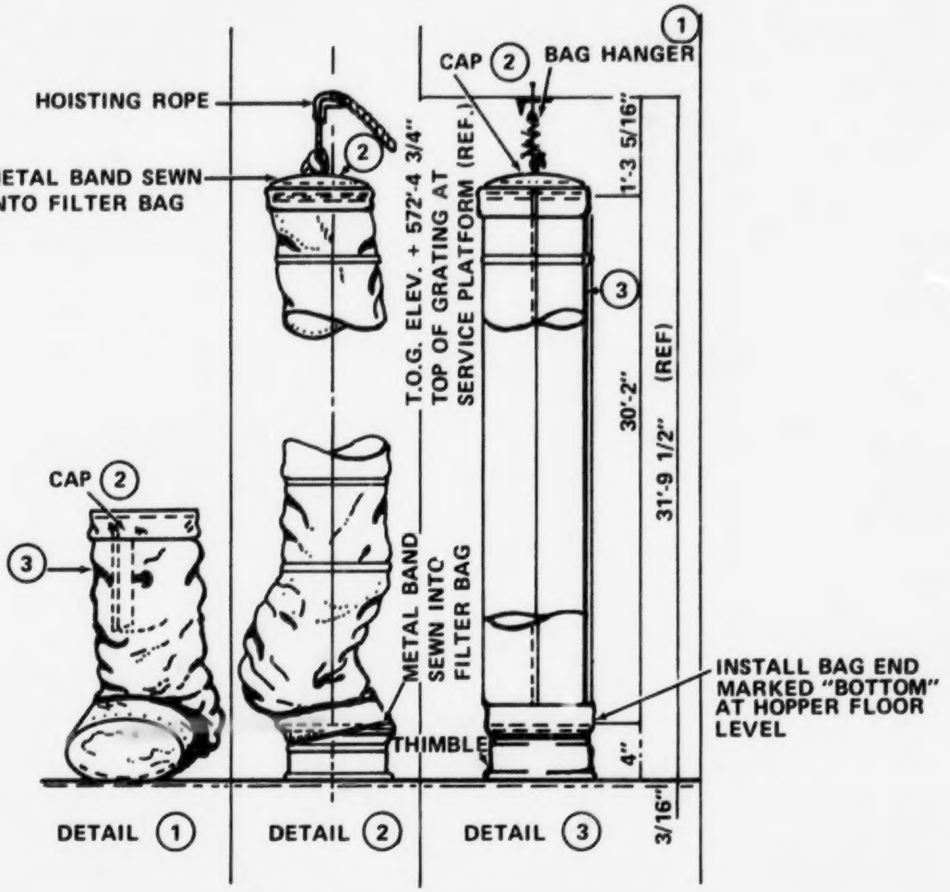
HOISTING ROPE
METAL BAND SEWN INTO FILTER BAG
②
CAP ②
③
DETAIL ①
METAL BAND SEWN INTO FILTER BAG
THIMBLE
DETAIL ②
T.O.G. ELEV. + 572'-4 3/4" TOP OF GRATING AT SERVICE PLATFORM (REF.)
CAP ② BAG HANGER
①
③
1'-3 5/16"
30'-2"
31'-9 1/2" (REF)
4"
3/16"
INSTALL BAG END MARKED "BOTTOM" AT HOPPER FLOOR LEVEL
DETAIL ③

INSTRUCTIONS FOR HANDLING AND INSTALLATION OF
GLASS CLOTH FILTER BAGS

HANDLING

GLASS CLOTH IS SOFT, FLEXIBLE, AND DURABLE. HOWEVER IT IS SUBJECT TO TYPES OF DAMAGE NOT ALWAYS ASSOCIATED WITH OTHER FABRICS. CARE IN ITS HANDLING WILL BE REPAID IN GREATER EFFICIENCY AND LONGER LIFE.

UNPACK BAGS CAREFULLY, ONE BY ONE, AS THEY ARE INSTALLED. AVOID CONTACT OF THE FABRIC WITH PROJECTIONS OF METAL OR ROUGH WOOD WHICH MAY CAUSE SNAGS OR TEARS.

NEVER LAY BAGS ON THE THIMBLE-PLATE OF THE BAGHOUSE WHERE THEY MAY BE WALKED UPON.

THE FABRIC SHOULD NEVER BE PULLED BY GRASPING BETWEEN THUMB AND FINGERS, WHICH MAY CAUSE SLIPPAGE OF THE YARNS.

FOLDED BAGS SHOULD NOT BE SUBJECTED TO HEAVY PRESSURE.

INSTALLATION

STEP ONE.-AFTER UNPACKING, PLACE FILTER BAG (3) IN BOX ON THIMBLE PLATE NEAR POSITION OF ASSEMBLY. RAISE ONE END OF FILTER BAG AND INSERT CAP (2) AS SHOWN IN DETAIL (1). ROTATE CAP 90° AND PULL UPWARD UNTIL METAL BAND SEWN INTO BAG CUFF FITS SNUGLY AGAINST ROLLED RIM OF CAP, AS SHOWN IN DETAIL (2).

STEP TWO.-HOOK ONTO CAP (2) WITH HOISTING ROPE AND RAISE BULK OF BAG (3) OFF THIMBLE PLATE. PLACE LOWER END OF BAG OVER THIMBLE, AS SHOWN IN DETAIL (2). PUSH BAG END DOWNWARD UNTIL THIMBLE RIM IS COMPLETELY COVERED. THEN GENTLY AND EVENLY, MOVE BAG END UPWARD UNTIL METAL BAND SEWN INTO BAG CUFF FITS SNUGLY AGAINST ROLLED RIM OF THIMBLE.

STEP THREE.-HOIST BAG TO FULL HEIGHT AND REPLACE ROPE WITH HANGER (1) AS SHOWN IN DETAIL(3). TIGHTEN HANGER TO DEVELOP 50 LBS. TENSION ON BAG - BY COMPRESSING HANGER SPRING 1-1/4 INCHES.

Figure 5. Installing filter bag

and started to provide forced ventilation. It normally takes 3 to 4 hours to ventilate the compartment sufficiently for men to enter. It is normally still necessary to wear a mask to prevent inhalation of sulfur dioxide. The compartment can then be entered and the failed bag replaced. The entire procedure (isolation and ventilating the compartment, finding the leak, replacing the bag, and returning the compartment to service) takes approximately 6 to 8 hours.

Detecting Bag Failures

Bag failures are detected by daily observations of the bolometer charts. When a bag has failed the bolometer senses the increased particulate emissions; generally, there is no visible stack discharge. The bolometer chart will indicate a periodic spike, in sequence with the cleaning cycle. There will be a decrease in bolometer reading when the compartment with the failed bag is removed from service, a spike when the compartment is returned to service, and a settling out to a higher than normal reading directly afterwards (Figure 6). Some spikes are not easily discernible and a careful study of each chart is necessary. Also some non-periodic spikes occur, but these do not indicate an abnormal condition.

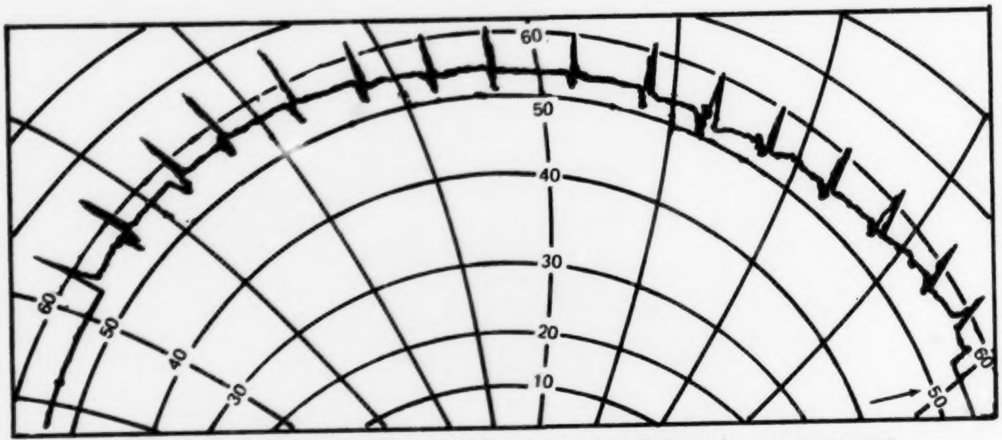

Figure 6. Bolometer chart - indicating a bag failure in compartment No. 14 of No. 2B baghouse

When it is determined what compartment has the failed bag, the compartment is taken out of service. The bolometer readings then return to normal. The compartment is entered, and each of the ninety bags is inspected. An accumulation of fly ash on the compartment floor is a tell-tale sign that there is an actual bag failure in the compartment. However, bag failures have been found in compartments with no fly ash accumulations. The bags are inspected by holding a flashlight at the bottom of the bag and shining it up the side of the bag. Any tears are illuminated in this manner. Also, a slight tap on the bag will, if there is a failure, cause a stream of fly ash to flow from the bag which is illuminated by the light, providing an additional check for failures.

The failed bag is replaced, the compartment floor is cleaned, and the compartment is returned to service.

Bag Failure Rate

As of May 1, 1976, a total of 37 bags have failed. A list of the failures is detailed in Table 4.

TABLE 4. BAG FAILURES[a]

Baghouse	1973	1974	1975	To May 1976	Total
1A	5	1	2	2	10
1B	0	6	2	2	10
2A	3	0	0	0	3
2B	4	7	2	1	14
				Total	37

Complete Bag Replacements

1A	3-20-75
1B	Bags never replaced
2A	11-20-74 (except for compartment No. 8)
2B	2-23-75

[a] Failures include neither those from faulty installation or damage during maintenance (about 23 bags) nor test bags.

As a precautionary measure, bags in three baghouses were replaced after approximately 2 years of service (dates are listed in Table 4). The 4th baghouse, No. 1B, still has its original set of bags. The bags will remain in service until an increased bag failure rate dictates their replacement.

Maintenance Problems

The collapse fans have been a continual problem. The fans were not designed to handle dirty gas. There is baffling in the hoppers to prevent the collapse fan from picking up dust. However, this has not been effective. The fan casings and blades are worn thin from the abrasiveness of the fly ash. This has caused excessive fan vibration and gas leakage from the fan. Frequent maintenance is required on the fans.

The air-operated dampers have caused continual problems. They are located in an environment of high temperatures (150°F to 200°F) and occasional dusting. This results in increased maintenance and occasional damper failure.

ECONOMICS

The initial installation cost of all four baghouse installations, including the fly ash removal system, was $5,500,100. Installation cost and yearly operating and maintenance costs are detailed in Table 5. Increased mechanical and electrical maintenance cost in 1975 was the result of increased collapse fan maintenance and the high pressure drop problem encountered on Baghouse No. 2A.

TABLE 5. INSTALLATION, OPERATION AND MAINTENANCE COSTS

Bag Filter Installation Cost

Expenditure Description	Total Cost, $
Western Precipitator Contract (4 Baghouses)	3,201,700.
Structures & Improvements	372,100.
Land & Land Rights	1,500.
Boiler Plant Equipment	1,190,000.
Ash Removal Equipment	
Precipitator Modifications	
Accessory Electrical Equipment	72,000.
Overhead	662,800.
Total Construction Cost	5,500,100.

(continued)

TABLE 5. (continued)

Estimated Operating & Maintenance Cost, @ $12/manhour Cost Description	Cost , $ 1973	 1974	 1975
Collapse Fan Power Consumption	18,600.	18,600.	18,600.
Air Compressor Power Consumption	3,000.	3,000.	3,000.
Instrument Department Labor	950.	950.	1,800.
Mechanical Maintenance Labor	2,130.	5,840.	15,678.
Electrical Maintenance Labor	7,410.	3,800.	6,000.
Construction Department Labor	3,950.	2,350.	2,000.
Complete Bag Replacement			
Material ($48,000/baghouse)		48,000.	96,000.
Labor ($11,000/baghouse)		11,000.	22,000.
TOTAL COST	36,040.	93,540.	165,078.

PERFORMANCE

In order to assess the performance of a fabric filter system as applied to a utility boiler, EPA asked for permission to perform efficiency tests after the Sunbury baghouses had been in service for a few months. Permission was granted and one set of tests was made in August 1973.[4] The results of these tests were impressive and further testing was scheduled to be done by GCA Corporation. The results of the GCA testing, performed in January, February, and March 1975, are discussed in this paper.[2]

Of greatest interest to EPA was the performance of the baghouse in the fine particulate range, i.e., below about 3 μm. Along with mass efficiency testing there were also measurements made with impactors and diffusion apparatus. The problems associated with the latter two types of devices led to some rather large error bands, but with over 30 tests made there is reasonable confidence in the results.

GCA performed their tests after the baghouses had been in service for approximately 2 years. Since bag changeover was to coincide with a scheduled outage, this situation allowed testing of bags at the end of their planned service life and also (for the new set of bags) at the beginning of their service life.

Mass Results

For 19 tests made at several combinations of fuel mix and boiler load, the average outlet concentration was 0.0017 gr/dscf or in terms of emission rate: 0.0041 lb/10^6 Btu. These tests were for the bags which had been in service for 2 years. Based on an average inlet loading of 2.6634 gr/dscf the average efficiency was 99.94%. For the new bags the average outlet concentration was 0.0024 gr/dscf; emission rate was 0.00543 lb/10^6 Btu.; average inlet loading was 2.2853 gr/dscf and average efficiency was 99.89%. The slightly higher outlet loading was consistent with slightly lower pressure drop through the new bags, and the new bags would be expected to have performance similar to the old bags after sufficient stabilization time. The results do indicate that baghouse efficiency does not deteriorate with time, and tends to get better through the service life of the bags.

For all 31 tests the range of outlet loadings was from 0.0013 to 0.0033 gr/dscf (0.0028 to 0.0101 lb/10^6 Btu).

Impactor Results

Apparent collection efficiency by particle size is shown in Figure 7. For the size range covered, 10 to 0.1 µm, it is apparent that the baghouse maintains nearly uniform, high reduction of particles entering the system. All sizes in the impactor range are collected with better than 99% apparent efficiency. There is some question as to whether or not particles can change their size as they go through the collection system, but the result at the baghouse outlet is a clear stack.

Condensation Nuclei Counter Results

A condensation nuclei counter (CNC) was used to count numbers of particles in the range from about 0.003 to 0.5 µm. Although the data are sketchy they indicate an apparent collection efficiency of between 93.0 and 99.7% for particles in this size range. It should be emphasized that this is a number efficiency and not a mass efficiency.

GENERAL COMMENTS

It is obvious that the Sunbury baghouses (as do the Nucla baghouses)[5] do a fine job at collecting particulate matter. The GCA testing also revealed that collection efficiency was not significantly affected by changes in fuel composition, boiler load, filtration velocity or cleaning regime within what might be normal limits of change. The baghouse seems to operate like a smoothing device; regardless of inlet variations the outlet showed very little change. For the changes that did occur, regression equations were formulated which showed particle penetration to be primarily a function of inlet concentration, percent moisture, filtration velocity and pressure drop.

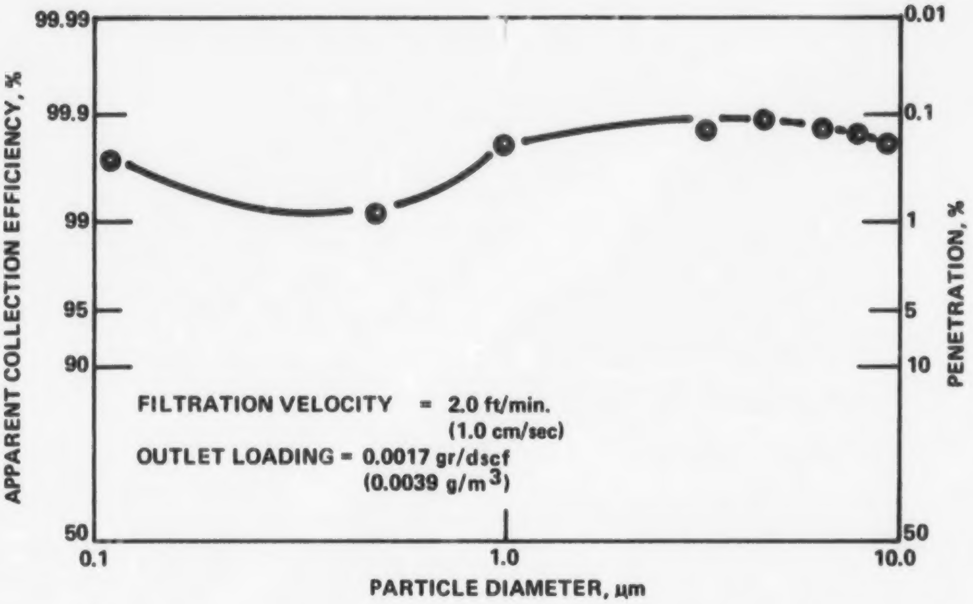

Figure 7. Baghouse performance at Sunbury Steam Electric Station

SUMMARY OF BAGHOUSE PERFORMANCE

As far as filtration performance is concerned, the Sunbury baghouses do an excellent job. Mass efficiency is 99.9%, grade efficiency is 99% or better in the impactor range, and the number efficiency for particles in the CNC range appears to be between 93 and 99.7%. Changes in process and collector operating variables have little effect on outlet concentration.

REFERENCES

1. Wagner, N.H., and D.C. Housenick. Sunbury S.E. Station — Units No. 1 & 2 Design and Operation of a Baghouse Dust Collector for a Pulverized Coal Fired Utility Boiler. Pennsylvania Power & Light Co., Allentown, Pa. May 1973.

2. Cass, R.W., and R.M. Bradway. Fractional Efficiency of a Utility Boiler Baghouse — Sunbury S.E. Station. GCA Corporation. EPA-600/2-76-077a, U.S. Environmental Protection Agency, Washington, D.C. 1976.

3. Operating Instructions for Therm-o-flex Filters for Pennsylvania Power & Light Co., Sunbury, Pa., Joy Manufacturing Company, Western Precipitation Division, February 1973.

4. Harris, D.B., and J.H. Turner. Particulate and SO_2/SO_3 Measurements Around an Anthracite Steam Generator Baghouse. Particulate and Chemical Processes Branch, Control Systems Laboratory, Office of Research & Development, Environmental Protection Agency, National Environmental Research Center, Research Triangle Park, N.C. November 8, 1973.

5. Bradway, R.M., and R.W. Cass. Fractional Efficiency of a Utility Boiler Baghouse — Nucla Generating Plant. GCA Corporation. EPA-600/2-75-013a. U.S. Environmental Protection Agency, Washington, D.C.

PAPER 11

SCRUBBER EXPERIENCE AT MOHAVE

John M. Johnson, Dale G. Jones,
Alexander Weir, Jr., and W. Carl Martin
Southern California Edison Co.

Seymour Calvert
Air Pollution Technology, Inc.

ABSTRACT

The performance of wet scrubbers in the removal of particulate was evaluated during a development test program conducted at the coal-fired Mohave Generating Station during 1974 and 1975. Data were obtained using three different scrubber configurations that were each sized for 170 MW. The Vertical TCA, the Vertical PPA and the Horizontal Cross-flow all received flue gas from a location downstream of cold-side electrostatic precipitators. A total of 154 inlet/outlet particulate samples were examined and compared to determine the effect of inlet particulate grain loading and variable scrubber operating conditions upon particulate removal performance. These scrubber variables included flue gas flowrate, circulating slurry flowrate, and internal packing configurations.

INTRODUCTION

Between July, 1971 when pilot plant testing was initiated at the Mohave Generating Station and July, 1975 when the 170 MW Test Modules Program was completed, the participants of the Navajo and Mohave Power Projects funded a scrubber development and evaluation project which has significantly advanced the understanding of scrubber technology. The results of this evaluation have been published, in part, at several EPA Flue Gas Desulfurization Symposium conferences.[1-4] The objectives of the 170 MW Test Modules Program were to evaluate the SO_2 and particulate removal performance of more than one full-scale scrubber, as well as to determine the practical feasibility of scrubbers for commercial service, including cost, operating flexibility, maintenance requirements, materials of construction, chemical control problems, and waste disposal factors.

The purpose of this paper is to describe the particulate removal characteristics of the 170 MW Mohave Test Modules. During the test program, a total of 154 inlet/outlet particulate samples were obtained during tests of three different 170 MW scrubber configurations. The scrubbers were located downstream from the cold-side electrostatic precipitators, and were designed to treat 450,000 scfm of flue gas (equivalent to 170 MW at the Mohave Generating Station).

TEST MODULE DESCRIPTION

The 170 MW Vertical Module, located on Unit 1, was tested in the Turbulent Contacting Absorber (TCA) configuration and the Polygrid Packed Absorber (PPA) configuration. The TCA configuration, shown in Figure 1, consisted of four stages of thermoplastic rubber balls supported on stainless steel grids at four-foot intervals. The balls were contained in compartments, with 15 compartments at each of the four levels. Although various levels of ball depths were tested, the compartments were initially filled to the one-foot level with approximately 1,600,000 balls. The TCA configuration was tested with both three and four stages of balls, and at ball depths of 6, 10, and 12 inches in the four stage configurations. The PPA configuration consisted of two and three stages of fixed "eggcrate" packing supported at four-foot intervals. The packing consisted of plastic grids 1¼ in. thick with 2-in. square openings, with the grids stacked to a depth of approximately 17 inches in each stage.

The 170 MW Horizontal Module, located on Unit 2, was tested with 1, 2, 3, 4 and 5 spraying stages. The basic four stage configuration, shown in Figure 2, consisted of crossflow spray discharged from a row of 36 externally-mounted nozzles at each stage. The Horizontal Module did not contain packing, but consisted of four stages of crossflow spray. The slurry was cycled through the scrubber in a countercurrent manner. That is, the fresh lime slurry from the mix tank was first sprayed across the flue gas at the fourth stage or discharge end of the scrubbing chamber. The same liquid was successively collected and pumped to the third, second, and first stages and successively depleted of alkalinity. By the time the slurry reached the first stage collection hopper for return to the lime mix tank, it was almost completely depleted of any excess alkalinity. The recirculating slurry flow rate was normally 9,000 gpm, but the slurry was mechanically pumped four times per circuit for a total installed pump capacity of 36,000 gpm.

Both the Horizontal and Vertical Modules were designed for identical test conditions, using the same sources of makeup water and removing particulate matter resulting from the combustion of low sulfur western coal from the Black Mesa Mine near Kayenta, Arizona.

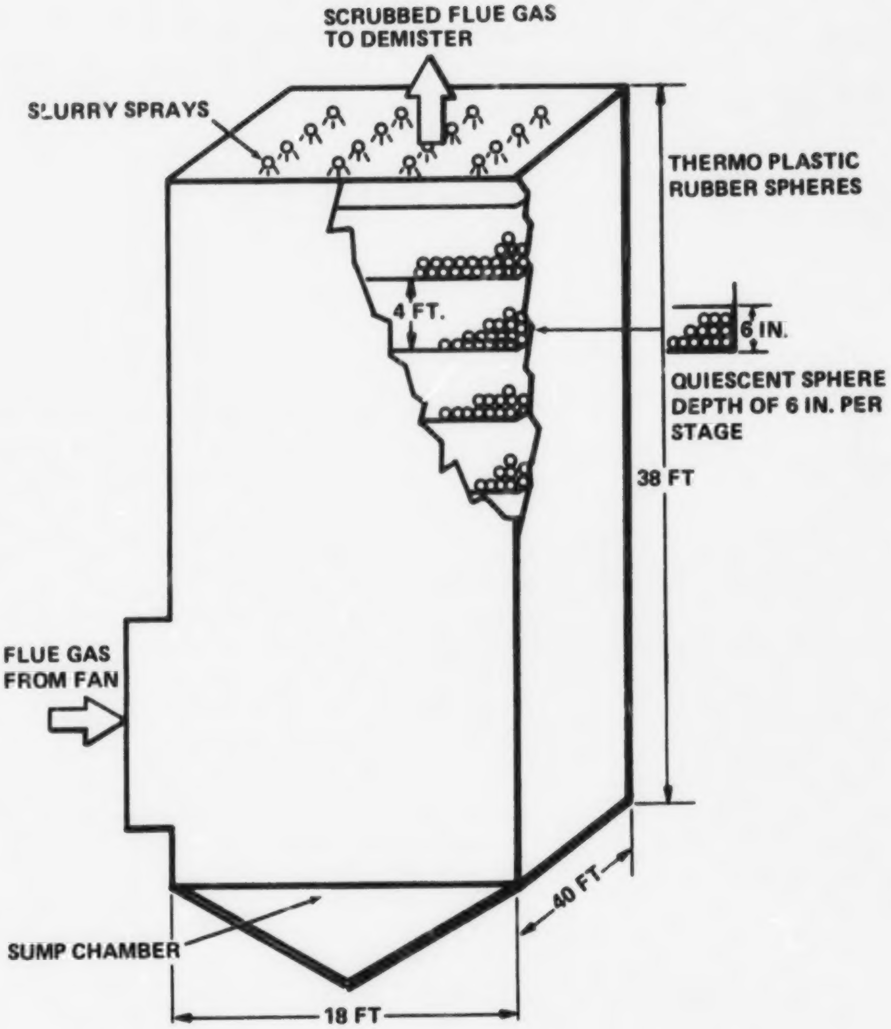
SCRUBBED FLUE GAS
TO DEMISTER
SLURRY SPRAYS
THERMO PLASTIC
RUBBER SPHERES
4 FT.
6 IN.
QUIESCENT SPHERE
DEPTH OF 6 IN. PER
STAGE
38 FT
FLUE GAS
FROM FAN
SUMP CHAMBER
40 FT
18 FT

Figure 1. 170 MW Vertical module (4-stage TCA)

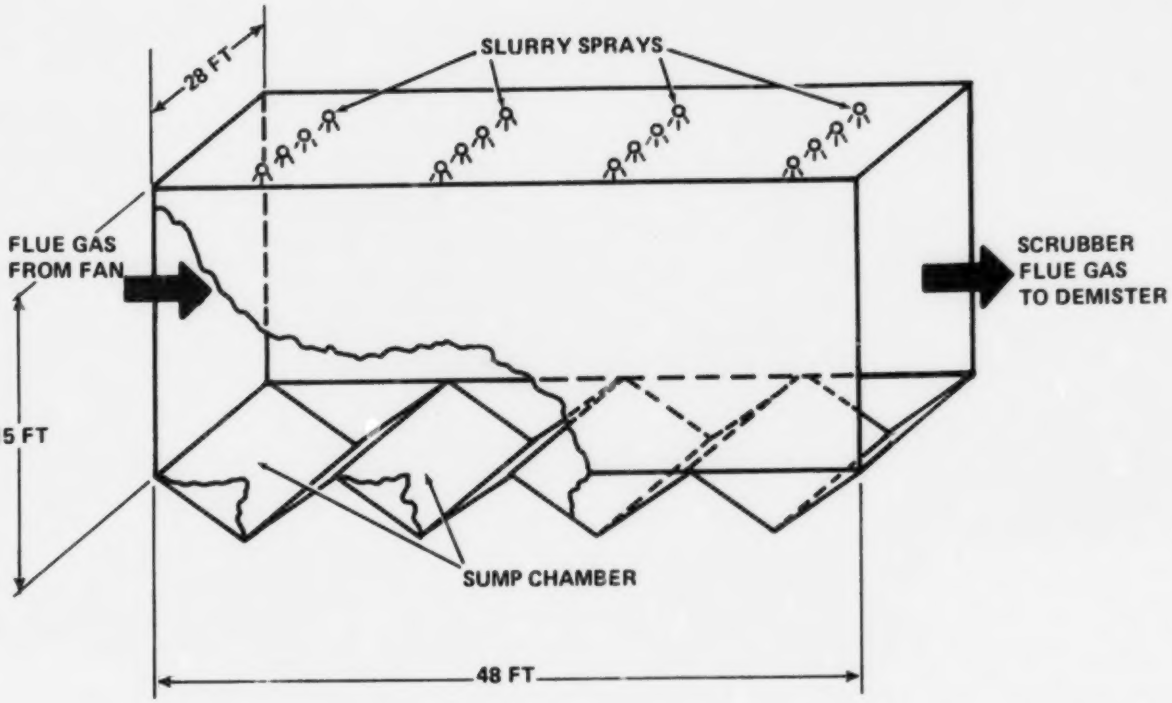

Figure 2. 170 MW Horizontal module (4-stage)

OBSERVED SCRUBBER PERFORMANCE

Particulate Removal at Design Operation Conditions

The observed operating conditions of the three full-scale scrubbers are indicated in Table 1. The outlet gas flowrate was greater than the inlet due to water vapor evaporated inside the scrubber. In addition, the Horizontal Module used an indirect reheater which injected approximately 80,000 scfm of hot ambient air into the outlet flue gas stream. The pressure drop indicated in Table 1 is the flue gas pressure drop across the scrubbing chamber itself, not including additional pressure drop due to ductwork, mist eliminator, and reheater restrictions. The electric power consumption in Table 1 is the total electric power measured for the entire scrubbing system, and includes control room lighting and air conditioning, thickener rake drive, tank agitators, process water pumps, and other miscellaneous power requirements. However, these miscellaneous factors are estimated to be about 5% of the total, while fan and slurry pump power requirements accounted for the remaining 95% of the total.

TABLE 1. OPERATING CONDITIONS AT DESIGN GAS FLOWRATE

	Horizontal	Vertical TCA	Vertical PPA
Inlet gas flowrate, scfm	450,000	450,000	450,000
Outlet gas flowrate, scfm	560,000	480,000	480,000
Number of stages	4	4	3
Circulating slurry flowrate, gpm	9,450	16,200	27,000
Scrubber gas velocity, ft/sec	22	12	12
Pressure drop, in. H_2O	1.0	14.0	12.2
Nozzle pressure, psig	35	15	30
Power consumption, MW	2.6	3.4	3.9
Type of reheat	Indirect	Direct	Direct

The observed outlet grain loadings obtained at the design operating conditions for the Horizontal, Vertical TCA, and Vertical PPA scrubbers are plotted as a function of inlet grain loading in Figures 3, 4, and 5, respectively. At an inlet grain loading of 0.10 gr/scf, all three scrubber configurations demonstrated a relatively high degree of particulate removal between 90% and 93%. As will be pointed out in the discussion, the percentage particulate removal changed with inlet grain loading due to changes in the average particle size and particle size distribution.

EFFECT OF TURNDOWN

During the Test Program, it was determined that the easiest method of operating the scrubbers was to maintain a constant liquid flowrate and allow the flue gas flowrate to change under simulated load-following conditions. From an engineering design standpoint, this simplification avoids the severe erosion problems encountered with slurry flow control valves. It was decided to determine the effect on particulate removal of gas flowrate turndown with the liquid flowrates held at the design values shown in Table 1.

The observed variation in percentage particulate removal at a constant inlet grain loading of 0.10 gr/scf is plotted as a function of the gas flowrate in Figure 6. Note that the particulate removal efficiency of the Horizontal Module increases as a function of turndown ratio.

One explanation for this is the change in energy input per unit of flue gas flowrate which occurs with increasing turndown ratio. The primary method of shattering slurry droplets and thus contacting particulate matter differs between the types of scrubbers tested.

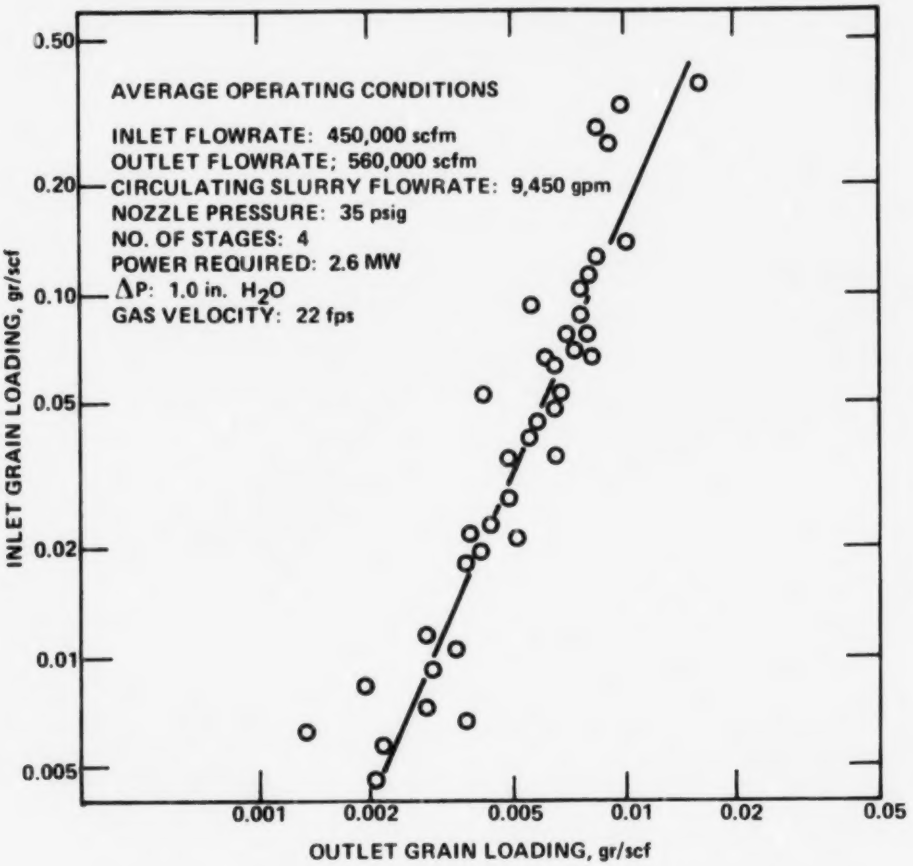

Figure 3. Inlet vs. outlet grain loading, 170 MW horizontal module

The Vertical TCA and PPA Modules require flue gas pressure drop to increase the tendency to shatter slurry droplets. The particulate removal was thus seen to decrease with decreasing pressure drop. For example, at 450,000 scfm, the particulate removal was about 90% at the design circulating slurry flowrates. Under these conditions the pressure drop was 14 inches of water in the TCA and 12.2 inches in the PPA. When the flue gas flowrate was decreased to one-third the design value, the pressure drop decreased to 3.5 inches of water in the TCA and 2.0 inches in the PPA. When the gas flow was reduced maintaining a constant circulating slurry flowrate, a given amount of flue gas was contacted by three times as many droplets at one-third load as at full load. In spite of this additional contacting, the particulate removal decreased to about 75% at one-third load.

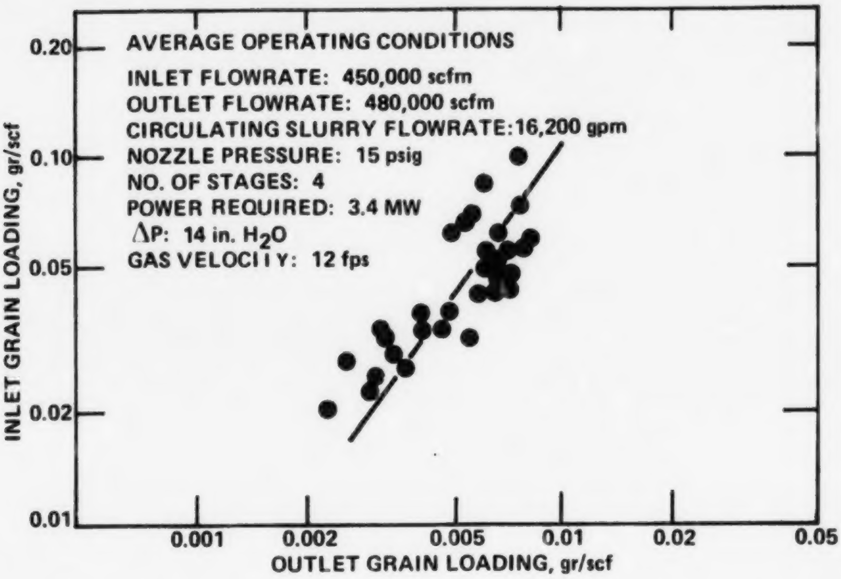

Figure 4. Inlet vs. outlet grain loading, 170 MW vertical TCA module

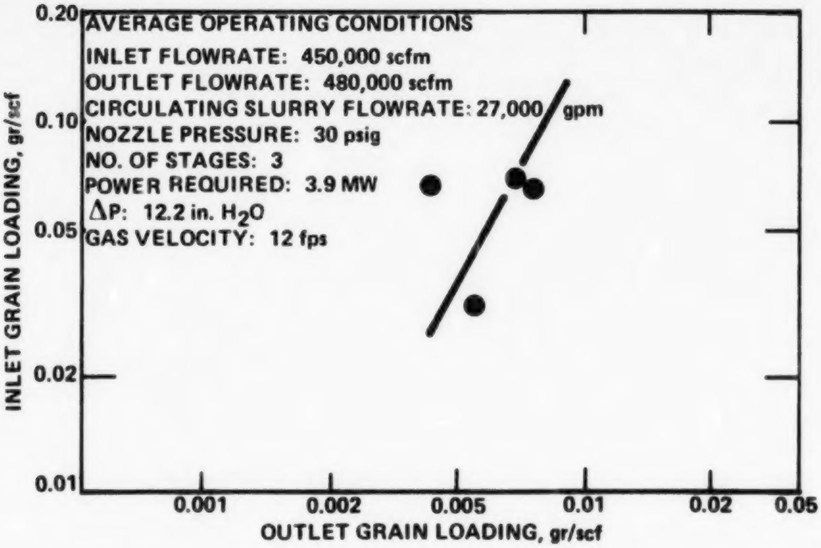

Figure 5. Inlet vs. outlet grain loading, 170 MW vertical PPA module

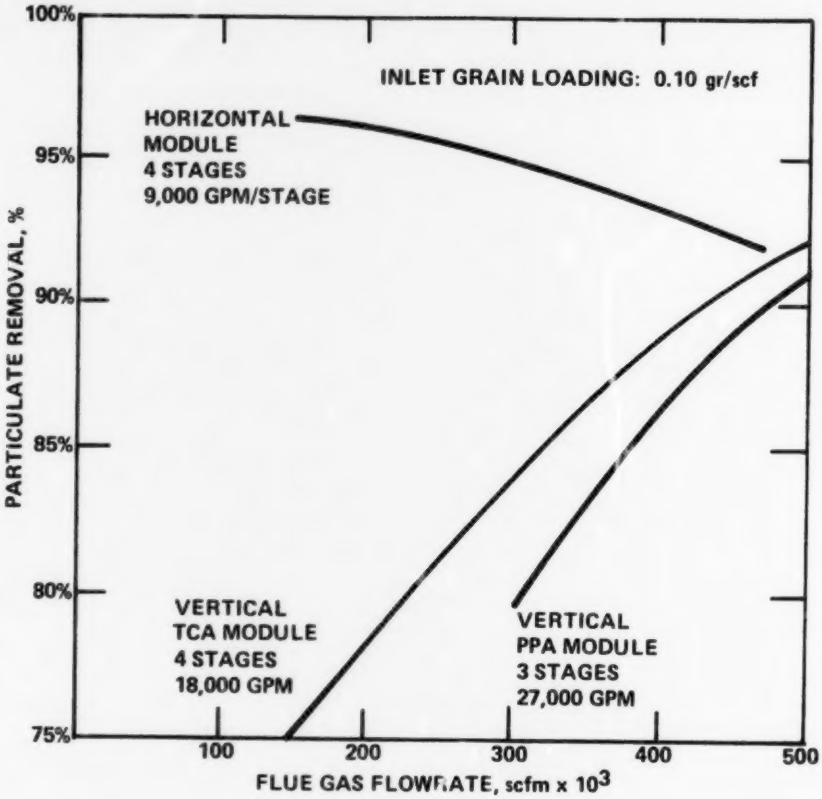

Figure 6. Effect of turndown ratio on particulate removal

The Horizontal Module utilized nozzle pressure to shatter the slurry droplets, and particulate removal was thus seen to increase with decreasing flue gas flowrate. As the flue gas flowrate was turned down from 450,000 scfm to 150,000 scfm, the pressure drop across the scrubbing chamber decreased from 1.0 inches of water to 0.10 inches. Since the liquid flowrate was constant, a given amount of flue gas was contacted by three times as many droplets at one-third load as at full load. The particulate removal efficiency was observed to increase from 92.5% at full load to 96.5% at one-third load.

Effect of Circulating Slurry Flowrate

The effect of various circulating slurry flowrates on Vertical TCA Module particulate removal is shown in Figure 7. It is seen that the percent particulate removal increased as the flowrate of the circulating slurry was increased. For example, the particulate removal achieved at 32,000 gpm is approximately 5% greater than that achieved at 16,000 gpm for both the 0.10 and 0.03 gr/scf inlet grain loading values.

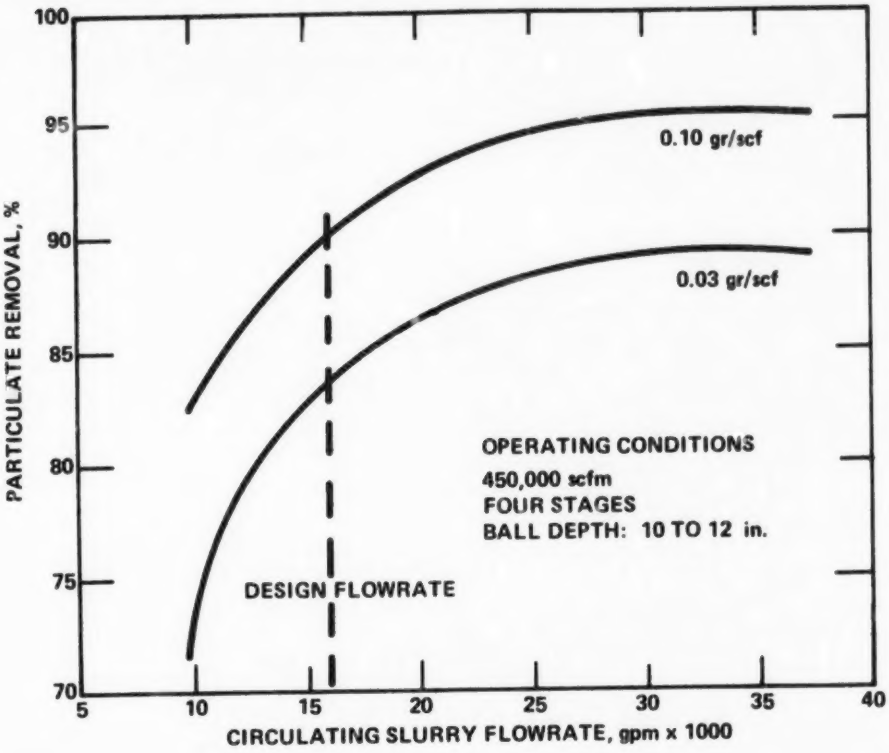

Figure 7. Effect of liquid flow rate on vertical TCA module particulate removal

With the Horizontal Module, particulate removal is also improved as the circulating slurry flowrate is increased. As shown in Figure 8, an increase in liquid flowrate from 5,000 gpm to 10,000 gpm would result in an increase in particulate removal from 81% to 93% at an inlet grain loading of 0.10 gr/scf and from 70% to 86% at an inlet grain loading of 0.03 gr/scf. These tests were conducted by shutting off individual nozzles to maintain 35 to 40 psig nozzle pressure, and although the spray coverage patterns were undoubtedly altered, the slurry droplet size probably did not change. The required liquid flowrate for a desired degree of particulate removal can thus be estimated from Figure 8.

Miscellaneous Effects

Several miscellaneous effects were investigated during the Test Program. For example, it was found that increasing the static ball depth from 6 in. to 12 in. in the Vertical TCA Module resulted in a minor increase in particulate removal.

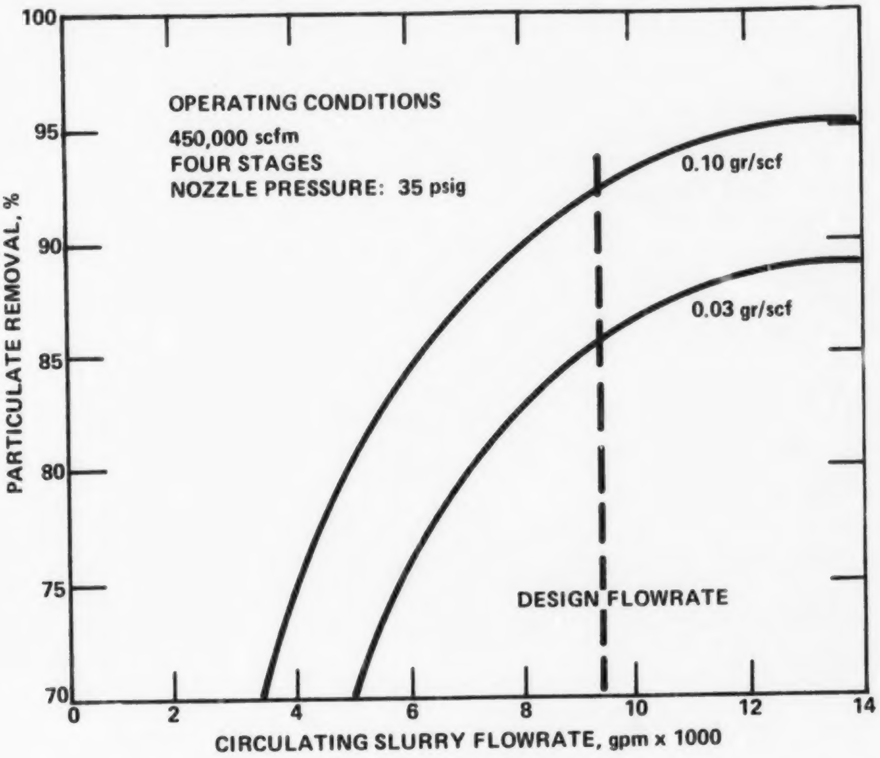

Figure 8. Effect of liquid flow rate on horizontal module particulate removal

The effect of variations in nozzle pressure was studied with the Horizontal Module. Particulate removal increased by 15 to 20 percent as the nozzle pressure was increased from 15 psig to 30 psig.

Finally, it was confirmed that increasing the number of contacting stages improves the particulate removal efficiency. For example, the particulate removal with the Vertical PPA Module increased as the number of packed stages was increased from two to three. Similar results were obtained with the Horizontal Module, where the effect of four versus five stages was studied in detail. A comparison of fractional collection efficiencies with four and five stages of scrubbing indicated that the extra stage increased the collection of particles less than 1.5 μm (aerodynamic). An interesting description of particulate collection in spray tower applications due to condensation effects can be found in Calvert, et al.[5] This may be a partial explanation for the high degree of particulate removal achieved with the Horizontal Module.

DISCUSSION

Data Acquisition and Reduction

It must be pointed out that it is not easy to obtain good particulate data by sampling in large ductwork with cross-sections of 200 square feet. Gas sampling crews of five persons working under ideal conditions were able to obtain one inlet and one outlet isokinetic particulate sample by probe traverse in one day. All testing was subject to unit outages and weather conditions ranging from 70 mph winds in the winter to 130° F temperatures in the summer. All testing was conducted by probe traverse, and electrical discharges from the metal probes to ground were observed at the inlet duct due to electrical charge carried on the inlet fly ash particles.

Grain loading measurements were conducted using an alundum thimble with a backup millipore filter, and gas volumes were metered and corrected for water vapor condensation in ice bath condensers. Particle size distribution measurements were obtained with both Andersen and University of Washington cascade impactors. Most of the particle size distribution measurements on the Vertical TCA Module were conducted with Andersen impactors without backup filters while similar measurements on the Horizontal Module were conducted primarily with University of Washington impactors with backup filters. It was found that physically identical impactors do not produce the same results from the same sample and must be individually calibrated using particles of a known size and instrumentation to measure the concentrations of particles upstream and downstream from the impactor.

Because of these differences, the particle penetration data for the Horizontal and Vertical TCA Modules at design operating conditions is difficult to compare directly. However, it can be stated with a reasonable degree of confidence that both the Horizontal and Vertical TCA Modules achieved approximately 65% collection of the 1.5 μm (aerodynamic) particles at design operating conditions. An examination of the slopes of Figures 3 and 4 would also suggest that the Horizontal Module at design conditions achieved a higher degree of collection efficiency for particles larger than 1.5 μm (aerodynamic) than the Vertical Module at design operating conditions.

The particle size data presented in Figure 10 refers to aerodynamic particle diameter as measured by a calibrated cascade impactor. The aerodynamic particle diameter takes into account particle density and shape factor. The term geometric standard deviation is used in Figure 9 to identify the distribution of particle sizes about an average size. For a log-normal particle size distribution, a geometric standard deviation of two means

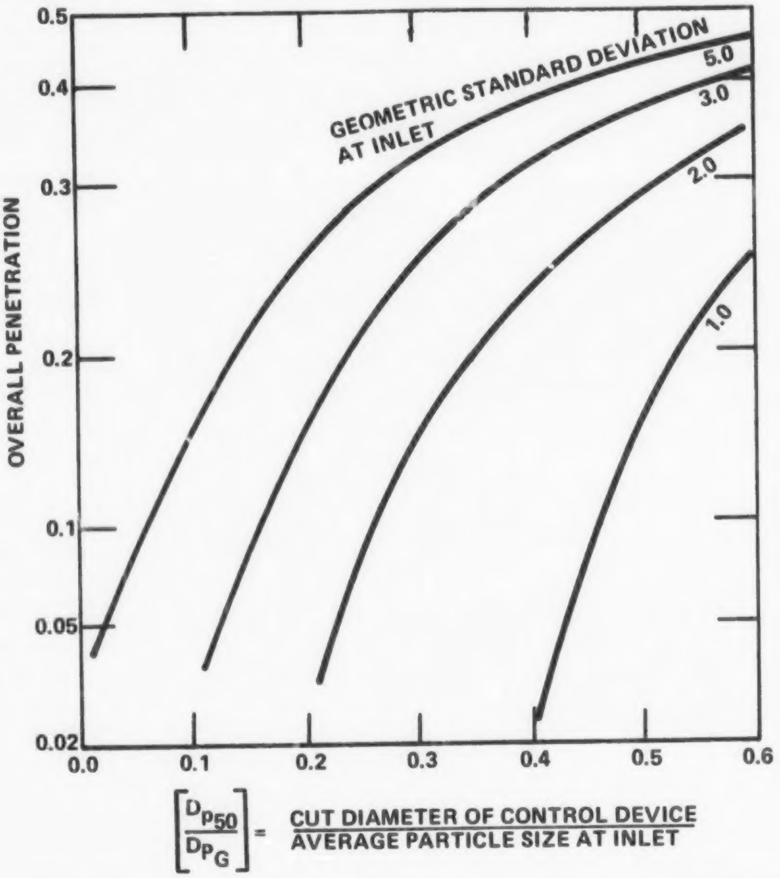

Figure 9. Overall penetration as predicted by impaction collection theory

that the size below which 84 weight percent of the particles are found is twice the average size. Thus, for a geometric standard deviation of one, all the particles are the same size.

As another prerequisite to obtaining high quality, accurate data, detailed grain loading and size distribution studies were conducted to determine the effects of stratification in the ductwork. It was found that below a grain loading of about 0.05 gr/scf, a variation of only ± 15% in geometric mean particle size and loading could be expected due to stratification at various points in the duct.

Performance Predicted By Inertial Impaction

If interest is restricted to particle diameters more than about 1.0 μm (aerodynamic), then Ranz and Wong[6] have shown that collection by inertial impaction is by far the most important collection mechanism. Particle penetration for many types of control equipment can be expressed as

$$P = \exp\left(-Kd_p^{B}\right) \qquad (1)$$

where K is a constant and
d_p is the aerodynamic particle size

Calvert[7,8] has indicated that the exponent B equals 2 for most types of packed towers, sieve plate columns, and venturi scrubbers. If the particle penetration is integrated over the entire size distribution, the average penetration can be determined by

$$PAV = \int_{0}^{W} P\,\frac{(dw)}{(w\ )} = \int_{0}^{W} \exp\left(-Kd_p^{\,2}\right)\frac{(dw)}{(w\ )} \qquad (2)$$

where w is the particle weight.

Following Calvert, equation (2) can be solved for a log-normal particle size distribution as a function of the inlet size distribution parameters and the so-called "cut diameter." The "cut diameter," dp50, is the particle diameter for which the collection efficiency of the control hardware is 50%. Therefore, more than half of the particles larger than the "cut diameter" will be collected. The "cut diameter" characterizes the overall particulate removal efficiency of a control device for known inlet particulate characteristics. The solution to equation (2) gives the overall penetration as a function of inlet particle size distribution characteristics and the "cut diameter" of the particulate control device.

Various "cut diameters" of the Horizontal and Vertical TCA Modules are plotted in Figure 10 as a function of the percent of electrical power required to operate the scrubber. Figure 10 was prepared from the data in Figures 7 and 8 as well as control room measurements of electric power requirements over a wide range of operating conditions. Since the "cut diameter" of a given scrubber depends on the energy supplied for droplet shattering and liquid/gas contacting, it is reasonable to expect that the "cut diameter" would correlate with percent of the electrical power required to operate the scrubber. A control device using less electrical power to achieve the same "cut diameter" would be a more efficient device in terms of particulate removal. The data in Figure 10 includes penalties for inefficient power consumption, such as pressure drop losses due to ductwork restrictions, pumping losses due to elevation differences and less than 100% mechanical efficiency of rotating equipment.

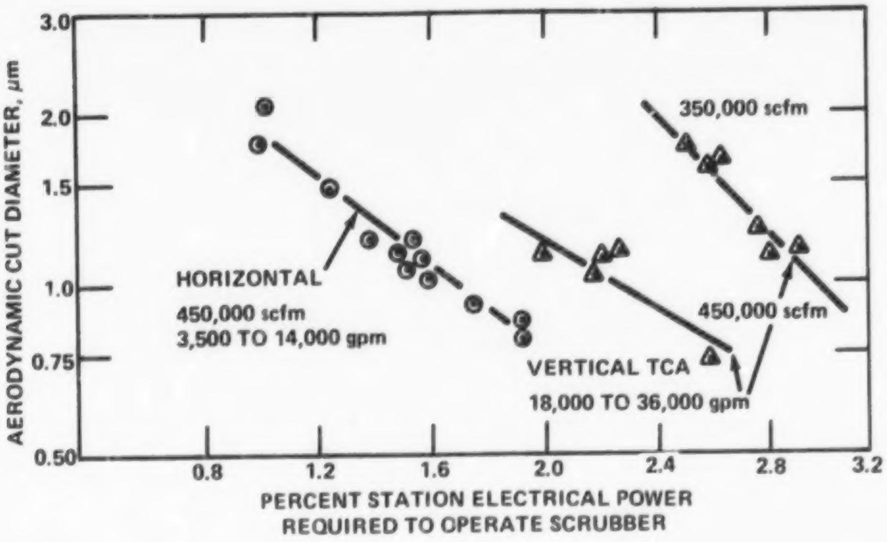

Figure 10. Comparison of power requirements to produce a given "cut diameter"

As shown in Figure 10, a "cut diameter" of 1.0 μm (aerodynamic) could be achieved at 450,000 scfm for an electric power consumption factor of 1.7% with the Horizontal Module and 2.3% with the Vertical TCA Module. Both scrubbers could achieve this result, but one is 35% less efficient than the other. When turndown with the Vertical TCA Module is taken into account, the electrical power comsumption resulting from an increased liquid flowrate required to achieve the same "cut diameter" increases significantly.

For the engineer, this method of predicting overall particulate removal knowing the inlet particulate characteristics, the type of scrubber and its electric power consumption characteristics can be a useful design tool. An example of this method is compared with test results.

Example Horizontal 170 MW Module

Assumptions:

Gas flow = 450,000 scfm
Power to operate scrubber = 2.6 MW
Inlet grain loading = 0.04 gr/scf
Average particle diameter = 4.0 aerodynamic micrometers (μm),
Geometric standard deviation (σ_g) = 2.8

Calculate:

Power consumption factor $\frac{2.6\ \text{MW}}{170\ \text{MW}} = 1.53\%$

"Cut diameter" from Figure 10 = 1.20 μm

$$\frac{\text{"Cut Diameter"}}{\text{Average Particle Diameter}} = \frac{1.20}{4.0} = 0.30$$

Prediction:

Overall penetration from Figure 9 = 0.125

Particulate removal = 100 - 12.5 = 87.5% removal

Test Data:

From Figure 3 (Inlet vs. Outlet Grain Loading)

$$\frac{(0.04 - 0.0054)}{0.04} \times 100 = \underline{86.5\%\ \text{removal}}$$

CONCLUSIONS

Several conclusions can be drawn from the data presented in this paper:

1. For the 170 MW scrubbers tested with Mohave Generating Station fly ash, more than 90% total particulate removal can be achieved with mobile bed, fixed bed and spray chamber scrubbers operating under design conditions at 450,000 scfm and an inlet grain loading at 0.1 gr/scf.

2. The effect of turning down the flue gas flowrate without changing the liquid flowrate increases the particulate removal of the Horizontal Module and significantly decreases the particulate removal of the Vertical TCA and PPA Modules. This could limit the particulate removal effectiveness of the Vertical Module configurations during normal load following operation.

3. The effect of changes in liquid flowrate on particulate removal is more pronounced with the Horizontal Module than the Vertical TCA Module.

4. Of all the miscellaneous effects tested with the Vertical Module, including stages of packing in the PPA configuration and static ball depth in the TCA configuration, only minor changes in particulate removal were observed.

5. Large increases in grain loading at the scrubber inlet cause relatively small increases in grain loading at the scrubber outlet. This is due to high collection efficiency for large particles. For example, at design operating conditions the Horizontal and Vertical TCA Modules both achieve more than 95% removal for particles larger than 6.0 μm (aerodynamic).

6. At design operating conditions, the Vertical TCA Module requires about 35% more electrical power than the Horizontal Module to achieve the same degree of particulate removal.

ACKNOWLEDGEMENTS

The Test Modules Program was a joint venture of the Navajo and Mohave Power Project participants who are listed below:

Salt River Project Agriculture Improvement
and Power District

Arizona Public Service Company

Department of Water and Power of the City of
Los Angeles

Nevada Power Company

Tucson Gas and Electric Company

Bureau of Reclamation of the U. S. Department of
the Interior

Southern California Edison Company

Funding for this program was provided by the participants in accordance with their respective megawatt entitlements in the Navajo and Mohave Power Projects. Southern California Edison Company was the project manager of the Test Modules Program.

The conclusions presented in this paper represent the personal opinions of the authors and are not intended to represent the opinions or position of any of the project participants.

REFERENCES

1. Shapiro, J.L., and W.L. Kuo. The Mohave/Navajo Pilot Facility for Sulfur Dioxide Removal. 2nd EPA Flue Gas Desulfurization Symposium, New Orleans, Louisiana, November 8, 1971.

2. Weir, A., and L.T. Papay. Scrubbing Experiments at the Mohave Generating Station. 3rd EPA Flue Gas Desulfurization Symposium, New Orleans, Louisiana, May 14, 1973.

3. Weir, A., J.M. Johnson, D.G. Jones, and S.T. Carlisle. The Horizontal Crossflow Scrubber. 4th EPA Flue Gas Desulfurization Symposium, Atlanta, Georgia, November 4, 1974.

4. Weir, A., L.T. Papay, D.G. Jones, J.M. Johnson, and W.C. Martin. Results of the 170 MW Test Modules Program. 5th EPA Flue Gas Desulfurization Symposium, New Orleans, Louisiana, March 8, 1976.

5. Calvert, S., J. Goldschmid, D. Leith, and N.C. Jhaveri. Feasibility of Flux Force/Condensation Scrubbing for Fine Particulate Collection. EPA-650/2-73-036, U.S. Environmental Protection Agency, Washington, D.C., 1973.

6. Ranz, W.E., and J.B. Wong. Impaction of Dust and Smoke Particles. Ind. Eng. Chem. 44(6):1371-1381, 1952.

7. Calvert, S. Engineering Design of Fine Particle Scrubbers. EPA/APT Fine Particle Scrubber Symposium, San Diego, California, May 28, 1974.

8. Calvert, S., J. Goldschmid, and D. Leith. Scrubber Performance for Particle Collection. A.I.Ch.E. Symposium Series 70 (137):357, 1974.

9. Jones, D.G., A. Weir, J.M. Johnson, W.C. Martin, and S. Calvert. Particulate Removal Characteristics of the 170 MW Mohave Scrubbers. EPA/EPRI Symposium on Particulate Control in Energy Processes, San Francisco, California, May 11, 1976.

PAPER 12

EVALUATION OF A PARTICULATE SCRUBBER ON A FULL SCALE UTILITY BOILER

D. S. Ensor
Meteorology Research, Inc.

L. E. Sparks
Industrial Environmental Research Laboratory
Environmental Protection Agency

S. Calvert
Air Pollution Technology, Inc.

D. V. Wallon and K. S. Campbell
Stearns-Roger, Inc.

ABSTRACT

The paper presents results of a performance test and engineering analysis of a mobile-bed scrubber on a full-scale coal-fired utility boiler. The scrubber nominally operated at the design particulate removal efficiency of 95% but the concentration of submicron particles was greatly influenced by mist entrainment. The entrainment resulted in a difference of aerosol penetration through the scrubber as a function of elemental composition and an outlet submicron particle concentration independent of pressure drop through the scrubber. The engineering analysis showed that the 1972 installed cost was $29/kW and the annual operating cost is 0.5 mills/kWh (75% availability). An initial decline in scrubber availability after start-up resulted from now-corrected minor design problems. Steadily improving reliability is attributed to the utility's providing maintenance and solving operating problems.

INTRODUCTION

Although scrubbers are commonly used for particulate control in many industries, they are not commonly used in the utility industry. Because scrubbers are not sensitive to dust resistivity, they may provide an acceptable means of controlling high-resistivity fly ash from combustion of low sulfur coal. In order to assess the potential of scrubbers for particulate control in the electric power industry, Industrial Environmental Research Laboratory-Research Triangle Park (IERL-RTP), sponsored an extensive evaluation of the TCA* scrubber at Public Service Company of Colorado's Cherokee Power Plant. A summary of the performance tests and engineering analysis of the evaluation is presented in this paper. Details of the tests and test results are reported by Ensor et al[1]

DESCRIPTION OF SYSTEM

Power Plant

The Cherokee Power Plant is located in north Denver, Colorado, near the South Platte River. The No. 3 unit has a name plate rating of 150 MW. The gas cleaning equipment consists of mechanical collectors, an electrostatic precipitator, and a wet scrubber arranged in series.

The unit normally burns coal or natural gas. The coal is mined in western Colorado and has a sulfur content of about 0.5%, an ash content of 9%, and a heating value of 2.492×10^7J/kg (10,712 Btu/lb).

Scrubber

The power plant was retrofitted in 1972 with a scrubber to treat flue gas from an existing electrostatic precipitator.

The Model 6700 Turbulent Contact Absorber Scrubber was designed by UOP, Air Correction Division. A diagram of the system is shown in Figure 1. The flue gas from the precipitator passes into two parallel induced draft fans. A bypass damper is used to direct the flue gas either into the stack or into the scrubber. The flue gas (under design conditions), 17,000 am^3/min, at 137°C (610,000 acfm at 280°F), enters the booster fans to offset the pressure drop through the scrubber. In the presaturator, 1440 ℓ/min (380 gpm) of makeup water is sprayed into the gas to reduce the temperature to approximately 50°C (125°F). From the presaturator, the gas enters the scrubber. The scrubber consists of three stages of fluidized beds packed with 3.8 cm (1.5 in.) diameter plastic balls arranged into three separated parallel scrubber sections. The two outer sections each handle 20% of the flow, while the center section handles the remaining 60%. All three sections can operate independently to provide flexibility of operation.

---

*Mention of manufacturers or brand names does not imply endorsement or recommendation for use by EPA.

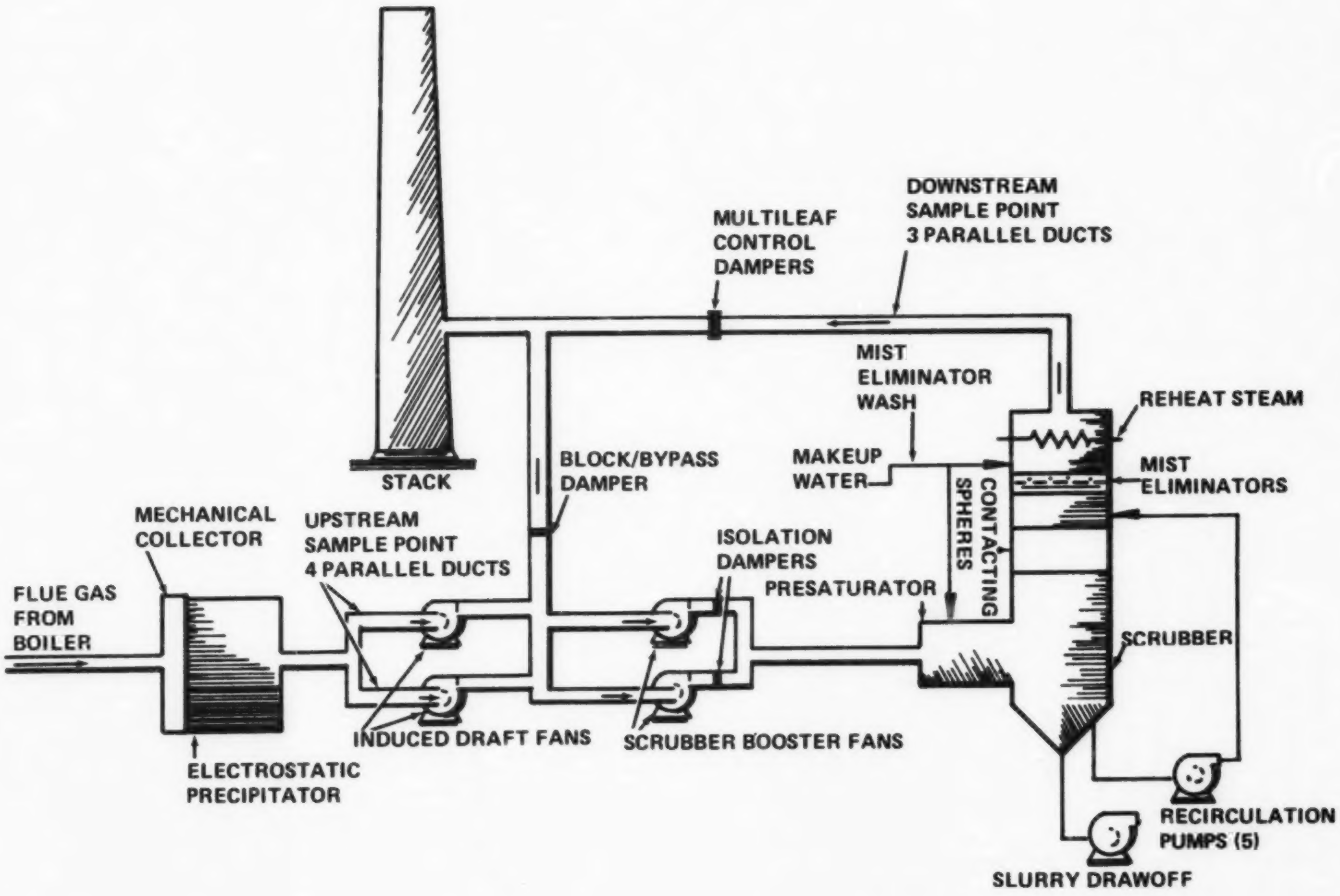
DOWNSTREAM
SAMPLE POINT
3 PARALLEL DUCTS
MULTILEAF
CONTROL
DAMPERS
MIST
ELIMINATOR
WASH
REHEAT STEAM
MAKEUP
WATER
MIST
ELIMINATORS
CONTACTING
SPHERES
STACK
BLOCK/BYPASS
DAMPER
MECHANICAL
COLLECTOR
UPSTREAM
SAMPLE POINT
4 PARALLEL DUCTS
ISOLATION
DAMPERS
PRESATURATOR
FLUE GAS
FROM
BOILER
SCRUBBER
INDUCED DRAFT FANS
SCRUBBER BOOSTER FANS
ELECTROSTATIC
PRECIPITATOR
RECIRCULATION
PUMPS (5)
SLURRY DRAWOFF

Figure 1. Scrubber system

The scrubbed gas passes through chevron-type mist eliminators made of fiberglass reinforced plastic where entrained droplets are removed. The mist eliminators are sprayed once a work-shift from the top to prevent accumulation of solids.

The gas is then heated by steam coils to 85°C (185°F) before entering the stack to prevent corrosion of the stack and duct work and to provide plume buoyancy after discharge into the atmosphere. The steam coils are equipped with two sets of soot blowers to remove fly ash from the heat transfer surfaces.

The scrubber was designed to the following specifications[2]:

Gas Flow	1,036,000 am^3/hr, 610,000 acfm 138°C (280°F)
Liquid-to-Gas Ratio	7.4 ℓ/m^3 (55 gal/100 ft^3)
ΔP	30.5 cm H_2O (12 in. H_2O)
Inlet Particulate Concentration	0.92 g/m^3 (0.40 gr/scf)
Outlet Particulate Concentration	0.046 g/m^3 (0.02 gr/scf)
Efficiency of Particulate Removal	95%

MEASUREMENT TECHNIQUES

Three measurement techniques were used during the tests to determine particle collection efficiency. These were: (1) diffusional techniques using condensation nuclei counters and screen diffusion batteries for determining concentration and size distribution on a number basis for particles having diameters less than approximately 0.2 µm; (2) inertial techniques using Meteorology Research, Inc. (MRI) cascade impactors for determining concentrations and size distributions on a mass basis for particles having diameters between approximately 0.3 µm and 20 µm, and (3) standard EPA Method 5 mass train measurements for determining outlet mass loadings. Details of the various instruments and test procedures are reported by Ensor *et al*[1].

Two Meteorology Research, Inc. (MRI) Plant Process Visiometers (PPV) were installed—one at the scrubber inlet and the other at the outlet. These instruments were used as real-time monitors to detect upsets and to determine in-stack opacity.

Impactor runs were conducted to obtain samples for elemental analysis by Ion-Excited X-Ray Analysis.

All impactor runs were conducted using Apiezon L high vacuum grease as a particle collection substrate. The Apiezon L was applied to light-weight collection discs. All weighings were conducted using a Cahn 400 analytical balance with a precision of 0.01 mg. Use of the Cahn balance and light-weight substrates was essential to reduce errors due to weighing.

The test program was divided into three phases in order to systematically evaluate the scrubber. The test phases were:

- Phase 1 - Evaluation of the distribution of aerosol mass concentration at the inlet. With the limited resources in manpower and equipment, the evaluation of the source was attacked one aspect at a time. All four inlet ducts were sampled at the same time. The cascade impactor trains were supplemented with in-stack filter probes to establish the consistency of the concentration.
- Phase 2 - Evaluation of outlet distribution of aerosol mass concentration. Similar parallel tests were used on the outlet of the scrubber to indicate the variation in the sections.
- Phase 3 - Simultaneous inlet-outlet tests for scrubber efficiency. The final phase of the field program was the simultaneous inlet-outlet tests with both primary and secondary tests.

The tests disclosed several problems with the scrubber which are discussed by Ensor et al[1].

SCRUBBER EFFICIENCY RESULTS

The Phase 3 tests were used to compute the efficiency of the scrubber. Sufficient data were taken to allow selection of the runs taken during steady-state plant conditions. The data used in the efficiency determinations are summarized in Table 1. The diffusion battery tests were restricted to section B at the outlet because of the relatively normal behavior of that section of the scrubber.

Total Mass Collection Efficiency

The mass collection efficiency was computed using only the cascade impactor data. The results are summarized along with some control room data in Table 1. The pressure drop across the system was reported to indicate the magnitude of the effect of the existence of the air reheaters. The outlet gas flow was the total for the system as determined from the velocity traverses. The lack of correlation between efficiency and pressure drop was an unexpected result.

TABLE 1. SCRUBBER COLLECTION EFFICIENCY

				SECTION A				SECTION B				SECTION C			
Date 1974	Load, MW	O_2, %	Outlet Gas Flow, am^3/hr	ΔP System, cm H_2O	ΔP Bed, cm H_2O	ΔP Mist Elimin., cm H_2O	Eff., %	ΔP System, cm H_2O	ΔP Bed, cm H_2O	ΔP Mist Elimin., cm H_2O	Eff., %	ΔP System, cm H_2O	ΔP Bed, cm H_2O	ΔP Mist Elimin., cm H_2O	Eff., %
11/20	166	3.6	[a]	41	9.9	0.76	ND	45	25	2.5	84.7	46	21	8.3	ND
11/21	164	3.4	[a]	39	9.6	0.76	ND	43	18	1.8	89.9	44	20	5.1	ND
12/10[b]	157	3.4	9.47×10^5	36	15.2	1.7	96.3	41	20.8	2.5	92.6	41	18.5	3.8	86.9
12/11	160	3.0	10.2×10^5	38	14.7	1.5	96.4	42	22.1	3.2	93.2	44	22.4	2.5	96.7
12/12	160	2.6	8.78×10^5	38	14.7	1.8	79.6	44	22.9	2.5	93.1	46	24.1	3.8	92.1

[a] Full velocity traverses were not taken.

[b] The control room data were incomplete. Interviews, data from other days and the log book were used to supplement available information.

The average efficiency of the December tests was 92%, slightly lower than the design efficiency of 95%.

Mass Penetration as a Function of Particle Diameter

The particle mass penetration as a function of particle diameter was determined for three days. These data are shown in Figures 2 to 4.

Generally, the size distributions and penetrations were consistent, though loadings fluctuated considerably. The maximum penetration (minimum efficiency) was achieved in the region of 0.2 μm actual diameter, similar to results for another scrubber as reported by Sparks et al[3].

Elemental Chemical Analysis

The measurement of the concentrations of a number of elements was intended mainly to provide data to aid in the interpretation of the scrubber performance. It was not planned to per-

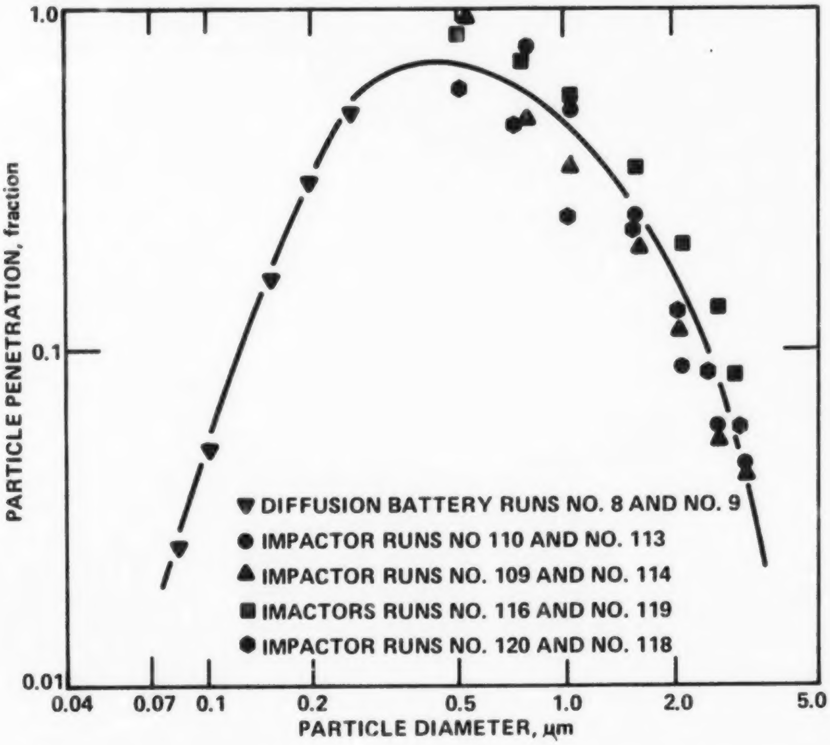

Figure 2. Combined penetrations for diffusion battery and cascade impactor (December 10, 1974)

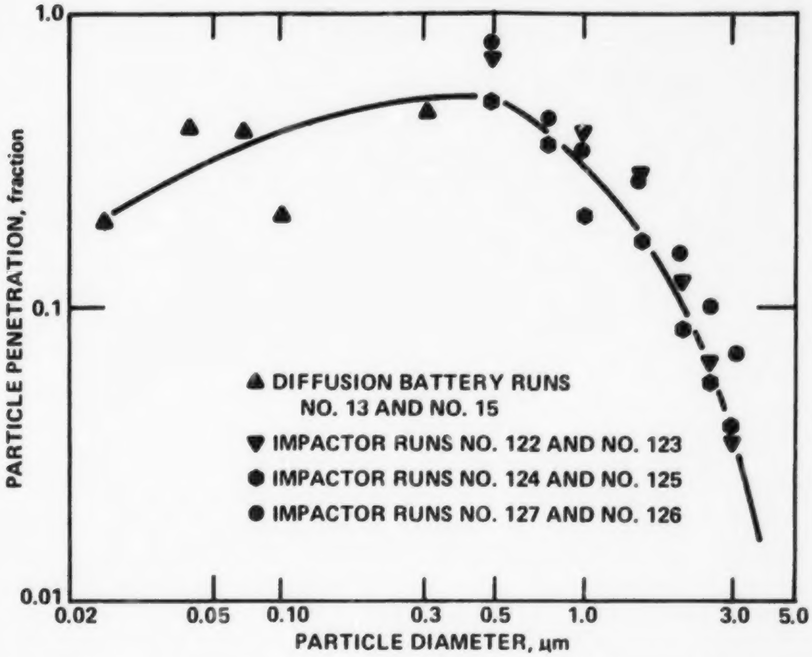

Figure 3. Combined penetrations of diffusion battery and cascade impactor (December 11, 1974)

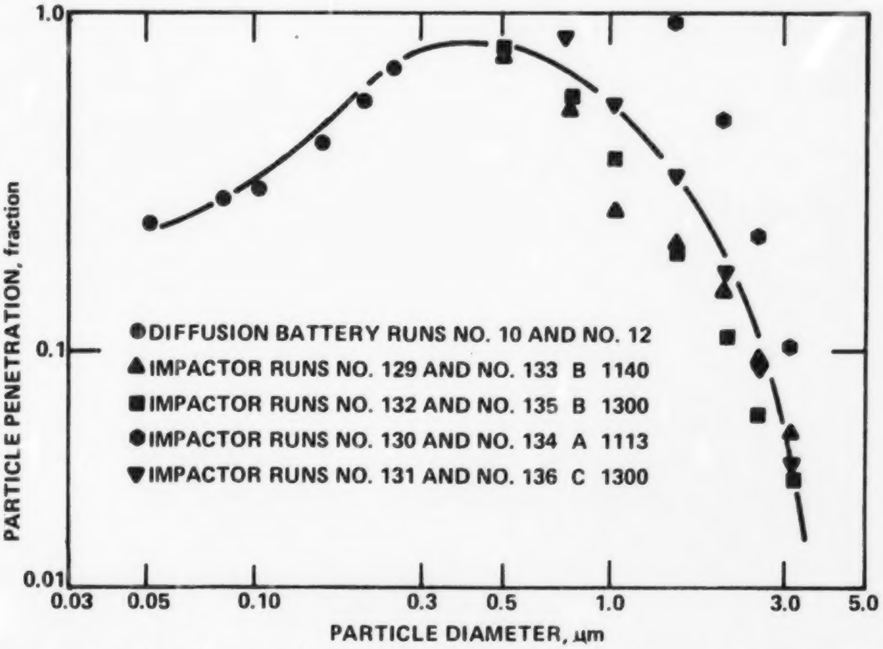

Figure 4. Combined penetrations for diffusion battery and cascade impactor (December 12, 1974)

form elemental balances or determine emission factors. The samples were taken during December 10-11, 1974. The overall penetrations of various elements are shown in Table 2. The penetration as a function of particle diameter for various elements is shown in Figure 5.

TABLE 2. PENETRATION OF ELEMENTS THROUGH THE SCRUBBER FOR DECEMBER 10, 1974

Element	Penetration	Average Outlet Concentration, micrograms/dsm^3 [b]
Al	0.029	326
Si	0.033	658
S	3.4[a]	1030
K	0.043	50
Ca	0.059	508
Ti	0.073	96
V	0.14	27
Cr	1.10[a]	57
Fe	0.18	1500
Ni	0.95	33
Cu	2.9[a]	668
Zn	1.5[a]	501
Br	0.28	5.7
Pb	0.64	120
For all elements	0.108	
Total mass	0.074	

[a] Penetrations greater than one indicate generation of particles in flue gas by evaporation of the scrubber liquor.

[b] Dry standard, 21.1°C, 760 mm Hg.

DISCUSSION

The scrubber performance results were analyzed in depth for trends and to allow comparison to data in the literature.

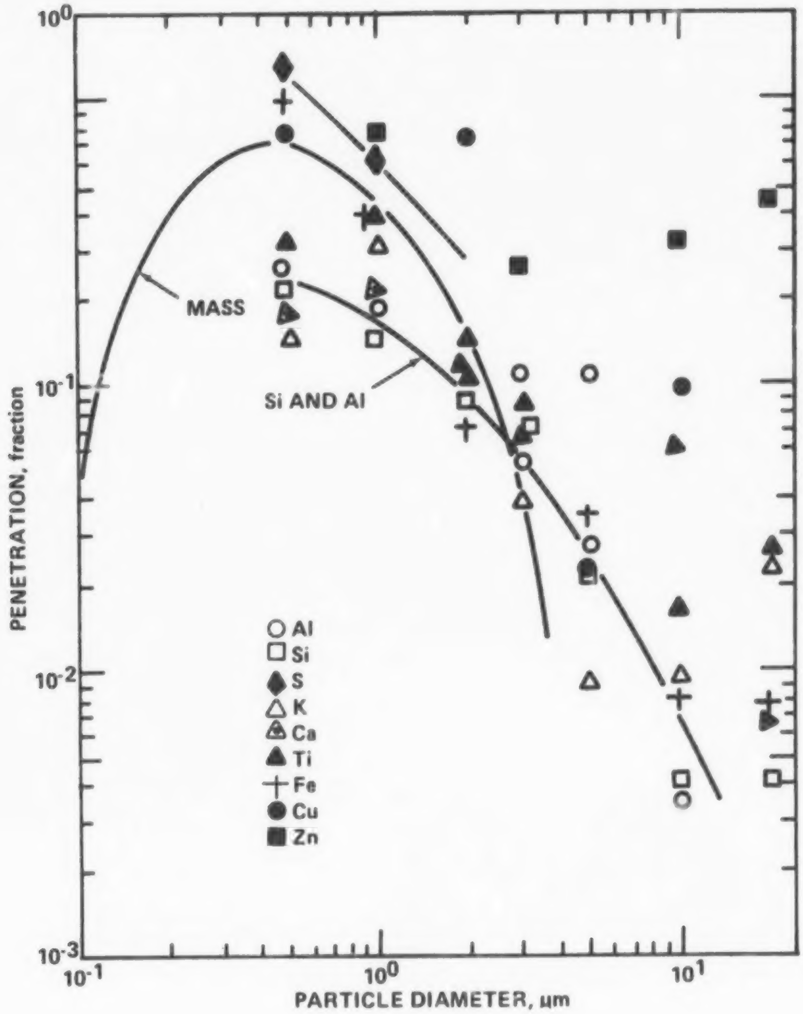

Figure 5. Scrubber penetrations for selected elements

Examination of the particle penetration data for each simultaneous pair of inlet and outlet runs shows a wide range of results, as summarized in Table 3.

TABLE 3. PARTICLE PENETRATION SUMMARY

Run No. In	Run No. Out	Section	d_{pc},[a] μm	ΔP, cm H_2O	Filter out / Filter in[b]
56	53	B	1.5	23.0	0.31
55	57	B	1.1	23.0	0.81
60	61	B	0.8	23.0	1.2
114	109	B	0.8	23.0	2.9
119	116	B	1.0	23.0	0.39
121	123	B	0.8	23.0	0.55
125	127	B	<0.5	23.0	1.2
133	129	B	0.8	23.0	2.0
135	132	B	0.8	23.0	0.47
124	125	B	0.6	23.0	3.1
113	110	A	1.0	--	0.81
127	126	A	0.8	15.0	0.41
134	130	A	2.0	9.0	6.7
115	119	C	<0.5	25.0	0.76
120	118	C	0.6	--	1.0
123	122	C	0.7	25.0	1.1
136	131	C	1.1	24.0	3.5

[a] Scrubber cut (50% penetration) diameter.

[b] Ratio of outlet filter to inlet filter particle concentrations $(mg/dsm^3)/(mg/dsm^3)$.

The scrubber performance cut diameter (i.e., particle diameter at 50% penetration), used to characterize efficiency, varied from less than 0.6 μm to 2.0 μm. No pattern of correlation between cut diameter and other parameters such as pressure drop was found. Thus, the variation was due to a combination of system fluctuations and measurement errors.

Penetrations found in this study are much higher than those reported in a previous study of the same scrubber (Calvert, et al.[4]), and of another mobile bed scrubber on a coal-fired power plant (Statnick and Drehmel[5]). For example, Calvert *et al.* reported a cut diameter of 0.35 μm and a penetration at 1.0 μm of about 0.09. Statnick and Drehmel reported that, for 25 cm of water scrubber pressure drop, penetration did not exceed 0.05 for any particle size and was about 0.02 for 1.0 μm particle diameter. These and some other points are compared in Table 4 with representative results from the present study.

TABLE 4. COMPARISON OF MOBILE BED STUDIES

Investigators	d_{pc}, μm	Penetration at Particle Diameter Shown			
		0.5 μm	0.8 μm	1.0 μm	2.0 μm
Present	0.8	0.8	0.5	0.4	0.15
Calvert, *et al.*[4]	0.35	0.3	0.15	0.08	0.02
Statnick and Drehmel[5]	--	0.07	0.03	0.02	0.002

Approximate mean values for all runs, exclusive of 56/53 and 134/130.

There is evidence that the high outlet particle concentration measured is due to entrainment from the scrubber. Facts which indicate the presence of outlet particles introduced by entrainment are as follows:

1. Outlet filter loadings are higher than inlets, based on the same gas sample volume, for many of the tests.
2. Penetrations in the present study are higher than those found by others.
3. Variations in penetration are not related to gas flow rate, pressure drop, or other known parameters, but can be attributed to variable entrainment.
4. Penetrations for scrubber section "A" are the same as for section "B" despite the gas pressure drop for "A" being about half that for "B".
5. Reheater and entrainment separator operating problems occurred during the test.
6. Elemental analyses of inlet and outlet particles showed an apparent "generation" of particles containing soluble elements as described in the previous section.

The overall conclusion is that the scrubber performance data obtained in this study are specific for the operating factors and scrubber condition which existed during the test period. It is not possible to establish a general mobile bed scrubber performance model from these data because of the overshadowing and undefined influence of liquid entrainment. It appears that both scrubber performance and reliability could be improved by improved entrainment separation.

ENGINEERING ANALYSIS

The objective of the engineering analysis was to assemble the following information:

Capital costs

Operating costs

Major maintenance problems

Scrubber reliability

Estimated cost required to minimize operating problems.

Capital Costs

The total installed cost in 1972 for the scrubber was \$4,400,000. Based on the boiler nameplate rating of 150 MW, the cost is \$29/kW or, based on the rated gas volume (see above), is \$4.18/1000 m^3/hr (\$7.10/1000 acfm). The detailed cost itemization is given by Ensor _et_ _al_.[1]. In 1975 dollars, the scrubber would cost \$5,800,000.

Operating Costs

The total operating costs are approximately \$495,000/yr (fourth quarter 1973 and the first three quarters of 1974) based on 75% availability of the scrubber or 0.50 mills/kWh.

Maintenance Problems

The scrubber had a number of maintenance problems, many of which were solved during start-up and operation. The problems mentioned here are the more persistent ones which have defied solution. The maintenance problems are discussed in detail by Ensor _et_ _al_.[1]. These include:

1. Breakage of Mobile Bed Contactors - The plastic mobile bed contactors have been a chronic problem due to breakage from wear. The desired lifetime of the spheres is 8000 hours; however, normally a lifetime of only 6000 hours was experienced.

Moreover, damage to the pump liners and plugging of the nozzles can result from the fragments entering the liquor recycle piping. Screens in the scrubber hopper have eliminated this problem with the penalty of adding screen cleaning to the required maintenance. Public Service Company of Colorado has tested a number of different packings and is currently using polyethylene spheres in the scrubber.

2. Migration of Mobile Bed Contractors - The mobile bed contactors will also migrate from one section of the scrubber to another if an opening the width of a contactor exists in the partitions. Poor distribution of the contactors causes channeling of flue gas and a reduction in particle collection efficiency.

3. Guillotine Dampers - The guillotine isolation dampers have caused problems due to breakage of the damper when closing against a buildup of fly ash and leakage.

4. Recirculation Pumps - The recirculation pumps have been a source of problems in the past due to mechanical failure. A new pump has been tested by Public Service Company of Colorado and has been providing good service.

5. Reheater Section - The scrubbed gases are heated by direct contact with three banks of steam coils. These coils are susceptible to pluggage and corrosion in the wet flue gas scrubber discharge. Addition of a second set of soot blowers and drying ash during periods of the scrubber shutdown with heavy soot blowing has had minimal effect. Corrosion problems have rendered the heaters inoperable. Both upper and lower layer reheat coils have been removed.

6. Weather-Related Problems - The freezing of lines has always been a problem during cold weather. All lines must be heat-traced and drained when the scrubber is shut down.

   Another solution is to enclose the scrubber in a weatherproof building. The major problem with this is the possibility of leakage of flue gas into the structure.

Scrubber Reliability

For this study, availability of the scrubber was defined as:

$$\text{Availability} = \frac{\text{hours of scrubber operation* -hours boiler was burning 100\% gas}}{\text{hours of boiler operation -hours boiler was burning 100\% gas}}$$

The reason that the hours the boiler was burning 100% gas was subtracted from the total hours of scrubber and boiler operation is that the scrubber is normally either left running with only water systems operating or completely shut down during periods of 100% gas burning operation.

It is interesting to note that the scrubber was out of service a majority of the time during August and September 1974, when the unit returned to mixed fuel burning. The reason for this is that after long periods of idleness, due to either maintenance or 100% gas burning, the scrubber usually experienced minor start-up problems. When start-up troubles with the scrubber were encountered, every effort was made to use any available gas on the unit. Consequently the scrubber had a poor percentage availability for the months involved, but the overall availability was not affected very much.

Values of availability are given for two capacity levels: 100% of capacity and 80% of capacity or greater. There is a significant amount of time that the scrubber operated at 80% of capacity. For example, in January of 1974, although the scrubber operated at 100% of capacity for only 175 hours, it did operate at 80% of capacity for 547 hours. Although the scrubber is not treating all of the boiler flue gas, it is felt that some credit should be given the scrubber for handling most of the flue gas. In most cases, running at 80% of capacity will probably allow PSCC to meet particulate emission standards.

The cumulative percent availability to date reflects the total hours of scrubber operation since start-up. This value is plotted by month in Figure 6. This figure shows that after an initial drop, the availability of the scrubber has been increasing steadily. This is typical of other PSCC scrubber operations. The initial drop is attributed to the many minor design problems which arose soon after start-up. The following increase in availability is attributed to the solving of these problems and the increased operating knowledge which was gained through operating experience.

As of November 30, 1974, the scrubber had operated at 100% capacity 59.9 percent of the time and at 80% capacity or greater 70.9 percent of the time.

---

*Hours of scrubber operation is related directly to the time the boiler was operating.

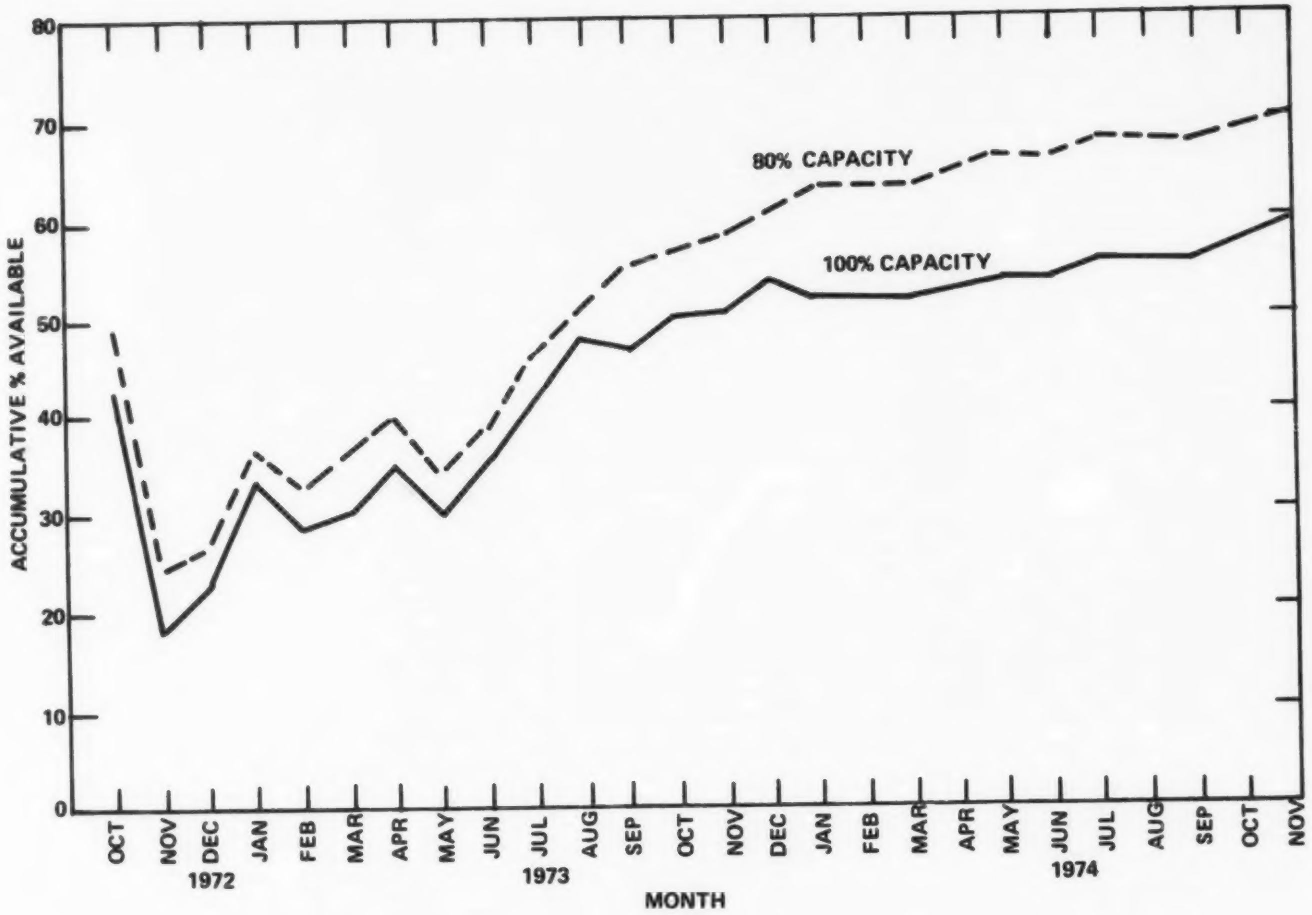

Figure 6. *Cherokee No. 3 scrubber accumulative availability from start-up to November 1974*

In order to more clearly see the increase in availability with time, after the first year when each new month was added to the log, only the previous 12 months availability was calculated. This value is plotted in Figure 7. Looking at the last month tabulated (November 1974) reveals that the scrubber operated at 100% of capacity 78.6 percent of the time and at 80% of capacity or greater 96.7 percent of the time during the previous year. The figure also shows that the scrubber had been operating at 80% of capacity or greater with over 90% availability since May of 1973.

The feasibility of using the design and operating experience to improve availability of the scrubber was investigated. The goal was to increase the availability of the scrubber, realizing that the maintenance required may slightly increase due to the extra equipment. The suggested modifications are summarized below:

		Estimated Availability, %
Identical scrubber	$5,800,000*	60-70
Extra 33-1/3% capacity section	1,200,000	10-15
Indirect reheat, incremental	200,000	
Scrubber enclosure	90,000	5-10
Miscellaneous charges	80,000	
	$7,370,000	75-95

The capital cost of $7,370,000 is $49/kW for a 150 MW unit.

The important aspect of maintaining and improving the availability of the scrubber system is the attitude of the plant operating and maintenance people in keeping the unit on line.

The steadily increasing availability of the Cherokee Scrubber is an indication that Public Service of Colorado is committed to solving the operating and maintenance problems.

---

*1975 dollars.

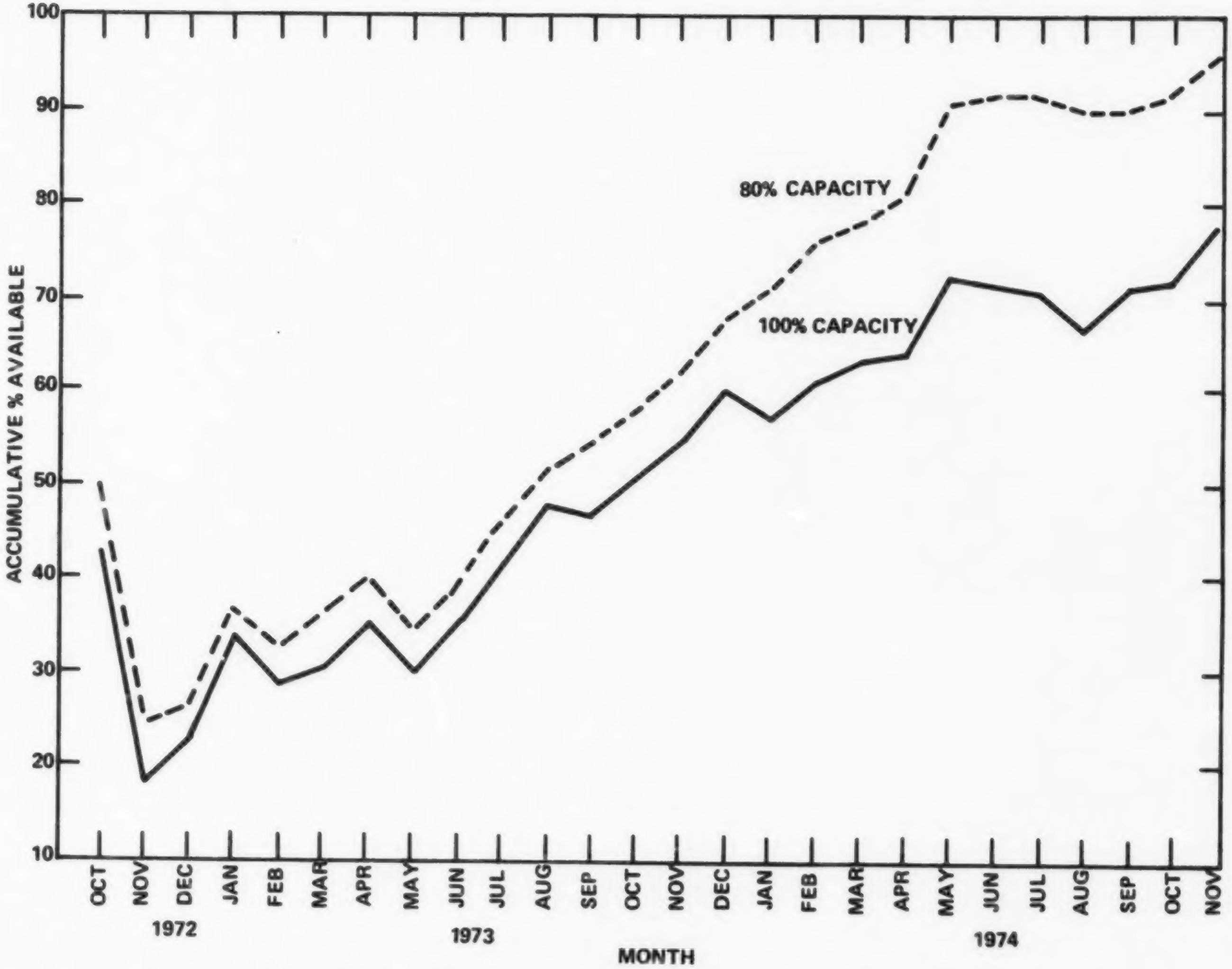

Figure 7. Cherokee No. 3 scrubber accumulative availability from start-up to November 1974 averaged over the previous year on a running basis

CONCLUSIONS

The performance data and engineering analysis indicate that scrubbers are capable of collecting fly ash from combustion of low sulfur coals. The Cherokee power plant was a successful retrofit with a scrubber to supplant the control with an existing electrostatic precipitator. The scrubber has a small physical space and the ability to connect with existing duct work. This is often a problem when retrofitting other control devices. Capital and operating costs for a scrubber are likely to be higher than similar costs for a moderately sized electrostatic precipitator. However, in applications where the dust resistivity requires a large-size electrostatic precipitator, a scrubber system is likely to be cost competitive.

ACKNOWLEDGEMENTS

The efforts of Public Service Company of Colorado personnel in providing assistance during the source test and the engineering evaluation were vital to the success of the Project. This work was conducted under EPA Contract 68-02-1802.

REFERENCES

1. Ensor, D.S., B.S. Jackson, S. Calvert, C. Lake, D.V. Wallon, R.E. Nilan, K.S. Campbell, T.A. Cahill, and R.G. Flocchini. Evaluation of a Particulate Scrubber on a Coal-Fired Utility Boiler, EPA-600/2-75-074, NTIS PB 249562/AS, U.S. Environmental Protection Agency, Washington, D.C., 1975.

2. Raben, I.A. Use of Scrubbers for Control of Emissions from Power Boilers. U.S. Paper No. 13. Proceedings, Symposium on Control of Fine Particulate Emissions from Industrial Sources. San Francisco, California. January 1974.

3. Sparks, L.E., J.D. McCain, and W.B. Smith. Performance of a Steam-Ejector Scrubber. J. Air Pollution Control Assoc. 24:958, 1974.

4. Calvert, S., N.C. Jhaveri, and C. Yung. Fine Particle Scrubber Performance Tests, EPA-650/2-74-093, NTIS PB 240325/AS, U.S. Environmental Protection Agency, Washington, D.C., 1975.

5. Statnick, R.M., and D.C. Drehmel. Fine Particle Control Using Sulfur Oxide Scrubbers. 67th Meeting of the Air Pollution Control Assoc., Denver, Colorado, Paper No. 74-231. June 1974.

METRIC CONVERSION FACTORS

To convert from	To	Multiply by
lb	kg	0.454
gr/ft^3	g/m^3	2.29
ft^3/min (cfm)	m^3/sec	0.000472
lbs/in.^{2}	kg/m^2	703.
°F	°C	(°F-32) × 5/9
ft^2/1000 cfm	m^2/(m^3/sec)	0.197
in. w.g.	mm Hg	1.868
gallons	liters	3.785
ft	m	0.3048
in.	m	0.0254
tons	kg	908.
in.^{3}	cm^3	16.39
ft^3	m^3	0.028
gal/min	l/sec	0.0631
ft^2	m^2	0.0929
in.^{2}	cm^2	6.452
gal/1000 ft^3	l/m^3	0.135
grams	grains	15.43
ft/min	cm/sec	0.508
ounces	grams	28.34
oz/yd^2	g/m^2	33.89
grains	grams	0.0647
gr/ft^2	g/m^2	0.698
lb force	dynes	4.44×10^5
lb/ft^2	g/cm^2	0.488
in. H_2O/ft/min	cm H_2O/cm/sec	5.00
Btu	calories	252